Optimization of the Axial Turbines Flow Paths

Anatoli Boiko Yuri Govorushchenko Alexander Usaty

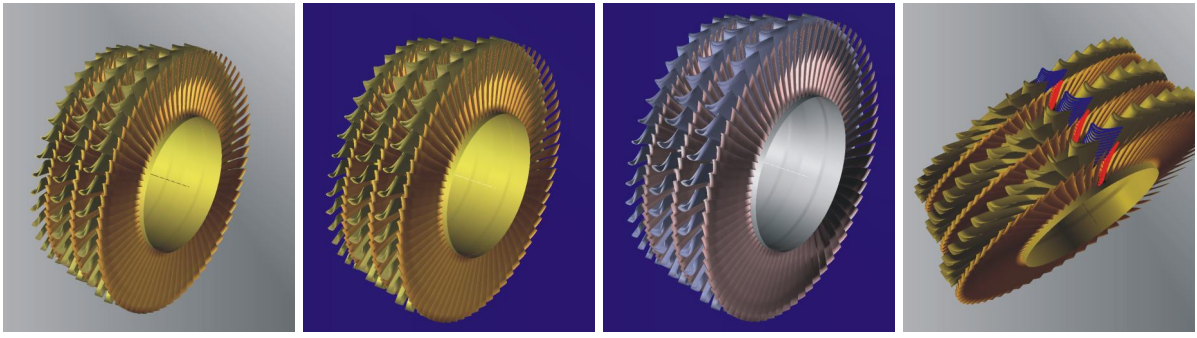

SciencePG
Science Publishing Group

Optimization of the Axial Turbines Flow Paths

Anatoli Boiko

Yuri Govorushchenko

Aleksander Usaty

SciencePG
Science Publishing Group

Published by

Science Publishing Group

548 Fashion Avenue
New York, NY 10018, U.S.A.

http://www.sciencepublishinggroup.com

ISBN: 978-1-940366-67-8

Preface

The decades of the 1970s and 1980s of the last century were marked by the emergence and rapid development of a new scientific direction in turbine manufacturing – optimal design. A summary of the approaches, models, and optimization methods for axial turbine flow path is presented in the monographs [13–15 and 24].

It should be noted that work on the optimal design of the flow path of axial turbines and the results obtained not only have not lost their relevance, but are now widely developing. Evidence of this is the large number of publications on the topic and their steady growth. Optimization of the turbomachine flow path is a priority area of research and development of leading companies and universities. Without the use of optimization, it is impossible nowadays to talk about progress made in the creation of high efficiency flow paths of turbomachines.

It is worth noting that the widespread use in power engineering of modern achievements of hydro-aerodynamics, the theory of thermal processes, dynamics and strength of machines, materials science, and automatic control theory, is significantly expanding the range of tasks confronting the designer and greatly complicating them.

The proposed book comprehensively addresses the problem of turbomachine optimization, starting with the fundamentals of the optimization theory of the axial turbine flow paths, its development, and ending with specific examples of the optimal design of cylinder axial turbines.

It should be noted that the mutual influence of designed objects of turbine installations and the many design parameters of each object, which the product's effectiveness depends on, is putting the task of multiparameter optimization on the agenda.

For turbines with extractions of working media for various needs, efficiency ceases to be the sole criterion of optimality. It is necessary to enable in the optimization process such important parameters as power supply. The task of optimal design of turbine has become multifaceted.

It should also be stressed that often the turbo installation mode of operation is far from nominal. So taking into account the operating mode in the optimization can significantly improve the efficiency of the turbine.

In the book, along with the widely used methods of nonlinear programming, taking into account the complexity of the task and the many varied parameters, the use of the theory of planning the experiment coupled with the LP sequence to find the optimal solution is discussed.

The first chapter of the book deals with general issues of the optimal design of complex technical systems and, in particular, the problem of optimization of turbomachines, using one of the approaches to the design of turbo installations – a block-hierarchical view of the design process. With this priority is given to flow path optimization of axial turbines. The task of object design and using mathematical models is formulated. A brief overview of optimization techniques, including the optimization method for turbines considering mode of operation is given.

The second chapter is devoted to the mathematical modeling of flow path elements of turbomachines. Special attention is paid to aerodynamic models of flow through the flow path, including flow through axial cascades of turbine profiles, one-dimensional and axial-symmetric flow through the turbine stage and multistage turbomachine cylinders; geometric and strength models; a model for creating a thermal scheme for a gas turbines and the computation of system equations is set out.

The results of the numerous calculations are compared with experimental data.

Chapter 3 examines one of the most important tasks in designing turbines – determination of the optimal number of stages and distribution between them of the heat drop.

The problem of parameter optimization of the axial turbine stage along the radius considering the slope and curvature of the working medium stream lines is the subject of the fourth chapter of the book. It assesses the impact of leaks on the optimal spin laws of the guides and working wheels of the axial turbine stages in a wide range of changes of bushing ratios, and the results of the effect of tangential slope on characteristics of axial turbine stage are presented.

Chapter 5 is devoted to optimal profile creation, starting from the choice of the main parameters and the consideration of their formation methods. The methods for optimal profile creation using geometrical quality criteria and minimum profile losses are described, and the results of experimental research of initial and optimal profiles are given.

The important problem of turbine blade shape optimization, using aerodynamic computation is covered in Chapter 6 of the book. The presentation of blade geometry, file formats for storage blades and grids, building up the lateral surfaces of blades and the three-dimensional parametric model of turbine cascades are discussed, an algorithm of spatial aerodynamic optimization of axial turbine cascades and the influence of simple and complex slopes on the flow in the ring cascade is described, and the reasons for increasing the efficiency of the optimized turbine cascade are analyzed.

The seventh chapter sums up the results of the developed optimization theory by applying it to the optimum design of flow parts of powerful modern steam turbine cylinders at nominal mode of operation and flow path of gas turbine installations, taking into account their operational mode.

It should be noted that in the book attention is paid to the verification of developed mathematical models of flow path elements of axial turbines as well as to the results offered by methods and algorithms for optimization. A comparison

of the results of calculations and optimization with experimental data of the modeling stages and with two stage air turbines as well as with the results of full-scale experimental research of powerful steam turbine in a wide range of modes of operation in a thermal power plant is performed.

The comparison of the results of experimental and calculated research data have convincingly confirmed that optimization calculations and designed and programmatically implemented mathematical models have a high degree of accuracy and adequately simulate the physical processes flow of the working medium in an axial turbine flow path.

The book convincingly shows that at the present stage of design and manufacturing of turbines (characterized by decades of accumulated positive experiences of creating high-performance flow paths) their further improvement is possible only using the most modern methods and software systems, capable of solving tasks of a multilevel object-oriented multicriterion and multiparameter optimization of the flow paths of axial turbines, taking into account their operational mode.

The book is intended for researchers and experts in design, calculation and research on turbomachines. It is useful for University faculty members, post-graduate students and senior undergraduate students of Technical Universities.

Authors express their sincere thanks to Director Engineering Institute Prof. Serbin S. I. for the kindly offered possibility of carrying out of CFD-calculations with usage ANSYS CFX at National Shipbuilding University named after Makarov. The authors also express gratitude to the junior scientist of National Technical University "Kharkiv Politecnical Institute" Naumenko Svetlana P. for her assistance on the final stage of work on the manuscript.

Contents

Key Symbols

a – local sound velocity, m/g; inter-blade channel throat, mm;

B – blade's profile axial chord, mm;

b – blade's profile chord, mm;

c, c_r, c_u, c_z – absolute velocity and its components in the cylindrical coordinate system, m/s;

C_0 – velocity, equivalent to stage or module heat drop, m/s;

C_p – specific heat capacity at constant pressure, J/(kg·grad); pressure coefficient;

C_v – specific heat capacity at constant volume, J/(kg·grad);

D (or d) – stage (or annular cascade) diameter, mm;

F – stage (or channel) cross-section area, m^2;

G – mass flow rate, kg/s;

H – specific rothalpy (Bernoully constant) in the relative frame; turbine heat drop, J/kg;

L_u – specific peripheral work, J/kg;

Δh – specific kinetic energy loss, J/kg;

i– specific enthalpy, J/kg; incidence angle, grad;

k – isentropic factor;

ℓ – blade height, mm;

M – Mach number;

N – stage power, W;

N_{it} – a predetermined number of iterations;

n– number of stages in the module; rotation speed, rev/min;

P – pressure, MPa;

R (or ρ') – reaction degree by static stage input parameters;

$\bar{R}$ (or ρ) – reaction degree by total stage input parameters;

Re – Reynolds number;

r – stage radius, mm; profile's edge radius, mm;

r, φ, z – cylindrical coordinate system's axes;

S – specific entropy, J/(kg·grad); axial distance, m;

s – length (along a streamline), mm;

T – temperature, K;

t – cascade's pitch, mm;

u – rotor annular velocity, m/s;

w – fluid velocity in the relative frame, m/s;

z– number of blades; last turbine's stage;

α_n – heat recovery factor of the n-stage module;

α, β – angles between c, w and rotation direction u; $\tilde{\beta} = 180^\circ - \beta$, grad;

β_r – profile's metal angle, grad;

β_s – profile's stagger angle, grad; $\beta_b = 90° - \beta_s$;

γ – angle in the meridional plane, grad;

ε (or θ) – flow turning angle in the cascade, grad;

ζ – loss factor, relative to dynamic head at the cascade outlet;

η_i – stage's internal efficiency;

η_u – stage's peripheral efficiency;

Λ – penalty coefficient; Lagrange's coefficient;

μ – crown mass exchange coefficient; exit velocity utilization factor;

ν – velocities ratio, u/C_0;

ξ – relative (to stage's heat drop) losses;

ρ – density, kg/m^3;

σ – entropy factor;

φ, ψ – velocity coefficients of stator and rotor blades;

χ – blockage factor;

Ψ – stream function;

Ψ^* – stream function at the tip;

ω – angular rotation speed, s^{-1};

$\aleph$ – stream line curvature, 1/м.

Indexes and Other Signs

0, 1, 2 – sections numbers at stage inlet, between vanes and at outlet;

abs – absolute;

add – additional;

as – additional stream;

bh – balance boles;

cons – constructive;

cr – critical;

cyl – cylinder;

def – defined;

e (or *eff*) – effective;

g (or *s*) – guide (stator) blade;

h (or *r*) – hub (root) radius;

i – stage number;

in – input;

j – section number;

l (or leak) – leakage;

ll – local losses;

m – module; at mean radius;

max – maximal;

min – minimal;

mix – mixture;

mod – module's;

ms – main stream;

n – nominal;

nom – nominal;

opt – optimal;

out – rotor output;

p (or *t*) – peripheral (tip) radius;

r – rotor;

r.c. – radial clearance;

s – stream;

spec – specified;

T – corresponding to isentropic (theoretic) fluid expansion;

t – tip;

u – circumferential direction projection.

Abbreviations

C	– Compressor
CAD	– Computer aided design system
CC	– Combustion chamber
CU	– Gas compressor unit
EFF	– Efficiency
FMM	– Formal mathematical model
FP	– Flow path
GT	– Gas turbine
GTU	– Gas turbine unit
GV	– Guide vane
HPC	– High pressure cylinder
HPT	– High pressure turbine
IPC	– Intermediate pressure cylinder
LPC	– Low pressure cylinder
LPT	– Low pressure turbine
OMM	– Original mathematical model
R	– Regenerator
RH	– Reheating
RTE	– Recycling turbine expanders
RV	– Rotor vane
S	– Stator

SC – Natural gas supercharger

TC – Thermal cycle

TE – Turbine expanders

1

Statement of the Axial Turbine's Flow Path Optimal Design Problem

The methodology of a turbine optimal design as a complex multi-level engineering system should support the operation with diverse mathematical models, providing for each design problem communication between the neighboring subsystems levels.

One approach to turbine design with using of block-hierarchical representation consists in the transition from the original mathematical models for the subsystems and numerical methods of optimization to "all-purpose" mathematical model and general method of parameters optimization.

1.1 Mathematical Models and the Object Design Problem

We will specify as original the mathematical model (OMM), which is a closed system of equations that describe the phenomena occurring in the designed object.

Regardless of the mathematical apparatus (algebraic, ordinary differential, integral, partial differential equations, etc.), OMM can be represented symbolically as follows:

$$\vec{Y} = \vec{Y}\left(\vec{B}, \vec{X}\right), \quad L\left(\vec{B}, \vec{X}\right) = 0, \tag{1.1}$$

where $\vec{X} = \left\{\vec{x}, \vec{u}\right\}$; $L\left(\vec{B}, \vec{X}\right)$ – the operator defining the model's system of equations.

The parameters $\vec{Y}$ characterize the quality indicators; $\vec{B}$ – entering the subsystems model from adjacent levels, the operational environment of the object. Parameters $\vec{X}$ can be either dependent, calculated by the OMM equation ($\vec{x}$) or independent, the choice of which provides the designer ($\vec{u}$). It is understood that the number of internal parameters of the object includes all internal parameters of the elements of underlying layers.

Significant simplification and unification of the subsystems description achieved by OMM approximation with a model, which we call a formal macromodel (FMM). We represent the FMM as a complete polynomial of the 2-nd degree, by which in many cases it is possible to approximate the output parameters with sufficient accuracy:

$$y(q) = A_0 + \sum_{i=1}^{n} (A_i + A_{ii} q_i) q_i + \sum_{i=1}^{n-1} \sum_{j=i+1}^{n} A_{ij} q_i q_j \ . \tag{1.2}$$

FMM parameters vector is expressed through the IMM parameters as

$$\vec{Q} = \vec{Q}(\vec{u}, \vec{B}). \tag{1.3}$$

hence FMM may be represented symbolically as follows:

$$y = y(\vec{B}, \vec{u}). \tag{1.4}$$

Comparing (1.4) and (1.1), we see that the FMM have no phase variables. The transformation of one model to another with a fewer number of variables or constraints, giving an approximated description of the investigated object or process compared to the initial, will be called *aggregation*. Thus, the FMM is aggregated with respect to (1.1).

The problems of the object's optimal design using models (1.1) and (1.4) will be called following:

$$\max_{\vec{u} \in U} Y_j(\vec{B}, \vec{x}, \vec{u}), \quad L(\vec{B}, \vec{X}) = 0; \tag{1.5}$$

$$\max_{\vec{u} \in U} y(\vec{B}, \vec{u}). \tag{1.6}$$

Suppose, that the problem (1.6) is solved for all possible values of the vector $\vec{B}$ that allows you to build approximation dependencies

$$y^{\text{opt}} = y^{\text{opt}}\left(\vec{B}\right), \quad \vec{u}^{\text{opt}} = \vec{u}^{\text{opt}}\left(\vec{B}\right), \tag{1.7}$$

containing information on all kinds of optimal designs. The model (1.7) is aggregated with respect to (1.4) and (1.5). The same could be made with the OMM: by virtue of solving the equations of the model would have disappeared phase, and by optimizing – control variables. Usually, however, this task is too complex for the numerical solution.

An approximate solution can be achieved with the help of disaggregation, i.e. mapping of aggregated variables in the model space of OMM. Substituting (1.7) to (1.1), we obtain:

$$Y_j = Y_j\left(\vec{B}, \vec{x}, \vec{u}^{\text{opt}}\left(\vec{B}\right)\right), \quad L\left(\vec{B}, \vec{X}\right) = 0,$$

where are $\vec{x}^{\text{opt}}$ and Y_j^{opt} – solution of OMM.

For example, in the optimal design of turbine cascade the quality criterion is the energy loss ratio, OMM – ideal gas motion and the boundary layer on the profile equations, phase variables – flow parameters, control – profile shape, cascade spacing and others.

In practice, instead of the loss calculation OMM various empirical loss calculation methods used, which, in fact, are FMMs of form (1.7), because does not take into account information about any and just about the currently best ("optimum") profile cascades. In this way, at higher design levels use only the information on the improved aerodynamic profiles loss ratio.

The approach described can be applied to multi-level design of complex systems.

1.2 Optimization of Complex Technical Devices

1.2.1 Design Hierarchy

Block-hierarchical representation of the design process, implemented with the creation of complex technical devices, leads to a problem of such complexity that can be effectively resolved by means of modern computing, and the results of the decision – understood and analyzed by experts. Typically, the design hierarchy of tasks is formed along functional lines for turbine can have the form shown in Fig. 1.1.

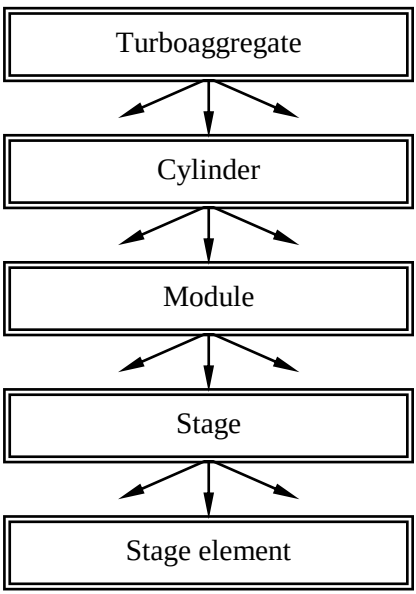

Figure 1.1 *Hierarchy of turbine design problems.*

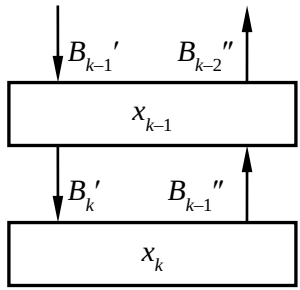

Figure 1.2 *Nearby hierarchy levels of optimization problems.*

The uniformity of mathematical models of the subsystems of the same level and local optimality criteria make it possible to organize the process of multi-level design, providing maximum global quality criterion of the whole system, in our case – the turbine. This process is based on the idea of so-called multilevel optimization approximation scheme that involves aggregation of mathematical models of the subsystems in the hierarchy when moving upward and disaggregation based on optimization results when moving downwards.

The problem of optimization the subsystem parameters described by OMM has the form (1.5). It can be solved by the methods of nonlinear programming and optimal control, depending on the form of the equations and the optimality criterion of the OMM.

Consider the solution order for the problems hierarchy of the system parameters optimization. Input parameters of *k*-level subsystem form of the set of internal and external parameters of the higher (*k*–1)-level subsystem. Feedback is carried out at the expense of the influence of the output parameters $\vec{B}_{k-1}''$ of the subsystem of *k*-level which with respect to the (*k*–1)-th subsystem is external. Complete vector of (*k*–1)-level external parameters, thus consists of a vector of external parameters $\vec{B}_{k-1}'$, coming from the higher-level and lower-level subsystems of vectors $\vec{B}_{k-1}''$ (Fig. 1.2).

Moving from the bottom up, we solve the problem of the form (1.6) at each *k*-level for all possible values of the vector of external parameters coming from a higher level. In this phase *k*-level variables are excluded from the internal parameters of the (*k*–1)-level model by effect of equations describing the *k*-level subsystem, and control – as a result of optimization. Thus, at each level above information is transmitted not about all, but only about the best projects of lower-level subsystems:

$$\vec{B}''_{k-1} = \vec{Y}_k^{\text{opt}}\left(\vec{B}'_k\right). \tag{1.8}$$

At the top, the 1-st level, from the problem (1.5) output parameters found, and predetermine external parameters of the level 2 subsystems, which makes it possible to restore the optimum parameters of the 2-nd level, solving the same problem (1.5). This disaggregation process extends to the lowest level, with the result that the optimal parameters are determined by all the subsystems that make up the complex technical systems.

To implement practically the described scheme is possible using FMM subsystems. In terms of the FMM problem (1.5) is written in a form similar to (1.6):

$$\max_{\vec{u}_k \in \vec{U}_k} y_k\left(\vec{u}_k, \vec{B}'_k\right), \tag{1.9}$$

which immediately follows

$$\vec{B}''_{k-1} = y_k^{\text{opt}}\left(\vec{B}'_k\right), \tag{1.10}$$

which is quite similar to (1.8), but has the advantage that it is a known polynomial of the form (1.2).

Methods based on the use of FMM is characterized in that before starting to solve the optimization problem on (*k*–1)-th level, it is replaced from the OMM

to FMM according to the condition (1.9). Driving multilevel optimization using FMM, is very flexible, allowing you to change the setting if necessary optimization tasks at any level due to changes in the components of vectors $\vec{Q}_k\left(\vec{u}_k, \vec{B}'_k\right)$.

1.2.2 A Numerical Method for the Implementation of the Multilevel Optimization Approximation Schemes

The current level of possibilities of computer technology and mathematics allow for a new approach to the organization of the block-hierarchical representation of the process of optimal design of axial turbine flow path (Fig. 1.1) and the information exchange between adjacent levels (Fig. 1.2). The essence of this approach lies in the application of the principle of recursion, provides automatic bypass facilities at all levels and solution for each object its local optimization problem in accordance with a predetermined scenario.

On the basis of this method created invariant subsystem of recursive object-oriented multi-criteria, multi-mode and multi-parameter optimization, providing solution of optimization problems, taking into account various types of parametric, structural, technological and functional limitations. Designed for its optimization techniques are universal, and the search for the optimal solution for each object is carried out in accordance with the scenarios of computing processes optimization.

Optimization scripts for all objects of all levels are formed and defined by set of components of the following vectors and lists:

- optX – address list parameters to be optimized;
- lXmin, lXmax – vectors defining the allowable range of variation of parameters to be optimized;
- lYcq – address list of the object settings and quality criteria;

- lYw – object quality criteria weight vector;
- lYfl – address list of parameters and functional limitations;
- flMin, flMin – functional limitations permissible change vectors;
- lYd – address list of settings – parametric constraints;
- dlMin, dlMin – parametric constraints permissible change vectors;
- lReg – list of regime (changing during the operation of the facility) parameters;
- sRegim – list of lines with the data on the values of operating parameters and the appropriate time of the object for these values;
- lLine – address list of parameters whose values are changed in the process of optimization by linear interpolation between the same type of parameters to be optimized nearby objects;
- optM – method for solving the optimization problem of the local object.

Forming all the lists, enumerated above, for all level objects and calling a recursive function, which includes a set of corresponding optimization algorithms, an automatic objects bypass and solving optimization problems for each of them is carried out.

1.3 Building Subsystems FMM

1.3.1 FMM Basics

As noted, the FMM is an approximation of the original model, which means it can be obtained by statistical processing of the results of numerical experiment using OMM. The complexity of solving the equations of the original model forces minimize the number of sampling points, which is practically achieved by using methods of the theory of experiment design. Get the response function in the form (1.2) can, in particular, on the basis of

three-level Box and Benken plans [1]. Special selection of sampling points on the boundary of the approximation

$$-1 \le q_l \le 1, \quad l = 1, \ldots, N \tag{1.11}$$

and in its center possible in accordance with the least squares method to obtain the values of the coefficients according to (1.2), without resorting to the numerical solution of the normal equations. The number of sampling points is in the range from 13 at N = 3 to 385 at N = 16.

Similarly, relations (1.2) can also be obtained by using the three-level saturated plans by Rehtshafner [2]. In this case, the dimension of the observation vector will vary from 16 at N = 4 to 232 at N = 20. The feature of these plans is that it is the most economical plans that require a minimum number of calculations to generate a vector of observations, i.e. the number of calculations (experiments) equal to the number of the coefficients according to (1.2).

When creating subsystems FMM quality criteria, should be noted, that at lower levels increases the degree of detailed description of the design objects, which leads to an increase in the dimension of $\vec{Q}_k$ vectors. If the dimension exceeds the permissible (N = 20), or for any reason is limited, for example, due to the complexity of OMM, it can be reduced by replacing a number of components of the control parameters vector defined by the laws of their change, by numbers of the same type subsystems (objects) at the considered design level. For example, in the formal macromodelling of the multi-stage turbine flow path efficiency, may be appropriate to change the degree of reaction, disposable heat drop and so forth linearly from stage to stage. To ensure information consistency between FMMs of adjacent levels, in a number of components of the vector $\vec{Q}_{k+1}$ should be required to include parameters that uniquely determine the position of the subsystems in the settings space of a higher k-level.

It should be noted that in addressing the increasingly complex, multi-parameter, multi-mode and multi-criteria problems of optimal design increases the likelihood of multimodal objective functions.

Using the dependency of the form (1.2) for the approximation of the objective functions and functional limitations in this case can lead to a decrease in the accuracy and adequacy of the obtained with its help optimal solutions for the projected objects or subsystems.

1.3.2 The Method of Improving the FMM Accuracy

The analysis of the structure of formula (1.2) shows, that its second term is a superposition of the parabola from each independent parameter that mainly determines the failure of functions of the form $\sum_{i=1}^{n}\left(A_i q_i + A_{ii} q_i^2\right)$ take into account the more complex nature of real dependencies, having, for example, bends and local extremes. We will use a second member according to (1.2) to reflect the independent effect of the parameters on the approximated function, and replace it with a more perfect form of addiction.

It is obvious that in the general case, the shape and structure of dependency, reflecting the influence of each parameter, is unique. Given that a priori a kind of dependency is not known, to solve this problem and ensure that the principle of universality, the second term of the form $\sum_{i=1}^{n}\left(A_i q_i + A_{ii} q_i^2\right)$ should be replaced with the superposition of interpolation cubic splines. As known, the interpolation cubic splines allow with a high degree of accuracy and adequacy to describe features of varying complexity, including multi-extremal. Thus, taking into account this replacement, the formal macromodel of the form (1.2) will be as follows:

$$y(q) = A_0 + \sum_{i=1}^{n}\left(a_{ij} + \left(b_{ij} + \left(\frac{c_{ij}}{2} + \Delta q_{ij}\cdot\frac{d_{ij}}{6}\right)\Delta q_{ij}\right)\Delta q_{ij}\right) + \sum_{i=1}^{n-1}\sum_{j=i+1}^{n} A_{ij} q_i q_j , \quad (1.12)$$

where $a_{ij}, b_{ij}, c_{ij}, d_{ij}$ – cubic spline coefficients of current (j-th) interpolation section of the i-th independent variable. For each independent normalized variable q_i there are several areas in the interpolation range between –1 and +1; Δq_{ij} – the distance between the current value q_i and coordinate of the initial node of j-th section of the spline, which q_i coordinate value is between the initial coordinates of (j-th) and final (j + 1-th) of its nodes.

Of course, for the coefficients $a_{ij}, b_{ij}, c_{ij}, d_{ij}$ of dependence (1.12) determination additional computational experiment is needed. This experiment carried out at the points of a normed space of independent variables q_i. The length of the interpolation areas and their nodes coordinates are the same for all the independent variables. The number of sections is given. The minimum required number of sections is four. In this case, an additional calculation of the objective functions at four points (1; 0.5; 0.5; 1) by each variable q_i is needed.

To ensure the principle of an independent effect of each variable, other variables in the calculation are assigned by the value 0 ($q_j = 0$), which corresponds to the center of the accepted range of their changes. It should also be noted that in the case of Rehtshafner's design plans to create more accurate FMM of form (1.12) the number of computations by OMM is reduced for each independent parameter of FMM by two and equal, accordingly, two, since the other two points coincide with the points of the Rehtshafner's plan and their corresponding calculations for OMM performed at the stage of creating a FMM

of form (1.2). For clarity, in Fig. 1.3 shows a comparison of the accuracy and the adequacy of the approximation of test functions of the form:

$$Z = 2 + 0.1X^2 + 0.1Y^2 - \sin X - \sin Y, \tag{1.13}$$

by formal macromodel of the form (1.2) and the form (1.12).

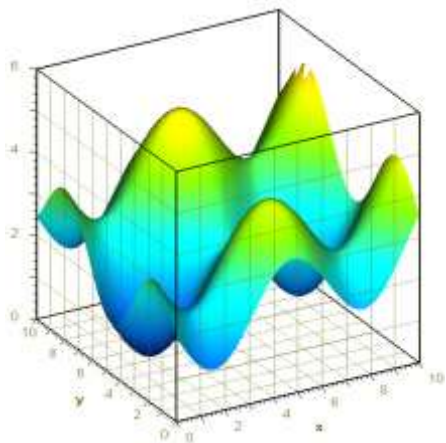

a

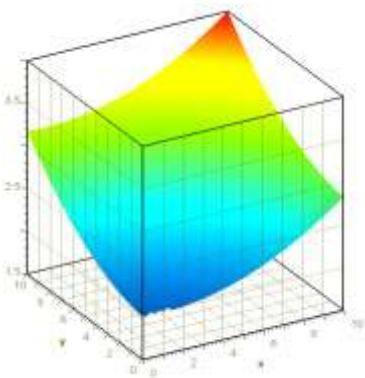

b

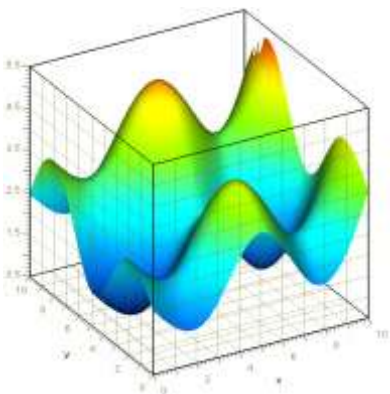

c

Figure 1.3 *Comparison of the accuracy of approximation of multimodal function using formal macromodel: a – test multimodal function of the form (1.13); b – approximation of functions of the form (1.13) using formal macromodel of the form (1.2); c – approximation of functions of the form (1.13) using formal macromodel of the form (1.12).*

1.4 Optimization Methods

1.4.1 General Information About the Extremal Problems

To solve problems with the single criterion of optimality rigorous mathematical methods are developed.

Direct methods of the calculus of variations – one of the branches of the theory of extreme problems for functional – reduce the problem of finding the functional extremum to the optimization of functions.

There are analytical and numerical methods for finding optimal solutions. As a rule, the real problems are solved numerically, and only in some cases it is possible to obtain an analytical solution.

Functions optimization using differentiation

Finding the extremum of the function of one or more variables possible by means of differential calculus methods. It's said that the $\hat{x}$ point gives to function $f(x)$ local maximum, if there is a number $\varepsilon > 0$ at which from the inequality $|x - \hat{x}| < \varepsilon$ the inequality $f(x) \le f(\hat{x})$ comes after.

The function is called one-extremal (unimodal) if it has a single extremum and multi-extremal (multimodal), if it has more than one extremum. The point at which the function has a maximum or minimum value of all local extrema, called a point of the global extremum.

A necessary condition for an extremum of a differentiable function of one variable gives the famous Fermat's theorem: let $f(x)$ – function of one variable, differentiable at the point $\hat{x}$. If $\hat{x}$ – local extreme point, then $f'(\hat{x}) = 0$.

The points at which this relationship is satisfied, called stationary. The stationary points are not necessarily the point of extreme. Sufficient conditions for the maximum and minimum functions of one variable – respectively $f''(\hat{x})<0$, $f''(\hat{x})>0$.

Before proceeding to the necessary and sufficient conditions for extrema of functions of several variables, we introduce some definitions.

The gradient of function $f(x)$ is a vector

$$\nabla f(x)=\begin{bmatrix}\dfrac{\partial f(x)}{\partial x_1}\\ \cdots\\ \cdots\\ \dfrac{\partial f(x)}{\partial x_n}\end{bmatrix},$$

$\nabla^T f(x)$ denotes the row vector

$$\nabla^T f(x)=\left\{\frac{\partial f(x)}{\partial x_1},\ldots,\frac{\partial f(x)}{\partial x_n}\right\}.$$

A square matrix of second derivatives

$$\nabla^2 f(x)=h(x)=\begin{bmatrix}\dfrac{\partial^2 f(x)}{\partial x_1^2} & \cdots & \dfrac{\partial^2 f(x)}{\partial x_1\partial x_n}\\ \cdots & \cdots & \cdots\\ \dfrac{\partial^2 f(x)}{\partial x_n\partial x_1} & \cdots & \dfrac{\partial^2 f(x)}{\partial x_2^n}\end{bmatrix}$$

is called the Hesse matrix or Hessian of function $f(x)$.

The real symmetric matrix H is called positive (negative) defined if $x^T = Hx > 0 (< 0)$ for every set of real numbers $x_1, x_2, \ldots, x_n$, not all of which are zero.

The necessary conditions for that $\hat{x}$ – the point of local extremum of n variables function $f(x)$, $x \in E^n$ are as follows:

1) the function $f(x)$ is differentiable in $\hat{x}$;

2) $\nabla f(x) = 0$, that is $\hat{x}$ – the stationary point; sufficient conditions for that $\hat{x}$ – local extreme point, but "1", "2" include the following;

3) Hessian is positive (negative) determined at the minimum (maximum), i.e. $\hat{x}^T H\hat{x} > 0 (< 0)$.

If the Hessian is positive (negative) defined for all $x \in E^n$, it is a sufficient condition of unimodality of the function. To test matrix A definiteness, Sylvester criterion is applied, according to which the necessary and sufficient condition for positive certainty are the inequalities:

$$a_{11} > 0, \begin{vmatrix} a_{11} & a_{12} \\ a_{21} & a_{22} \end{vmatrix} > 0, \ldots, \begin{vmatrix} a_{11} & \ldots & a_{1n} \\ \ldots & \ldots & \ldots \\ a_{n1} & \ldots & a_{nn} \end{vmatrix} > 0,$$

as to the negative certainty

$$-a_{11} > 0, \begin{vmatrix} a_{11} & a_{12} \\ a_{21} & a_{22} \end{vmatrix} > 0, \ldots, (-1)^n \begin{vmatrix} a_{11} & \ldots & a_{1n} \\ \ldots & \ldots & \ldots \\ a_{n1} & \ldots & a_{nn} \end{vmatrix} > 0.$$

Tasks for conditional extremum of function

This case involves determining the extremum in an infinite change range of variables $x_1, x_2, \ldots, x_n$. If optimized function imposed additional conditions (restrictions), talk about the problem of conditional extremum. In general, you want to find extremum $f(x)$, $x \in E^n$ under the constraints

$$\left.\begin{aligned} h_j(x) = 0, \quad j = 1, \ldots, m; \\ g_j(x) \geq 0, \quad j = 1, \ldots, p. \end{aligned}\right\} \tag{1.14}$$

To solve the problem (1.14) only with restrictions in the form of equations a method of Lagrange multipliers is used, which is based on the conduct of the Lagrange's function $L(x, \lambda) = f(x) + \sum_{j=1}^{m} \lambda_j h_j(x)$, where λ_j – undetermined Lagrange multipliers. We write the necessary conditions for optimality in the problem of conditional extremum with equality constraints

$$\left.\begin{aligned} \frac{\partial L}{\partial x_i} = \frac{\partial f}{\partial x_i} + \sum_{j=1}^{m} \lambda_i \frac{\partial h_j}{\partial x_i} = 0, \quad i = 1, \ldots, n; \\ \frac{\partial L}{\partial \lambda_i} = h_j(x) = 0, \quad j = 1, \ldots, m. \end{aligned}\right\} \tag{1.15}$$

It is a system of $n + m$ equations from which can be determined x_i, $i = 1, \ldots, n$, λ_j, $j = 1, \ldots, m$. A rigorous proof of the Lagrange conditions set out in the specific manuals. Explain the meaning of the method as follows. On the one hand, for all of x which satisfy the constraints $h_j(x) = 0$, $j = 1, \ldots, m$, obviously $L = (x, \lambda) = f(x)$.

On the other hand, the extreme point of the Lagrange function also satisfies these conditions (the second equation (1.14), and therefore, finding an extremum $L(x, \lambda)$, we simultaneously obtain a conditional $f(x)$ extremum. To

address the issue of the presence of a stationary point to be a local extremum in the problem of conditional extremum, let us expand Lagrange function in a Taylor series with a subject to the satisfaction of relations $h_j(x)=0$.

$$f(\bar{x}+\xi)-f(\bar{x})=L\left(\bar{x}+\xi,\hat{\lambda}\right)-L\left(\bar{x},\hat{\lambda}\right)=$$
$$=\sum_{i=1}^{n}\frac{\partial L}{\partial x_i}\xi_i+\frac{1}{2}\sum_{i=1}^{n}\sum_{j=1}^{m}\frac{\partial^2 L}{\partial x_i\partial x_j}\xi_i\xi_j+o(\|\xi\|^2), \quad (1.16)$$

and according to (1.15) the first term on the right side is zero. The expansion of a Taylor series $h_j(x)$ in the neighborhood of a stationary point $\bar{x}$ yields

$$\sum_{i=1}^{n}\frac{\partial h_j}{\partial x_i}\xi_i+o(\|\xi\|^2)=0,\quad j=1,\ldots,m, \quad (1.17)$$

Neglecting terms of higher order, write (1.16), (1.17) in the form

$$f(\bar{x}+\xi)-f(\bar{x})=\frac{1}{2}\sum_{i=1}^{n}\sum_{j=1}^{m}\frac{\partial^2 L}{\partial x_i\partial x_j}\xi_i\xi_j;\ \sum_{i=1}^{n}\frac{\partial h_j}{\partial x_i}\xi_i=0,\ j=1,\ldots,m. \quad (1.18)$$

If from the second equation (1.18) the dependent variables ξ_i, $i=1,\ldots,m$, can be expressed through independent ξ_k, $k=m+1,\ldots,n$, then substituting them in the first equation (1.18), we obtain a quadratic form relatively independent increments $\xi_{m+1},\ldots,\xi_n$. The stationary point $\bar{x}$ is a local conditional minimum (maximum), only if it is positive (negative) defined.

Optimization with constraints in the form of inequalities

Classical methods of finding the conditional and unconditional extrema of functions discussed above, in some cases, allow to solve problems with inequality constraints.

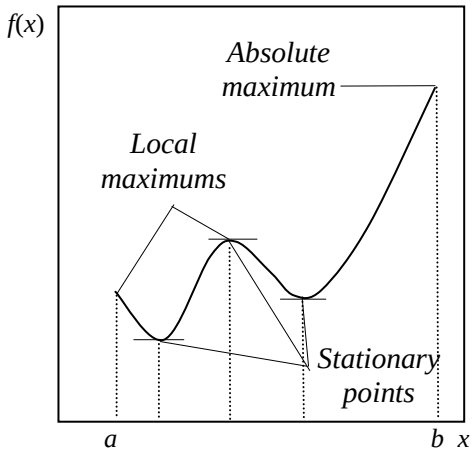

Figure 1.4 *For extremum determination of the functions of one variable in the interval.*

Let the task of finding the maximum of a function of one variable $f(x)$ on the interval $a \le x \le b$. Using the necessary optimality conditions, we find the roots of $f'(x)=0$ which lie in the interval $[a,b]$; We check the suffi-ceent conditions for maximum $f''(\hat{x})<0$ and choose the points corresponding to the maximum. Also, we compute the function values at the borders of a segment, where it can take higher values than the interval (Fig. 1.4).

We turn now to the case of several variables and consider the optimization problem: find a maximum $f(x)$, $x \in E^n$, subject to the constraints:

$$\left.\begin{aligned} h_j(x)=0, \quad j=1,\ldots,m<n; \\ x_i \ge 0, \quad i=1,\ldots,n. \end{aligned}\right\} \tag{1.19}$$

In the first stage of the solution by the method of Lagrange multipliers, we find all stationary points lying in the positive octant of *n*-dimensional space and isolate the maximum points on the basis of sufficient conditions for an extremum. Then we explore the positive octant boundary, in turn equating to

zero in all sorts of combinations of $1, 2, \ldots, n-m+1$ variables, and each time solving the optimization problem with equality constraints. As a result of the computing process, the complexity of which is obvious, the largest of all the extrema should be selected.

A more general problem, find the maximum

$$f(x),\ x \in E^n \tag{1.20}$$

under constraints $h_j(x)=0$, $j=1,\ldots,m$; $g_i(x)\geq 0$, $i=1,\ldots,p$, can be reduced to just considered by the introduction of additional variables y_i , $i=1,\ldots,p$, such that

$$g_i(x)-y_i=0,\quad y_i\geq 0. \tag{1.21}$$

The extremum can be achieved in a region, where $y_i>0$, or at its borders, where $y_i=0, i=1,\ldots,p$. Lagrange function for the constrained optimization problem (1.20), (1.21) has the form

$$L(x,y,\lambda)=f(x)+\sum_{i=1}^{m}\lambda_i h_i(x)+\sum_{i=1}^{p}\lambda_{m+i}\left(g_i(x)-y_i\right).$$

In the optimum point its partial derivatives by x_j, y_j, λ_j vanish, including

$$\frac{\partial L}{\partial y_j}=\hat{\lambda}_{m+j}=0,\quad j=1,\ldots,p.$$

This condition means that if at the point of extremum $\hat{y}_j>0$, then $\hat{\lambda}_{m+j}=0$, on the other hand, if $\hat{y}_j=0$, that is on the border area $\hat{\lambda}_{m+j}\neq 0$, as the corresponding limit should be considered. Thus, the property

$\hat{y}_j \dfrac{\partial L}{\partial y_j} = 0, \quad j = 1, \ldots, p$ is proved. Obviously, the problem (1.20) and (1.21) are completely identical to (1.24) and can be solved in the same way.

For the problem can be written necessary optimality conditions (generalized Lagrange multiplier rule), however, it is rarely used because of the complexity of solving the resulting system of equations.

1.4.2 Nonlinear Programming

Subject of nonlinear programming

Nonlinear programming – branch of applied mathematics dealing with finding the extremum of function of many variables in the presence of non-linear constraints in the form of equalities and inequalities, i.e. solution of the problem (1.14), discussed in the previous section [3].

Classical methods of optimization are part of it, along with disciplines such as linear, quadratic, separable programming. However, of the greatest practical interest to us are the numerical or direct methods of nonlinear programming, especially intensively developed in recent years.

None of the proposed algorithms is absolutely the best, so the choice of a numerical method is dictated by the content of a specific problem, which must be solved. Computational methods are classified according to some peculiarity of the problem (no restrictions, with equality constraints, inequalities and so on), the nature of methods of solutions (e.g., with or without the use of derivatives), the type of computers, programming language, and so on.

Search of one variable function extremum

A number of methods of finding an extremum of function of many variables use as a part the procedure for the one-dimensional optimization. In the case then function of one variable is multi-extremal, the only correct method of

finding the global extremum is a direct enumeration of a number of values with some step in its change.

Obviously, the function can vary sharply, the smaller should be chosen the grid. After a rough determination of the neighborhood of extremum, begin to search its exact value. For this purpose, one-dimensional algorithms for searching the extremes of unimodal functions in a given interval are used.

One of the most effective methods is the so-called golden section. Recall that if a segment divided into two parts, so that the ratio of the lengths at a greater relative length equal to the length of most of all segment, obtain the so-called golden ratio (is approximately 0.38: 0.62). Golden section method just based on the multiple division of uncertainty interval, i.e. the interval in which the extremum enclosed in an appropriate ratio.

Suppose that in some approximation known interval Δ_i in which the function extremum exists. Divide it by points y_1^i, y_2^i in the proportion of the golden section. If $y_2^i > y_1^i$ we discarded x_2^i, indicating $x_2^{i+1} = y_2^i$ a segment Δ_{i+1} share in the proportion of the golden section, and so on. To reduce the range of uncertainty in the 100 times 11 calculations is required, in the 10000 times – 21 calculations. For comparison, the bisection method (dichotomy) leads to a corresponding narrowing of the range of 14 and 28 function evaluations.

The advantage of the golden section is that it works equally well for smooth and non-smooth functions. It was found that, in the case of smooth functions by a polynomial approximation possible to quickly determine the number of extreme at the same accuracy as that by the golden section.

If the optimized function is defined and unimodal on the entire real axis, there is no need to worry about selecting the initial uncertainty interval. For example, in the method of Davis, Sven and Campy (abbreviated as DSC), from a certain

point, it becomes increasing steps until extremum is passed, and then made quadratic interpolation on the basis of information about the functions in the past three points is determined extremum of the interpolation polynomial.

The *Powell's algorithm* of quadratic polynomial interpolation is carried out in three arbitrary points, approximate extremum is found, dropped one of the four points and the procedure is repeated until convergence. The most effective is a combination of the described algorithms, or the so-called method of *DSC-Powell*. In accordance with this first algorithm DSC sought interval in which the extremum, three points are selected and carried there through parabola. Approximate value at an extremum is calculated as in the method of Powell:

$$\bar{x} = \frac{1}{2}\frac{\left(x_2^2 - x_3^2\right) f\left(x_1\right) + \left(x_3^2 - x_1^2\right) f\left(x_2\right) + \left(x_1^2 - x_2^2\right) f\left(x_3\right)}{\left(x_2 - x_3\right) f\left(x_1\right) + \left(x_3 - x_1\right) f\left(x_2\right) + \left(x_1 - x_2\right) f\left(x_3\right)}.$$

If the value of the function at the point $\bar{x}$ of optimum values $f\left(x_1\right)$, $f\left(x_2\right)$, $f\left(x_3\right)$ differ by less than a predetermined accuracy, complete calculations, otherwise discard the worst of the points $x_1, x_2, x_3, \bar{x}$, and carry out a new parabola. For functions that are sufficiently close to quadratic efficiency DSC-Powell is very high: as a rule, the decision to an accuracy $10^{-5} \ldots 10^{-6}$ is achieved 6–8 calculations of the objective function.

Methods for unconstrained optimization

Consider the problem of finding the maximum of a function of several variables without restrictions. Find maximum $f\left(x\right)$, $x \in E^n$. One of the most famous is the gradient methods to solve this problem. They are based on the fact that the promotion of the objective function to the extreme in the space E^n made by the rule

$$x_{k+1} = x_k + \Delta x_k . \tag{1.22}$$

There Δx_k – transition vector from point x_k to the point x_{k+1}, $\Delta x_k = \lambda_k s_k$, where s_k – the unit vector in the direction Δx_k; λ_k – a scalar.

Vector s_k sets another search direction and λ_k – the length of a step in this direction. Obviously, λ_k should be chosen so as to move as close as possible to the extreme. Various methods of selecting the direction of the search are used. The simplest of these is that the movement of the point x_k is made in the direction of the greatest magnification of $f(x_k)$, i.e. in the direction of a gradient function at a given point.

According to this method, called the method of *steepest descent*,

$$s_k = \frac{\nabla f(x_k)}{\left\| \nabla f(x_k) \right\|},$$

where $\left\| \nabla f(x_k) \right\| = \sqrt{\sum_{i=1}^{n} \left(\frac{\partial f(x_k)}{\partial x_i} \right)^2}$, and the formula of the transition from x_k to x_{k+1} has the form

$$x_{k+1} = x_k + \lambda_k \frac{\nabla f(x_k)}{\left\| \nabla f(x_k) \right\|} . \tag{1.23}$$

Consider a geometric interpretation of the steepest descent method in the case of two variables. Transition from formula (1.21) does not allow to come to a point extremum by one step; the procedure should be repeated many times until it reaches a maximum, i.e., conditions $\left\| \nabla f \right\| = 0$ are fulfilled. Partial derivatives of the function calculation at points generally performed numerically. Search step, you can select a constant, but it is better to define it in terms of

$$\max_{\lambda_k} f\left(x_k + \lambda_k s_k\right)$$

using the previously discussed methods of one-dimensional search.

The theory shows, and the practice of calculation confirms that the steepest descent method is not very effective in cases where the level curves of the objective function is strongly stretched, i.e. there are deep ravines while searching a minimum or ranges when searching maximum. The steepest descent direction is almost orthogonal to the best direction of the search, as a consequence, the optimal step reduced all the time, and the algorithm "get stuck" without reaching the extreme. The way out of this situation can be a scaling of variables, at which the level lines would get kind of close to the circle.

In order to reduce the amount of computations of the objective function, associated with a numerical definition of partial derivatives, sometimes used method of *coordinate descent*, which is also called a relaxation or Gauss-Seidel method. Let e_i – axis x_i unit vector, and $x = \{x_1, \ldots, x_n\}$ – the starting point of the search. One iteration of coordinate descent is to take steps: $x_{k+1} = x_k + \lambda_k e_k$, $k = 1, \ldots, n$.

Step as in the method of steepest descent is determined by the condition $\max_{\lambda_k} f\left(x_k + \lambda_k s_k\right)$. The Gauss-Seidel method suffered from the same flaw as the steepest descent method, – a bad convergence in the presence of ravines.

One way to overcome the computational difficulties associated with the gully structure of the objective function involves the use of information not only on its first derivative, but also higher order, contained in the second partial derivatives. An arbitrary function can be represented by its quadratic expansion in a Taylor series in the neighborhood of point *x*:

$$f\left(x+\Delta x\right)=f\left(x\right)+\nabla^{T}f\left(x\right)\Delta x+\frac{1}{2}\left(\Delta x\right)^{T}H\left(x\right)\Delta x.$$

The minimum in the direction Δx is obtained by differentiation for each of the components of the vector Δx, which gives

$$\Delta x=-H^{-1}\left(x\right)\nabla f\left(x\right). \tag{1.24}$$

If we substitute (1.23) into (1.21), we obtain an expression for the minimum point of the quadratic function

$$x=x-H^{-1}\left(x\right)\nabla f\left(x\right). \tag{1.25}$$

In the case where the objective function from the outset is a quadratic, the optimum point is found by one step, but if the function is arbitrary, this fails to achieve the minimum and should be repeatedly use the formula (1.25):

$$x_{k+1}=x_{k}-H^{-1}\left(x_{k}\right)\nabla f\left(x_{k}\right). \tag{1.26}$$

Even better, by analogy with gradients instead of (1.25) to use the relation

$$x_{k+1}=x_{k}+\lambda_{k}s_{k}=x_{k}+\lambda_{k}\frac{H^{-1}\left(x_{k}\right)\nabla f\left(x_{k}\right)}{\left\|H^{-1}\left(x_{k}\right)\nabla f\left(x_{k}\right)\right\|}, \tag{1.27}$$

and the step λ_{k} choose from the $\min\limits_{\lambda_{k}} f\left(x_{k}+\lambda_{k}s_{k}\right)$ minimum condition.

Equations (1.26) or (1.27) are applied iteratively until the end calculation process criterion is reached, called *Newton's method*. Difficulties of using Newton algorithm associated, firstly, with Hessian matrix inversion, and secondly, with the computation of the second partial derivatives, which restricts its practical use.

The methods of conjugate directions are without drawbacks of gradient methods and have the convergence rate close to Newton's method. At the same time, they are the methods of the first order, as the gradient. Positive defined

quadratic form of *n* variables is minimized conjugate gradient method for no more than *n* steps. The conjugate gradient method is suitable for minimization of non-quadratic functions, only when they are iterative.

Two vectors *x*, *y* in the space E^n called conjugate relative to the matrix *H*, if $x^T Hy = 0$. Consider the quadratic function of the *n* variables

$$f(x) = a + x^T b + \frac{1}{2} x^T Hx \tag{1.28}$$

with a positive defined matrix *H*. Let's apply for function $f(x)$ minimization iterative process $x_{k+1} = x_k + \lambda_k s_k$. The direction of descent to *k*-th step is one of the vectors of conjugate vectors $s_0, s_1, \ldots, s_{n-1}$. If you select λ_k from the minimum of $f(x_k + \lambda_k s_k)$, i.e. $\frac{\partial f(x_k + \lambda_k s_k)}{\partial \lambda_k}$, that, differentiating by step (1.27), we obtain

$$\lambda_k = -\frac{\nabla^T f(x) s_k}{s_k^T H s_k}. \tag{1.29}$$

Applying the formula (1.28), (1.29), on n-th step of the iterative process will find

$$x_n = x_0 + \sum_{k=0}^{n-1} \lambda_k s_k = x_0 - \sum_{k=0}^{n-1} \frac{\nabla^T f(x) s_k}{s_k^T H s_k}. \tag{1.30}$$

We can say that the point x_n is the exact minimum of the function $f(x)$, i.e. $x_n = \widehat{x} = -H^{-1} b$, which means that the process (1.30) with the choice of λ_k by (1.28) does give the opportunity to find the minimum of a quadratic function by *n* steps.

There are different ways of constructing conjugate directions. In particular, Fletcher and Reeves proposed a method, called the conjugate gradients method, according to which the subsequent direction of the search is a linear combination of the direction of steepest descent and the previous direction, i.e.,

$$s_k = -\nabla f\left(x_k\right) + \beta_{k-1} s_{k-1}. \tag{1.31}$$

As the initial search direction $s_0 = -\nabla f\left(x_0\right)$ is chosen. The weighting factors β_{k-1} are determined so that the directions $s_0, s_1, \ldots, s_{n-1}$ were conjugated. It can be shown that

$$\beta_{k-1} = \frac{\left\|\nabla f\left(x_k\right)\right\|^2}{\left\|\nabla f\left(x_{k-1}\right)\right\|^2}.$$

Since the direction of the search is conjugated to a quadratic function, the Fletcher-Reeves method leads to the solution of no more than *n* steps. In the case of an arbitrary function is recommended after every *n* steps "upgrade" the search direction by setting $s_n = -\nabla f\left(x_n\right)$ and repeat the process (1.30) with replacement of x_0 to x_n.

Some methods do not use the derivatives of functions, and the optimization direction in which tis determined only on the basis of successive calculations of the objective function. In cases where the determination of the objective function derivatives is difficult, *search algorithms* may be preferable. In the case of one-dimensional analogue of the search method is the method of golden section, and the method of using derivatives – DSC-Powell method.

Methods of optimization with constraints

In addition to the previously described method of Lagrange multipliers for finding the extremum of functions with restrictions a number of numerical

methods developed. The first approach to the construction of algorithms for constrained optimization is monotonous motion to the optimum of the objective function and at the same time striving to meet the exact or approximate limits. Methods of this type are numerous, but the complexity, lack of flexibility and a large amount of computational work limit their use in practical calculations.

More elegant, easy to implement and effective the methods based on the reduction of problems with constraints to the solution of a sequence of unconstrained optimization – the so-called penalty function methods. There are several variations of these methods.

Let's begin their consideration with the interior point method for problems with inequality constraints:

find the maximum $f(x),\ x \in E^n$

with restrictions $g_j(x) \geq 0, \quad j = 1, \ldots, p.$ (1.32)

To determine the conditional extremum built the so-called attached objective function

$$I_k^*(x, \Lambda_k) = f(x) - \Lambda_k \sum_{j=1}^{p} \frac{1}{g_j(x)}, \tag{1.33}$$

where Λ_k – a number, called penalty factor; $\sum_{j=1}^{p} \frac{1}{g_j(x)}$ – penalty function.

The algorithm for solving the problem (1.32) is the following: allowable point x_0 at which everything $g_j(x_0) \geq 0$ is selected, and a monotonically decreasing sequence of positive penalties Λ_k; for every $k = 1, 2, \ldots,$ starting with the point $\hat{x}_{k-1}$, it solves the problem of unconstrained optimization function (1.33).

If for every k it is possible to find the maximum of I_k^* by x, the sequence $\{\hat{x}_k\}$ converges to the solution of the problem (1.33).

The organization of numerical maximum search of (1.29) must be such that the point does not leave the feasible region. This shortage is deprived the *external penalty function method*, which for the problem of the form (1.33) involves the construction of the associated objective function

$$I_k^*(x, \Lambda_k) = f(x) - \Lambda_k \sum_{j=1}^{p} \left(g_j^+(x)\right)^2, \tag{1.34}$$

Where $g_j^+(x) = \min\{0, g_j(x)\}$.

Thus, inside the allowable region, where $g_j(x) \geq 0$, $g_j^+(x) = 0$, and $g_j^+(x) = g_j(x)$ outside.

In contrast to (1.33), the function (1.34) is defined for all $x \in E^n$.

The algorithm for solving the problem is as follows: take an arbitrary point x_0, and monotonically increasing sequence of numbers $\Lambda_k \to \infty$; for $k = 1, 2, \ldots,$ starting from $\hat{x}_{k-1}$, it solves the problem of unconstrained optimization function (1.34), with the result that is determined the new approach $\hat{x}_k$.

It can be shown that the sequence of points $\hat{x}_k$ converges to the solution of the problem (1.33), but in contrast to the interior point method to the extreme movement takes place outside the feasible set, and is taken from the name of the method of exterior penalty functions. This method is also applicable to the general problem of nonlinear programming (1.14), for which used attached objective function

$$I_k^*(x, \Lambda_k) = f(x) - \Lambda_k \left[\sum_{j=1}^{m} h_j^2(x) + \sum_{j=1}^{p} \left(g_j^+(x) \right)^2 \right]. \quad (1.35)$$

Algorithm of solution is the same as for the problem (1.34).

The solution of nonlinear programming problems with constraints using penalty function method is complicated by the fact that as the penalty function coefficient is increasing, (1.35) expressed gully structure. As previously shown, not all the methods of unconditional optimization solution can cope with such problems, and therefore the choice of the method of finding the extremum of the attached objective function is of fundamental importance.

An important role is also played the strategy of the penalty factor change, because if you choose it immediately large, constraints of the problem satisfied well, but the objective function does not improve. In contrast, if too small values of Λ_k, motion occurs in the direction of improvement of the objective function, but practically does not take into account the constraints that can lead to failure in the E^n areas where the objective function and constraints are not defined.

For example, if in the objective function or in limitations members of the form x^a are present, it is unacceptable entering the zone $x \le 0$. Get rid of the zone uncertainty, resulting in the computer calculations for emergencies can sometimes be the introduction of a suitable change of variables. In particular, to meet conditions $x > 0$ the replacement $x = e^z$ is suitable, which already $z \in E^1$. If such a reception is impossible, it should be carefully selected constants of unconditional search methods as the length of the step in the direction of descent, change of this step in the process to find a one-dimensional vector of variables did not leave the area where the objective function and constraints of the problem identified.

In conclusion, we consider the possibility of nonlinear optimization methods usage in order to solve systems of nonlinear equations. Suppose that in the problem (1.14) there are no restrictions in the form of inequalities, and the number of variables equal to the number of restrictions in the form of equations, i.e., in fact, the task of solving the system of *m* equations with *m* unknowns. We form the function

$$I^* = -\sum_{j=1}^{m} h_j^2(x) \tag{1.36}$$

and find its maximum. If the system of equations $h_j(x) = 0$, $j = 1, \ldots, m$, has a solution, then, obviously, at the same time with the maximum of I^* is the root of the system of equations. In particular, if the functions $h_j(x)$ are linear, function (1.36) is obtained quadratic and can be effectively solved by Newton's and conjugate gradient method.

Replacement of the problem of systems of linear equations solution to extremum problems is justified in cases where the matrix of the system is ill-conditioned (e.g., in the problem of approximation by least squares) and can not be solved by conventional methods, in particular, by process of elimination.

The values $h_j(x)$ in (1.35) are called residuals, and the solution of nonlinear equations is replaced by *minimizing the sum of squared residuals*.

1.4.3 Methods for Optimization of Hardly Computable Functions

In some problems, when the calculation of the value of the objective function may take minutes, hours or even days of the computer, the range of acceptable methods of optimization significantly narrowed.

These problems, in particular, include aerodynamic optimization of turbine blades using CFD.

The Nelder-Mead method (Nelder A.-Mead R.), also known as the flexible polyhedron method or the simplex method is a method of unconditional optimization of functions of several variables. Without requiring computation of the gradient function, it is applicable to non-smooth, noisy functions, and is particularly effective in small (up to 6) number of variable parameters. Its essence lies in the follow-successive movement and deformation of the simplex around the point of extreme. The method is a local extremum and can "get stuck" in one of them. If you still need to find a global extremum, one can try to select other initial simplex.

A more developed approach to the exclusion of local extrema offered algorithm based on the Monte-Carlo method, as well as evolutionary algorithms.

The genetic algorithm (GA) – is a global search heuristic method, used to solve optimization problems and modeling, by random selection, combination and variation of the required parameters with the use of mechanisms that resemble biological evolution. GA usage assumes its careful adjustment on special test functions, which, however, does not guarantee the effectiveness of the algorithm and the accuracy of decisions of the function.

This algorithm is well suited to the study of noisy functions, but requires a large number of CFD – calculations and therefore more time on optimization. The last forcing researchers to use coarse meshes and not quite accurate, but easily calculated turbulence models, which will inevitably leads to loss of the numerical calculations precision.

Monte-Carlo (random search) methods allows you to find the extremes of multimodal and noisy functions; use various constraints during optimization; is particularly effective when a large number of variable parameters; requires careful adjustment for test functions; it is one of the most common methods of optimization and solution of various problems in mathematics, physics, economics, etc. However, the method requires tens of thousands of the objective

function computing and practically not applicable for direct optimization based on CFD – calculations. To improve the efficiency of random search used quasi-random sequence of numbers (LPτ [4] Sobol), Faure, Halton et al.). Increased efficiency is achieved by eliminating clustering that occurs in a random search that is by more even distribution of points in the search study area of the function extremum.

Recently, in the optimization algorithms the methods of experiment planning are widely used. Using the methods of the theory of experimental design (Design of the Experiment – DOE), the original mathematical model can be approximated by a quadratic polynomial. One of the relevant planning schemes of the experiment described in Section 1.3. These quadratic polynomials can be used to further optimization with the use of a universal and reliable global search method using a quasi-random sequences.

1.5 The Practice of Numerical Methods Usage for Local Leveled Optimization Problems Solution

To solve demanded by practice of axial turbines design multi-criteria problems, multi-parameter and multi-mode optimization of the multistage flow path further development and improvement of appropriate numerical methods and approaches required.

It should be noted some features of numerical solution of problems related to the optimization of design objects based on their modes of operation, multimodal objective functions, as well as issues related to the multi-objective optimization problems.

Some aspects of the above problems solutions are given below.

1.5.1 Solution of the Multi-Criteria Optimization Problems

Set out in section 1.4 are the basic optimization techniques. However, depending on the formulation of the optimization problem, as well as the selected design object there are some features of numerical implementation of these methods and their applications.

It is known that the actual design object is usually characterized by a number of quality indicators and improvement in one of them leads to a deterioration in values of other quality criteria (Pareto principle). In such cases it is necessary to consider the optimization problem from many criteria.

The authors offer a well-established practice in solving multi-objective optimization problems – "convolution" of partial objective function weighted by μ_i depending on the importance of a particular quality criteria in a comprehensive quality criteria based on the following

$$\left\| Y^*\left(\vec{x}_d, \vec{x}_p\right)\right\| = \sqrt{\sum_{i=1}^{n}\left(\mu_i Y_i^*\left(\vec{x}_d, \vec{x}_p\right)\right)^2}, \tag{1.37}$$

where Y_i^* – the components of the vector criterion (partial indicators of quality of the object); $\vec{x}_d, \vec{x}_p$ vectors of design parameters and operational parameters, respectively, which together define a design decision.

In fact, (1.37) is the magnitude of the partial criteria of quality, taking into account their weights (μ_i).

Thus, in the *n*-dimensional normalized criterial space each variant of definitely best design object is characterized by a corresponding so-called Pareto point, whose distance to the center of coordinate proportional to the value of the module $\left\| Y^*\left(\vec{x}_d, \vec{x}_p\right)\right\|$ of vector quality criterion.

The experience of steam turbines cylinder optimization with the flow extraction for the purposes of regeneration and heating shows that there is needed to consider at least two criteria of quality – the efficiency of the flow of the cylinder and the power, generated by them.

1.5.2 The Numerical Solution of the Optimization Problem with the Multimodal Objective Function

In some cases it is necessary to check the objective function on multimodality.

In the developed subsystem of multi-criterial and multi-level multi-parameter optimization of design objects to find the optimal solution the search is always performed in two stages whether unimodal or multimodal objective function.

Thus, the first (preliminary) stage is used to determine suspicious extremum points, to find which method is used ideas swarm (Bees Algorithm), the first work of which were published in 2005 [5, 6]. The method is an iterative heuristic multi-agent random search procedure, which simulates the behavior of bees when looking for nectar.

The criterion for the selection of points and their respective sub-areas, in which will be specified by the relevant decision of optimization problems, is the Euclidean distance $R_{ab} = \left\| \vec{x}_a - \vec{x}_b \right\|$ in the space of optimized parameters between the compared points from the set LPτ sequence.

If the Euclidean distance R_{ab} between two points of LPτ sequence $\left(\vec{x}_a, \vec{x}_b \right)$, less than some fixed value R_{set}, then point with the large value of the objective function is selected.

Criteria evaluation for quality and functional limitations at the preliminary stage is performed by using FMM (of the form (1.2) or (1.12)). After processing

all of the set of LPτ sequence points by a "swarm" algorithm suspicious extremum point are defined.

These points are then used as initial approximations of the final (refining) stage of the optimal solution finding. When refining the optimal solutions around the extremum suspicious spot, in a recursive optimize algorithm it is provided the transition from the evaluation criteria of quality and functional limitations by using FMM to their evaluation by appropriate OMM. It uses a method of coordinate descent or conjugate gradient method, for example, Fletcher-Reeves. Thus found several points of local optima are sorted by the value of the objective function, and the best solution given the status of optimal.

1.5.3 The Method of Optimization Taking into Account Turbine Operating Modes

The above (1.37) convolution vector type of the objective function allows to take into account the specific feature of the problem of optimal design of facilities intended for use as a constant, and the variable modes. In the case of optimization taking into account the variability of operating loads, function (1.37), on the one hand, carries information about the overall effectiveness of the design in all modes of operation, and on the other hand, it emphasizes the Pareto signs of the competitive effect of 'individual' quality criteria for each of the operating modes on the final result.

Below is a description of the developed method, which provides the solution of problems of optimum design of turbomachinery, operated at a predetermined range of modes.

This method is based on the integration of formal macromodels of the objective functions.

When included in the examination of the alleged operation modes, created FMM criteria of quality and functional limitations are functions of the design

and operational parameters. Ranges of change of regime parameters are selected in accordance with the proposed schedule changes and they do not change in the course of iterations to refine the optimal solutions.

Such FMM usage at the step of finding the optimal solutions necessitates multiple evaluation of quality criteria and functionality limitations for each sampling point (corresponding to a combination of structural parameters), the number of calculations of each FMM considered equivalent to the number of operating modes. Obviously, the increased number of calculations requires additional computing resources in the search for the best design.

The decision of the problem marked can be achieved by eliminating the regime parameters of the vector of varied FMM parameters (1.2). To eliminate the regime parameters it is necessary to carry out the FMM integration. In this case, the new FMM coefficients of integral quality criterion obtained from the following relationship:

$$Y(q) = A_0 + \sum_{i=1}^{N_c} A_i q_i + \sum_{j=1}^{N_m} A_j \int_0^1 q_j(t)\,dt + \sum_{i=1}^{N_c-1} \sum_{k=i+1}^{N_c} A_{ik} q_i q_k + \\ + \sum_{j=1}^{N_m-1} \sum_{m=j+1}^{N_m} A_{jm} \int_0^1 q_j(t) q_m(t)\,dt + \sum_{i=1}^{N_c} \sum_{j=1}^{N_m} A_{ij} q_i \int_0^1 q_j(t)\,dt + \\ + \sum_{i=1}^{N_c} A_{ii} q_i^2 + \sum_{j=1}^{N_m} A_{jj} \int_0^1 q_j^2(t)\,dt, \qquad (1.38)$$

where N_c, N_m – numbers of structural and operational parameters, respectively; t – time.

The new FMM of form (1.38) contains integrals of regime parameters, which can be calculated from the charts of regime parameters $\left(q_j(t)\right)$ and converted to the form:

$$Y_m(q) = A_{0m} + \sum_{i=1}^{N_c} \left(A_{im} q_i + A_{ii} q_i^2 \right) + \sum_{i=1}^{N_c-1} \sum_{k=i+1}^{N_c} A_{ik} q_i q_k, \qquad (1.39)$$

where

$$\left.\begin{aligned} A_{0m} &= A_0 + \sum_{j=1}^{N_m}\left(A_j \int_0^1 q_j(t)\,dt + A_{jj}\int_0^1 q_j^2(t)\,dt \right) + \\ &+ \sum_{j=1}^{N_m-1}\sum_{m=j+1}^{N_m} A_{jm}\int_0^1 q_j(t)\,q_m(t)\,dt; \\ A_{im} &= A_i + \sum_{j=1}^{N_m} A_{ij}\int_0^1 q_j(t)\,dt. \end{aligned}\right\} \tag{1.40}$$

FMM form (1.39) is more convenient to use in the optimization algorithms for quality criteria and functional constraints evaluation, as presented macromodel depends only on the design parameters that do not change their values when changing the operating mode of the FP. Thus, the account of the expected schedule change duty operation is performed due to the fact, that the operating parameters are integrally included in the new coefficients FMM (1.40).

2

Mathematical Modelling of the Turbomachine Flow Path Elements

2.1 Equations of State

The equation of state can be written in different forms depending on the independent variables taken. Numerical algorithms should allow to calculate and optimize the axial turbine stages, both with an ideal and a real working fluid. It uses a single method of calculating the parameters of the state of the working fluid, in which as the independent variables are taken enthalpy *i* and pressure *P*:

$$T = T(P, i); \quad \rho = \rho(P, i); \quad S = S(P, i). \tag{2.1}$$

For a perfect gas equation of state with *P* and *i* variables are very simple:

$$T = \frac{1}{C_p} i; \quad \rho = \frac{C_p}{R} \frac{P}{i}; \quad S = S_0 + C_p \ln i - R \ln P. \tag{2.2}$$

For the water steam approximation formula proposed in [7] is used, which established a procedure to calculate parameters of superheated and wet fluid.

It is easy to verify that the knowledge of the value of the velocity coefficient $\psi = w/w_T$ allows to determine the value of losses at the expansion $i - i_T = \frac{1-\psi^2}{\psi^2} w^2 \Big/ 2$ and obtain an expression that relates the enthalpies i_T and *i* at the end of the isentropic and the actual process of expansion, as well as stagnated enthalpy in relative motion $i_w^* = H + u^2/2 = i + w^2/2$:

$$\left(1 - \psi^2\right) i_w^2 - i + \psi^2 i_T = 0. \tag{2.3}$$

The last expression in combination with isentropic process equation from point 1 with parameters P_1, i_1 and the value of the relative velocity

$$S(P_1, i_1) = S\left(P_{w1}^*, i_{w1}^*\right) = S\left(P, i_T\right). \tag{2.4}$$

allows to come, deleting from (2.3), for example i_T, to the following process equation with unknowns *P*, *i*:

$$S\left(P, \frac{1}{\psi^2}\left[i-\left(1-\psi^2\right)i_w^*\right]\right)-S\left(P_{w1}^*, i_{w1}^*\right)=0\,. \tag{2.5}$$

With the help of the equation (2.5) can be solved a number of problems related to the thermal calculations of stages, which statement depends on which parameter of the unknown is a given. If we assume a known specific enthalpy *i* at the end of expansion, we obtain the equation (2.5) relative to the pressure *P*. This problem arises, for example, based on a predetermined degree of reaction or determining the counter pressure by the theoretical enthalpy drop per stage.

Solution of equations of the form (2.5) with one unknown is carried out by means of minimizing the residual square using one-dimensional search of extreme.

2.2 Aerodynamic Models

2.2.1 Axisymmetric Flow in the Axial Turbine Stage

Assume that in the flow path of the turbine:

- the flow is steady relatively to the impeller, rotating at a constant angular velocity ω about the *z*-axis or stationary guide vanes.
- the fluid is compressible, non-viscous and not thermally conductive, and the effect of viscous forces is taken into account in the form of heat recovery in the energy and the process equations, i.e., friction losses are accounted energetically.
- if the working fluid is real (wet steam) it is considered the equilibrium process of expansion.

- the flow is axisymmetric, i.e., its parameters are independent of the circumferential coordinate.

Under these assumptions the system of equations describing the steady axisymmetric compressible flow motion, includes:

1. The equation of motion in the relative coordinate system in the Crocco form

$$-\vec{W}\times\left[\nabla\times\vec{W}\right]+2\vec{\omega}\times\vec{W}=T\nabla S-\nabla H+\vec{F}+\vec{f}\,, \tag{2.6}$$

where $H=i+w^2/2-u^2/2=i+c^2/2-uc_u$ – rothalpy; $\vec{F}$ – blade force; $\vec{f}=-\vec{W}\dfrac{T}{w^2}\left(\vec{W},\nabla S\right)$ – friction force.

2. Continuity equation

$$\nabla\left(\chi\rho\vec{W}\right)=0\,, \tag{2.7}$$

where χ – blockage factor.

3. The equation of the process or system of equations describing the process

$$\left.\begin{array}{c}\left(1-\psi^2\right)\left(H+u^2/2\right)-i+\psi^2 i_T=0;\\ S_{in}-S_T\left(P,i_T\right)=0.\end{array}\right\} \tag{2.8}$$

4. The equations of state

$$T=T\left(P,i\right);\quad \rho=\rho\left(P,i\right);\quad S=S\left(P,i\right). \tag{2.9}$$

5. The equation of the flow surface

$$\left(\vec{W},\vec{n}\right)=0\,, \tag{2.10}$$

where $\vec{n}$ – normal to the S_2 surface (Fig. 2.1).

6. The equation of blade force orthogonality to the flow surface

$$\left[\vec{n}, \vec{F}\right] = 0. \tag{2.11}$$

Projections of the vortex in the relative motion $\mathrm{rot}\,\vec{W} = \nabla \times \vec{W}$ to be determined by the formulas:

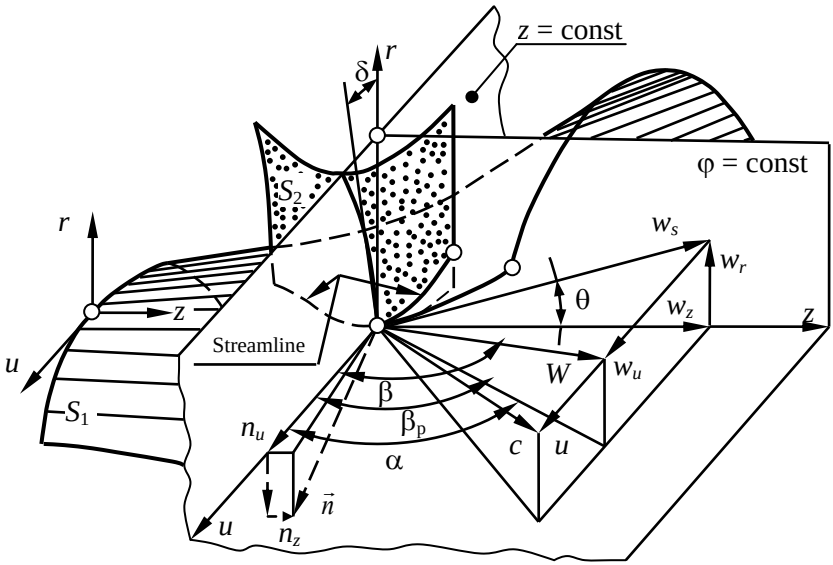

Figure 2.1 *The surfaces of the three-dimensional flow, relative flow angles and velocity components.*

$$\left.\begin{aligned} \mathrm{rot}_r\,\vec{W} &= \frac{1}{r}\left(\frac{\partial w_z}{\partial \phi} - \frac{\partial\left(r w_u\right)}{\partial z}\right); \\ \mathrm{rot}_u\,\vec{W} &= \frac{\partial w_r}{\partial z} - \frac{\partial w_z}{\partial r}; \\ \mathrm{rot}_z\,\vec{W} &= \frac{1}{r}\left(\frac{\partial\left(r w_u\right)}{\partial r} - \frac{\partial w_r}{\partial \phi}\right). \end{aligned}\right\} \tag{2.12}$$

Taking into account (2.12), projection of the equation of motion (2.6) on the axes of cylindrical coordinate system can be written as follows:

- on the *r* axis (radial equilibrium equation)

$$-\frac{w_u}{r}\frac{\partial(rw_u)}{\partial r}-w_z\left(\frac{\partial w_r}{\partial z}-\frac{\partial w_z}{\partial z}\right)-2\omega w_u=T\frac{\partial S}{\partial r}-\frac{\partial H}{\partial r}+F_r+f_r; \qquad (2.13)$$

- on the *u* axis:

$$\frac{w_r}{r}\frac{\partial(rw_u)}{\partial r}+w_z\frac{\partial w_u}{\partial z}+2\omega w_r=F_u+f_u; \qquad (2.14)$$

- instead of the projection on the *z* axis will use energy conservation equation:

$$\frac{\partial H}{\partial s}=0. \qquad (2.15)$$

The components of the relative velocity based on the designated flow angles (Fig. 2.1) can be written as

$$\left.\begin{aligned} w_z &= w_s\cos\theta = w\sin\beta\cos\theta;\\ w_u &= w_s\operatorname{ctg}\beta = w\cos\beta;\\ w_r &= w_s\sin\theta = w\sin\beta\sin\theta. \end{aligned}\right\} \qquad (2.16)$$

From the relation $\left[\vec{n},\vec{F}\right]=0$ will have:

$$n_rF_u=n_uF_r;\quad n_zF_u=n_uF_z;\quad n_zF_r=n_rF_z.$$

We express the ratio of the normals projections through the flow angles (Fig. 2.2):

$$\operatorname{tg}\delta=-\frac{n_r}{n_u};\quad \operatorname{tg}\theta=-\frac{n_z}{n_r};\quad c\operatorname{tg}\beta_p=\frac{n_z}{n_u}.$$

Than we can write

$$F_r=-\operatorname{tg}\delta F_u;\quad F_z=-\operatorname{tg}\theta F_r;\quad F_z=-c\operatorname{tg}\beta_pF_u. \qquad (2.17)$$

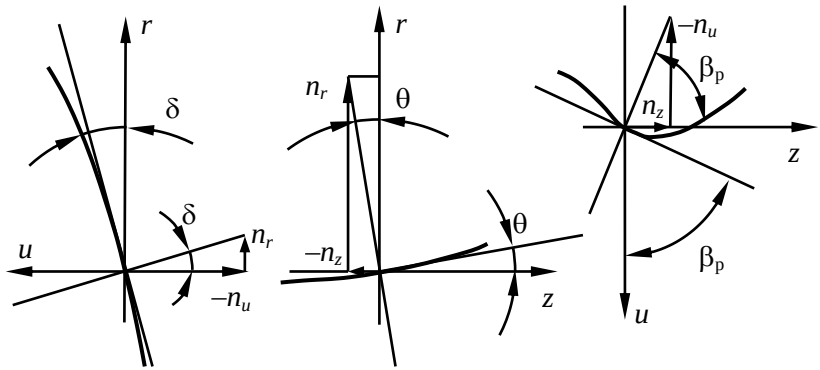

Figure 2.2 *The normal projections to the* S_2 *surface.*

Transforming the radial equilibrium equation

Using the relationship between the coordinates *z*, *r* and *s*, *r* in the meridian plane $\frac{\partial}{\partial z} = \frac{1}{\cos\theta}\left(\frac{\partial}{\partial s} - \sin\theta\frac{\partial}{\partial r}\right)$, and the ratio (2.16), the second term of the equation of radial equilibrium (2.13) can be converted

$$w_z\left(\frac{\partial w_r}{\partial z} - \frac{\partial w_z}{\partial r}\right) = w_s^2\left(\aleph\cos\theta + \sin\theta\frac{\partial \ln w_s}{\partial s} - \frac{\partial \ln w_s}{\partial r}\right). \qquad (2.18)$$

where $\aleph = \partial\theta/\partial s$ – the curvature of the meridian stream line.

To determine the $\partial \ln w_s/\partial s$ member use the continuity equation for an axisymmetric flow:

$$\frac{\partial\left(r\rho\chi w_r\right)}{\partial r} + \frac{\partial\left(r\rho\chi w_z\right)}{\partial z} = 0; \qquad (2.19)$$

which by means of (2.16) and the connecting relations between the cylindrical system of coordinates *z*, *r* and the coordinates of *s*, *n* in the natural grid (stream line *s* in the meridian plane and normal to it *n*)

$$\frac{\partial}{\partial z}=\frac{\partial}{\partial s}\cos\theta-\frac{\partial}{\partial n}\sin\theta,\quad \frac{\partial}{\partial r}=\frac{\partial}{\partial s}\sin\theta-\frac{\partial}{\partial n}\cos\theta$$

transformed into

$$\frac{\partial\theta}{\partial n}+\frac{\partial}{\partial s}\ln\left(\chi r\rho w_s\right)=0\,.$$

The last expression, in turn, by shifting from the coordinates *s*, *n* to coordinates *s*, *r* is represented as:

$$\frac{\cos\theta}{r}\frac{\partial\left(r\mathrm{tg}\,\theta\right)}{\partial r}-\aleph\mathrm{tg}\,\theta+\frac{\partial\ln\chi}{\partial s}+\frac{\partial\ln\rho}{\partial s}+\frac{\partial\ln w_s}{\partial s}=0\,,\qquad(2.20)$$

since

$$\frac{\partial\theta}{\partial n}=\frac{1}{\cos\theta}\left[\frac{\partial\theta}{\partial r}-\sin\theta\frac{\partial\theta}{\partial s}\right]=\frac{1}{\cos\theta}\frac{\partial\theta}{\partial r}-\aleph\mathrm{tg}\,\theta\,.$$

To determine the $\partial\ln\rho/\partial s$ member, engage the energy equation (2.15), where, according to (2.6) and Fig. 2.1

$$H=i+\frac{c^2}{2}-uc_u=i+\frac{c_u^2}{2}+\frac{w_s^2}{2}-uc_u=\mathrm{const}\,.$$

Then we have

$$\frac{\partial i}{\partial s}+c\frac{\partial c}{\partial s}-\frac{\partial\left(uc_u\right)}{\partial s}=\frac{\partial i}{\partial s}+w_s^2\frac{\partial\ln w_s}{\partial s}+c_u\frac{\partial c_u}{\partial s}-\frac{\partial\left(uc_u\right)}{\partial s}\,.\qquad(2.21)$$

The expression for $\partial i/\partial s$ defined differently depending on whether we are dealing with an ideal or a real working fluid.

The first term of (2.13) with (2.16), as well as Fig. 2.1 can be written as:

$$-\frac{w_u}{r}\frac{\partial(rw_u)}{\partial r}=-\frac{w_s^2\mathrm{ctg}^2\beta}{r}-w_s\mathrm{ctg}^2\beta\frac{\partial w_s}{\partial r}-\frac{w_s^2}{2}\frac{\partial\mathrm{ctg}^2\beta}{\partial r};$$

$$-\frac{w_u}{r}\frac{\partial(rw_u)}{\partial r}=-\frac{c_u r-\omega r^2}{r^2}\frac{\partial(c_u r)}{\partial r}+2\omega\frac{c_u r-\omega r^2}{r}.$$

Radial equilibrium equation (2.13) can now be converted to the form:

- *for a given* $c_u r$ (inverse problem):

$$w_s^2\left(\aleph\cos\theta+\sin\theta\frac{\partial\ln w_s}{\partial s}-\frac{\partial\ln w_s}{\partial r}\right)-$$
$$-\frac{c_u r-\omega r^2}{r^2}\frac{\partial(c_u r)}{\partial r}=T\frac{\partial S}{\partial r}-\frac{\partial H}{\partial r}+F_r+f_r; \qquad (2.22)$$

- in the gap between vanes (free channel):

$$w_s^2\left(\aleph\cos\theta+\sin\theta\frac{\partial\ln w_s}{\partial s}-\frac{\partial\ln w_s}{\partial r}\right)=$$
$$=-\frac{c_u r-\omega r^2}{r^2}\frac{\partial(c_u r)}{\partial r}+T\frac{\partial S}{\partial r}-\frac{\partial H}{\partial r}; \qquad (2.23)$$

- for a given β:

$$w_s^2\left[\aleph\cos\theta+\sin\theta\frac{\partial\ln w_s}{\partial s}-\frac{\mathrm{ctg}^2\beta}{r}-\frac{1}{2}\frac{\partial\mathrm{ctg}^2\beta}{\partial r}-\left(1+\mathrm{ctg}^2\beta\right)\frac{\partial\ln w_s}{\partial r}\right]-$$
$$-2\omega w_s\mathrm{ctg}\beta=T\frac{\partial S}{\partial r}-\frac{\partial H}{\partial r}+F_r+f_r. \qquad (2.24)$$

The projection of the equation of motion in the circumferential direction

Let us now consider the projection of the equation of motion (2.6) in the circumferential direction (2.14). Using (2.16), and the relationship between the coordinates *z*, *r* and *s*, *r* in the meridian plane

$$\frac{\partial}{\partial z}=\frac{1}{\cos\theta}\left(\frac{\partial}{\partial s}-\sin\theta\frac{\partial}{\partial r}\right),$$

equation (2.14) becomes:

- *for a given* $c_u r$ (inverse problem):

$$F_u = \frac{w_s}{r}\frac{\partial(c_u r)}{\partial s} - f_u; \tag{2.25}$$

- in the gap between vanes (free channel):

$$\frac{\partial(c_u r)}{\partial s} = 0; \tag{2.26}$$

- for a given β:

$$F_u = w_s^2\left[\frac{\sin\theta\,\mathrm{ctg}\,\beta}{r} + \frac{\partial \mathrm{ctg}\,\beta}{\partial s} + \frac{\partial \ln w_s}{\partial s}\mathrm{ctg}\,\beta\right] + 2\omega w_s \sin\theta - f_u. \tag{2.27}$$

These equations enable us to determine the projection of the blade force F_u in the circumferential direction. The radial component F_r is expressed through the circumferential according to (2.17).

The projections of the friction force on the coordinate axes

The expression for the friction force $\vec{f} = -\vec{W}\frac{T}{w^2}\left(\vec{W}, \nabla S\right)$ can be transformed by using the expression (2.16) and the binding ratio between the cylindrical coordinates *z*, *r* and the coordinates *s*, *r*:

$$\vec{f} = -\frac{\vec{W}}{w}\sin\beta T\frac{\partial S}{\partial s}, \tag{2.28}$$

whence we get the projection of the friction force on the coordinate axes:

$$f_r = -\sin^2\beta\sin\theta\, T\frac{\partial S}{\partial s}; \quad f_u = -\sin\beta\cos\beta\, T\frac{\partial S}{\partial s}.$$

The continuity equation is advisable to use in a form

$$d\psi = \frac{dG}{2\pi} = \chi r \rho w_s dn,$$

or, using the obvious relation $dn = dr\cos\theta$ (Fig. 2.3), we have:

$$\frac{\partial \psi}{\partial r} = r\rho w_s \cos\theta\, \chi. \tag{2.29}$$

If the working fluid can be considered as ideal gas, for which the equations of the state and of the process are simple expressions, using the equation [8] $i\sigma^{k-1}\rho^{1-k} = \text{const}$, we obtain

$$\frac{\partial i}{\partial s} = a^2\left(\frac{\partial \ln \rho}{\partial s} - \frac{\partial \ln \sigma}{\partial s}\right), \tag{2.30}$$

where $a^2 = (k-1)i = kRT$ – local sound velocity square.

Substituting (2.30) into (2.21), solving (2.21) and (2.20) as a system of linear equations with unknowns $\partial \ln w_s / \partial s$ and $\partial \ln \rho / \partial s$, we obtain for a given $c_u r$:

$$-\frac{\partial \ln w_s}{\partial s} = \frac{1}{1-\mathrm{M}_s^2}\left[\frac{\cos\theta}{r}\frac{\partial (r\,\mathrm{tg}\,\theta)}{\partial r} - \aleph\,\mathrm{tg}\,\theta + \right.$$
$$\left. + \frac{\partial \ln \chi}{\partial s} - \frac{c_u}{a^2}\frac{\partial c_u}{\partial s} + \frac{1}{a^2}\frac{\partial (uc_u)}{\partial s} + \frac{\partial \ln \sigma}{\partial s}\right]. \tag{2.31}$$

Note that

$$c_u \frac{\partial c_u}{\partial s} = \frac{c_u}{r}\frac{\partial (c_u r)}{\partial s} - \frac{c_u^2}{r}\sin\theta, \tag{2.32}$$

since $\partial r / \partial s = \sin\theta$, $\mathrm{M}_s = w_s / a$.

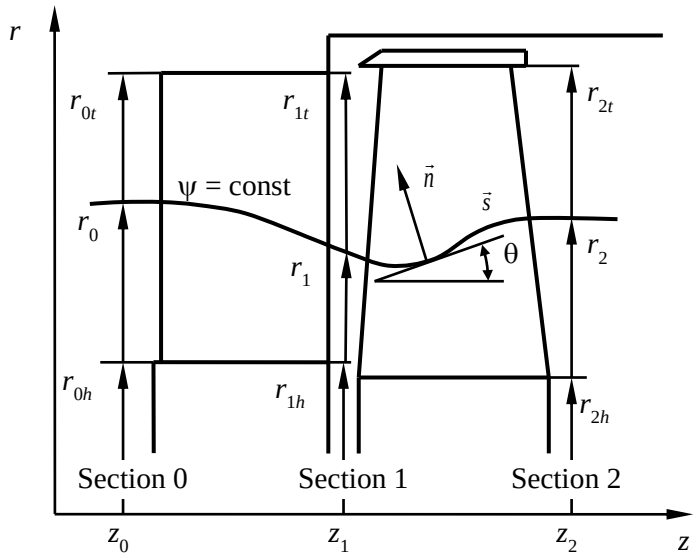

Figure 2.3 *Axial turbine stage meridian projection. Symbols used in the simplified stage calculation procedure.*

For a free channel from the projection of the equation of motion in the absolute coordinate system to the circumferential direction, obtain, that the circulation $c_u r = \text{const}$ along the meridian streamline and $\partial(c_u r)/\partial s = 0$.

Then *for a free channel* $(\chi = 1)$ from (2.31) we have:

$$-\frac{\partial \ln w_s}{\partial s} = \frac{1}{1-\mathrm{M}_s^2}\left[\frac{\cos\theta}{r}\frac{\partial(r\mathrm{tg}\theta)}{\partial r} - \aleph\mathrm{tg}\theta + \frac{(c_u r)^2}{a^2 r^3}\sin\theta + \frac{\partial \ln\sigma}{\partial s}\right]. \quad (2.33)$$

2.2.2 Aerodynamic Calculation of the Axial Turbine Stage in Gaps

The considered above in the general formulation, the problem of calculation of axisymmetric flows of a compressible fluid in the flow path of the axial turbine can be simplified and reduced to the calculation in gaps [9]. The flow in the axial gap is seen at the main proposals set out above. Within axial gap in the space free of the blades $\chi = 1$; because of its small length in the axial direction

the entropy S locally do not changes along the meridian streamlines (i.e. $\partial S/\partial s = 0$); it is possible to force components $F_r = f_r = 0$; stream keeps the direction of motion, telling him by blades (i.e., the angle of the flow β is set).

In these assumptions the radial equilibrium equation will differ from (2.24) in the absence of the right side of F_r and f_r:

$$w_s^2\left[\aleph\cos\theta+\sin\theta\frac{\partial\ln w_s}{\partial s}-\frac{\mathrm{ctg}^2\beta}{r}-\frac{1}{2}\frac{\partial\mathrm{ctg}^2\beta}{\partial r}-\left(1+\mathrm{ctg}^2\beta\right)\frac{\partial\ln w_s}{\partial r}\right]-$$
$$-2\omega w_s\mathrm{ctg}\beta-T\frac{\partial S}{\partial r}+\frac{\partial H}{\partial r}=0. \qquad (2.34)$$

From the energy equation (2.21), using (2.32), considering the fact that $\chi = 1$ and along the stream lines $\partial\left(c_u r\right)/\partial s = 0$ obtain

$$\frac{\partial\ln w_s}{\partial s}=\frac{1}{\left[1-w_s^2\left(\frac{\partial\rho}{\partial P}+\frac{\partial\ln\rho}{\partial i}\right)\right]}\left[\aleph\mathrm{tg}\theta-\frac{\cos\theta}{r}\frac{\partial\left(r\mathrm{tg}\theta\right)}{\partial r}-\right.$$
$$\left.-\frac{\left(c_u r\right)^2}{r^3}\sin\theta\left(\frac{\partial\rho}{\partial P}+\frac{\partial\ln\rho}{\partial i}\right)+T\frac{\partial S}{\partial s}\frac{\partial\rho}{\partial P}\right]. \qquad (2.35)$$

Radial equilibrium equation (2.34), written about the speed *w* (that gets rid of the derivative $\partial\mathrm{ctg}^2\beta/\partial r$) by going to the new independent variable ψ by a ratio

$$\frac{d}{dr}=r\rho w_s\cos\theta\frac{d}{d\psi},$$

takes the form

$$\frac{dw}{d\psi}=-\frac{\sin\beta}{r\rho\cos\theta}\left(B\sin\theta-\aleph\cos\theta+\frac{\mathrm{ctg}^2\beta}{r}+\frac{2\omega\mathrm{ctg}\beta}{w\sin\beta}\right)+$$

$$+\frac{1}{w}\left(\frac{dH}{d\psi}-T\frac{dS}{d\psi}\right). \tag{2.36}$$

The continuity equation can be represented as:

$$\frac{dr}{d\psi}=\frac{1}{r\rho w\sin\beta\cos\theta}. \tag{2.37}$$

Thus, flow in the gap of the turbine stage described by the system of two ordinary first order differential equations (2.36), (2.37) with the boundary conditions $r(0)=r_h$, $r(\psi^*)=r_t$.

The values $B=-\partial\ln W_S/\partial s$ are determined by (2.35), and the enthalpy – according to the equation energy

$$H=i+\frac{w^2}{2}-\frac{u^2}{2}=i+\frac{c^2}{2}-uc_u=\text{const}.$$

To calculate the temperature, density and entropy from the formulas (2.9) need to know other than the enthalpy *i* also pressure *P*, which for some *w* can be found from the second equation (2.8):

$$S_{in}=S_T\left(P, H+\frac{u^2}{2}-\frac{w^2}{2\psi^2}\right). \tag{2.38}$$

Consequently, the system of equations, describing the steam flow in the axial turbine stage gaps are as follows:

- after the guide vanes:

$$\left.\begin{aligned} \frac{dr_1}{d\psi} &= \frac{1}{r_1\rho_1 c_1 \sin\alpha_1 \cos\theta_1}; \\ \frac{dc_1}{d\psi} &= -\frac{\sin\alpha_1}{r_1\rho_1\cos\theta_1}\left(B_1\sin\theta_1 - \aleph_1\cos\theta_1 + \frac{\mathrm{ctg}^2\alpha_1}{r_1}\right) + \\ &+ \frac{1}{c_1}\left[\frac{di_0^*}{d\psi} + T_1\frac{dS_1}{d\psi}\right], \end{aligned}\right\} \tag{2.39}$$

where

$$B_1 = -\partial \ln w_{1s}/\partial s; \quad i_1 = i_0^* - c_1^2/2; \quad T_1 = T_1\left(i_1, P_1\right);$$

$$\rho_1 = \rho_1\left(i_1, P_1\right); \quad S_1 = S_1\left(i_1, P_1\right); \quad S_0^* = S_{1T}\left(P_1, i_0^* - c_1^2/\left(2\phi^2\right)\right).$$

Boundary conditions

$$r_1(0) = r_h; \; r\left(\psi^*\right) = r_s;$$

- after the rotor:

$$\left.\begin{aligned} \frac{dr_2}{d\psi} &= \frac{1}{r_2\rho_2 w_2 \sin\beta_2 \cos\theta_2}; \\ \frac{dw_2}{d\psi} &= -\frac{\sin\beta_2}{r_2\rho_2\cos\theta_2}\left(B_2\sin\theta_2 - \aleph_2\cos\theta_2 + \frac{\mathrm{ctg}^2\beta_2}{r_2} + \right. \\ &\left. + \frac{2\omega\,\mathrm{ctg}\,\beta_2}{w_2\sin\beta_2}\right) + \frac{1}{w_2}\left[\frac{di_0^*}{d\psi} - \frac{d\left(u_1 c_{1u}\right)}{d\psi} + T_2\frac{dS_2}{d\psi}\right], \end{aligned}\right\} \tag{2.40}$$

where

$$B_2 = -\partial \ln w_{2s}/\partial s; \quad i_2 = i_0^* - u_1 c_{1u} + u_2^2/2 - w_2^2/2; \quad T_2 = T_2\left(i_2, P_2\right);$$

$$\rho_2 = \rho_2\left(i_2, P_2\right); S_2 = S_2\left(i_2, P_2\right); S_1 = S_{2T}\left(P_2, i_{2w}^* - w_2^2/\left(2\psi^2\right)\right); i_{2w}^* = i_2 + w_2^2/2.$$

Boundary conditions:

$$r_2(0) = r_{2h};\ r_2(\psi^*) = r_{2t}.$$

The numerical realization of the stage thermal calculation problem

Mathematical models of axial turbine stages, discussed above, allow their calculation by setting some additional (closing) relations, for example, the distribution of the angles β and α (direct problem), the quantities $c_u r$, ρc_z, et al. (inverse problems).

To solve the direct problem of stage calculation in gaps the following information is required:

- form of the stage meridian contours, i.e. external and internal radii of axial sections;
- rotor speed ω;
- stagnation parameters at the stage input P_0^* and i_0^*;
- the geometrical characteristics of the blades: entry and exit angles, as well as blades count in the crowns, the chord, edge thickness and other parameters necessary for determining the velocity coefficients along the blade length;
- if the velocity coefficients are predefined – their distribution along the blade length.
- streamline slope angles θ and their curvature ℵ in fixed axial sections.

There are varieties of the direct problem with a given flow rate *G* and with a specified back pressure P_2. Solution of the problem with a fixed flow easier because the integration of the equations (2.39), (2.40) is made for a known $\psi^* = G/(2\pi)$ value and mathematically formulated as a two-point boundary value problem for a system of two ordinary first order differential equations of the form:

$$\left.\begin{aligned}\frac{dw}{d\psi} &= f_1(\psi, w, r);\\ \frac{dr}{d\psi} &= f_2(\psi, w, r),\end{aligned}\right\} \tag{2.41}$$

with boundary values: $r(0) = r_h$; $r(\psi^*) = r_t$.

Right sides of equation (2.41) are calculated according to the formula of the system of equations (2.39), (2.40).

The decision imposed positivity of w (unseparated flow condition).

From physical considerations it is known that problem (2.41) can have either two solutions, corresponding sub- and supersonic flow mode, either one or do not have a solution.

One way of solving the problem (2.41) is to reduce it to finding the root of the transcendental equation, which serves for the selection of the missing boundary condition at the hub $w(0) = w_h$. Indeed, setting a boundary condition w_h and integrating (2.41) as the Cauchy problem with the initial conditions $r(0) = r_h$; $w(0) = w_h$, we obtain at ψ^* an approximate value of the outer radius $r(\psi^*) = \tilde{r}_t$. Considering $\tilde{r}_t$ as a function w_h we obtain the equation with one unknown w_h:

$$\tilde{r}(w_h) - r_t = 0. \tag{2.42}$$

Thus, for the solution of the direct problem of the stage calculation with a given flow rate is required to solve the system of transcendental equations:

$$\left.\begin{aligned}&\tilde{r}_{1t}(c_{1h}) = r_{1t},\\ &\tilde{r}_{2t}(c_{1h}, w_{2h}) = r_{2t}.\end{aligned}\right\}. \tag{2.43}$$

The solution of (2.43) is made in two stages: first, the first equation is solved and the distribution of the flow in fixed axial gap is found, then, knowing the parameters entering the impeller can solve the second equation. That is, the problem is reduced to determining the roots of the equation with one unknown for each of the two equations (2.43). For the calculation of the subsonic solutions of (2.43) can be successfully used the methods of nonlinear programming. The system (2.43) is solved by sequential minimization of residuals

$$\left.\begin{aligned} \Delta_1^2 &= \left[\tilde{r}_{1t}\left(c_{1h}\right) - r_{1t}\right]^2, \\ \Delta_2^2 &= \left[\tilde{r}_{2t}\left(w_{2h}\right) - r_{2t}\right]^2. \end{aligned}\right\} \tag{2.44}$$

using one of the described one-dimensional extremum search methods.

Solution of the problem with a given back pressure P_2 (flow rate unknown) is more complicated. To determine the unknown mass flow G to the system of equations (2.43) is necessary to add one more thing – a limit on the heat drop.

In this formulation of the problem it seems appropriate to set the mass flow averaged pressure according to the formula

$$\int_0^{\psi^*} P_2 d\psi = \psi^* P_{2m.def.}. \tag{2.45}$$

In view of (2.45) to calculate the level with a given back pressure is needed to solve a system of three equations with three unknowns:

$$\left.\begin{aligned} \Delta_0 &= h\left(c_{1h}, w_{2h}, \psi^*\right) - h_0 = 0; \\ \Delta_1 &= \tilde{r}_1\left(c_{1h}, \psi^*\right) - r_{1t} = 0; \\ \Delta_2 &= \tilde{r}_2\left(c_{1h}, w_{2h}, \psi^*\right) - r_{2t} = 0. \end{aligned}\right\} \tag{2.46}$$

Numerically, the problem is solved to minimize the sum of squared residuals

$$I^* = \Delta_0^2 + \Delta_1^2 + \Delta_2^2 \tag{2.47}$$

on three variables c_{1h}, w_{2h}, ψ^* using one of the multidimensional extremum search methods.

A maked up mathematical model describing the flow in the axial gaps of turbomachine (equation (2.39), (2.40)), allows the calculation of supersonic flow (including the transition through the speed of sound), which $M_s < 1$, i.e., in the case of the meridional component of velocity less than the velocity of sound. Specified the conditions satisfy all existing stages of powerful steam turbines.

Calculation of supersonic stages must be performed with a given back pressure, because otherwise does not provide a unique solution of the equation of the form (2.41). At the same time, the system of transcendental equations (2.46) in the variables c_{1h}, w_{2h}, ψ^* in contrast to (2.43) has a unique root.

Another feature of the supersonic stages calculation is the need to consider the flow deflection in an oblique cut at Mach numbers higher than unity. For this purpose it is possible to use a method of determining the flow deflection angle in an oblique cut comprising in equating flow rate into the throat section and behind the blade [10, 11].

In this case, to calculate the residuals of equations (2.44), (2.46) it is necessary to integrate the system of ordinary differential equations of the form (2.41), namely (2.39), (2.40). These equations are due to the complexity of the form of the right sides in the general case can be integrated numerically. When integrating (2.39) (2.40) should be borne in mind that at each step of pressure shall be determined by solving the equations of the form (2.38), which greatly complicates the task.

Finally, we note that because of the existence of the right sides of (2.38), (2.40), a member $T\partial S/\partial\psi$, the system, generally speaking, can not be considered as written in the form of Cauchy, as these non-linear supplements are some of the functions w_2 or c_1, r and their derivatives. When integrating these terms are determined by successive approximations.

The important point is the choice of numerical methods for integrating systems of the form (2.41). Extensive experience in solving such problems suggests the possibility of partitioning the integration interval to a small number of steps (5–10). As a result of numerical experiments comparing different methods, preference was given to the modified Euler's method [12], which has the second order of accuracy for the integration step.

The leakage calculation is necessary to conduct together with a stage spatial calculation, the results of which are determined the parameters along a height in the calculation sections, including the meridian boundaries of the flow part.

The stage capacity depends on the value of clearance (or leakages), in connection with which calculation of the main stream flow is made by mass flow amplification at fixed the initial parameters and counter-pressure on the mean radius, or with counter-pressure elaboration at fixed initial parameters and mass flow.

The need for multiple steps in optimization problems requires a less labor-capacious, but well reflecting the true picture of the flow, methods of axisymmetric stage calculation. Its main point is to calculate the stage parameters in the axial gaps supplemented by the algorithm of stream lines slope and curvature refinement in the design sections.

When calculating the stage taking into account leakage, the continuity equation is convenient to take the form:

$$\frac{\partial \psi}{\partial r} = \mu r \rho w_s \cos\theta\,, \tag{2.48}$$

where μ – mass transfer coefficient, which allows to take into account changes in the amount of fluid passing through the crowns, and at the same time to solve a system of ordinary differential equations in sections in front of and behind the impeller like a constant mass flow rate.

As shown, the calculation of spatial flow in the stage with the known in some approximation the shape of the stream lines is reduced to the solution in the sections $z_1 = \text{const}$ and $z_2 = \text{const}$ (Fig. 2.3) of a system of ordinary differential equations (2.39) and (2.40), where as independent variable a stream function ψ is taken. Thus, the equations describing the flow in the axial gap, presented in the form of:

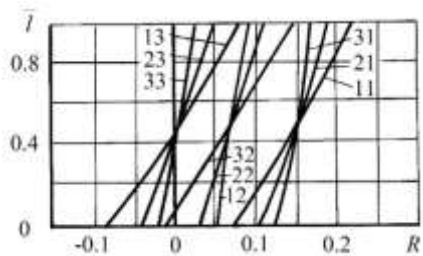

Figure 2.4 *Estimated distribution of the reaction degree in a series of stages with* $D_m/l = 19$ *[13].*

- in the section after the guide vanes:

$$\left.\begin{aligned} \frac{dr_1}{d\psi} &= f_{11}(\psi, r_1, c_1); \\ \frac{dc_1}{d\psi} &= f_{12}(\psi, r_1, c_1); \\ r_1(0) &= r_{1h}; \quad r_1(\psi^*) = r_{1t}; \end{aligned}\right\} \tag{2.49}$$

- in the section after rotor:

$$\left.\begin{aligned} &\frac{dr_2}{d\psi} = f_{21}\left(\psi, r_1, c_1, r_2, w_2\right); \\ &\frac{dw_2}{d\psi} = f_{22}\left(\psi, r_1, c_1, r_2, w_2\right); \\ &r_2\left(0\right) = r_{2h}; \quad r_2\left(\psi^*\right) = r_{2t}. \end{aligned}\right\} \tag{2.50}$$

The solution of the boundary problems (2.49), (2.50) for a given mass flow rate is reduced to finding the roots of the two independent transcendental equations (2.43) with respect to the hub velocities c_{1h}, w_{2h}.

For a given backpressure to the number of defined values the mass flow ψ^* is added and the problem reduces to solving a system of three equations. As a third equation the stage heat drop constraint is added (2.45) that can be symbolically written as

$$h\left(c_{1h}, w_{2h}, \psi^*\right) - h_0 = 0.$$

Systems of equations are solved using the methods of nonlinear programming.

An approximate method of meridian stream lines form amplification using their coordinates in the three sections, is to construct an interpolation cubic spline at a given slopes at the flow path boundaries. In order to accelerate the convergence the stream line curvature is specified with lower relaxation. Previous calculations showed that the interpolation process converges with sufficient accuracy in 3…5 iterations.

Mass flow rates through crowns carried out in parallel with the streamlines construction. The algorithm allows to solve the direct problem of the spatial stage calculation in the gaps in various statements, with given or variable in the process

of calculating the streamlines, velocity and flow coefficients of crowns, at various ways of flow angles distribution along the height, for a perfect gas or steam.

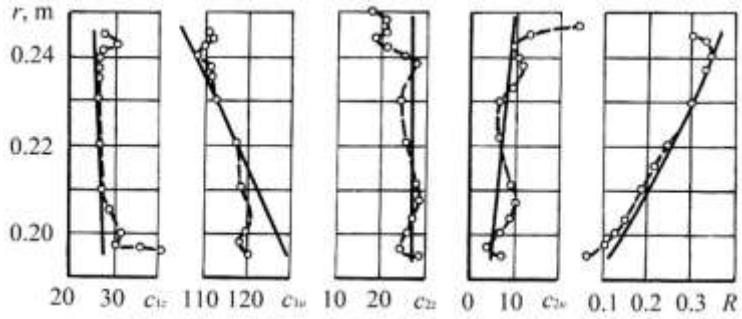

Figure 2.5 *Estimated (——) and experimental (---- o ----) distribution of parameters in the M1 stage gaps* $D_m/l = 8.3$ *[13].*

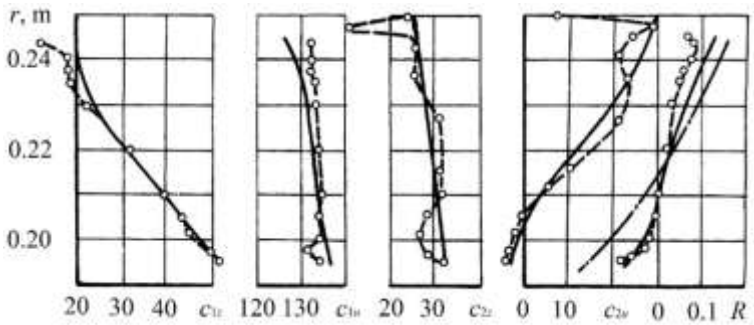

Figure 2.6 *Estimated (——) and experimental (---- o ----) distribution of parameters in the P3 stage gaps* $D_m/l = 8.3$ *[13]: —• ——calculation of cylindrical theory.*

The algorithm was tested by comparing the calculation results with the exact solutions, as well as with the experimental data obtained for a large number of stages of the experimental air turbines in the turbine department of NTU "KhPI" [13–14, 15]. The results of calculations and experiments illustrated in Fig. 2.4–2.12. It should be stated a good calculations agreement with the experimental result for the various stages of the different elongation, meridian shape contours, twist laws and the reaction degree at the mean radius.

The greatest difficulty to calculate present stages with the steep opening of the flow path (Fig. 2.12), and the cylindrical stages with inversely twisted guide vanes (Fig. 2.4, 2.6–2.8).

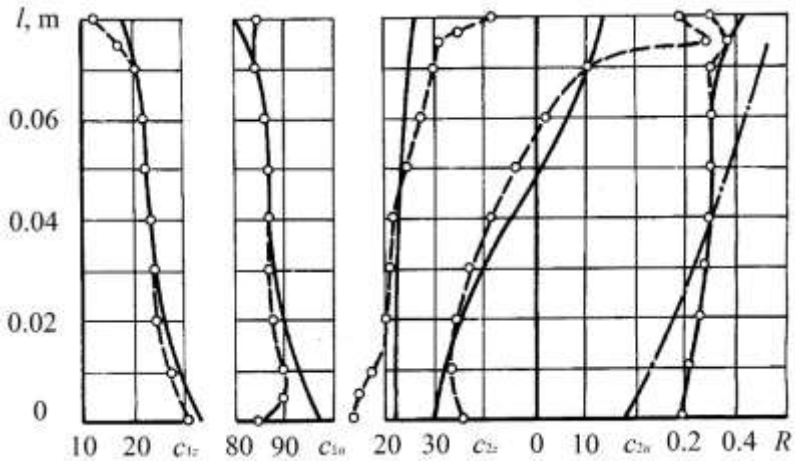

Figure 2.7 *Estimated (——) and experimental (---- o ----) distribution of parameters in the stage 41 gaps with* $D_m/l = 5.13$ *[13]; —• —– calculation of cylindrical theory.*

The calculation of stages with inverse twist using the proposed method allows to obtain a valid gradient of reaction degree and circumferential velocity component of the stage, while the calculation provided in assumption of cylindrical flow gives results that differ significantly from the experimental data (Fig. 2.6–2.8). The technique allows to take into account also the effect of the law of the impeller's twist on the distribution of parameters in the gap between guide vane and rotor. This is evidenced by the comparison stages 41 and 42 (Fig. 2.7, 2.8) with the same nozzle unit, the first of which has a cylindrical impeller, and the second – twisted by constant circulation law.

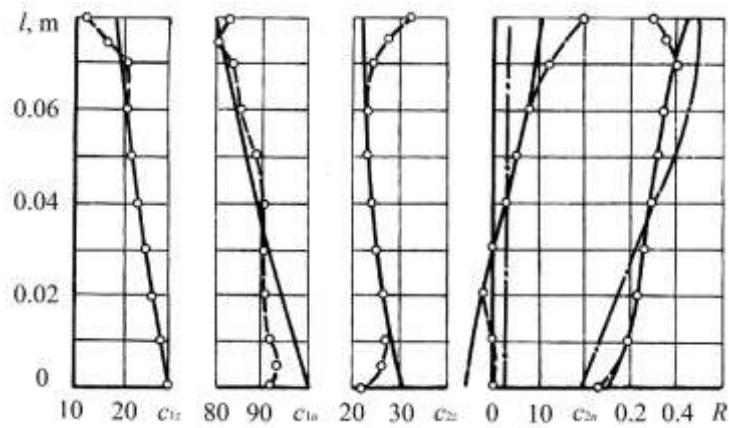

Figure 2.8 *Estimated (——) and experimental (---- o ----) distribution of parameters in the stage 42 gaps* $D_m/l = 5.13$ *[13]; —• —– calculation of cylindrical theory.*

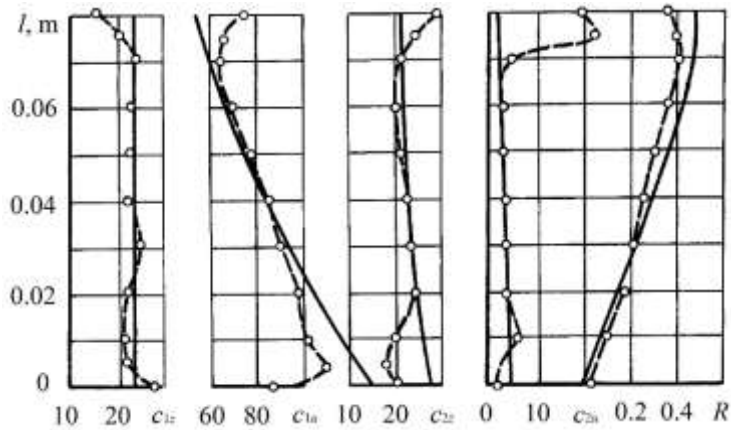

Figure 2.9 *Estimated (——) and experimental (---- o ----) distribution of parameters in the stage 32 gaps* $D_m/l = 5.13$ *[13].*

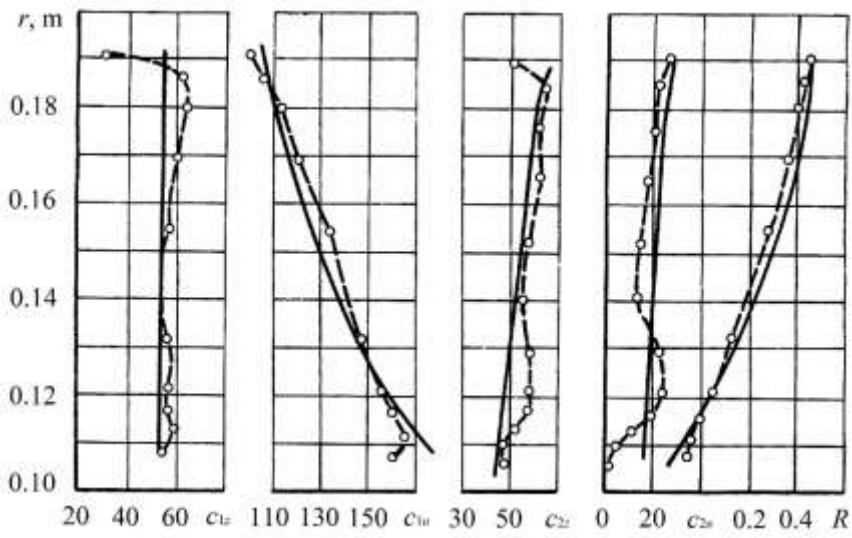

Figure 2.10 *Estimated (——) and experimental (---- o ----) distribution of parameters in the stage I gaps* $D_m/l = 3.6$ *(the author's tests).*

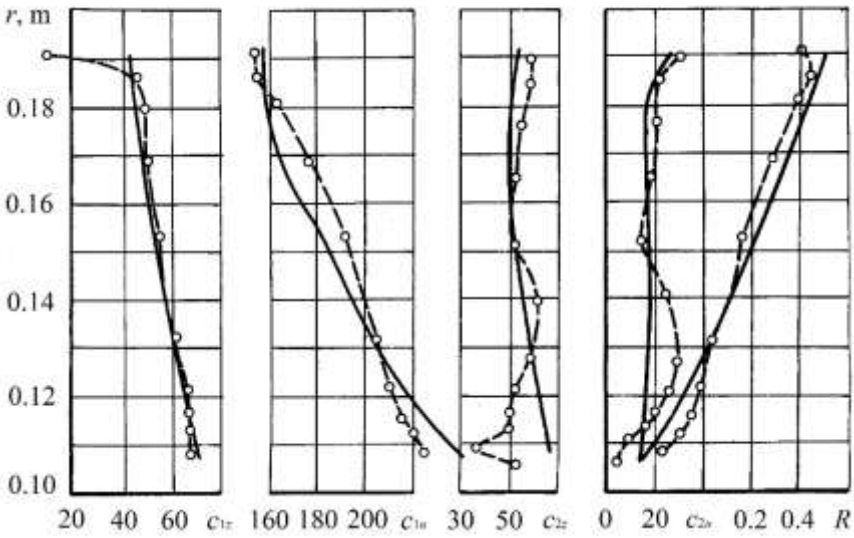

Figure 2.11 *Estimated (——) and experimental (---- o ----) distribution of parameters in the stage gaps II* $D_m/l = 3.6$ *(the author's tests).*

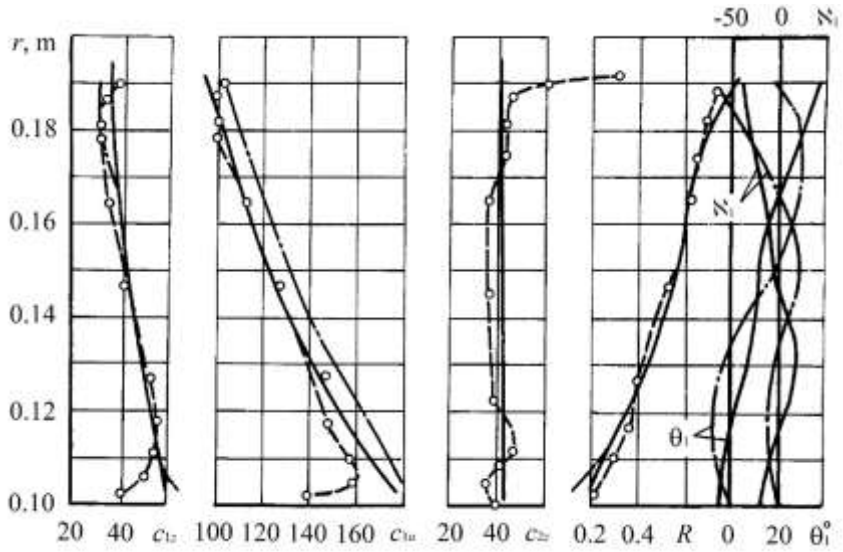

Figure 2.12 *Estimated (——) and experimental (---- o ----) distribution of parameters in the stage 33 gaps* $D_m/l = 3.2$ *[13]; —• —– full axisymmetric statement calculation.*

2.2.3 Off-Design Calculation of Multi-Stage Steam Turbine Flow Path

Formulation of the problem

The off-design analysis problem is to determine the gas-dynamic characteristics derived from the design calculation such as the size of the flow path (FP) and the parameters that determine the long-term (steady) operation of the turbine. The need to analyze FP off-design modes arises when assessing aero- and thermodynamic, power, strength parameters of the turbine in extreme operating conditions, the choice of method for control and calculation of steam distribution, for turbines designed to operate at changing the regime parameters (speed, unregulated steam extraction and so on).

The specifics of these problems requires a gas-dynamic calculations in a direct statement, which is more labor intensive than the calculations commonly

used in the design stage. In connection with this methods designed for use with a computer optimization procedures must meet several requirements:

- to base on the equations of motion of a real working fluid in the flow path of the multi-stage turbine;
- to consider with the required accuracy the influence of geometrical and operational parameters on the loss factors of the FP elements;
- to allow to conduct calculations with varying from section to section the mass flow rates;
- to be highly reliable and economical in terms of consumption of computer resources, i.e. make it possible to carry out multi-variant and optimization calculations.

To calculate high, medium and, to a lesser extent, the low-pressure parts of powerful steam turbines, justified the use of one-dimensional gas dynamics calculations using the simplified radial equilibrium equations in a axial clearance, the leaks balance at the root of the diaphragm design stages and the calculation method of the FP moisture separation. Accounting for the loss of kinetic energy and efficiency assessment should be carried out by successive approximations based on the current results of the gas-dynamic calculation and empirical relationships, and reliability of the results – achieved by comparison with experimental results and the introduction of necessary adjustments.

Should be regarded as a satisfactory the accuracy of coincidence of calculated and experimental values of the relative losses in the range of 5…7% for FP made with straight or twisted by constant circulation law blading in the absence of the sharp curvature of the meridian contours. When the actual loss levels of 10...30% error in determining the efficiency, thus lies in the range of 0.5...2% [15].

Method of calculation

One-dimensional steady-state equilibrium adiabatic motion of water vapor in the flow path in a coordinate system rotating with angular velocity ω, sought a system of equations:

- energy

$$H = i + \frac{w^2 - u^2}{2}; \tag{2.51}$$

- continuity

$$G = F\rho w_z; \tag{2.52}$$

- process

$$S_0 - S\left(P, \frac{1}{\psi^2}\left[i - \left(1 - \psi^2\right) i_w^*\right]\right) = 0; \tag{2.53}$$

- state

$$T = T(P, i);\ \rho = \rho(p, i);\ S = S(p, i);\ P = P(i, S);\ i = i(P, S); \tag{2.54}$$

- flow kinematic parameters relations.

The solution to this system of equations for an isolated axial turbine stage in a direct statement requires:

- stage input enthalpy i_0^*;
- stage output pressure P_{2def};
- angular rotational speed ω;
- mean diameters of sections D_{1m}, D_{2m} and blade lengths l_1, l_2;
- cascade's output effective angles α_{1e}, β_{2e};

- data to estimate blades velocity factors: chords, number of blades, edge thickness, geometry entry angles so on;
- the data for the calculation of additional energy losses, such as the types of seals and their sizes, the values of axial and radial clearances, the number of bonding wires, etc.

The two main statements involve mass flow G_0 determination at certain stagnated pressure P_0^* at stage inlet, or the P_0^* definition at known flow rate. It is also possible the solution of the problem with given at the same time G_0 and P_0^* changing angles α_{1e} or β_{2e}, in particular, makes it possible to simulate the nozzle assembly with rotary blades. In all cases, subject to the definition of the flow speed c_1 and w_2.

For definiteness we shall consider the problem with fixed P_0^* and mass flow determination. We transform the equation of continuity (2.52) for the nozzle in view of (2.51), (2.53), (2.54):

$$G = \rho_1 \left(P\left(i_0^* - \frac{c_1^2}{2\phi^2}, S_0^*\left(P_0^*, i_0^*\right)\right), i_0^* - \frac{c_1^2}{2}\right) c_1 \sin\alpha_1 F_1 \tag{2.55}$$

with unknown c_1 and G.

Similarly, after the impeller

$$G = \rho_2 \left(P\left(H + \frac{u_2^2}{2} - \frac{w_2^2}{2\psi^2}, S\left(P_1, i_1\right)\right), H + \frac{u_2^2}{2} - \frac{w_2^2}{2}\right) w_2 \sin\beta_2 F_2, \tag{2.56}$$

where

$$H = i + \frac{c_1^2}{2} - u_1 c_{1u};\ P_1 = P\left(i_0^* - \frac{c_1^2}{2\phi^2}, S_0^*\right);\ i_1 = i_0^* - \frac{c_1^2}{2}.$$

This equation contains the unknown c_1, G, w_2.

Under α_1 and β_2 at subsonic flow understood the cascade's effective angles, and at supersonic – flow angles in the oblique cut-off by the Ber formula.

The third equation is:

$$P\left(H+\frac{u_2^2}{2}-\frac{w_2^2}{2\psi^2}, S\left(P_1, i_1\right)\right)=P_{2def}. \tag{2.57}$$

Under certain velocity factors φ and ψ to determine the unknown c_1, G, w_2, there are three equations (2.55)–(2.57), which in general terms be written as follows:

$$\left.\begin{aligned} &g_1\left(G, c_1\right)=0;\\ &g_2\left(G, c_1, w_2\right)=0;\\ &h\left(G, c_1, w_2\right)=0. \end{aligned}\right\} \tag{2.58}$$

The system (2.58) is solved numerically by minimizing the sum of squared residuals $g_1^2+g_2^2+h^2$ using the conjugate gradient method.

Calculation of multistage flow path does not differ systematically from the stage calculation. An equation of (2.58) is written for each of the stages, which leads to a system of the form

$$\left.\begin{aligned} &g_{1j}\left(G, c_{1j}, c_{1j-1}, \ldots, w_{2j-1}, w_{2j-2}, \ldots.\right)=0;\\ &g_{2j}\left(G, c_{1j}, c_{1j-1}, \ldots, w_{2j}, w_{2j-1}, \ldots.\right)=0,\ j=1, \ldots, n;\\ &h\left(G, c_{1n}, \ldots, c_{11}, w_{2n}, \ldots,\ w_{21}\right)=0, \end{aligned}\right\} \tag{2.59}$$

where j – stage index; n – number of stages in the FP.

The numerical solution is carried out by minimizing the function

$$\sum_{j=1}^{n}\left(g_{1j}^2+g_{2j}^2\right)+h^2$$

by $2n+1$ unknowns $c_{1j}, w_{2j}, (j=1,\ldots,n), G$.

Sections may have different mass flows because of the leaks, district heating or regenerative steam extraction, moisture separation and so on. In the equations (2.59) in this case instead of a mass flow rate *G* in the relevant sections should take the current value

$$G_k = G_{k-1} + \Delta G_k,$$

where ΔG_k – given or confirmed in iterations the mass flow change in the transition from $(k-1)$ section to the *k*-th $(k=1\ldots2n)$.

The unknown is considered the G_0 mass flow at the FP entrance.

After the solution of (2.58) or (2.59) all the parameters of the flow calculated, loss factors and the actual mass flows in sections adjusted. The required number of iterations is usually equal to 3...4.

Kinetic energy loss determination

Losses associated with the leakage of the working fluid are considered separately. The remaining components are divided into losses in cascade and auxiliary, which are allocable to the stage heat drop.

Methods of assessing the losses in cascades based on research [8, 16] with a corresponding adjustment of empirical dependencies using test data about profiles used in the turbine building [17, 18].

Following [16], the loss factor in the cascade $X=\left(1-\psi^2\right)/\psi^2$ is the sum of the factors of profile X_p and secondary X_s losses, which are defined as follows:

$$X_p = X_{pb} N_{\mathrm{Re}} N_i N_{iy} N_t + \Delta x_t + \Delta x_{\mathrm{M}} + \Delta x_y , \tag{2.60}$$

where X_{pb} – base profile loss; N_{Re} – Reynolds number correction; N_i – incidence angle correction; N_{iy} – correction for the angle of attack associated with the elongation of the leading edge profile; $N_t, \Delta x_t$ – trailing edge thickness corrections; Δx_{M} – Mach number correction at $\mathrm{M} > 1$; Δx_y – correction due to the elongation of the input portion of the profile with a zero angle of attack.

$$X_s = X_{sb} N_{\mathrm{Re}} N_{b/l} N_\delta , \tag{2.61}$$

where X_{sb} – base secondary loss; $N_{b/l}$ – relative blade height correction; N_δ – an amendment to the length of hanging visor.

Corrections for the Reynolds number, angle of attack, the thickness of the trailing edge, at supersonic flow are taken over without change [19]. The amendment to the angle of attack in the profiles provided with an extension of the leading edge, is estimated according to experimental studies on the standard nozzle profiles and the impact of the extension on the profile loss – NPO CKTI the procedure [20].

The basic component of the profile X_{pb} obtained by a corresponding adjustment to the loss level of graphic dependence [16]. Basic secondary loss is determined by the corrected chart [16], an amendment to the ratio of the chord to the height of the blade $N_{b/l}$ – according to [16], and the coefficient N_δ taking into account the length of the visor hanging over the trailing edge of the blade – based on experimental data on nozzle standard profiles test data.

When assessing the energy losses in the rotor blades, can be taken into account the effect of the periodic incident flow unsteadiness caused by the

presence of traces of the previous nozzle cascade, as amended N_γ. The degree of non-uniformity of the incoming flow is taken over [8].

Additional energy losses are the disc friction and ventilation, extortion, humidity, the presence of the wire bonding and friction in the open and closed axial clearance in accordance with the guidelines [21].

Leak sand leakage losses calculation

It is estimated that losses caused by leakage of the working fluid into the gaps of the flow path, associated with a decrease in the mass flow rate through the crowns, aerodynamic and thermodynamic mixing with the main flow losses, as well as the deviation of the kinematic parameters in the gaps comparing to the design.

To determine the thermodynamic parameters near the flow path margins, needed to calculate the leaks mass flows, a simplified equation of radial equilibrium $\partial P = \frac{\rho c_u^2}{r}\partial r$ is involved. In the gap between vanes considered that $c_u r = \text{const}$, $\rho_1 = \text{const}$, and behind the stage $c_{2u} = \text{const}$, $\rho_2 = \text{const}$.

Leaks in the root area of multistage flow paths are the solution of the mass flow balance equations through diaphragm, root seals and discharge holes taking into account given dependences of the gaps flow factors and friction coefficients of the regime and geometrical parameters, changes in pressure and flow swirling in the disk chambers along the radius at the presence of the working fluid flow etc.

Evaluation of leakages based on a calculation of the anterior chamber only, first, does not allow correct balance the mass flows along the FP, and secondly, may lead to considerable errors as the leakage values and axial forces, particularly at the off-design operation.

The algorithm is developed for the calculation of leakages in multistage FP, in which can be built leaks circuit within the cylinder based on the majority of the factors, influencing them [14]. Calculation of mixing the main flow with leaks through tip and root gaps is based on the balance equations for flow, enthalpy, and entropy. Raising the equations of motion for the evaluation of aerodynamic mixing losses allows, under certain assumptions, take into account the impact on the mixing loss of the blowing working fluid angle.

The third group of losses factors, caused by leaks, mainly, through a change of velocity coefficient of cascades after gaps, where mixing occurs, due to variations of inlet flow angles.

2.2.4 Simulation of Axisymmetric Flow in a Multi-Stage Axial Turbine

To solve this problem, we used a combined one-dimensional and axisymmetric approach.

A mathematical model of a coaxial flow of the working fluid in the flow part of a multi-stage axial turbine

This model belongs to the class of quasi- two-dimensional models, and is a logical continuation of the one-dimensional model of the FP shown in subsection (2.2.3). All equations, methods and techniques of assessment of energy dissipation in the elements of FP used in the one-dimensional model, have been fully utilized in the development of quasi- two-dimensional model of the coaxial FP.

A distinctive feature of the coaxial model is the fact that the system of equations (2.59) are determined not to cross-sections corresponding to the mean radius of the multistage FP crowns, and for each current streams along its midline.

The system of equations (2.59) in a coaxial FP model in a general form as follows:

$$\begin{cases} g_{1(i,\,j)}\left(G, c_{1(i,\,j)}\right)=0; \quad g_{2(i,\,j)}\left(G, c_{1(i,\,j)}, w_{2(i,\,j)}\right)=0; \quad (i=1); \\ g_{1(i,\,j)}\left(G, c_{1(i,\,j)}, w_{2(i-1,\,j)}\right)=0; \quad g_{2(i,\,j)}\left(G, c_{1(i,\,j)}, w_{2(i,\,j)}\right)=0; \quad (i=2); \\ \ldots\ldots\ldots\ldots\ldots\ldots\ldots\ldots\ldots\ldots\ldots\ldots\ldots\ldots\ldots\ldots\ldots\ldots \\ g_{1(n,\,m)}\left(G, c_{1(n,\,m)}, w_{2(n-1,\,m)}\right)=0; \quad (i=n); \\ g_{2(n,\,m)}\left(G, c_{1(n,\,m)}, w_{2(n,\,m)}\right)=0; \quad (i=n); \\ (i=1,\ldots,n); \\ h\left(G, c_{1(n,\,j)}, c_{1(n-1,\,j)}, \ldots, c_{1(1,\,j)}, w_{2(n,\,j)}, w_{2(n-1,\,j)}, \ldots, w_{2(1,\,j)}\right)=0; \\ (j=1,\ldots,m), \end{cases} \tag{2.62}$$

where m – is equal to increased by two the number given sections (streamlines) along the radius of the blades; j – number of cross-section along the blade height (the first cross section is located at the root level).

Accordingly, the dimension of the system of equations in a mathematical model of a coaxial flow in the FP is equal to $(n + 1)m$.

The marked increase in the number of sections required for a significant approaching of the root and near-the-tip stream lines to the root level and the peripheral area, respectively. With the same purpose the cross sectional area of the extreme stream lines assigned minimum values (1% of area of the corresponding vane). For the first iteration the remaining cross-sectional areas between the stream lines are equal and are determined as follows:

$$S_{(k,\,j)}=0.98S_{(k)}(m-2),$$

where $S_{(k)}$ – cross-section area of k-th vane.

After determining the $S_{(k,\,j)}$ are determined the radii of mean lines of all flow streams, angular velocities and the values of all the geometric characteristics of the cascades at those radii. In subsequent iterations, the average radius of the stream lines, and all the characteristics of cascades and the working flow determined in accordance with the obtained distribution of the mass flow the radius of corresponding vanes. This ensures the equality of the working fluid (including the extractions and leakages) along the respective stream lines.

Considering that the system of equations (2.62) is based on the one-dimensional flow theory for each stream line, where there is no equation of radial equilibrium, it becomes apparent that the above-described method of stream tubes sizing, is most accurate by using this model, it will be possible to evaluate the characteristics of the axial turbines, which vane's twist corresponds to the $c_u r = \text{const}$ law, or close to it. For practical tasks coaxial mathematical model is most suitable when assessing the characteristics of the high pressure cylinder (HPC) flow path.

Despite the fact that the flow of working fluid along each stream tube in consideration of coaxial mathematical model of the FP is modeled in accordance with the one-dimensional theory, when calculating the flow kinematics the slope angles of each stream line are taken into account (curvature of the streamlines is not considered) and identifies all components of the flow velocity in axial gaps. To determine the angles of the middle line of the stream tubes cubic spline interpolation is used. A well-known feature of these splines is the coincidence of the first and second derivatives of the neighboring areas in the nodes of the spline coupling. It allows us to describe the midline of a stream line using dependence, which provides its most smooth shape.

Because in the outer iteration loop of the multistage axial turbine FP coaxial mathematical model (as well as in the one-dimensional mathematical model of

the FP), the quantities of moisture separation, tip leakage and near-the-hub leakages and the working fluid extractions to the heating system and feed-water heating refer to the entire stage, and not to each stream tube, the question of adequate distribution of the marked mass flow changes between the stream tubes arise.

In this case, there are two variants of distribution of leaks and the working fluid extractions between the stream tubes:

1) The total change in the mass flow of the working fluid in the transition from one vane to another distributed between streams in proportion to their cross-section areas (1-st iteration).

2) The distribution of mass flow changes in proportion to the stream tube mass flow, the size of which is determined from the condition that the mass flow of each stream tube in accordance with the law of the flow rate changing along the radius of the stage, obtained in the previous iteration.

Additionally, there are also two versions of the distribution of secondary loss of height of the blade:

1) The secondary losses are concentrated at the ends of the blades.

2) The secondary losses are evenly distributed among all streams tubes (proportional to the mass stream tube mass flow).

Integral indicators of each stage in the coaxial model are determined by the relationships below

$$\begin{cases} G_{0(i)} = \sum_{j=1}^{m} g_{0(i,\,j)}; \quad G_{1(i)} = \sum_{j=1}^{m} g_{1(i,\,j)}; \quad G_{2(i)} = \sum_{j=1}^{m} g_{2(i,\,j)}; \\ N_{st(i)} = \sum_{j=1}^{m} N_{str(i,\,j)}; \quad N_{(i)} = \left(\sum_{j=1}^{m} g_{1(i,\,j)} \cdot h_{(i,\,j)} \right) \Big/ G_{1(i)}; \\ \eta_{(i)} = \left(\sum_{j=1}^{m} g_{0(i,\,j)} \cdot \eta_{(i,\,j)} \right) \Big/ G_{0(i)}; \quad Lu_{(i)} = \left(\sum_{j=1}^{m} g_{0(i,\,j)} \cdot lu_{(i,\,j)} \right) \Big/ G_{0(i)}; \\ \Phi^2_{(i)} = \left(\sum_{j=1}^{m} g_{1(i,\,j)} \cdot \phi^2_{(i,\,j)} \right) \Big/ G_{1(i)}; \quad \psi^2_{(i)} = \left(\sum_{j=1}^{m} g_{2(i,\,j)} \cdot \psi^2_{(i,\,j)} \right) \Big/ G_{2(i)}, \end{cases} \tag{2.63}$$

where $g_{0(i,\,j)}, g_{1(i,\,j)}$ and $g_{2(i,\,j)}$ – working fluid mass flows of the *j*-th stream tube entering the *i*-th stage and through its nozzle and working cascade, respectively; $N_{str(i,\,j)}, h_{(i,\,j)}, lu_{(i,\,j)}$ – power, heat drop and disposable work of the *j*-th stream tube of *i*-th stage; $\eta_{(i,\,j)}, \phi^2_{(i,\,j)}, \psi^2_{(i,\,j)}$ – the efficiency, the velocity coefficients squares of the nozzle and working cascades along the *j*-th stream tube of the *i*-th stage. Similarly other integral indicators of the axial turbine FP stages are determined.

A mathematical model of an axisymmetric flow of the real working fluid in a multi-stage axial turbine FP

Despite the fact that the coaxial mathematical model of the flow of the working fluid in the FP, as described in the previous section, has a fairly narrow range of independent use, yet it has a sufficiently high potential. If the formation of the transverse dimensions of the stream tubes to carry the light of the decision of the radial equilibrium equation (sections 2.2.1, 2.2.2), this model can be successfully used in the calculation of axisymmetric flow in a multi-stage axial turbine FP with virtually any kind of its crowns twists.

The use of coaxial FP model to evaluate the distribution of the static pressure behind the rotor blades to determine disposable heat drops of each stage that you

need to solve the axisymmetric problem "with a given back pressure". It is known that only in such a setting is possible to find the correct solution to supersonic stages. Marked problems for each crown of multi-stage flow path solved by the means of stream line curvature method. Thus, in view of (2.46) and the system of equations (2.62), the scheme for solving the problem "with a specified back pressure" for a multi-stage axial flow turbine parts will be as follows:

- Using a coaxial FP model made an initial assessment of the static pressure distribution along the radius of the stages working crowns.
- Relations obtained according to the static pressure of the stages as the boundary conditions are transferred to the axisymmetric simulation unit (sections 2.2.1, 2.2.2).
- As a result of solution of the boundary value problems (2.49) and (2.50), for each stage the distributions of the mass flow of the working fluid along the nozzle and working crowns radii for all FP stages are formed.
- The resulting distributions of the mass flow of the working fluid along the radii of the crowns are used to determine the average of the radii of new stream tubes and areas of cross-sections for the coaxial FP model.
- Calculation of coaxial FP model with the new values of the transverse dimensions of the stream tubes is performed.

For clarity, the above-described sequence of solving axisymmetric problem "with a given back pressure" for multi-stage FP is shown in Fig. 2.13.

Consider some features of the numerical solution of axisymmetric problem for multi-stage FP. First, in dealing with this problem it is necessary to determine the parameters of the working fluid along the streamlines for multi-stage FP with variable from crown to crown mass flow of the working fluid. The marked change often occurs in the steam turbines FP, where the extraction

of the working fluid is carried out between the stages, for example, for the feed water heating or a heat supply needs.

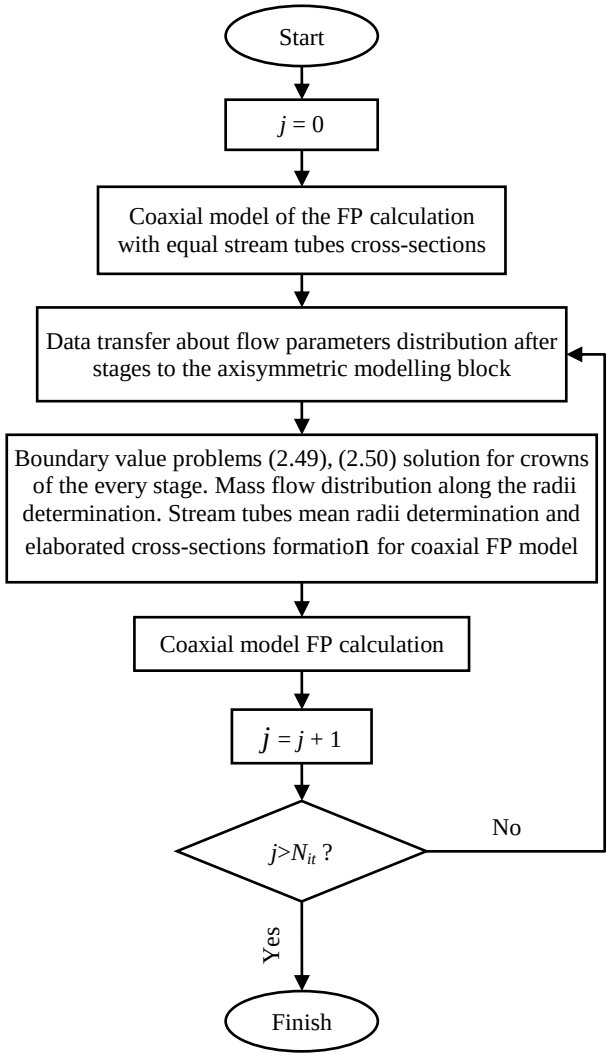

Figure 2.13 *A block diagram of a multistage axial turbine FP axisymmetric problem solving with coaxial models.*

Considering that the equations (2.49) and (2.50), describing axisymmetric flow, valid for one stream line with a constant stream function along it, which value for the single-stage and multi-stage FP without extraction of the working fluid varies from $\Psi = 0$ to $\Psi = G_0 / (2\pi)$, there is a need to adjust the definition of the stream function with the extraction of the working fluid.

In this case, the most appropriate is the idea lies in the fact that the maximum value of the stream function for all crowns drive must be the same. With this in mind, is quite clear the Ψ^* definition

$$\Psi^* = \left(\frac{G_{0(i)}}{2\pi} \right) \Big/ G_{0(i)} = \frac{1}{2\pi}. \tag{2.64}$$

Thus, for the solution of (2.49) and (2.50), the boundary conditions for nozzle and the rotor in this case will be as follows:

$$\begin{cases} r_1(\Psi = 0) = r_{1h}; \quad r_1\left(\Psi = \Psi^* = \dfrac{1}{2\pi}\right) = r_{1t}; \\ r_2(\Psi = 0) = r_{2h}; \quad r_2\left(\Psi = \Psi^* = \dfrac{1}{2\pi}\right) = r_{2t}. \end{cases} \tag{2.65}$$

Numerical integration of the equations (2.49), (2.50) is carried out by the Runge-Kutta third order accuracy method. The algorithm for determining streams tubes mean radii and their cross-sectional areas described below.

Using dependencies $r_1 = r_1(\Psi)$ and $r_2 = r_2(\Psi)$, as result of two-point boundary value problems for nozzle and rotor solutions, define, first of all, the root and tip stream tubes sizes. We assume that the mass flow through the stream tubes will be equal to 1% of the flow through the respective vanes. In this case, the current value of the Ψ function for the mean line of the root stream tube will be equal to

$$\Psi_1 = \Psi^* \cdot 0.005 = \frac{0.005}{2\pi}, \tag{2.66}$$

and for tip stream tube, respectively,

$$\Psi_m = \Psi^* - \Psi_1 = \frac{0.995}{2\pi}. \tag{2.67}$$

Using linear interpolation algorithms on the received values of the stream functions corresponding to the utmost stream tubes mean lines, determine their radii. For other stream tubes the values of the stream functions and the mean line radii will be defined similarly by condition of equal mass flow rates for all stream tubes, which values are determined from the following relationship:

$$g_{(i,\,j)} = 0.98 g_{(i)} (m-2). \tag{2.68}$$

As the result of boundary problems solutions (2.49) and (2.50), the mean radii of stream tubes for all the crowns of multistage FP are transmitted to the coaxial model, where for the new stream tube's cross-sectional areas, angular velocities, and all the geometric characteristics of the nozzle and working blades, the FP calculation is carried out and the new static pressure distribution after working stages crowns is determined.

The FP calculation results using the algorithm corresponding to the coaxial model again transferred to the block of boundary problems solutions (2.49) and (2.50). Described iterative process continues as long as the results of the calculation for both FP calculation algorithms differ less than a prescribed accuracy. Thus, the FP coaxial model and boundary value problems (2.49) and (2.50) complement each other in solving the axisymmetric problem, eliminating the "alignment" on the results of the one-dimensional calculation and more adequately assess the value of disposable heat drop of FP stages.

It should be noted that the numerical implementation of the axisymmetric mathematical model of the working fluid flow in the FP in the form of alternate

use of coaxial mathematical model and boundary problems, can with a high degree of adequacy and accuracy to model the processes in the FP with stages with relatively long blades and having a twisted crowns substantially different from the law $c_u r = \text{const}$. As an example, in Fig. 2.14 are shown the shape of the flow lines resulting from the calculation of LPC FP of powerful steam turbine using the above axisymmetric mathematical model.

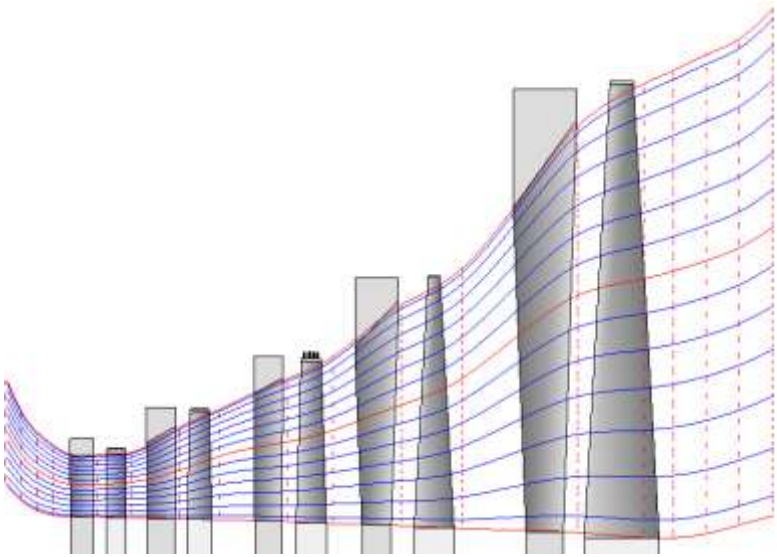

Figure 2.14 *Stream lines of the flow in the powerful steam turbine LPC FP.*

2.2.5 Cascades Flow Calculation

For the design of high efficiency axial flow turbines flow path it is important to have accurate, reliable and fast method for calculation of cascade flow and friction loss on the profile surfaces.

In the calculation of subsonic flows of an ideal liquid in the cascades long used an approach based on the reduction of partial differential equations to Fredholm integral equation of the 1-st or 2-nd kind [8, 22]. Available numerical implementation of solutions to these equations are facing a number of problems

that do not allow a sufficient degree of reliability or accuracy of the calculated arbitrary configuration cascades.

For example, for a long time, we used the method of calculation [22] reduces to the solution of the integral equation of the second kind with respect to the speed potential. It is possible to solve a number of important practical problems of cascade optimization, but had important shortcomings: the complexity of the integral equation kernel normalization, which led to difficulties in calculating thin and strongly curved profiles, as well as the need for numerical differentiation calculated potentials, which brings an additional error in the profile velocity distribution.

Later, we developed a method for cascades potential flow numerical calculating with an approximate view of the ideal gas compressibility based on the solution of the Fredholm equation of the 2-nd kind with respect to speed on the rigid surface, and a program for the PC is designed to work interactively.

Friction loss on the profile is carried out by calculating the compressible laminar, transitional and turbulent boundary layers using one-parameter Loitsiansky method [23]. To improve the accuracy of the results obtained on the basis of the recommendations given in the literature, calculated buckling points and end of the transition from laminar to turbulent boundary layer depending on the pressure gradient, the degree of free-stream turbulence and of profile surface roughness.

The developed algorithms for an ideal fluid flow calculation in the cascade and the boundary layer on the surface of the profile give a good qualitative and quantitative agreement between the calculated and experimental data for different types of cascades at different inlet angles, relative pitch, Mach and Reynolds numbers, characterized by high speed and are therefore suitable for use in problems of optimizing the axial turbomachinery blades shape.

2.2.6 Computational Fluid Dynamics Methods

Aerodynamic optimization of turbine cascades is directed search a large number (hundreds to thousands) variants for their geometry, which increases with the number of variable parameters. The most reliable source of objective data on the flow of gas in a turbine cascade – physical experiment – obviously can not provide a sufficiently deep extreme.

Therefore, currently in the works for aerodynamic optimization it is the most popular approach in which to obtain data on the nature and parameters of the flow of the working fluid in the tested inter-blade channels numerically solve the Navier-Stokes equations, or their modifications [24].

Navier-Stokes equations written in conservative form is as follows:

$$\frac{\partial U}{\partial t}+\frac{\partial F_i}{\partial x_i}+\frac{\partial G_i}{\partial x_i}=B\,, \tag{2.69}$$

where U, F_i, G_i, B – ordered sets of combinations of basic variables

$$U=\begin{bmatrix}\rho\\ \rho V_j\\ \rho E\end{bmatrix};\quad F_i=\begin{bmatrix}\rho v_i\\ \rho v_i v_j+p\delta_{ij}\\ \rho E v_i+p v_i\end{bmatrix};\quad G_i=\begin{bmatrix}0\\ -\tau_{ij}\\ -\tau_{ij}v_j+q_i\end{bmatrix};\quad B=\begin{bmatrix}0\\ \rho F_j\\ \rho F_j v_j\end{bmatrix}.$$

Since the analytical solution of this system of equations associated with insurmountable mathematical difficulties, such a direction as computational fluid dynamics (CFD) arose, which deals with the numerical solution of the Navier-Stokes equations. The numerical solution of the equations of fluid dynamics involves replacing the differential equations of discrete analogs. The main criteria for the quality of the sampling scheme are: stability, convergence, lack of nonphysical oscillations. Computational fluid dynamics is a separate discipline, distinct from theoretical and experimental fluid dynamics and complement them. It has its own methods, its own sphere of applications, and its own difficulties.

Given the speed of modern computers, the most appropriate approach is based on a system of Reynolds-averaged Navier-Stokes (RANS) equations. It involves some additional turbulence modeling using some complimentary to the system (2.69) equations, which are called turbulence model.

The reliability obtained by the CFD results requires a separate analysis. As an example, compare the results of experimental studies of stages with $D/l = 3.6$ (Fig. 2.15–2.17) with the calculations in one-dimensional, axisym-metric (for gaps) and 3*D* CFD statements [19].

Table 2.1 *Main parameters of the test stages.*

Parameter	**Value**	
Stage design	**MI**	**MII**
Inlet pressure, Pa	117000	130000
Inlet temperature, K	373	373
Outlet pressure, Pa	100000	100000
Rotation frequency, 1/s	7311	8212
Nozzle vane mean diameter, m	0.2978	0.2978
Nozzle vane length, m	0.0822	0.0822
Blade mean diameter, m	0.2986	0.2986
Blade length, m	0.0854	0.0854
Nozzle vane outlet gauging angle near hub, deg.	20	17.2
at mean radius, deg.	24	17.5
at peripheral radius, deg.	28	17.8
Blade outlet gauging angle near hub, deg.	32	41
at mean radius, deg.	29.7	26
at peripheral radius, deg.	26	19

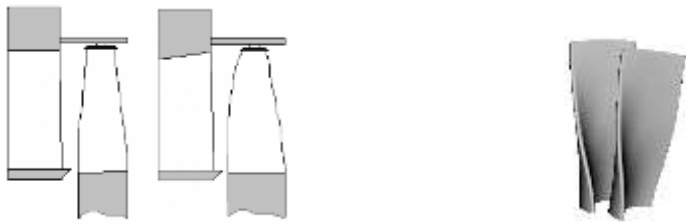

a b

Figure 2.15 *Sketches of MI (left) and MII (right) stage design (a) and stage MI blades (b).*

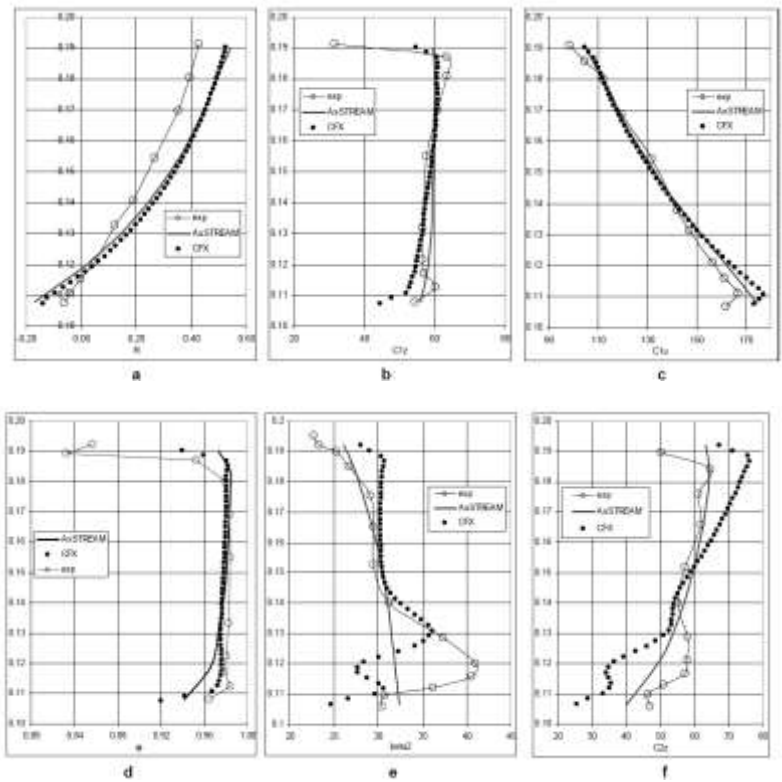

Figure 2.16 *Computation vs experiment (comparison for stage MI).*

Flow parameters distribution along nozzle vane and blade height:

a – reaction; *b* – axial velocity component after nozzle vane;

c – tangential velocity component after nozzle vane; *d* – nozzle vane velocity coefficient; *e* – blade exit flow angle in relative motion; *f* – axial velocity component after blade

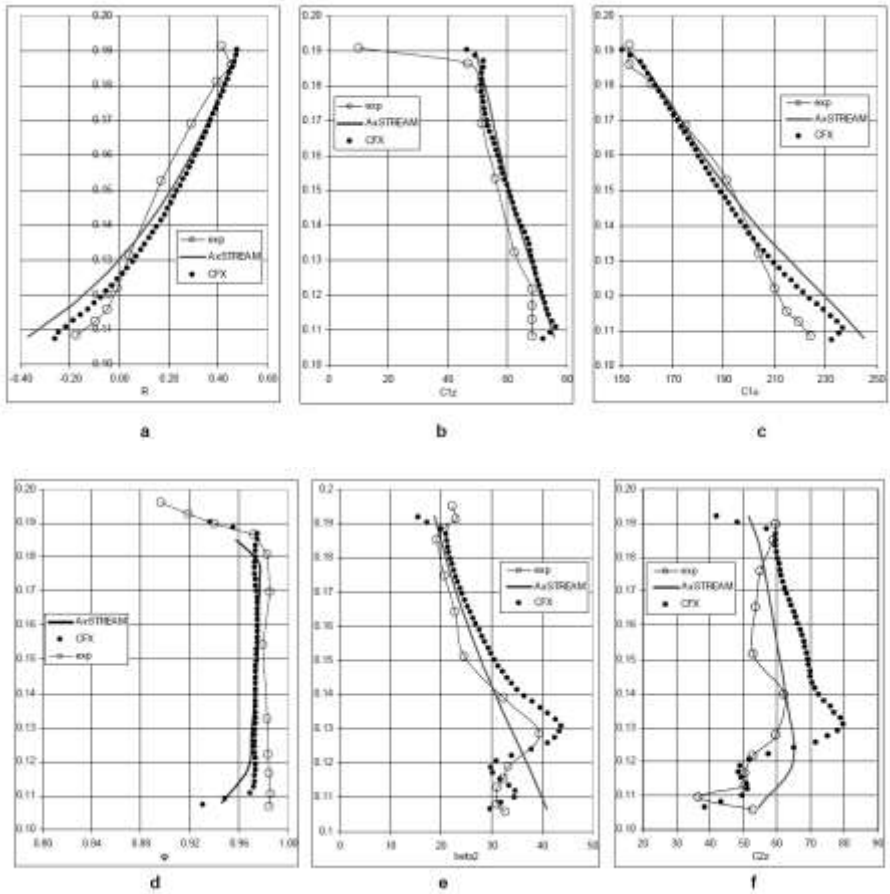

Figure 2.17 *Computation vs experiment (comparison for stage MII).*

Flow parameters distribution along nozzle vane and blade height:

a – reaction; *b* – axial velocity component after nozzle vane;

c – tangential velocity component after nozzle vane; *d* – nozzle vane velocity coefficient; *e* – blade exit flow angle in relative motion;

f – axial velocity component after blade

Table 2.2 *Comparison of stages MI and MII parameters at minimum radial clearance.*

Parameter	Stage MI			Stage MII		
	2*D* AxSTREAM	**3*D* CFX**	**Experiment**	**2*D* AxSTREAM**	**3*D* CFX**	**Experiment**
$(u/C_0)_{opt}$	0.6	0.627	0.62	0.55	0.550	0.55
ξ_s, %	3.5	4.0	2.7	4.9	5.2	3.1
ξ_r, %	2.2	2.1	2.4	2.1	3.0	4.6
ξ_{out}, %	10.8	13.9	11.9	6.8	9.0	7
η_i, %	82.3	80.0	83	84.9	82.8	85.3

It was shown that proper unidimensional and axisymmetric models combined with proven empiric methods of loss calculation provide the accuracy of the turbine flow path computation sufficient for optimization procedures in a bulk of practice valuable cases. Comparative analysis of the experiment and simulation results indicates an untimely nature of the assertion that 3*D* CFD analysis is already capable to substitute physical experiments.

2.3 Geometric and Strength Model

2.3.1 Statistical Evaluation of Geometric Characteristics of the Cascade Profiles

For accurate estimates of the size of the blades, which takes into account not only their aerodynamic properties and conditions of safe operation, it is required to calculate the set of dependent geometric characteristics of the profiles (DGCP) as a function of a number of parameters that determine the shape of the profile. When the shape of the profiles is not yet known, to assess DGCP should use statistical relations. From the literature are known attempts to solve a similar problem [25, 26] on the basis of the regression analysis.

The DGCP include: f – area; I_e and I_n – minimum and maximum moments of inertia; I_u – moment of inertia about an axis passing through the center of gravity of the cross section parallel to the axis of rotation *u*; φ – the angle between the central axis of the minimum moment of inertia and the axis *u*;

X_{gc}, Y_{gc} – the coordinates of the center of gravity; β_i – stagger angle; l_e, l_{ss} – the distance from the outermost points of the edges and suction side to the axis *E*; l_{in}, l_{out} – the distance from the outermost points of the edges to the axis *N*; $W_e, W_{ss}, W_{in}, W_{out}$ – moments of profile resistance.

The listed DGCP values most essentially dependent on the following independent parameters (IGCP) β_{1g} – geometric entry angle; β_{2eff} – effective exit angle; b – chord; t/b – relative pitch; r_1, r_2 – edges radii; ω_1, ω_2 – wedge angles.

Formal macromodelling techniques usage tends to reduce the IGCP number, taking into account only meaningful and independent parameters. In this case, you can exclude from consideration the magnitude of r_1, r_2, ω_2, taking them equal $r_1 = 0.03b$; $r_2 = 0.01b$; $\omega_2 = 0.014K_\omega\omega_1/(0.2+\omega_1)$, $K_\omega = 1...3$, depending on the type of profile [26].

We obtained basic statistical DGCP relationships using profiles class, designed on the basis of geometric quality criteria – a minimum of maximum curvature of high order power polynomials [15] involving the formal macromodelling technique. Approximation relations or formal macromodel (FMM) are obtained in the form of a complete quadratic polynomial of the form (1.2):

$$y(\vec{q}) = A_0 + \sum_{i=1}^{n}(A_i + A_{ii}q_i)q_i + \sum_{i=1}^{n-1}\sum_{j=i+1}^{n} A_{ij}q_iq_j \ .$$

The response function $y(\vec{q})$ values (DGCP) corresponding to the points of a formal macromodelling method, calculated by the mathematical model of cascades profiling using geometric quality criteria.

Analysis of profiles used in turbine building reveals, that two of remaining four IGCP β_{1g} and *t*/*b* highly correlated.

It is advisable to use in place of these factors their counterparts – the flow rotation angle in the cascade θ and the parameter $\Delta t = t/b - T$, where $T = 1.08 - 0.004\theta$ – linear regression equation that specifies the statistical relationship between the relative pitch and angle of rotation of the flow, the resulting data for typical turbine cascade.

Thus, informal macromodelling as IGCP were taken: $\theta, \beta_{2e}, \omega_1, \Delta t$, relatively in ranges 20…120, 10…30, 20…30, –0.2…0.2. In normalized form in the range of –1…1 the factors are calculated as follows:

$$q_1 = \frac{\theta - 70}{50}, \quad q_2 = \frac{\beta_{2e} - 20}{10}, \quad q_3 = \frac{\omega_1 - 25}{5}, \quad q_4 = \frac{\Delta t}{0.2}. \tag{2.70}$$

During macromodelling were designed 25 turbine cascades with $b = 1$ and with IGCP values, corresponding to the points in the of numerical experiment plan, were calculated DGCP values and the dependencies on the form (1.2) built for them. Calculation of flow diagrams and loss factors confirms the high aerodynamic quality of the 25 profile cascades.

In Tables 2.3, 2.4 the FMM coefficients and variance of the cascades DGCP FMM are given. In the tables FMM coefficients increased by 10^4.

Similar relationships were also obtained for a special class of nozzle profiles with an elongated front part [26].

Table 2.3 *DGCP macromodels coefficients.*

A(i, j)	$\ln(F)$	$\ln(I_e)$	$\ln(I_n)$	$\ln(I_u)$	φ	β_i
A(0)	–26530	–87000	–53800	–64034	320	9010
A(1)	4049.2	16769	4241.7	13055	–68.183	–3422.5
A(2)	–45	53.333	37.5	4423.8	–13.683	–1920.8
A(3)	807.5	1200.8	579.17	727.58	–0.5833	–68.333
A(4)	–538.33	–1075	–228.33	–3982.6	83.917	726.67

Table 2.3 *DGCP macromodels coefficients (continuation).*

A(1, 1)	4716.7	6769.2	4024.2	6248.7	–162.02	–1454.6
A(2, 2)	1207.9	2385.4	715.42	1000.2	4.7333	–342.08
A(3, 3)	194.17	711.67	55.418	41.169	–15.867	81.666
A(4, 4)	–204.58	–542.08	–198.33	–1300.1	11.133	186.67
A(1, 2)	562.5	602.5	690	–1472	–120.55	–567.5
A(1, 3)	147.5	–367.5	175	148.5	25.25	–32.5
A(1, 4)	572.5	1412.5	445	1584.8	30.25	–12.5
A(2, 3)	342.5	552.5	180	53	21	–40
A(2, 4)	810	2520	522.5	3917.8	–91.5	–400
A(3, 4)	–7.5	52.5	–2.5	–36.75	–2	12.5

Table 2.4 *DGCP macromodels coefficients (continuation).*

A(i, j)	X_{gc}	Y_{gc}	l_e	I_{ss}	I_{in}	l_{out}
A(0)	2927	5540	1371	882	3726	6090
A(1)	1090.1	–213.75	1093.8	635.14	–63.5	165.75
A(2)	976.42	–657.33	–25.508	–31.008	157.42	–99.667
A(3)	49.417	2.0833	9.2333	47.708	–23.5	26
A(4)	–344.75	237.83	23.558	–32.825	–84.25	61.75
A(1, 1)	433.04	–399.42	324.87	405.3	237.33	–207.75
A(2, 2)	14.292	–135.04	93.692	142.72	–1.2918	–9.8752
A(3, 3)	–30.708	48.583	15.58	19.396	–5.668	9.8748
A(4, 4)	–65.958	34.958	–22.688	–29.929	20.042	18.5
A(1, 2)	–68.75	–500	4.275	51.4	227.5	–241.5
A(1, 3)	19.5	4.75	31.05	29.6	–24.25	19
A(1, 4)	38.5	118	61.825	61.375	–40.25	44.75
A(2, 3)	–5	–10	25.75	22.425	1.5	–3.5
A(2, 4)	192	8.5	79	90.8	35.25	–13.5
A(3, 4)	–6.75	12	5	1.6	5.25	5

2.3.2 Strength Models

On the choice of cascade's optimal gas dynamic parameters significantly affect the strength limitations, which, in turn, is largely dependent on the flow path design.

For example, the calculation of splitted diaphragms strength based on using a simplified scheme, according to which the diaphragm is considered as a semi-circle rod (band with a constant cross-section), loaded with unilateral uniform pressure and supported on the curved outer contour[27]. This approach allows us to evaluate the maximum stress in the diaphragm and is sufficient to assess the strength of the diaphragm at the stage of conceptual and technical design.

Calculation of the blades strength is carried out using the beam theory that restrict computer time to evaluate the tensile and bending stress, for example, using statistical data on profiles, as shown in Section 2.3.1.

To ensure the vibration reliability of blading, rotor blades requires detuning from resonance, i.e., the natural frequencies of the blades should not coincide with the frequency of the disturbing forces that are multiples of the frequency of rotation. The required for detuning dynamic (depending on rotation speed) the first natural frequency of the blade is defined by a simplified formula.

2.4 Flow Path Elements Macromodelling

Macromodels are dependencies of the "black box" type with a reduced number of internal relations. This is most convenient to create such dependence in the form of power polynomials. Obtaining formal macromodels (FMM) as a power polynomial based on the analysis of the results of numerical experiments conducted with the help of the original mathematical models (OMM).

Therefore, the problem of formal macromodelling includes two subtasks:

1. The FMM structure determining.

2. The numerical values of the FMM parameters (polynomial coefficients) finding.

As is known, the accuracy of the polynomial and the region of its adequacy greatly depend on its structure and order. At the same time, obtaining polynomials of high degrees requires analysis of many variants of the investigated flow path elements, which leads to significant computer resources cost and complicates the process of calculating the coefficients of the polynomial.

To create FMM it is advisable to use the mathematical apparatus of the design of experiment theory to significantly reduce the number of computing experiments with OMM, i.e. obtain sufficient information with a minimum dimension of the vector of observations Y'. We use two types of FMM – (1.2) and (1.12). To get them methods of the design of experiment theory applied (three-level Boxing-Benkin plans and saturated Rehtshafner's plans) and cubic spline interpolation.

In a particular implementation of a formal macromodelling methodology need to perform the following steps:

1) the choice of the IMM of the flow path element;

2) the appointment of its performance criteria;

3) choice of OMM parameters, whose influence on performance criteria of the flow path element is necessary to study in detail and the formation on their basis vector of varied parameters $\vec{Q}$;

4) macromodelling area appointment (ranges of components of the vector $\vec{q}$);

5) DOE matrix formation;

6) active numerical experiments conducting and evaluation of the components of observations vector Y' for each criterion;

7) the processing of the experimental results and the determination of the FMM coefficients.

Steps 1–4 are not amenable to formalization and their implementation should take into account the specific features of macromodelling objects and existing experience of designing elements of axial turbines flow path.

2.5 Thermal Cycles Modelling

Imagine the process of analyzing the thermal cycle in the example of gas turbine unit (GTU) (Fig. 2.18) in the following sequence:

- the structure diagram presentation as a set of standard elements and connections between them;
- entering the input data on the elements;
- generation of computer code in the internal programming language based on the chosen problem statement;
- processing;
- post-processing and analysis of results.

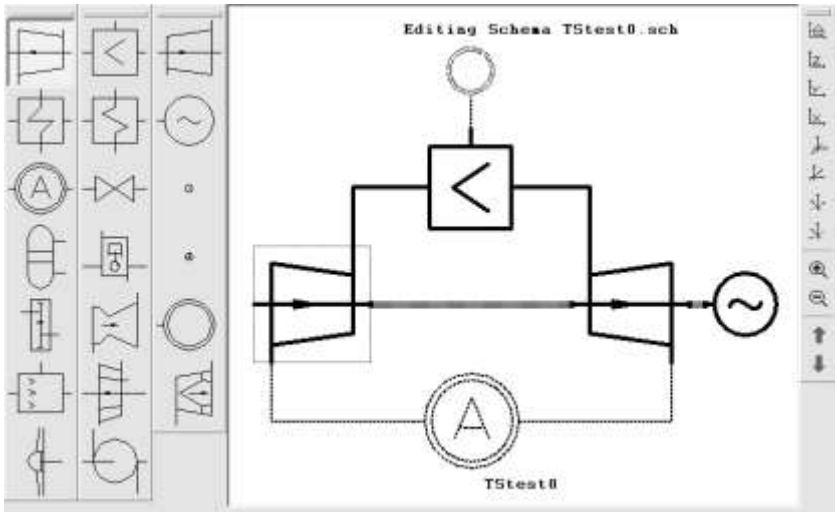

Figure 2.18 *Thermal schemes graphical interactive editor window.*

This sequence of actions combines a high degree of automation of routine operations (input-output and storage of data, programming, presentation of the results of calculations, and so on) with the possibility of human intervention in the process of calculations at any stage (editing of data, changing the program code in the domestic language, writing additional custom code for non-standard calculations performing, etc.).

A key element of the algorithm, allows it to compile a more or less broad class of configurations, is the stage of code generation, based on a graphic description of the scheme (a set of elements and relations between them), i.e., parsing. The problem is that it is pointless to try to solve the problem of the scheme calculation for the arbitrary, sometimes physically implemented schemes. Therefore, the goal of the analyzer is also identification of semantically incorrect scheme descriptions using heuristics embedded in it.

The analyzer's task is to draw up code for solving the system of algebraic equations that describe the problems of cycle analysis in one of the selected language. This system of equations must be linked to energy balances of

different types (for example, flows of working fluids or shafts power) and, therefore, from the graph scheme should provide specific elements chains and use them to make a chain of appropriate formulas. Code generation is based on the information on the scheme chosen by the parser from the internal data structures of elements and connections.

This information includes, in particular, the total number of elements in the cycle, the number of elements of each type, chain elements attached to one shaft, the chain members having regard for air and gas. In addition, there is the total number of connections found and created a list of links with the types and numbers of adjacent elements, as well as the types of energy source. For the efficient operation of the analyzer is required to implement rather complex and flexible dynamic data structure to describe the types and implementation elements, links, as well as types and implementations of data elements and relationships.

Cycle element is an object that is indivisible (in terms of the cycle calculation) for modeling processes of energy conversion and exchange or energy flows. In fact the element is quite complex and multifaceted structure which includes information about the external and the internal representation of its mathematical model, a set of data divided into input and output (and, depending on the type of problem to be solved), a list of associated interface functions etc.

The cycle consists of elements and links between them. Cycle description is stored in a special text file format that contains data by elements, links and service information. Since a sufficiently large number of elements in the scheme, the appointment of links is time-consuming operation, which requires a lot of attention to the formation of the schema file, is desirable to have an interactive graphical schema editor, with which the elements and their relationship just "drawn" on the screen (Fig. 2.18). During the graphical information and elements data input the online preliminary control of the integrity and correctness of the scheme is performed.

Schema data includes collection of data of its elements and links that are relevant to the mathematical modeling of physical processes occurring in the cycle. In connection with this set of data is determined by the requirements of the codes, implementing these models – in our case – a "closed" to the user kernel. External modules available to the user (files of elements and schemes, interpreted code), when changed the set of data of a particular element, should be modified, preferably through means provided by the system or, in extreme cases, manually.

The program of thermal schemes calculation organized in such a way that the graphical user interface and substantive part (solver) would be relatively independent of each other. This makes it possible, on the one hand, to use a solver as a standalone program or as part of other systems, and the other – to connect other solvers to the interface for pre- and post-processing. Therefore solver and interface program have independent data structures.

Solver is a dynamic link library that provides a set of procedures, sufficient for data input and output, as well as organizing the process of setting up and solving the balance equations of thermal cycle. The interpreter has the ability to access these functions, and thus becomes a real calculation procedure described above.

Mathematical modeling of cycles based on predetermined mathematical models of its constituent elements. This approach usually allows to simplify and speed up the calculations. Each of the circuit elements is a more or less complicated object, which can be described with varying degrees of detail.

There are significant differences in the simulation of the elements in the schemes calculation at design and off-design operation modes. In the latter case, the properties of the elements are given as characteristics (maps), i.e. dependency of the output parameters of the regime one. In some cases the characteristics building (especially for the compressors) is a fairly time-consuming task.

3

Determining the Optimal Stages Number of Module and the Heat Drop Distribution

3.1 Analytical Solutions

An important objective in the design of a multi-stage axial turbine is to determine the optimal number of stages in the module and the distribution of heat drop between stages.

Typically, a given quantity is the module's heat drop, and should vary the number of stages and the rotational speed (diameter). It should be understood that the circumferential velocity reduction, and hence the diameters of the stages, reduces the disc friction losses, increase height of the blades (and therefore reduce the proportion of end losses), decrease the flow path leakage. At the same time it leads to an increase in the optimal number of stages, which causes an increase in losses due to discs friction and an additional amount of the turbine rotor elongation. Immediately aggravated questions of reliability and durability (the critical number of revolutions), materials consumption, increase cost of turbine production and power plant construction.

A special place in the problem of the number of stages optimization is the correct assessment of the flow path shape influence, keeping its meridional disclosure in assessing losses in stages. As you know, the issue is most relevant for the powerful steam turbines LPC. It is therefore advisable for the problem of determining the optimal number of stages to be able to fix the form of the flow path for the LPC and at the same time to determine its optimal shape in the HPC and IPC.

It should also be noted that the choice of the degree of reaction at the stages mean radius (the amount of heat drop also associated with it) must be carried out with a view to ensuring a positive value thereof at the root. Formulated in this section methods and algorithms:

- may serve as a basis for further improvement of the mathematical model and complexity of the problem with the accumulation of experience, methods and computer programs used in the algorithm to optimize the flow of the axial turbine;
- allow the analysis of the influence of various factors on the optimal characteristics of the module, which gives reason for their widespread use in teaching purposes, the calculations for the understanding of the processes taking place in stages, to evaluate the impact of the various losses components on a stage operation;
- allow to perform heat drop distribution between stages and to determine the optimal number of stages in a module within the modernization of the turbine, i.e. at fixed rotational speeds (diameters) and a given flow path shape or at the specified law or the axial velocity component change along the cylinder under consideration.

A possible variant of the form setting of *n* stages group of the flow path can be carried out by taking the known axial and circumferential velocity components in all cross-sections, which the numbering will be carried out as shown in Fig. 3.1.

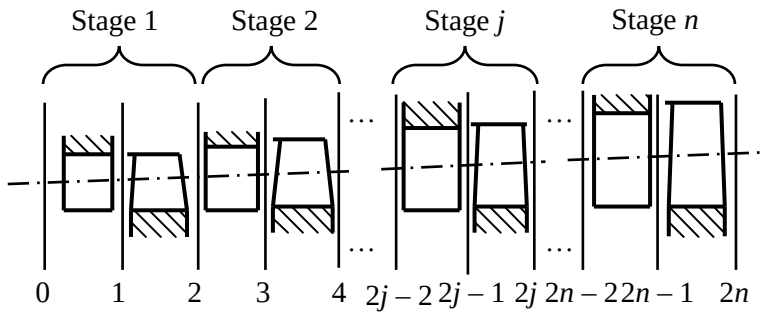

Figure 3.1 *The sections numbering in the turbine flow part section, consisting of n stages.*

The axial velocity components we refer to the axial velocity at the entrance to the stages group:

$$c_{jz} = K_{jz} c_{0z}, \quad \left(j = \overline{1, 2n}\right), \tag{3.1}$$

where K_{jz} – specified values.

The shape of the flow path center line determined by the introduction of coefficient

$$K_{jz} = u_j / u_0, \quad \left(j = \overline{1, 2n}\right), \tag{3.2}$$

By satisfying the conditions (3.1), (3.2) after optimization using the continuity equation $G = c_{0z}\rho_0 F_0 = c_{jz}\rho_i F_j, \quad \left(j = \overline{1, 2n}\right)$ we can determine the shape of the flow path boundaries.

Assuming that we know the initial parameters of the working fluid at the turbine module inlet and the outlet pressure, i.e. theoretical heat drop in the group of *n* stags is known. Thermal process in the group of stages with the help of *hs*-diagram is shown in the Fig. 3.2.

Peripheral efficiency of the stages group determined by the formula

$$\eta_u = \frac{\sum_{j=1}^{n} L_u^{(j)}}{H_0} = \frac{\sum_{j=1}^{n} L_u^{(j)}}{i_0^* - i_{2TT,n}}$$

or taking into account (3.1) and (3.2) in a dimensionless form according to the expression

$$\eta_u = 2\nu_0^2 \bar{c}_{0z} \sum_{j=1}^{n} \left(K_{2j-1,u} K_{2j-1,z} \operatorname{ctg}\alpha_{2j-1} - K_{2j,u} K_{2j,z} \operatorname{ctg}\alpha_{2j} \right), \qquad (3.3)$$

where $\nu_0 = u_0 / C_0$; $C_0^2 = 2H_0$; $\bar{c}_{0z} = c_{0z} / u_0$.

We take into account the loss in the blades by applying velocity coefficients $\phi_j, \psi_j, \left(j = \overline{1,n} \right)$. Also, assume that the output of the intermediate stage a portion of the output energy may be lost. This fact will take into account by introducing a factor by which the output loss is defined as

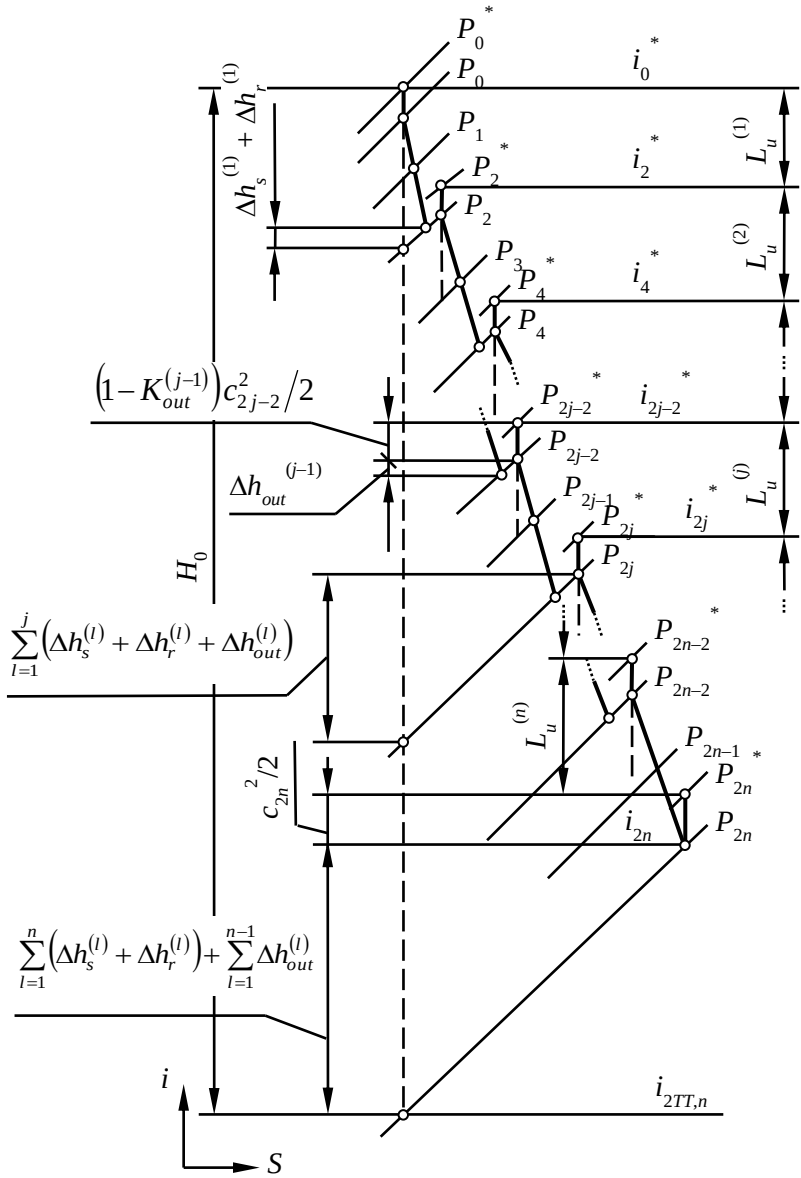

Figure 3.2 *The thermal process in the hs-diagram for the group of n stages.*

by introducing a factor by which the output loss is defined as

$$\Delta h_{out}^{(j)} = K_{out}^{(j)} \frac{c_{2j}^2}{2}, \quad \left(0 \le K_{out}^{(j)} \le 1; \quad j = \overline{1,n}\right), \tag{3.4}$$

Calculating losses in the guide vane and the rotor by formulas

$$\Delta h_s^{(j)} = \frac{1-\phi_j^2}{\phi_j^2} \frac{c_{2j-1}^2}{2}, \quad \Delta h_r^{(j)} = \frac{1-\psi_j^2}{\psi_j^2} \frac{w_{2j}^2}{2}, \quad \left(j = \overline{1,n}\right)$$

taking into account the factor of heat recovery α_n, the limit for the heat drop in the group of *n* stages can be written as:

$$A_3 = \left(1+\alpha_n\right) H_0 - \sum_{j=1}^{n} L_u^{(j)} - \sum_{j=1}^{n} \left(\Delta h_s^{(j)} + \Delta h_r^{(j)}\right) - \sum_{j=1}^{n-1} \Delta h_{out}^{(j)} - \frac{c_{2n}^2}{2} = 0. \tag{3.5}$$

Dividing equation (3.5) by u_0^2, taking into account (3.1), (3.2), as well as well-known kinematic correlations between velocity and flow angles after obvious transformations we obtain an expression for the limitation A_3 in the dimensionless form:

$$\begin{aligned} A_3 = {} & 2\bar{c}_{0z} \sum_{j=1}^{n} \left(K_{2j-1,u} K_{2j-1,z} \operatorname{ctg} \alpha_{2j-1} - K_{2j,u} K_{2j,z} \operatorname{ctg} \alpha_{2j}\right) + \\ & + \sum_{j=1}^{n} \left\{ \frac{1-\phi_j^2}{\phi_j^2} K_{2j-1,z}^2 \bar{c}_{0z}^2 \left(1+\operatorname{ctg}^2 \alpha_{2j-1}\right) + \frac{1-\psi_j^2}{\psi_j^2} \left[K_{2j,z}^2 \bar{c}_{0z}^2 \left(1+\operatorname{ctg}^2 \alpha_{2j}\right) - \right.\right. \\ & \left.\left. - 2K_{2j,u} K_{2j,z} \bar{c}_{0z} \operatorname{ctg} \alpha_{2j} + K_{2j,u}^2 \right] \right\} + \sum_{j=1}^{n-1} K_{out}^{(j)} K_{2j,z}^2 \bar{c}_{0z}^2 \left(1+\operatorname{ctg}^2 \alpha_{2j}\right) + \\ & + K_{2n,z}^2 \bar{c}_{oz}^2 \left(1+\operatorname{ctg}^2 \alpha_{2n}\right) - \frac{\left(1+\alpha_n\right)}{\nu_0^2} = 0. \end{aligned} \tag{3.6}$$

The task of definition of the angles α_j so that, given the parameters $\nu_0, \bar{c}_{0z}, K_{ju}, K_{jz}, \left(j = \overline{1,2n}\right)$ and taken on the basis of some considerations (or defined by one of the possible methods), the quantities of velocity coefficients

$\phi_j, \psi_j, K_{out}^{(j)}, \left(j = \overline{1, n}\right)$ reaches its objective function (3.3) maximum and satisfies the constraint (3.6).

Mathematically the formulated problem reduces to finding:

$$\max_{\text{ctg}\,\alpha_j} \eta_u = \frac{\sum_{j=1}^{n} L_u^{(j)}}{H_0}, \quad \left(j = \overline{1, 2n}\right)$$

under the constraint (3.6).

Using the penalty functions method, you can reduce the problem of finding the extremum in the presence of constraints to the problem without limitation for the attached objective function

$$I^* = \eta_u - \Lambda A_3^2, \tag{3.7}$$

where Λ – penalty coefficient.

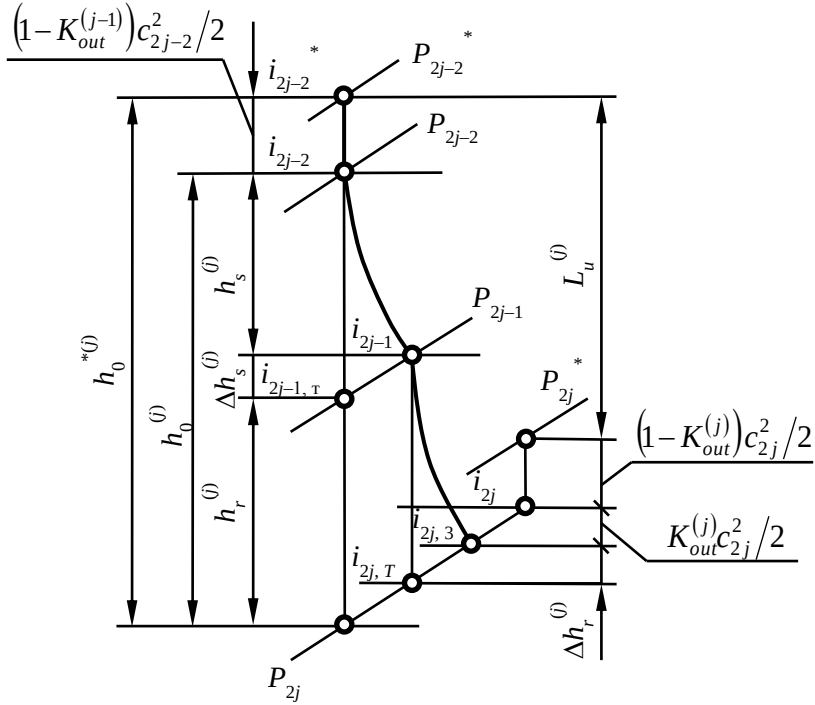

Figure 3.3 *The thermal process in hs-diagram for an intermediate j-th stage.*

Given the values of the velocity coefficients ϕ_j, ψ_j along the module, solution of the problem is simplified due to the possibility of its decision by indefinite Lagrange multipliers method. Differentiating the Lagrange function by variables $\operatorname{ctg}\alpha_j, \left(j=\overline{1,2n}\right)$

$$\tilde{L}=\eta_u+\Lambda A_3, \tag{3.8}$$

where Λ – Lagrange multiplier, we find the following necessary optimality conditions

$$\frac{1}{\Lambda}=-\frac{1}{v_0^2}\left(1+\frac{1-\phi_j^2}{\phi_j^2}\frac{K_{2j-1,\,z}}{K_{2j-1,\,u}}\bar{c}_{0z}\operatorname{ctg}\alpha_{2j-1}\right),\quad \left(j=\overline{1,n}\right); \tag{3.9}$$

$$\frac{1}{\Lambda}=-\frac{1}{\nu_0^2}\left(\frac{1}{\psi_j^2}-\left(\frac{1-\psi_j^2}{\psi_j^2}+K_{out}^{(j)}\right)\frac{K_{2j,z}}{K_{2j,u}}\bar{c}_{0z}\operatorname{ctg}\alpha_{2j}\right),\quad \left(j=\overline{1,n-1}\right);\tag{3.10}$$

$$\frac{1}{\Lambda}=-\frac{1}{\nu_0^2\psi_n^2}\left(1-\frac{K_{2n,z}}{K_{2n,u}}\bar{c}_{0z}\operatorname{ctg}\alpha_{2n}\right).\tag{3.11}$$

Expressing all $\operatorname{ctg}\alpha_j\ (j\neq 2n)$ through $\operatorname{ctg}\alpha_{2n}$, and excluding Λ according to the third formula, we get:

$$\operatorname{ctg}\alpha_{2j-1}=\frac{1}{\mu_j}\frac{K_{2j-1,u}}{K_{2j-1,z}}\left(\frac{1-\psi_n^2}{\bar{c}_{0z}}-\frac{K_{2n,z}}{K_{2n,u}}\operatorname{ctg}\alpha_{2n}\right),\quad \left(j=\overline{1,n}\right);\tag{3.12}$$

$$\operatorname{ctg}\alpha_{2j}=\frac{1}{\chi_j+\psi_n^2K_{out}^{(j)}}\frac{K_{2j,u}}{K_{2j,z}}\left(\frac{\psi_n^2-\psi_j^2}{\psi_j^2\bar{c}_{0z}}+\frac{K_{2n,z}}{K_{2n,u}}\operatorname{ctg}\alpha_{2n}\right),\quad \left(j=\overline{1,n-1}\right),$$

Where $\mu_j=\psi_n^2\dfrac{1-\phi_j^2}{\phi_j^2}$; $\chi_j=\psi_n^2\dfrac{1-\psi_j^2}{\psi_j^2}$.

Substituting found in this manner $\operatorname{ctg}\alpha_{2j-1}$ and $\operatorname{ctg}\alpha_{2j}$ in the equation (3.6), we get the quadratic equation in the parameter $\operatorname{ctg}\alpha_{2n}^{opt}$

$$D\operatorname{ctg}^2\alpha_{2n}^{opt}+E\operatorname{ctg}\alpha_{2n}^{opt}+F=0,\tag{3.13}$$

where

$$D=\frac{K_{2n,z}^2}{K_{2n,u}}\frac{\bar{c}_{oz}^2}{\psi_n^2}\left(\sum_{j=1}^{n}\frac{K_{2j-1,u}^2}{\mu_j}+\sum_{j=1}^{n-1}\frac{K_{2j,u}^2}{\chi_j+\psi_n^2K_{out}^{(j)}}+K_{2n,u}^2\right);$$

$$E=-2\frac{K_{2n,z}}{K_{2n,u}}\frac{\bar{c}_{oz}}{\psi_n^2}\left(\sum_{j=1}^{n}\frac{K_{2j-1,u}^2}{\mu_j}+\sum_{j=1}^{n-1}\frac{K_{2j,u}^2}{\chi_j+\psi_n^2K_{out}^{(j)}}-K_{2n,u}^2\right);$$

$$F=\frac{c_{0z}^2}{\psi_n^2}\left[\sum_{j=1}^{n}\mu_j K_{2j-1,z}^2+\sum_{j=1}^{n-1}K_{2j,z}^2\left(\chi_j+\psi_n^2K_{out}^{(j)}\right)+K_{2n,z}^2\right]+$$
$$+\sum_{j=1}^{n}\frac{1}{\mu_j}\left(\frac{1}{\psi_n^2}-\psi_n^2\right)K_{2j-1,u}^2-\sum_{j=1}^{n-1}\frac{K_{2j,u}^2}{\chi_j+\psi_n^2K_{out}^{(j)}}\left(\frac{\psi_n^2}{\psi_j^4}-\frac{1}{\psi_n^2}\right)+$$
$$+\sum_{j=1}^{n}K_{2j,u}^2\frac{1-\psi_j^2}{\psi_j^2}-\frac{1+\alpha_n}{\nu_0^2}.$$

Using the solution of this equation, then define all the optimal angles $\operatorname{ctg}\alpha_j^{opt}\left(j=\overline{1,2n-1}\right)$ with (3.12), as well as optimal efficiency as a function of the set parameters with the help of (3.3).

Consider the important special case when $K_{j,u}=K_{j,z}=1$; $K_{out}^{(j)}=K_{out};\left(j=\overline{1,n-1}\right)$; $\phi_j=\phi,\psi_j=\psi,\left(j=\overline{1,n}\right)$. In this case, the formula (3.12) will have the form

$$\left.\begin{aligned}\operatorname{ctg}\alpha_{2j-1}&=\frac{1-\psi^2}{\mu\bar{c}_{0z}}-\frac{1}{\mu}\operatorname{ctg}\alpha_{2n},\quad\left(j=\overline{1,n}\right);\\ \operatorname{ctg}\alpha_{2j}&=\frac{\operatorname{ctg}\alpha_{2n}}{1-\psi^2\left(1-K_{out}\right)},\quad\left(j=\overline{1,n-1}\right),\end{aligned}\right\}\tag{3.14}$$

Where $\mu=\psi^2\frac{1-\phi^2}{\phi^2}$.

After the substitution of (3.14) into (3.6) we have a quadratic equation of the form (3.15) with the following values of the coefficients:

$$D=\frac{\bar{c}_{0z}^2}{\psi^2}\left[\frac{n}{\mu}+\frac{n-1}{1-\psi^2\left(1-K_{out}\right)}+1\right];$$

$$E=-2\frac{\bar{c}_{0z}}{\psi^2}\left[\frac{n}{\mu}+\frac{n-1}{1-\psi^2\left(1-K_{out}\right)}+1\right];$$

$$F=\frac{\bar{c}_{0z}}{\psi^2}\left\{1+n\mu+(n-1)\left[1-\psi^2\left(1-K_{out}\right)\right]\right\}+\frac{n}{\psi^2}\left[\frac{1-\psi^4}{\mu}+\left(1-\psi^2\right)\right]-\frac{1+\alpha_n}{\nu_0^2},$$

of which there is an optimal value $\operatorname{ctg}\alpha_{2n}$, then $\operatorname{ctg}\alpha_j\ \left(j=\overline{1,2n-1}\right)$ and from (3.13) the optimal efficiency

$$\eta_u=2\nu_0^2 n\left\{\frac{1-\psi^2}{\mu}-\bar{c}_{0z}\operatorname{ctg}\alpha_{2n}\left[\frac{1}{\mu}+\frac{n-\psi^2\left(1-K_{out}\right)}{n\left[1-\psi^2\left(1-K_{out}\right)\right]}\right]\right\}, \qquad (3.15)$$

optimal velocity ratios of the stages

$$\nu_j=\frac{u_j}{c_{0j}}=\left[2\bar{c}_{0z}\operatorname{ctg}\alpha_{2j-1}+\frac{1-\phi^2}{\phi^2}\bar{c}_{0z}^2\left(1+\operatorname{ctg}^2\alpha_{2j-1}\right)+\right.$$

$$\left.+\frac{\bar{c}_{0z}^2}{\psi^2}\left(1+\operatorname{ctg}^2\alpha_{2j}\right)-\frac{2\bar{c}_{0z}}{\psi^2}\operatorname{ctg}\alpha_{2j}+\frac{1-\psi^2}{\psi^2}\right]^{\frac{1}{2}}, \qquad (3.16)$$

optimal reactions

$$R=\frac{\phi^2-\bar{c}_{0z}^2\left(1+\operatorname{ctg}^2\alpha_{2j-1}\right)\nu_j^2}{\phi^2\left[1-\bar{c}_{0z}^2\left(1+\operatorname{ctg}^2\alpha_{2j-2}\right)\left(1-K_{out}\right)\nu_j\right]}. \qquad (3.17)$$

If adopted above conditions, we see that all the stages except the last, are the same. The final stage is different from all that is connected with the need to reduce the exit velocity loss that is completely lost at this stage $\left(K_{out}^{(n)}=1\right)$.

Using formulas (3.14)–(3.17) for values $\phi^2=0.96$, $\psi^2=0.9$ over a wide range $\bar{c}_{0z}$ from 0.2 to 1.0 and K_{out} from 0 to 1 the calculations were carried out, the results of which at values $\bar{c}_{0z}=0.4$ and $K_{out}=0.1$ are shown in Fig. 3.4.

Calculations have shown that for each value $\nu_0 = u/C_0$, i.e. heat drop for a given amount H_0 at a fixed circumferential speed *u*, an optimum number of stages exists at which the maximum efficiency of the module is reached.

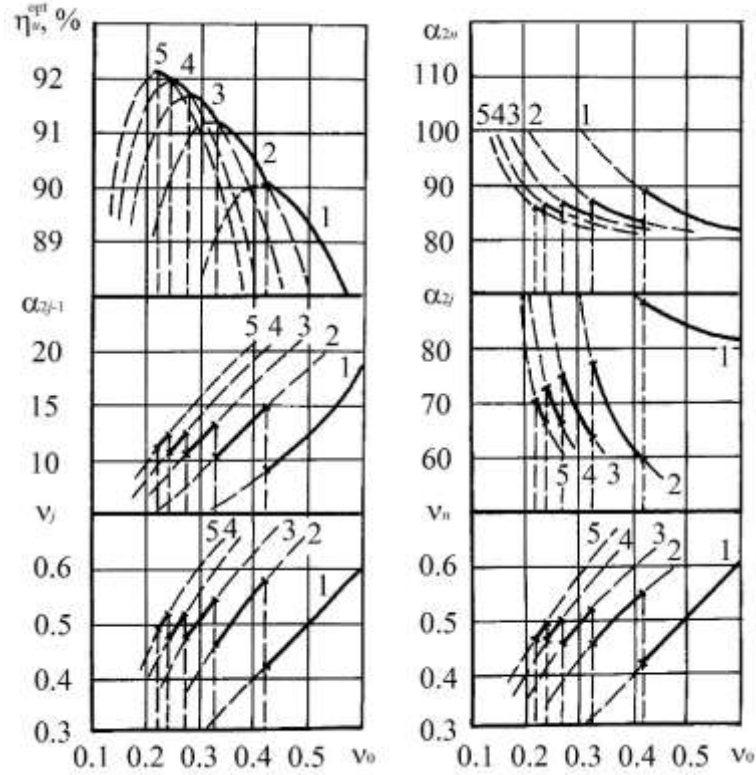

Figure 3.4 *The calculated optimal exit flow angles α, velocity ratios ν of intermediate and last stages, module efficiency η for different values of the heat drops* ($\bar{c}_{0z} = 0.4$, $\phi^2 = 0.96$, $\psi^2 = 0.9$, $K_{out} = 0.1$; $\left(j = \overline{1, n-1}\right)$). *The numbers on the curves indicate the number of stages in the module. The bold line shows the envelope of the parameters, corresponding to the maximum efficiency.*

Assuming full utilization of the output velocity of the intermediate stages $\left(K_{out} = 0\right)$ the rotor exit angles of the intermediate stages α_{2j} $\left(j \neq n\right)$ can be very different from 90°.

The last stage flow exit angle α_{2n} in accordance with the calculation results must be done close to 90°, which corresponds with a minimum loss of output velocity. Angles downstream of the guide vanes lie in the range 10...17°, the optimum value of the velocity ratio in the range of 0.48...0.58. With increasing of number of stages in the module the range of acceptable changes of these values is narrowed.

In the case of output velocity loss in the intermediate stages $\left(K_{out} > 0\right)$ the picture somewhat changes. Increases the value of the heat drop, in which it is advisable to go to a larger number of stages, angles downstream of the intermediate stages α_{2j} are also close to 90°. There is a decrease in the velocity ratio values ν_j, the exit flow angles of the guide vanes α_{2j-1}, resulting in a slight drop in the optimum degree of reaction for the intermediate and for the last stages.

In the case of a *single stage*, assuming n = 1 peripheral stage efficiency is given by

$$\eta_u = \frac{L_u}{h_0} = \frac{u_1 c_{1u} - u_2 c_{2u}}{i_0^* - i_{2TT}}.$$

From (3.3) we obtain in the dimensionless form

$$\eta_u = 2\nu_{0z}^2 \bar{c}_{0z} \left(K_{1u} K_{1z} \operatorname{ctg} \alpha_1 - K_{2u} K_{2z} \operatorname{ctg} \alpha_2\right). \tag{3.18}$$

For restrictions $\vec{A}_1$, $\vec{A}_2$ and $\vec{A}_3$ from equations (3.13), (3.6) is written (see notation on Fig. 3.1):

$$\left.\begin{aligned} A_1 &= i_0^* - i_1 - c_1^2/2 = 0; \\ A_2 &= i_0^* - i_2 - L_u - c_2^2/2 = 0; \\ A_3 &= i_0^* - i_{2TT} - L_u - \Delta h_s - \Delta h_r - c_2^2/2 = 0. \end{aligned}\right\}. \tag{3.19}$$

Drawing on the kinematic relations between velocities and flow angles, using the velocity triangles have

$$A_1 = 1 - \frac{i_1}{i_0^*} - \frac{k-1}{k+1}\lambda_0^2 K_{1z}^2 \frac{1+\mathrm{ctg}^2\alpha_1}{1+\mathrm{ctg}^2\alpha_0} = 0. \tag{3.20}$$

$$A_2 = 1 - \frac{i_2}{i_0^*} - \frac{k-1}{k+1}\lambda_0^2 K_{2z}^2 \frac{1+\mathrm{ctg}^2\alpha_2}{1+\mathrm{ctg}^2\alpha_0} -$$
$$-2\frac{k-1}{k+1}\frac{\lambda_0^2}{\bar{c}_{oz}\left(1+\mathrm{ctg}^2\alpha_0\right)}\left(K_{1u}K_{1z}\,\mathrm{ctg}\,\alpha_1 - K_{2u}K_{2z}\,\mathrm{ctg}\,\alpha_2\right) = 0. \tag{3.21}$$

$$A_3 = 2K_{1u}K_{1z}\bar{c}_{0z}\,\mathrm{ctg}\,\alpha_1 - 2\frac{K_{2u}K_{2z}}{\psi^2}\bar{c}_{0z}\,\mathrm{ctg}\,\alpha_2 +$$
$$+\frac{1-\phi^2}{\phi^2}\bar{c}_{0z}^2 K_{1Z}^2\left(1+\mathrm{ctg}^2\alpha_1\right) + \frac{K_{2Z}^2}{\psi^2}\bar{c}_{0z}^2\left(1+\mathrm{ctg}^2\alpha_2\right) +$$
$$+\frac{1-\psi^2}{\psi^2}K_{2u}^2 - \frac{1}{\nu_0^2} = 0. \tag{3.22}$$

Here for convenience introduced a dimensionless ratio

$$\lambda_0 = \frac{C_0}{a_*}, \tag{3.23}$$

where C_0 – stage inlet velocity defined by c_{0z} and α_0; $a_* = \sqrt{2\frac{k-1}{k+1}i_0^*}$ – velocity, equivalent to the critical value, for the ideal working fluid.

In the case of a perfect gas λ_0 is a reduced velocity at the stage inlet.

The stage optimization problem is solved using conjugate gradient method by maximizing the attached objective function $I^* = \eta_u - \Lambda A_3^2$, where Λ – penalty coefficient.

In the case of fixed velocity ratios φ and ψ from (3.12) we obtain the relationship between α_1^{opt} and α_2^{opt} analytically

$$\operatorname{ctg}\alpha_1^{opt}=\frac{1}{\mu}\frac{K_{1u}}{K_{1z}}\left(\frac{1-\psi^2}{\bar{c}_{0z}}-\frac{K_{2z}}{K_{2u}}\operatorname{ctg}\alpha_2^{opt}\right), \tag{3.24}$$

where denoted $\mu=\psi^2\dfrac{1-\phi^2}{\phi^2}$.

To determine the $\operatorname{ctg}\alpha_2^{opt}$ is needed to use the quadratic equation (3.13), which coefficients in the case of single stage are given by:

$$D=\frac{\bar{c}_{0z}^2K_{2z}^2}{\psi^2}\left(1+\frac{1}{\mu}\frac{K_{1u}^2}{K_{2u}^2}\right);$$

$$E=-\frac{2K_{2u}K_{2z}\bar{c}_{0z}}{\psi^2}\left(1+\frac{1}{\mu}\frac{K_{1u}^2}{K_{2u}^2}\right);$$

$$F=\frac{1-\psi^4}{\psi^2}\frac{K_{1u}^2}{\mu}+\frac{\bar{c}_{0z}^2K_{2z}^2}{\psi^2}\left(1+\mu\frac{K_{1z}^2}{K_{2z}^2}\right)+\frac{1-\psi^2}{\psi^2}K_{2u}^2-\frac{1}{\nu_0^2}.$$

The reaction degree *R* of single stage is given by:

$$R=\frac{h_0-\frac{1}{2}\left(\frac{c_1}{\phi}\right)^2}{h_0-\frac{C_0^2}{2}}=\frac{1-\frac{K_{1z}}{\phi^2}\bar{c}_{0z}^2\nu_0^2\left(1+\operatorname{ctg}^2\alpha_1\right)}{1-\bar{c}_{0z}^2\nu_0^2\left(1+\operatorname{ctg}^2\alpha_0\right)}. \tag{3.25}$$

In the case where φ and ψ are functions of flow parameters, for a single stage the solution of the problem of determining the optimal parameters can be simplified by using the method of successive approximations:

1. Set the initial approximation φ, ψ and define the parameters for the stage using derived formulas.

2. The velocity coefficients are recalculated according to the obtained parameters and calculations are renewed from the item 1.

Calculations have shown that this process converges with high accuracy in a few iterations.

To investigate the influence of dimensionless parameters on the optimum stage performance computational study was conducted under various assumptions about the loss in the stage. The velocity coefficients were taken into account as a constant or dependent of the flow parameters. In the latter case, their determination was made using simplified dependency [28] with a bit increased losses on the rotor blades:

$$\left.\begin{aligned}\phi^2 &= 1-0.025\left[1+\left(\frac{\varepsilon_\alpha}{90}\right)^2\right];\\ \psi^2 &= 1-0.040\left[1+\left(\frac{\varepsilon_\beta}{90}\right)^2\right].\end{aligned}\right\}. \tag{3.26}$$

The increase in losses on the rotor blades in the presence of negative degree of reaction produced artificially by the formula

$$\psi^2 = \begin{cases}\psi^2, \text{ determined using (3.26), if } w_1 \le w_2;\\ \dfrac{\psi^2}{\psi^2 + \dfrac{w_1^2}{w_2^2}\left(1-\psi^2\right)}, \text{if } w_1 > w_2.\end{cases} \tag{3.27}$$

The most complete calculations are made for the important special case when $K_{jz} = K_{ju} = 1 \quad (j = 1, 2)$.

Computational study has allowed to determine the optimal parametric dependencies of efficiency, angles α_1 and α_2, reaction R, velocity coefficients

φ, ψ and loss factors ξ_s, ξ_r, ξ_{out} on $\bar{c}_{0z}$ and ν_0. The calculation results are shown in Fig. 3.5–3.7.

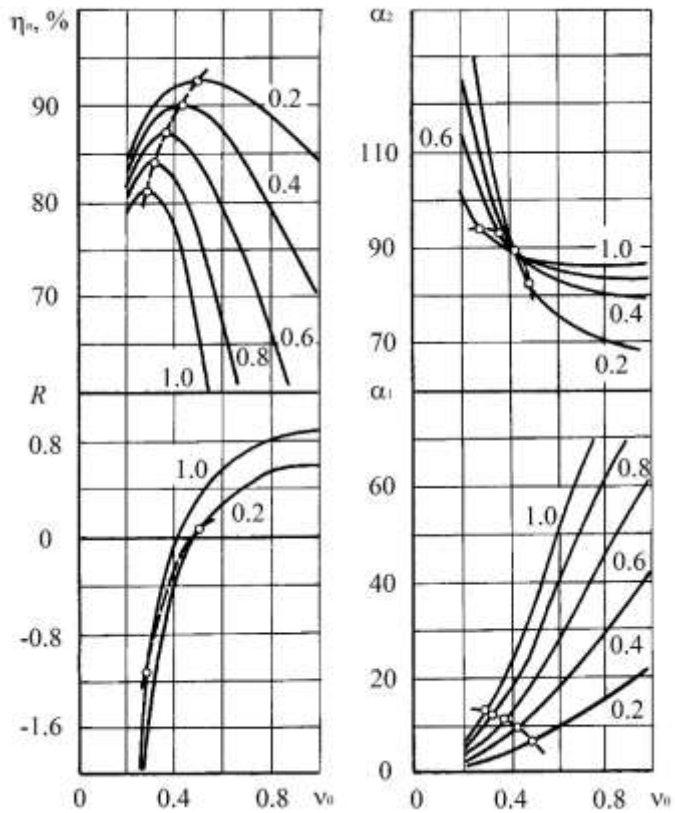

Figure 3.5 *Optimal characteristics of the turbine stage ($\phi^2 = 0.96$, $\psi^2 = 0.9$). The numbers refer to $\bar{c}_{0z}$ values. Circles mark the optimal parameters at optimal heat drop in the stage.*

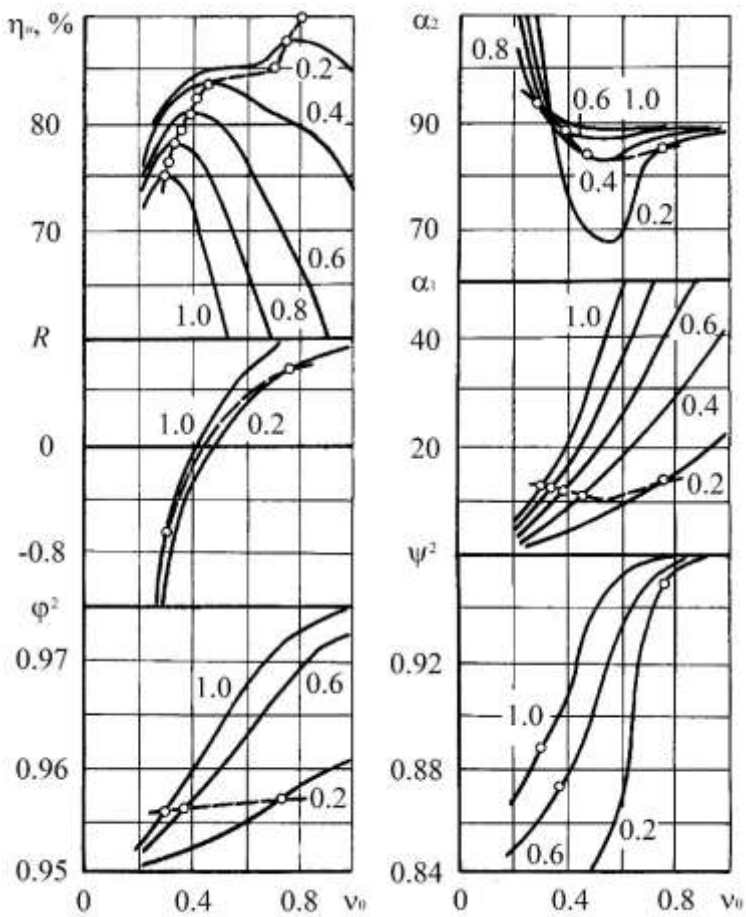

Figure 3.6 *Optimal characteristics of the turbine stage with velocity ratio, calculated by the formula (3.26). The numbers refer to* $\bar{c}_{0z}$ *values. Circles mark the optimal parameters at optimal heat drop in the stage.*

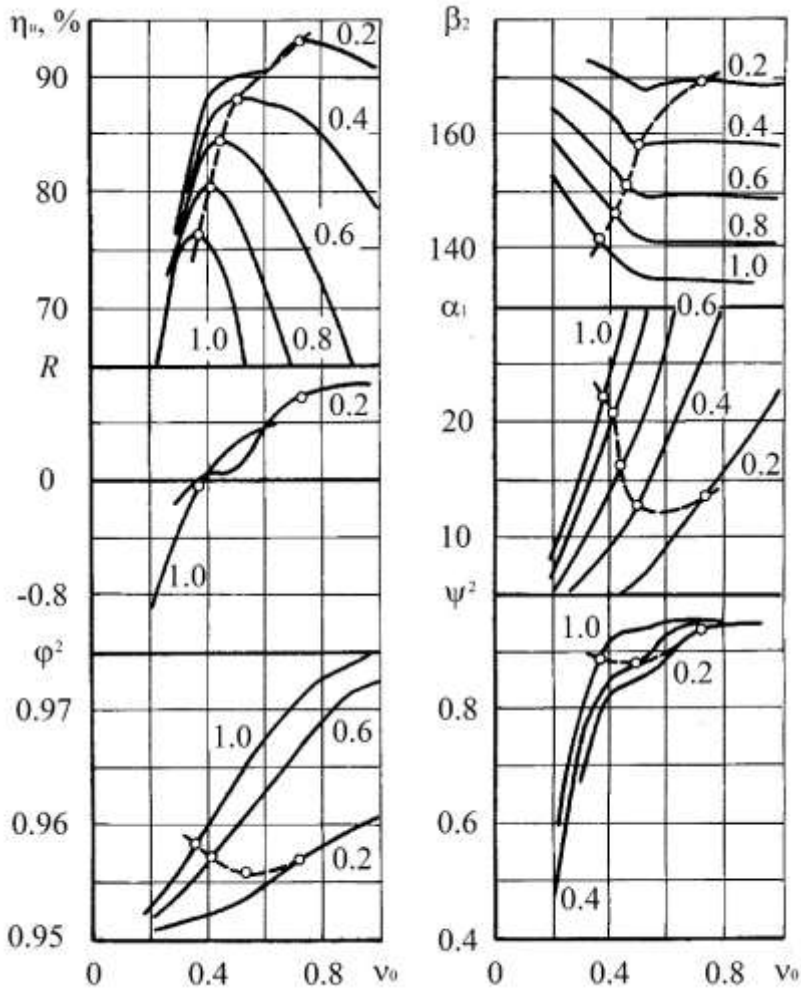

Figure 3.7 *Optimal characteristics of the turbine stage (φ, ψ calculated by the formula (3.26)) with ψ recalculated according to (3.27). The numbers refer to* $\bar{c}_{0z}$ *values. Circles mark the optimal parameters at optimal heat drop in the stage.*

3.2 Preliminary Design of the Multistage Axial Flow Turbine Method Description

In the early stages of the flow path (FP) design of the turbine, when determined the diameter, the blade heights, heat drops and other main

characteristics of the stages, required to study alternatives with a view to the design solution, in the best sense of a quality criterion.

Most effectively, this problem is solved within the created turbine flow path CAD systems, because manage: to achieve a rational division of the designer, defining the strategy and computer, quickly and accurately perform complex calculations and presents the results in human readable numeric or graphical form; to take into account many different factors influencing the efficiency, reliability, manufacturability, cost and other indicators of the quality of the design being created; organize dialogue or fully automatic determination of optimal parameters, etc [29].

Most methods of the multi-stage turbine parameters optimization is designed to select the number of gas-dynamic and geometric parameters on the basis of the known prototype, the characteristics of which are taken as the initial approximation.

When using complex mathematical models, a large number of variables and constraints, the solution of such problems requires considerable computer time and for the purposes of CAD that require quick response of the system is often unacceptable.

It is desirable to have a method of design that combines simplicity, reliability and speed of obtaining results with an accuracy of the mathematical model, a large number of factors taken into account and optimized, the depth of finding the optimal variant. This inevitably certain assumptions, the most important of which are: the synthesis parameters of "good", competitive structure without attracting accurate calculation models; in-depth analysis and refinement of the parameters are not taken into account at the first stage; optimization of the basic parameters by repeatedly performing the steps of the synthesis and analysis.

Design of the FP in such a formulation will be called preliminary (PD). PD does not claim to such a detailed optimization of parameters, as in the above-mentioned methods of optimal design. Its goal – to offer a workable, effective enough design, the characteristics of which, if necessary, can be selected as the initial approximation for more accurate calculations.

Major challenges in creating a PD method are:

- a rational approach to the problem of the preliminary design, the selection of the quality criteria and the constraints system;
- development of a method for the multi-stage flow path basic parameters selection;
- formation of requirements for a mathematical models complex describing different aspects of turbines and their efficient numerical implementation;
- selection of the appropriate algorithm for finding the optimal solution;
- a flexible software creation for a dialog based solution of the design problems in various statements and visual representation of the results.

It is assumed that FP PD will be conducted immediately after the calculation of the turbine thermal cycle under known for each of the cylinders steam parameters i_0^*, P_0^* at the inlet, the backpressures for modules P_{2j}, mass flows G_j $\left(j = 1, \ldots, n_{\text{mod}}\right)$ and rotor frequency ω.

The task is selecting the number of stages in the modules n_j, root diameter D_{hj} and stages blades heights so as to achieve the maximum power of the cylinder, while ensuring reliability, manufacturability, or any other (material consumption, cost, size, etc.) pre-specified requirements.

The minimum acceptable reliability limits regulated (including safety factors) by static stresses in the blades and diaphragms, as well as detuning rotor blades

of constant cross-section of the resonance. Technological constraints are reduced to a certain FP embodiment, task specific surface finish, as well as the use of standardized components – profiles, shanks, etc.

Common to powerful steam turbines HPC and IPC is the requirement of blading unification, when all stages are formed by trimming the top of the nozzle and rotor blades of the last stage of the module. At the same time it maintained a constant root diameter, angles α_{1h} and β_{2h}, as well as the root degree of reaction R_h at the uniform heat drops distribution between the stages and the constant axial velocity component in sections.

Consider ways of forming the cylinder FP, consisting of sections, satisfying, in particular, the above requirements of the unification. The idea of the method repeatedly expressed earlier. We apply it to the computer-aided FP design and make some modifications and generalizations.

3.2.1 Methods of the FP Synthesis

Consider one of the formulations of the PD problems, which we call the task I, in relation to the module.

Suppose that the root diameter D_h, root degree of reaction R_h and angle α_{1h} are known. The nozzle and rotor blades are considered to be twisted by law $c_u r = \text{const}$, which gives:

$$r_1 \operatorname{ctg} \alpha_1 = \text{const}; \quad r_2 \operatorname{tg} \beta_2 = \text{const}, \tag{3.28}$$

and to change the degree of reaction along the radius the relation is applicable

$$R_m = 1 - \frac{\bar{c}_z}{\phi}\frac{u}{C_0}\left[1 - \left(\frac{D_h}{D_h + l_1}\right)^2\right] - \left(\frac{D_h}{D_h + l_1}\right)^2 (1 - R_h)$$

or the approximate formula [10]

$$R_m = 1-(1-R_h)\left(1-\frac{l_1}{D_h+l_1}\right)^{1.8}. \tag{3.29}$$

First of all, the estimated process of steam expansion in the module is build. As we know neither the number nor the geometrical characteristics of the stages, it can be done only very approximately, evaluating the module efficiency η_{im}, such as by method [30]. This makes it possible to find the parameters of steam at the end of the actual process of expansion and, taking this process as linear, to evaluate the thermodynamic parameters at any pressure

$$P_{2n,\,\mathrm{mod}} \le P \le P_0^*.$$

To select the number of stages in the module let allow approximately uniform breakdown of the heat drops by the stages. Then, by setting the velocity ratio u/C_0 or evaluating its "optimal" (i.e. corresponding to the axial outlet flow from the stage – α_2 = 90) value, for example, by the formula [10]

$$\nu_0 = \frac{u}{C_0} = \frac{\phi\cos\alpha_1}{2\sqrt{1-R_m}} \quad \text{or} \quad \nu_h = \frac{u_h}{C_0} = \frac{\phi\cos\alpha_{1h}}{2\sqrt{1-R_h}}, \tag{3.30}$$

you can get

$$n = \frac{H_0 - \frac{c_{in}^2}{2}}{\frac{1}{8}\left(\frac{\omega D_h}{\nu_h}\right)^2 - \frac{c_{in}^2}{2}}, \tag{3.31}$$

where H_0 – module disposable heat drop; c_{in} – velocity at the inlet of the module; n – stage number – rounded up to the nearest integer.

Velocity c_{in}, which is equal to the axial component is determined by taking into account (3.30) according to the formula

$$c_{in} \approx c_{1z} = c_{1h} \sin \alpha_{1h} = \sqrt{2H_0 \left(1 - R_h\right) \sin^2 \alpha_{1h}} =$$
$$= \sqrt{\frac{4u_h^2 \left(1 - R_h\right)^2 \sin^2 \alpha_{1h}}{\phi^2 \cos^2 \alpha_{1h}}} = \omega \frac{D_h}{\phi} \left(1 - R_h\right) \mathrm{tg}\, \alpha_{1h}, \qquad (3.32)$$

where φ is assumed equal to 0.96...0.98.

Introducing the notation

$$\Delta i = \frac{i_0^* - \frac{c_{in}^2}{2} - i_{2n_{\mathrm{mod}}}}{n}; \quad \Delta S = -\frac{S_0^* - S_{2n_{\mathrm{mod}}}}{n},$$

on the proposed steam expansion process for each of the stages the parameters in the gap between vanes without much error is determined based on the relationships:

$$P_{1j} = P\left(i_0^* - \frac{c_{in}^2}{2} - \left(j - 1\right)\Delta i + \frac{c_{1z}^2}{2} - \right.$$
$$\left. -\left(1 - R_{mj}\right)\left(\frac{\Delta i}{\eta_{im}} + \frac{c_{1z}^2}{2} \right), \quad S_0^* + \left(j - 1\right)\Delta S + \left(1 - R_{mj}\right)\Delta S \right), \qquad (3.33)$$

$$i_{1j} = i\left(P_{1j}, S_0^* + \left(j + 1\right)\Delta S + \left(1 - R_{mj}\right)\Delta S\right), \qquad (3.34)$$

$$\rho_{1j} = \rho\left(P_{1j}, i_{1j}\right), \quad j = 1, \ldots, n. \qquad (3.35)$$

Pressures downward the stages are equal

$$P_{2j} = P\left(i_0^* - \frac{c_{in}^2}{2} - j\Delta i, \quad S_0^* + j\Delta S \right).$$

Nozzle vanes heights are determined from the continuity equation

$$G_j = \pi l_{1j} \left(D_h + l_{1j}\right) \rho_{1j} c_{1z}, \qquad (3.36)$$

where c_{1z} taken from (3.32).

Solving (3.36) as a quadratic equation, we find

$$l_{1j} = \frac{1}{2}\left(-D_h + \sqrt{D_h^2 + \frac{4G_j}{\pi \rho_{1j} c_{1z}}} \right). \tag{3.37}$$

Since the value of R_{mj}, entering into (3.33)–(3.35), depends on the height of the blades, the iterative refinement of all the values determined by formulas (3.29), (3.33)–(3.35), (3.37) is needed. Taking as an initial approximation $R_h = 0$ typically achieve convergence of 2–4 iterations.

Instead of α_{1h} may be set, for example, the ratio D_m / l of the 1-st stage. We call this formulation as the problem II. In this case, immediately we find the height of the blades of the 1-st stage

$$l_1 = \frac{D_h}{\frac{D_m}{l} - 1}$$

and the 1-st stage degree of reaction at the mean radius using (3.29).

Angle α_1 of the 1-st stage is determined based on the continuity equation

$$G = \pi \rho_1 c_1 \sin \alpha_1 \left(D_m + l_1 \right) l_1, \tag{3.38}$$

the obvious relation

$$c_1^2 = \phi^2 C_0^2 \left(1 - R_m \right) = \frac{\phi^2 \omega^2 \left(D_h + l_1 \right)^2 \left(1 - R_m \right)}{4\nu^2} \tag{3.39}$$

and the conditions (3.30), what after simple calculations gives

$$\operatorname{tg} \alpha_1 = \frac{G}{\pi \rho_1 \left(D_h + l_1 \right)^2 l_1 \left(1 - R_m \right) \omega}. \tag{3.40}$$

Furthermore, deleting C_0 from (3.39) using (3.30), we obtain

$$c_1 = \frac{\omega\left(D_h + l_1\right)\left(1 - R_m\right)}{\cos\alpha_1}; \quad c_{in} \approx c_1 \sin\alpha_1 . \tag{3.41}$$

The most advantageous number of stages in a module is determined by (3.31). Otherwise method II does not differ from the method I.

With the introduction of the coefficient

$$K_z = \frac{c_{1z,\,n}}{c_{in}}$$

methods I and II can be generalized to the case where the axial velocity components linearly vary from stage to stage. For this purpose, in the equations (3.33), (3.36) and (3.37) c_{1z} should be replaced by the value

$$c_{1z,\,j} = c_{in}\left[1 + \frac{\left(K_z - 1\right)\left(j - 1\right)}{n_m - 1}\right].$$

It should be borne in mind that when $K_z \neq 1$ the blade system unification condition ($\alpha_{1h} = \text{const}$, $\beta_{2h} = \text{const}$) is not satisfied.

Thus, as a result of solving PD problems in the statement I (II) certain basic characteristics of the FP are defined: the number of stages *n*, stages counter-pressures $P_{2\,j}$, root – level reaction degrees R_h , root diameter D_h , height of nozzle vanes $l_{1\,j}$, angles α_{1h} (ratio D_m / l of the 1-st stage).

3.2.2 Detailed Thermal Calculation

Next, to a more accurate assessment of the created design quality criteria and calculation of all required parameters is proposed to solve the inverse one-dimensional problem of thermal calculation of the FP for each of the stages of the cylinder. Known at this point data is not enough for this calculation.

Additionally, you need to specify the height of rotor blades, the geometric characteristics of the cascades, seals, etc.

Selection of missing values must be based on the design adopted, strength, technological and other requirements. For example, the height of the rotor blade can be obtained on the ground of information about the standard overlap or through the strict implementation of the conditions $\beta_{2h} = \text{const}$ in the group of stages. Using standard profiles data or generalized dependencies for the profile characteristics of arbitrary shape allows you to create a cascade, satisfying the requirements of efficiency, reliability and manufacturability. Selection of the main cascade parameters (a chord, stagger angle, pitch, etc.) it is advisable to carry out during the refinement of the velocity coefficients of crowns in the one-dimensional inverse problem of the FP thermal calculation. It's quite a complicated independent problem which deserves special consideration.

The results of this calculation are the kinematic parameters of the flow in the gaps, the effective angles, cascade's components of the kinetic energy loss and power parameters of stages. It also calculated the magnitude of stresses in the elements of design, weight, size and other characteristics. This information is sufficient to draw a conclusion about the quality of the built structure and the need to continue the design process.

A proximity in the selection of the basic FP parameters in the first PD stage compensated with the detailed account of the most factors affecting the quality parameters of the turbine in the model of thermal calculation. However, it should be borne in mind that during the synthesis of the FP should be set a number of parameters which are precisely determined only at the second calculation step. Therefore, there may be some differences in the parameters $u/C_0, \alpha_2, \eta_{i,\,\text{mod}}$.

The most significant differences between the set and the refined α_{1h} value, which can reach 0.5...1.0° or more because of the stages number rounding to the nearest integer in the formula (3.31) and, as a consequence, the deflection u/C_0 in the formula (3.30) from the optimum. For this reason, and also because of methodologically inappropriate to set as the initial parameter, which subsequently must be determined (angle α_{1h}), the PD problem formulation II seems more rational.

3.2.3 Optimization

The desire to automate the PD process leads to the development of an algorithm for finding the optimal combination of the basic parameters of the flow path. With regard to the formulation II it is $D_h, R_h, \nu_h, D_m/l$ of the 1-st stage, and in case of failure of the unification – also K_z. The total number of variables to variable cylinder consisting of n_m modules thus does not exceed $5n_{\text{mod}}$.

They imposed restrictions

$$\left.\begin{aligned} &D_{h\min} \le D_h \le D_{h\max};\\ &R_{h\min} \le R_h \le R_{h\max};\\ &\nu_{h\min} \le \nu_h \le \nu_{h\max};\\ &\left(D/l\right)_{\min} \le \left(D/l\right) \le \left(D/l\right)_{\max};\\ &K_{z\min} \le K_z \le K_{z\max}. \end{aligned}\right\} \tag{3.42}$$

When selecting cascade's profiles during the detailed thermal calculation may be presented restrictions on static strength of the diaphragm and the rotor blades of the type

$$\sigma \le [\sigma], \tag{3.43}$$

design

$$\left.\begin{array}{l}\alpha_{1h} \geq \alpha_{1h\min};\\ \beta_{2h} \geq \beta_{2h\min};\\ n \geq n_{\max}\end{array}\right\} \tag{3.44}$$

and other.

To automatically design the FP, optimal in terms of the selected quality criteria, the designer must specify ranges of variable parameters and the required number of points in the search space defined by the conditions (3.42).

Sampling points generation is conducted using the LPτ sequences. Clarification of the optimal solution is achieved by reducing the ranges in the search. Typically, the amount of the search points ranges from a few dozen to several hundreds. Since the synthesis and thermal design of one point takes a few seconds, the maximum time to find the optimal variant is not more than a few minutes on a standard PC.

4

Optimization of the Axial Turbine Parameters Along the Stage Radius

4.1 Formulation of the Problem

Mathematical models of gas and steam turbines stages, discussed above, allow to put the task of their geometry and gas-dynamic parameters optimization. This optimization problem is solved by the direct problem of stage calculation. The reason for this are the following considerations:

- it is most naturally in optimizing to vary the geometry of the blades;
- in the streamlines form refinement it is convenient to use well-established methods for the solution of the direct problem in the general axisymmetric formulation;
- only a direct problem statement allows to optimize the stage, taking into account the off-design operation;
- For the stages to be optimized, assumed to be given:
- the distribution of the flow at the stage entrance;
- the form of the meridian contours;
- the number of revolutions of the rotor;
- mass flow of the working fluid;
- averaged integral heat drop.

In general, you want to determine the distribution along the certain axial sections of angles α_1 and β_2 to ensure maximum peripheral efficiency of the stage:

$$\eta_u = \int_0^{\psi^*} L_u d\psi \Big/ \int_0^{\psi^*} h_0 d\psi \,, \tag{4.1}$$

Where $L_u = u_1 c_{1u} - u_2 c_{2u}$; $h_0 = L_u + \Delta h_s + \Delta h_r + c_2^2/2$.

Restriction on the heat drop, that determines the back pressure, is given in the form:

$$\int_0^{\psi^*} h_0 d\psi = h_{0m}\psi^* . \tag{4.2}$$

The effective angles of cascades may be restricted:

$$\alpha_{1\max} \geq \alpha_1 \geq \alpha_{1\min}; \quad \beta_{2\max} \geq \beta_2 \geq \beta_{2\min} . \tag{4.3}$$

Here the inlet geometric angle of the rotor we assume equal to the angle of the inlet flow. Selection of the optimal angle β_{1g} can be achieved solving an optimal profiling problem.

The objective function (4.1) can be calculated with the known distribution of the kinematic parameters of the flow in the gaps, which are determined by solving the direct problem of the stage calculation using the models set out in Chapter 2.

Mathematically, the assigned stage optimization problem has been reduced to a problem of the theory of optimal control of distributed parameter systems, including integrated criterion of quality (4.1) and system of constraints, which comprises:

- a system of equations in section 1 for the nozzle (2.39);
- a system of equations in section 2 of the rotor (2.40);
- isoperimetric condition (4.2), ensuring operation at a given stage heat drop;
- restrictions on the control variables (4.3).

The velocities c_1 and w_2, and the radii r_1 and r_2 are the phase variables; the independent variable stream function ψ plays the role of time.

From physical considerations it is obvious that the control functions $\alpha_1(\psi)$ and $\beta_2(\psi)$ must be sufficiently smooth, at least continuously differentiable, i.e. does not have discontinuities of the first kind, and kinks. For this purpose it is convenient to use parametric angles as dependencies

$$r_1^{m_1}\operatorname{ctg}\alpha_1 = \text{const}; \quad r_2^{m_2}\operatorname{ctg}\beta_2 = \text{const}, \tag{4.4}$$

which allow to investigate the influence of coefficients m_1 and m_2 on the stage efficiency.

The parameters m_1 and m_2 characterize twist angles gradients. For $m > 0$ are obtained the angles increasing to the periphery (direct twist) and for $m < 0$ – decreasing (reverse twist). Twist law $c_u r = \text{const}$ corresponds to the values $m_1 = 1$, $m_2 = -1$, that under the simplified equation of radial equilibrium, provides a minimum of the output velocity losses for the stage with cylindrical contours.

4.2 The Impact of Leaks on the Axial Turbine Stages Crowns Twist Laws

Significant impact on the stage efficiency have leakage of the working fluid through the seal gaps and discharge openings. The dependence of the leakage (and associated losses) of the stage bounding surfaces parameters can dramatically affect the distribution of the optimal parameters along the radii and, hence, the spatial structure of the flow therein. The latter, in turn, is determined by the shape and twist law of guide vane and impeller.

Development of algorithms for the axial turbine stages crowns twist laws optimization demanded the establishment of appropriate in the terms of computer time methods for calculating the quantities of leaks and losses on

them, allowing the joint implementation of the procedure for calculating the spatial parameters of the flow in the stage.

The leakage calculation is necessary to conduct together with a spatial calculation step, as the results of which the parameters in the calculation sections are determined, including the meridian boundaries of the flow path. The flow capacity depends on the clearance (or leakages) values, in connection with which main stream flow calculation is made with the mass flow amplification at fixed the initial parameters and counter-pressure on the mean radius, or clarifying counter-pressure at fixed initial parameters and mass flow. The need for multiple stage spatial parameters calculation (in the optimization problem the number of direct spatial calculations increases many times) demanded a less time-consuming, but well reflecting the true picture of the flow, methods of spatial stage calculation in the gaps described above (Fig. 2.3).

When calculating stage in view of leakage the continuity equation is convenient to take as [8]:

$$\frac{\partial \psi}{\partial r} = \mu r \rho w_s \cos\theta , \tag{4.5}$$

where μ – the mass transfer coefficient, which allows to take into account changes in the amount of fluid passing through the crowns, and at the same time to solve a system of ordinary differential equations in sections in front of and behind the impeller like with a constant flow rate.

The leakage mass transfer coefficients [13] is defined as follows

$$\mu_{1leak} = \frac{G_0}{G_1} = 1 + \frac{G_d}{G_1};$$

$$\mu_{2leak} = \frac{G_0}{G_2} = 1 + \frac{G_d}{G_2} + \frac{G_r}{G_2} - \frac{G_h}{G_2}.$$

In the case of wet steam flow with loss of moisture, crown overall mass transfer coefficient is given by

$$\mu_i = \mu_{i,\,leak}\psi_{m,\,i}, \quad (i=1,\,2),$$

where $\psi_{m,\,i}$ – flow coefficient, is usually determined in function of the degree of humidity and pressure ratio [8].

As shown in Chapter 2, the calculation of stage spatial flow with the known in some approximation the shape of the streamlines is reduced to the solution in the sections $z_1 = \text{const}$ and $z_2 = \text{const}$ (Fig. 2.3) a system of ordinary differential equations (2.39) and (2.40), wherein as the independent.

As discussed in Chapter 2, the solution of (2.54) (2.55) for a given flow rate is reduced to finding the roots of the two independent transcendental equations in the hub velocities c_{1h}, w_{2h}.

For a given backpressure to the number of defined values the parameter ψ^* is added and the problem reduces to solving a system of three equations. As a third equation the heat drop constraint (2.45) is added which can be symbolically written as

$$h\left(c_{1h}, w_{2h}, \psi^*\right) - h_0 = 0. \tag{4.6}$$

Systems of equations are solved using the methods of nonlinear programming.

The calculation of stages with reverse twist using the proposed method allows to obtain a valid reaction degree gradient and circumferential velocity component of the stage, while the calculation provided cylindricality flow gives results that differ significantly from the experimental data. The technique allows to take into account also the effect of the rotor twist law on the parameters

distribution in the gap after stator. This is evidenced by comparison of stages with the same nozzle assembly.

Effect of D_m/l ratio

With the methods described above, you can put the task of the stage parameters optimization along the height, taking into account the spatial flow and leakages. To explain the physical meaning of certain optimum blade units twist laws depending on different characteristics of stages, such as D/l ratio, radial gap, level of reaction degree at the mean radius, the presence of suction, and other factors, there is convenient to use the angle dependencies in the form (4.4).

The stages characteristics changing may be presented as constant level lines (isolines or topograms) in the plane of the variables m_1 and m_2. Computational studies were subjected to axial turbine stages with $D_m/l = 19\ldots3.2$, which have been tested on an experimental air turbine [13]. Some of them are at the same axial dimension and D_m/l have different levels of reaction at the mean radius that allows us to estimate the impact of the last factor on the crowns optimal twist laws. Separately the impact of radial clearance and suction at the root on optimal stage parameters was studied.

Influence of leakage through the radial gap

An important part of the kinetic energy loss in the axial turbine stage is a loss from radial clearance leakage, which is defined on the one hand, design and dimensions of the peripheral seal of the rotor blade and on the other – the pressure difference in the axial clearance in the outer radius. The analysis shows that in the stages of steam turbines for the amount of leakage significantly affects the D_m/l ratio: in the stages with relatively short blades, where δ_r/l_b is large, leakage losses greater of stages with a small D_m/l ratio, despite the

higher degree of reaction at the outer radius of the latter. Higher losses from leaks have stage without rim seals.

Large turbine units operating experience shows, that the radial clearances may increase from 1.5 mm to 5 mm, which results in reduced efficiency due to leaks more than 2 %. In some turbines due to increased near-the-shroud gaps efficiency drops 2…3 % or even 5 %.

In order to analyze the impact of the radial clearance leakage losses to optimal axial turbine stage crowns twist laws calculation were conducted for the above stages with all sorts of combinations of parameters m_1 and m_2 and the radial clearance values. As a result of numerical experiments parameters level lines built that characterize the efficiency in the plane of m_1, m_2.

As an example, the results of the calculations are shown in Fig. 4.1, 4.2. Each point of the topogram was produced by the method of the spatial calculation in gaps with the streamlines refinement. The calculations were performed in different statements: with a given flow rate with a predetermined heat drop, with a predetermined flow rate and heat drop adjusting when you change the angle α_{1m}.

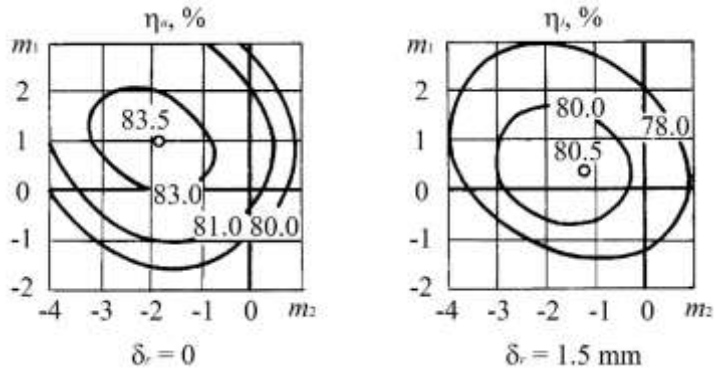

a

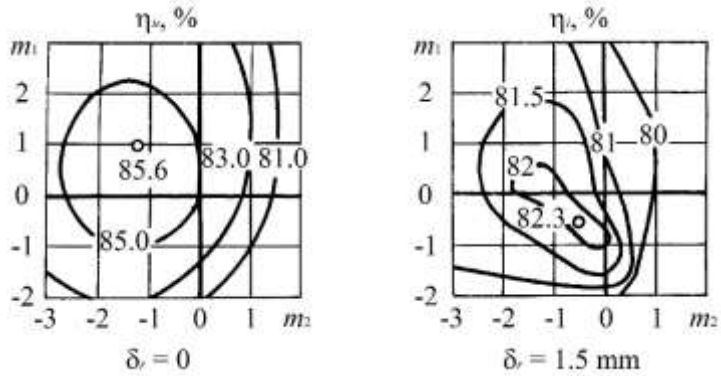

b

Figure 4.1 *Dependencies of stages I and II efficiency with a different relative cascades width values with the* $D_m/l = 3.6$ *on the blades twist laws at different radial clearances.*

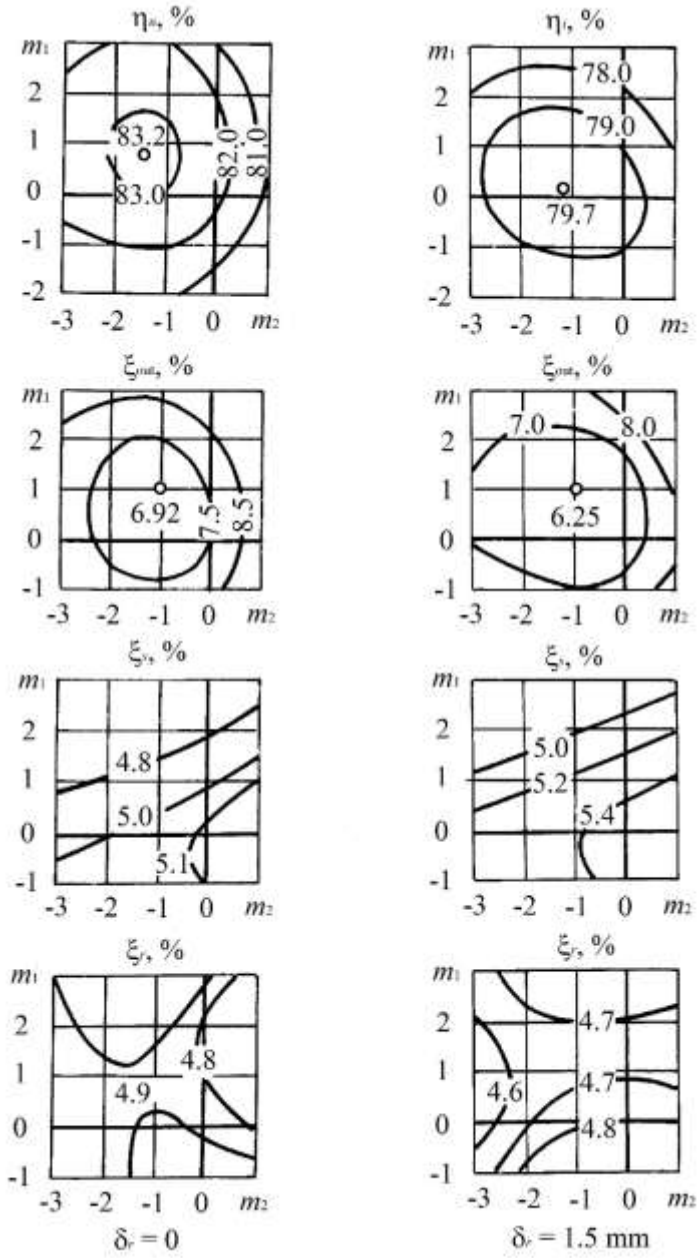

Figure 4.2 *Dependence of the relative losses in stage II with* $D_m/l = 3.6$ *on the blades twist laws at different radial clearances.*

Effect of parameters m_1, m_2 on the reaction gradient degree varies with different diameter to blade length ratios. Thus, for stages with relatively long blades ($D_m/l<5$) substantial reaction gradient alignment has been observed when $m_1=-1$, whereas for short blades ($D_m/l>10$), requires values m_1 reduction up to −8…−10. Significant impact on the reaction gradient degree with the reverse twist of the guide blades have also stage axial dimensions, especially nozzle relative width (or chord). At lower values the effect of the reaction gradient degree leveling is stronger. Reaction gradient degree alignment not only affects the magnitude of flow leakage and loss of these, but also manifested in the increase of uneven circumferential velocity component along the radius for the rotor, which leads to increased losses from the exit velocity the more (depending on m_1 and m_2) the smaller the D_m/l ratio. The value of the leakage losses in the radial gap determined by the relative leakage flow rate, which depends, inter alia, on the radial clearance size and its design.

The results of numerous calculations indicate that the crowns optimum twist laws (parameters m_1 and m_2) for the stages of the various D_m/l ratio at different values of radial clearance is mainly determined by the ratio between the amount of output velocity losses, and losses from leaks in the radial clearance. Influence of hydraulic losses in the guide vane and the rotor has a significant impact on the level of the degree of reaction for very small leak quantities into over-shroud space.

At zero clearance maximum of peripheral efficiency of the cylindrical stage for small D_m/l located in a neighborhood of the point with a minimum exit loss (Fig. 4.1, 4.2): the guide vanes twist close to the $c_u r=\text{const}$ law, and impeller should be twisted a little more intense ($m_2=-1\ldots-2$).

With increasing D_m/l ratio the maximum peripheral efficiency shifts toward twist laws with $m_1 > 1$ due to the hydraulic losses influence. The amount of displacement depends on the method of calculation (with a given flow rate or heat drop) and the reaction degree at the mean radius: offset is stronger when calculating with a predetermined flow rate due to changes in the angle α_1 at the middle (on flow rate) radius as a result of the streamlines lifting, as well as an increase in the average reaction degree.

The increase of the relative radial clearance leads to a shift of the maximum internal stage efficiency point in the direction of m_1 downward and m_2 increase, which is a sharper, then D_m/l relation is greater. This entails the reaction degree gradient alignment due to the streamlines inclination to the hub after the stator and some thrown at the periphery of the impeller. For example, in sages with $D_m/l = 8.3$ in the absence of leakage in a radial gap some flow preload to the periphery in the gap between the vanes is expedient. As the radial clearance increases it is appropriate to decrease the level of the reaction degree at the mean radius and its gradient. When $\delta_r = 1.5$ mm is advantageous to almost completely eliminated the reaction gradient ($m_1 = -4\ldots-5$, $m_2 = 0\ldots1$). The calculated results are in good agreement with the experimental study [13].

In the stages with even shorter blades ($D_m/l = 19$) for large radial clearances m_1 optimum value drops to –9…–11, and m_2 increases to 4…5. For large D_m/l values the stages with reverse twist for all real values of clearance have higher efficiency than the stages of traditional design. Winning increases with decreasing gap and the degree of reaction at the mean radius. Experimental research of stages $D_m/l = 19$ [13] fully confirms the conclusions.

The character of the stage relative loss change qualitatively is the same for all types of stages, with both small and large D_m/l ratios (Fig. 4.2). Isolines of the exit velocity loss form closed curves, surrounding the minimum point with $m_1 = 1$, $m_2 = -1$, corresponding to the constant circulation twist law. Isolines of the relative hydraulic loss regardless of the size of radial clearance are in the nature of saddle points: the relative losses in the guide vanes have in the saddle point m_1 maximum and m_2 minimum, while the relative losses in the rotor blades on the contrary, have m_1 minimum and m_2 maximum. With the D_m/l ratio increase hydraulic losses in the crowns becoming less dependent on the laws of another crown twist, acquiring the form of lines extended along the respective axes. This applies in particular to losses in the guide vane.

The leakage losses in the radial clearance in the plane of the variables m_1, m_2 achieved the highest value in the upper left corner of the topogram, where the peripheral degree of reaction is maximal, and the least – in the lower right corner, where the reaction degree gradient is minimal.

Influence of suction in the near-the-hub gap

To investigate the suction effect on the crowns best twist laws at fixed parameters on the mean radius were selected three experimental air turbine stages, with different blades elongation and reaction degree at the mean radius ($D_m/l = 3.6, 8.3, 14.1$ and $R_m = 0.2, 0.02, 0.01$, respectively). Calculations were made for various values of the radial gap and flow suction introduced by changing the reduced gap of the diaphragm seal, to provide thereby suction value in stages with $D_m/l = 3.6$ – 0.5 %, with $D_m/l = 8.3$ – 1 % and with $D_m/l = 14.1$ – 2 %.

The influence of the flow suction does not change the conclusions regarding the optimal crown twist laws made above. It should be borne in mind that in actual turbine stages discharge holes presence results in a large impact on the suction flow of the pressure difference at the inner radius of the impeller. When properly selected reaction degree in the root and the appropriate size of the discharge holes relative flow rate of the jet can be almost reduced to zero.

4.3 The Axial Turbine Stage Optimization Along the Radius in View of Leakages

The above numerical study results, confirmed experimentally, show, that leakages significantly affect the axial turbine stage crowns optimal twist laws. With a decrease in the length of the rotor blade (increase of D_m/l ratio) this effect is amplified.

In this regard, the problem arises of determining the guide vanes and rotor optimal twist laws for a given stage geometry, inlet parameters, the rotor angular velocity, flow rate and heat drop. We restrict ourselves to the task of practically important case of the blades angles specification in the form (4.4). At the same time, while setting the flow and heat drop together, thermal calculation is performed by adjusting one of the angles α_{1m} or β_{2m}. Described below optimization technique based on repeated conduct this kind of thermal calculations for the purpose of calculating the internal stage efficiency depending on one of α_{1m}, β_{2m} angles, and the exponents m_1, m_2 in the expression (4.4).

Assume that the control variables are β_{2m}, m_1 and m_2, whereby the back pressure at a predetermined flow rate must be specified by changing the angle

α_1 at the mean radius. The problem of the thermal stage calculation is written as

$$r_1' = f_{11}(\alpha_{1m}, r_1, c_1); \quad c_1' = f_{12}(\alpha_{1m}, r_1, c_1);$$
$$r_1(0) = r_{1m}; \quad r_1(\psi^*) = r_{1t};$$
$$r_2' = f_{21}(\alpha_{1m}, r_2, w_2); \quad w_2' = f_{22}(\alpha_{1m}, r_2, w_2);$$
$$r_2(0) = r_{2h}; \quad r_2(\psi^*) = r_{2t}; \quad h(c_{1h}, w_{2h}, \alpha_{1m}) = 0,$$

and its numerical solution is based on finding the roots of transcendental equations

$$\left.\begin{aligned} &\tilde{r}_{1t}(c_{1h}, \alpha_{1m}) = r_{1t}; \\ &\tilde{r}_{2t}(c_{1h}, w_{2h}, \alpha_{1m}) = r_{2t}; \\ &h(c_{1h}, w_{2h}, \alpha_{1m}) = 0. \end{aligned}\right\} \tag{4.7}$$

After the solution of (4.7), which is conducted with the specification form of the stream lines, leakage values, velocity and flow rate coefficients, internal stage efficiency calculated as a function of three variables β_{2m}, m_1, m_2.

Thus, the stage optimal design problem with a maximum internal efficiency reduced to a nonlinear programming problem:

find
$$\max_{\beta_{2m}, m_1, m_2} \eta_i = \frac{N}{h_0}, \tag{4.8}$$

where h_0 is calculated by the formula [13]:

$$h_0 = N + \Delta h_s + \Delta h_r + \Delta h_{out} + \Delta h_d G_d + \Delta h_r |G_r| + \Delta h_{bh} |G_{bh}| +$$
$$+ \left[\Delta h_h + \frac{1}{2}(c_h \sin\gamma_h)^2 \right] |G_h| + \Delta h_{mix}, \tag{4.9}$$

Unconditional maximization (4.8) does not meet the fundamental difficulties. Physically seems justifiable division of the optimization problem (4.8) on two related subtasks:

- determination of optimal angles at the mean radius under the certain blades twist laws;
- selection of optimal parameters m_1 and m_2 at specified angles.

Thus, the general problem (4.8) can be solved iteratively by alternately solving subtasks:

$$\max \eta_i = \frac{N}{h_0} \quad \text{at} \quad m_1, m_2 = \text{const}; \tag{4.10}$$

$$\max_{m_1, m_2} \eta_i = \frac{N}{h_0} \quad \text{at} \quad \beta_{2m} = \text{const}; \tag{4.11}$$

This approach is analogous to the component-wise optimization, which is a special case of the known method of the coordinate descent (Gauss-Seidel). The first of the sub-tasks (4.10) is solved by searching the extremes of functions of one variable. The second sub-task (4.11) can be solved by direct search of two variables function extremum. The combination of a one-dimensional search of the best angles at the mean radius and a direct search of optimum parameters m_1, m_2 was the most reliable way of the problem (4.8) numerical solution, providing the finding of the global maximum of the objective function even in the presence of local extrema in the topogram plane.

As a practical application of the developed technique of the turbine stage spatial optimization in view of leaks were upgraded cylinders of high and intermediate pressure of the steam turbine with 200 MW capacity. Relation D_m/l varies from 25 (II stage of HPC) to 4.8 (VII last stage of IPC) (control stage was not considered), the number of stages in the HPC and IPC was 6 and

7, respectively. As initial were taken the stages with the manufacture's blade angles at the mean radius. If $D_m/l > 10$, rotor blades assumed cylindrical, and if $D_m/l < 10$ – twisted by constant circulation law. Modernization was carried out at regular radial gaps ($\delta_r = 0.001 D_t$).

The data allowed to build dependence of the parameters m_1 and m_2, characterizing crowns twist laws on the ratio D_m/l (Fig. 4.3).

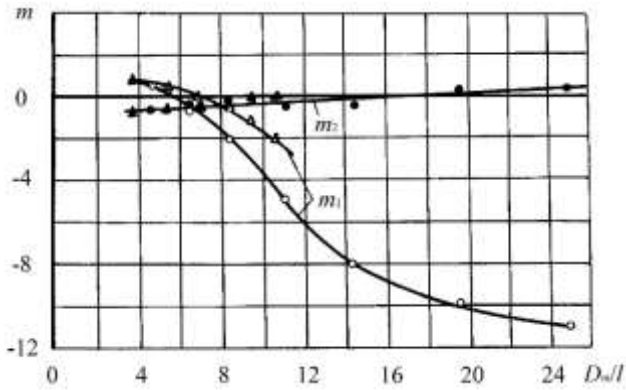

Figure 4.3 *Dependencies of the parameters m_1 and m_2, defining the crowns twist laws of powerful steam turbine HPC and IPC stages on the D_m/l ratio.*

Comparison of the effectiveness of IPC sections, consisting of original and optimized stages showed that efficiency of the last 0.65% above baseline. With increased radial clearances the gain increases.

The possibilities of this optimization method can also be illustrated by modern powerful (500 MW) steam turbine IPC upgrading example. 500 MW turbine intermediate pressure cylinder consists of 11 stages in the range $D_m/l = 10.8 \ldots 3.6$.

Optimization calculations have shown the expediency of the crowns twist with m_1 and m_2, the values and the magnitude of which change depending on

D_m/l are denoted with triangles in Fig. 4.3. Reducing exponents m_1 for stages with the same D_m/l values from the turbine 500 MW compared to 200 MW turbine can be explained narrower guide vanes (lower B_t/l values) in the IPC of the first turbine. Carried out optimization calculations have shown 0.45% improved cylinder efficiency.

4.4 The Effect of Tangential Lean on the Characteristics of Axial Turbine Stage

One means of the flow control in the axial turbine stage is the use of blades with non-radial setting. In this case, there is a non-zero the blade surface lean angle.

Vortex equation for the case of flow in a rotating crown can be written as:

- projected on the radial direction:

$$\left(1+\mathrm{ctg}^2\beta\right)w_s\frac{\partial w_s}{\partial r}-w_s^2\left(x\cos\theta+\frac{\partial \ln w_s}{\partial s}\sin\theta-\frac{\mathrm{ctg}^2\beta}{r}-\frac{1}{2}\frac{\partial \mathrm{ctg}^2\beta}{\partial r}\right)+$$

$$+2\varpi w_s\mathrm{ctg}\,\beta=\frac{\partial H}{\partial r}-T\frac{\partial s}{\partial r}-F_r-f_r; \tag{4.12}$$

- in the projection on the circumferential direction:

$$F_u=w_s^2\left(\frac{\sin\theta\mathrm{ctg}\,\beta}{r}+\frac{\partial \mathrm{ctg}\,\beta}{\partial s}+\frac{\partial \ln w_s}{\partial s}\mathrm{ctg}\,\beta\right)+2\varpi w_s\sin\theta-f_u, \tag{4.13}$$

where

$$\mathrm{ctg}\,\beta=\mathrm{ctg}\,\beta_p\cos\theta+\mathrm{tg}\,\delta\sin\theta; \tag{4.14}$$

$$F_r=-\mathrm{tg}\,\delta\,F_u. \tag{4.15}$$

Substituting (4.13) in (4.12) with (4.14), (4.15) and neglecting friction forces $f_r\approx f_u\approx 0$, we get the following equation of the radial equilibrium:

$$w\frac{\partial w}{\partial r}-w_s^2\left[x\cos\theta+\frac{\partial \ln w_s}{\partial s}\sin\theta-\frac{\operatorname{ctg}^2\beta}{r}+\right.$$
$$\left.+\operatorname{tg}\delta\left(\frac{\sin\theta\operatorname{ctg}\beta}{r}+\frac{\partial\operatorname{ctg}\beta}{\partial s}-\frac{\partial \ln w_s}{\partial s}\operatorname{ctg}\beta\right)\right]+$$
$$+2\varpi w_s\left(\operatorname{ctg}\beta-\sin\theta\operatorname{tg}\delta\right)=\frac{\partial H}{\partial r}-T\frac{\partial s}{\partial r}. \qquad (4.16)$$

Turning to the new independent variable ψ – the stream function, we write (4.16) in final form:

$$w'=\left(\mu r\rho\cos\theta\right)^{-1}\left\{\left[x\cos\theta+\frac{\partial \ln w_s}{\partial s}\sin\theta-\frac{\operatorname{ctg}^2\beta}{r}+\right.\right.$$
$$\left.+\frac{\sin\theta\operatorname{ctg}\beta\operatorname{tg}\delta}{r}+\frac{\partial\operatorname{ctg}\beta}{\partial s}\operatorname{tg}\delta+\frac{\partial \ln w_s}{\partial s}\operatorname{ctg}\beta\operatorname{tg}\delta\right]\sin\beta-$$
$$\left.-2\frac{\varpi}{w}\left(\operatorname{ctg}\beta-\sin\theta\operatorname{tg}\delta\right)\right\}+\frac{1}{w}\left(H'-TS'\right). \qquad (4.17)$$

Equation (4.17) for given geometrical parameters of the surface S_2' forms a closed system of ordinary differential equations in cross-section $z=\text{const}$ together with the continuity equation:

$$r'=\left(\mu r\rho w_s\cos\theta\right)^{-1}. \qquad (4.18)$$

Consider a three sections stage calculation which located on the entrance and exit edges of the guide vane and on the trailing edge of the impeller. Derivative $\partial \ln w_s/\partial s$ is defined in terms of the flow of the working fluid in the free space (right side of the design section):

$$\frac{\partial \ln w_s}{\partial s}=\frac{1}{\mathrm{M}_s^2-1}\left[\frac{\cos\theta}{r}\frac{\partial\left(r\operatorname{tg}\theta\right)}{\partial r}-x\operatorname{tg}\theta+\frac{\mathrm{M}_u^2}{r}\sin\theta\right]. \qquad (4.19)$$

In the absence of lean $\left(\operatorname{tg}\delta=0\right)$ the equation (4.17) coincides with the previously obtained. Upheld algorithm for the stage calculation by sections and

supplements it by specifying the lean angles of the guide and rotor blades output edges. Agreed $\delta(r) = \text{const}$.

Of particular interest is the study of the guide vane lean in order to assess its effect on the degree of reaction gradient and as a consequence, the amount of leakage in the radial space over rotor blades for different types of guide vane twists $\beta(r)$.

To determine $\partial \operatorname{ctg}\beta/\partial s$ the profile's backbone line appears as a parabola $u = u(z) = az + bz^2$, that gives approximately:

$$\frac{\partial \operatorname{ctg}\beta}{\partial s} \approx \frac{\operatorname{ctg}\beta_2 - \operatorname{ctg}\beta_1}{H}, \tag{4.20}$$

where H – the width of the blade.

Estimated study shows that the lean most strongly affects the flow conditions in the stage just because a member $\frac{\partial \operatorname{ctg}\beta}{\partial s}\operatorname{tg}\delta$. If there δ is positive, an alignment of reaction gradient happens, and, as can be seen from (4.20), the stronger, the smaller the α_1 angle and narrower the blade. Analysis (4.17) shows that the pressure compensation in the gap due to nozzle reverse twist occurs because of the appearance of the curvature of the stream lines in the gap, i.e. this influence is indirect and requires specification of the form of the stream lines in the stage calculation.

On the contrary, the effect of the lean angle on the degree of reaction gradient in the equation (4.17) manifests itself through the curvature of the surface in the oblique cut area, which allows the stage calculation even within a cylindrical theory.

Calculations were performed to determine the effect of the nozzle tangential lean on the characteristics of the experimental air turbine stage with high load $D_m/l = 14$, with the value of the radial gap $\delta_r = 1.5$ mm.

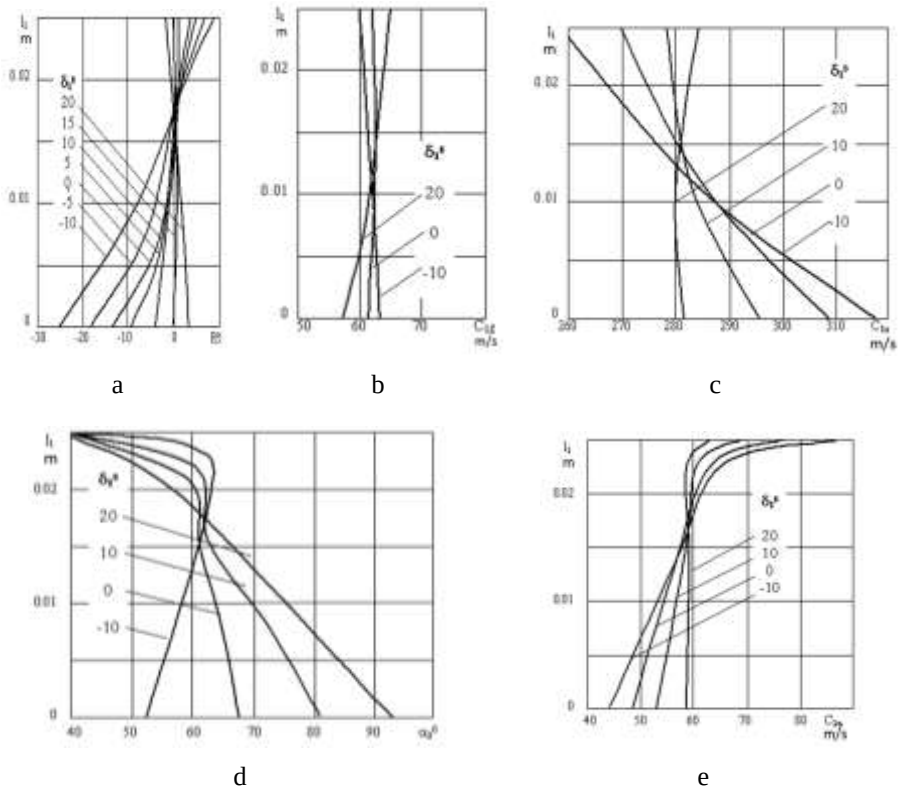

Figure 4.4 *The impact of the lean on the stage performance with m = 1.*

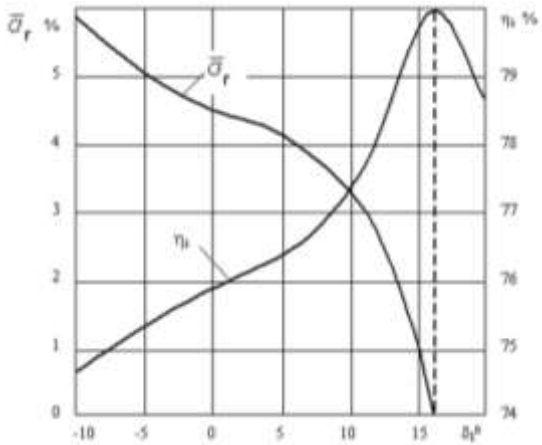

Figure 4.5 *Dependence of the radial clearance relative mass flow and stage internal efficiency on the lean angle for m = 1.*

Vane twist law was set in the form (4.4) and the lean angle ranged –10°…+20°. The results of calculations for $m = 1$ (the constant circulation law), and $m=-8$ (reverse twist, optimal when this value of radial clearance in the absence of the lean) are shown in Fig. 4.4, 4.5 and Fig. 4.6, 4.7. The figures show that the lean is a powerful tool in controlling the stage flow, in some cases giving an opportunity to significantly increase its efficiency.

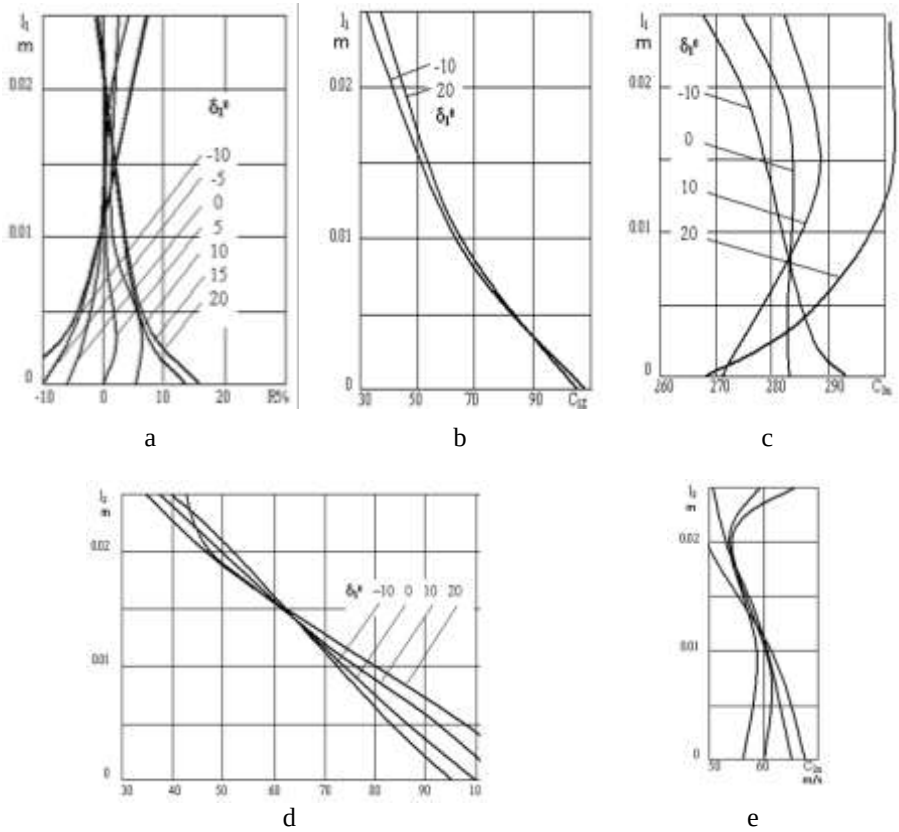

Figure 4.6 *The impact of the lean on the stage performance at m = –8.*

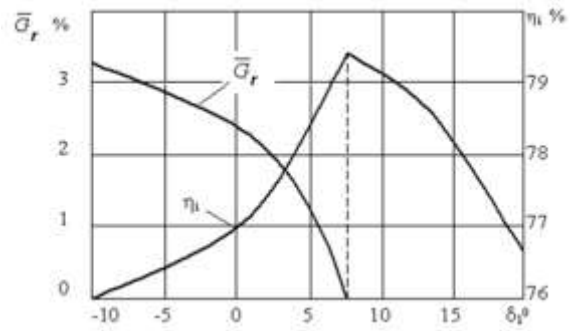

Figure 4.7 *Dependence of the relative mass flow in the radial clearance and stage internal efficiency on the lean angle at m = –8.*

5

Optimal Cascades Profiling

There are two different approaches to determining the optimal parameters of planar cascades of profiles for the designed axial turbine flow path.

The first one which is suitable for the early stages of design, does not takes into account the real profile shape, i.e. based on the involvement of empirical data on loss ratio, geometrical and strength characteristics depending on the most important dimensionless criteria (the relative height and pitch, geometric entry and exit angles, Mach and Reynolds numbers, relative roughness, etc.). The advantages of this approach are shown in the calculation of the optimal parameters of stages or groups of stages, as allow fairly quickly and accurately assess the mutual communication by various factors – aerodynamics, strength, technological and other, affecting the appearance of created design – and make an informed decision.

The second approach involves a rigorous solution of the profile contour optimal shape determining problem on the basis of a viscous compressible fluid flow modeling with varying impermeability boundary conditions of the profile walls. In practice, the task is divided into a number of sub-problems (building the profile of a certain class curve segments, the calculation of cascade fluid flow, the calculation of the boundary layer and the energy loss) solved repeatedly in accordance with the used optimization algorithm, designed to search for the profile configuration that provides an extremum of selected quality criteria (e.g., loss factor) with constraints related to strength, and other technological factors.

5.1. The Cascade's Basic Geometry Parameters Optimization

The importance of solving the problem of the cascade's basic characteristics definition can be seen from the following considerations. Let designed axial turbine stage blades at a predetermined height. Under certain parameters before

and behind the stage is usually determined the number of blades and profile chords so that with an energy loss minimum satisfy strength and vibration requirements. The simplest solution is to select the "optimal" *t*/*b* ratio using known empirical relationships and determining the chords provide reliable operation. Upon closer examination the situation is not so simple: first, the optimum ratio *t*/*b* is determined by many factors (the relative thickness of the edge, the Reynolds number and the relative roughness of the surface, relative height and others); secondly, the permissible loss and the vibration characteristics depend on the influence of the previous cascade; third, the stage design can be carried out both from the set of standard profiles or suggest subsequent entirely new cascades profiling. Consideration of these circumstances makes the task of optimization of the basic cascade parameters quite challenging and promising in terms of using hidden in complicated situations reserves to increase efficiency and reduce consumption of materials in the created turbomachine design.

The calculation of the kinetic energy loss on the basis of empirical relationships has repeatedly been considered and, as experience shows, in the form set out in Chapter 2, is a reliable tool to assess the various components of the losses in the cascade. Calculation of the geometric characteristics of the profiles is carried out using a dependency suitable for working and nozzle profiles, including an elongated front portion. The stresses in the diaphragms, nozzle and rotor blades, as well as restrictions on the vibrational reliability calculated by the well-known and, as far as possible, the exact dependence.

When optimizing an isolated cascade the following problem statements species are considered.

I. Profile presentation method

I.1. Standard profile. The geometric characteristics are determined by the tabular data and restated for a specific profile stagger in the cascade, which provides the desired output stream angle at a known relative pitch.

I.2. "Macromodel". The form of the profile is not known beforehand, but its defining geometrical characteristics can be estimated by empirical dependence of the type [26].

I.3. Profiling. In addition to the previous statement can be built demo profile, designed by a faster way. It is possible geometrical and strength characteristics evaluation on its configuration.

II. Variable parameters.

II.1. Optimization of chord when t/b = const.

II.2. Optimization of t/b when b = const.

II.3. The chord and the relative pitch optimization. In constructing the cascade of the standard profiles the profiles chord selection is in sequential enumeration of profiles of this type, but of different size [20, 33].

III. Boundary conditions.

III.1. Geometric, kinematic and gas-dynamic parameters in the first approximation are given from stage thermal calculation.

III.2. Cascade optimization process is conducted directly to the stage (multistage flow path) thermal calculation and optimization. In this case, the design of the cascade is embedded in an iterative process instead of the verifying energy losses in cascades, as is usually done.

Optimization is made by LP- search, and where this is not possible, brute force at defined ranges of variable parameters and the number of sampling

points. The calculation is carried out in designer's dialogue with a computer, which significantly reduces the time to find an acceptable solution.

5.2 Profiles Cascades Shaping Methods

The resulting thermal calculations of optimal geometry and gas-dynamic parameters of the working fluid at the inlet and outlet of the blade row let you go to the next stage of optimization of the turbine flow path – the blade design. The solution of the latter problem, in turn, can be divided into two stages: the creation of planar profiles cascades and their reciprocal linkage also known as stacking [25].

The optimal profiling problem formulated as follows: to design optimal from the standpoint of minimum aerodynamic losses profiles cascade with desired geometrical characteristics, provides necessary outlet flow parameters and satisfying the requirements of strength and processability.

To optimize the cascade's profile shape profiling algorithm is needed, satisfying contradictory requirements of performance, reliability, clarity and high profiles quality.

Earlier, considerable effort has been expended to develop such algorithms [25]. Analyzing the results of these studies, the following conclusions may be done. First, great importance is the right choice of a class of basic curves, of which profiles build (which may be straight line segments and arcs, lemniscate, power polynomial, Bezier curves, etc.), which primarily determines the reliability and visibility of solutions. The quality of the obtained profiles associated with the favorable course of the curvature along the contours, the choice of which is carried out using the criteria of "dominant curvature", minimum of maximum curvature, and other techniques.

First, consider the method of profiles constructing with power polynomials [15, 34]. The presentation will be carried out in relation to the rotor blade.

5.2.1 Turbine Profiles Building Using Power Polynomials

Initial data for the profile construction. Analysis of the thermal calculation results (entry β_1 and exit β_2 angles, values of flow velocities W_1 and W_2), and the requirements of durability and processability lead to the following initial profiling data (Fig. 5.1): β_{1g} – constructive entry angle; f – cross-sectional area; b – chord; t – cascade pitch. Optimal relative pitch of the cascade can be determined beforehand on the recommendations discussed in [25]; a – inter-blade channel throat; ω_1 – entry wedge angle; r_1 – the radius of the leading edge rounding; r_2 – the radius of the trailing edge rounding; ω_2 – exit wedge angle; β_s – profile stagger angle; β_{2g} – constructive exit angle; δ – unguided turning angle.

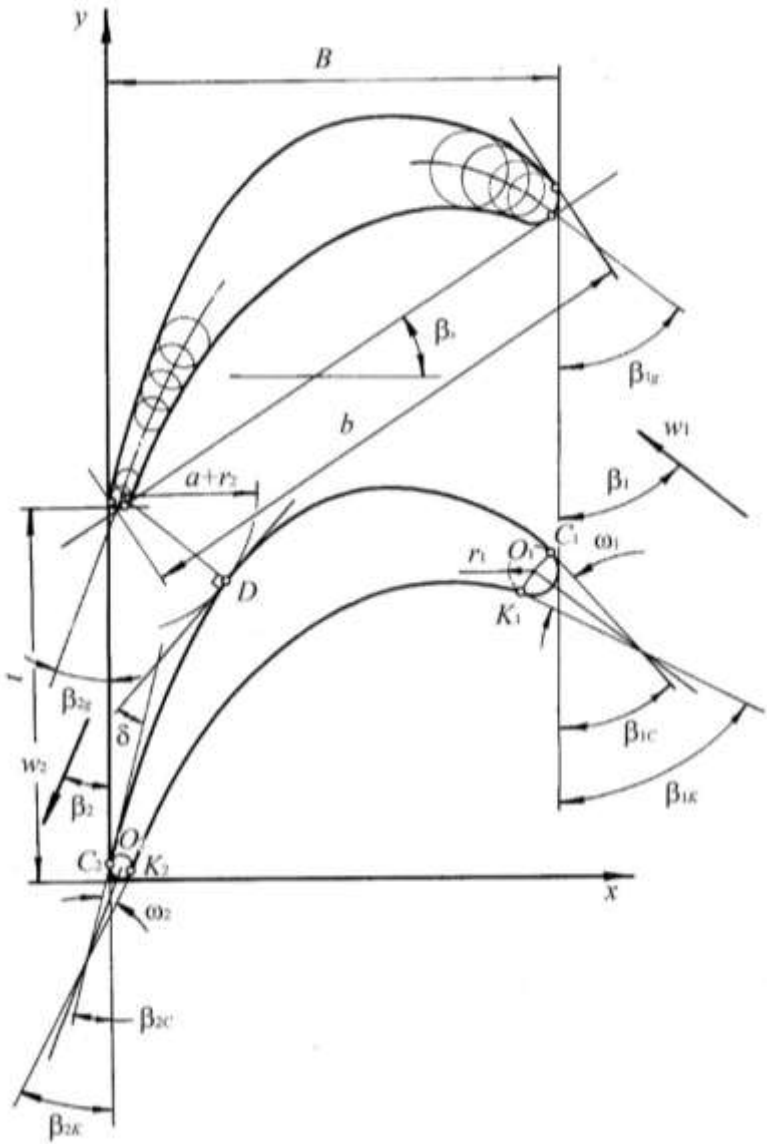

Figure 5.1 *The design parameters of the profile cascade.*

Of the last six parameters three (r_1, r_2, ω_2) are determined by calculation, the remaining three (β_s , β_{2g} , δ) can also be determined in the first approximation by the empirical formula [25]. In further at constructor's option last three

parameters or part of them, may be maintained constant during the profiling, or changed, as variable parameters. As a first approximation for the profile stagger angle β_s the next relationship can be recommended:

$$\beta_s = 13.59 + 0.682\left(\beta_{1g} - \beta_{2g}\right) - 0.0028\left(\beta_{1g} - \beta_{2g}\right)^2.$$

Profile is built in a Cartesian coordinate system. Coordinates of the circle center of input and output edges, as is easily seen, is given by (Fig. 5.1):

$$\left.\begin{aligned} &x_{0_2} = r_2; \quad y_{0_2} = r_2; \\ &x_{0_1} = x_{0_2} - r_1\left(\sin\beta_s + \cos\beta_s\right) + r_2\left(\sin\beta_s - \cos\beta_s\right) + b\cos\beta_s; \\ &y_{0_1} = y_{0_2} - r_1\left(\sin\beta_s - \cos\beta_s\right) - r_2\left(\sin\beta_s + \cos\beta_s\right) + b\sin\beta_s. \end{aligned}\right\} \quad (5.1)$$

The coupling coordinates of the edges circles with convex and concave sides of the profile C_1, C_2, K_1, K_2 and their derivatives at these points are defined as follows:

$$\left.\begin{aligned} &x_{C_1} = x_{0_1} + r_1\cos\beta_{1C}; \\ &y_{C_1} = y_{0_1} + r_1\sin\beta_{1C}; \\ &y'_{C_1} = \mathrm{tg}\left(90^\circ - \beta_{1C}\right); \\ &x_{C_2} = x_{0_2} - r_2\cos\beta_{2C}; \\ &y_{C_2} = y_{0_2} + r_2\sin\beta_{2C}; \\ &y'_{C_2} = \mathrm{tg}\left(90^\circ - \beta_{2C}\right); \end{aligned}\right\}, \quad (5.2)$$

$$\left.\begin{aligned} x_{K_1} &= x_{0_1} - r_1 \cos\beta_{1K}; \\ y_{K_1} &= y_{0_1} - r_1 \sin\beta_{1K}; \\ y'_{K_1} &= \mathrm{tg}\left(90^\circ - \beta_{1K}\right); \\ x_{K_2} &= x_{0_2} + r_2 \cos\beta_{2K}; \\ y_{K_2} &= y_{0_2} - r_2 \sin\beta_{2K}; \\ y'_{K_2} &= \mathrm{tg}\left(90^\circ - \beta_{2K}\right), \end{aligned}\right\} \tag{5.3}$$

Where $\beta_{1C} = \beta_{1g} - \omega_1/2; \quad \beta_{1K} = \beta_{1g} + \omega_1/2;$

$$\beta_{2C} = \beta_{2g} - \omega_2/2; \quad \beta_{2K} = \beta_{2g} + \omega_2/2.$$

The wedge angle of the leading edge ω_1 in first approximation can be determined using the guidelines [25]:

$$\omega_1 = 2.5\frac{C_{\max} - 2r_1}{b}, \tag{5.4}$$

Where $C_{\max} = 1.3f/b$.

The trailing edge wedge angle ω_2 can be set by the designer or determined by the expression:

$$\omega_2 = K_\omega \frac{0.14\omega_1}{0.2 + \omega_1}. \tag{5.5}$$

In the formulas (5.4), (5.5) the angles are in radians. The K_ω value is often taken as equal to 1. It can influence the position of the center of gravity of the profile. In the process of profile building angle ω_1 specified from the conservation of a given area.

Preserving the value of the throat *a*, for point *D* we have:

$$\left.\begin{aligned} x_D &= x_{0_2} + (a + r_2)\cos(\beta_{2C} + \delta); \\ y_D &= y_{0_2} - (a + r_2)\sin(\beta_{2C} + \delta) + t; \\ y_D &= \operatorname{ctg}(\beta_{2C} + \delta). \end{aligned}\right\} \tag{5.6}$$

In the construction of the profile convex and concave parts must first achieve coupling of describing their curves with circumferential edges, while the profile's convex part with the circumference of the throat at the point *D*. This means that these curves must satisfy the boundary conditions which are defined by formulas (5.2), (5.6) to the convex and (5.3) for the concave portions of the profile.

As for the convex part the number of these conditions is six, and for the concave – four, in order to have an opportunity to widely vary the outline profile to produce a minimum loss, the convex portion of the profile should be described by a polynomial of higher than 5-th, and the concave portion – than 3-d degree.

Let the order of the polynomial is *n*. In this case, the question of choosing the correct *n*-5 boundary conditions for the convex portion of the profile and *n*-3 boundary conditions for the concave part. As such one can take, for example, the high-order derivatives (second and higher) in the points C_2 and K_2. Not stopping until the solution of this problem, assume that the boundary conditions are somehow chosen.

Due to the fact that the number of points at which the boundary conditions are given, may be different for the convex portion and the concave profile (as mentioned above), for generality, we consider the task of determining the coefficients of the polynomial in the case of setting the boundary conditions in any number of points.

This problem is formulated as follows:

required to find the coefficients of the polynomial

$$y = a_0 + a_1 x + a_2 x^2 + a_3 x^3 + \ldots + a_n x^n , \tag{5.7}$$

satisfying in the k points to $n + 1$ boundary condition

$$\text{at } x = x_1 : \; y = y_1, y' = y'_1, \ldots, y^{(k_1 - 1)} = y_1^{(k_1 - 1)};$$

$$\text{at } x = x_2 : \; y = y_2, y' = y'_2, \ldots, y^{(k_2 - 1)} = y_2^{(k_2 - 1)};$$

$$\ldots\ldots\ldots\ldots\ldots\ldots\ldots\ldots\ldots\ldots\ldots\ldots\ldots\ldots$$

$$\text{at } x = x_k : \; y = y_k, y' = y'_k, \ldots, y^{(k_k - 1)} = y_k^{(k_k - 1)};$$

$$\left(k_1 + k_2 + k_3 + \ldots + k_k = n + 1\right).$$

Differentiating (5.7) $\ell = \max\left\{(k_1 - 1), (k_2 - 1), \ldots, (k_k - 1)\right\}$ times by x. We assume in (5.7) and in the first $k - 1$, obtained by differentiating (5.7), the equations $x = x_1$, then (5.7) in the first and $k_2 - 1$ equations $x = x_2$, etc. until you go through all the k points at which the boundary conditions are given. Every time we get a system of algebraic equations, which for the m-th point can be written as:

$$\left.\begin{array}{l} a_0 + x_m a_1 + x_m^2 a_2 + \ldots + x_m^n a_n = y_m; \\ a_1 + 2x_m a_2 + \ldots + n x_m^{n-1} a_n = y'_m; \\ \ldots\ldots\ldots\ldots\ldots\ldots\ldots\ldots\ldots\ldots \\ 1 \cdot 2 \cdot 3 \cdots (k_m - 1) a_{k_m - 1} + 2 \cdot 3 \cdot 4 \cdots k_m x_m a_{k_m} + \ldots + \\ + (n - k_m + 2)(n - k_m + 3) \ldots n x_m^{n - k_m + 1} a_n = y_m^{(k_m - 1)}; \end{array}\right\} \tag{5.8}$$

In the matrix form, this system can be presented as

$$C \cdot A = B ,$$

where C – matrix of coefficients (5.8); A – unknown parameters column $a_0, a_1, a_2, \ldots, a_n$; B – right-hand sides of equations (5.8) column.

It is easy to see the elements of the matrix *C*, and the right-hand part column B may be determined by the following formulas:

$$\left.\begin{aligned} &C_{i,\,j} = 0, \left(\begin{matrix} j = 1, 2, 3, \ldots, k_m \\ i > j \end{matrix} \right); \\ &C_{1,\,j} = x_m^{j-1}, \left(j = 1, 2, 3, \ldots, n+1 \right); \\ &C_{i,\,j} = x_m^{j-1} \prod_{S=1}^{i=1} \left(j - S \right), \left(\begin{matrix} j = 2, 3, 4, \ldots, k_m \\ j = i, i+1, \ldots, n+1 \end{matrix} \right); \\ &b_i = y_m^{(i-1)}, \left(j = 1, 2, 3, \ldots, k_m \right). \end{aligned} \right\} \tag{5.9}$$

Now, if the index *m* in (5.8) will run from 1 to *k*, we arrive at a system of linear algebraic equations of order *n* + 1 relatively of unknowns $a_0, a_1, a_2, \ldots, a_n$, the elements of the coefficient matrix and the right sides of the column which are determined by formulas (5.9). Solving this system of linear equations, we will determine the coefficients of the polynomial (5.7) separately for convex and concave profile parts.

The area is calculated using the difference between the integrals of the curves describing the convex and concave portion of the profile. Be aligned with a given area can be varying wedge angle of the leading edge ω_1, repeating at the same time building a profile with the formulas (5.2), (5.3).

The developed method of turbine profiles design allows the construction of an oblique cut with straight section. Such profiles can be used for supersonic expiration and work well in conditions other than nominal.

5.2.2 Profiles Building Using Besier Curves

A more simple and clear way to build the base curve is a Bezier curve (which is especially convenient for interactive construction of complex curves), but to automate profiling with its help some special measures should be taken. There

is no doubt also the fact that that the minimum of maximum curvature is a prerequisite for high aerodynamic qualities of turbine profiles cascades. In many cases, probably this criterion prevails over the condition of the absence of curvature jumps, as evidenced by still competitive CKTI profiles [33], designed from arcs and line segments.

Based on these considerations, we will build a profile consisting of two circles describing the input and output edges and three Bezier curves, one of which forms the pressure side, and the other two – convex part, respectively, from the trailing edge to the throat and from the throat to the leading edge.

Bezier curve that passes through two given end points and having at these points specified derivatives, will be called the base curve (BC).

The simplest base curve satisfying the above requirements, a Bezier curve, based on the polygon consisting of two segments passing through the given points with a given slope (Fig. 5.2). It is not difficult to assume that the use of the support polygon of the two segments gives BC, having a very large maximum curvature. In addition, when the angle between segments tends to be zero, the maximum curvature increases indefinitely.

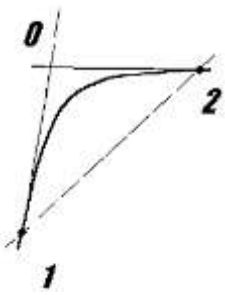

Figure 5.2 *Construction of Bezier curve by 2 points.*

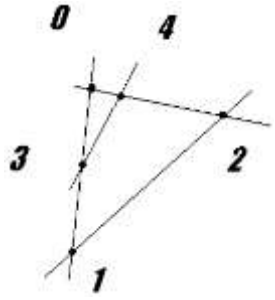

Figure 5.3 *Construction of Bezier curve in three basic segments.*

The next (and decisive) step to improving the base curve is the addition of one more segment, intersecting the first two (Fig. 5.3).

We introduce relationship

$$\frac{|1-3|}{|1-0|} = f; \quad \frac{|2-4|}{|2-0|} = g\,.$$

The course of the base curve generated by polygon *1-3-4-2* much smoother. Furthermore, it is obvious that there must be optimum values of the parameters *f* and *g*. Indeed, at *f* and *g*, aspiring to unity, we have the case of two basic segments and a very large curvature in the central part of the curve, while *f*, and *g*, tending to zero, greatly increasing curvature at points *1* and *2*.

A disadvantage of the third order base curve construction is the need to determine the optimal combination of parameters *f*, *g*, which greatly slowed the process of the profile design. Fortunately, the coefficients can be calculated only once and tabulated for different combinations of angles (Table 5.1). Since the optimum base curves do not depend on the polygon orientation or the size, the calculations can be made for the polygon, whose base is the unit interval, which lies on the *Ox* axis. In addition, due to the obvious condition

$$f_{opt}(\beta_1, \beta_2) = g_{opt}(\beta_2, \beta_1),$$

it is enough to store the data for only one optimal ratio. If you have a table of dependencies, the basic curves of sufficient quality are built almost instantly.

Table 5.1 *Optimal f and g coefficients for different angles.*

10	**20**	**30**	**40**	**50**	**60**	**70**	**80**	**Angles**
0.66	0.60	0.70	0.76	0.80	0.80	0.78	0.75	**10**
0.95	0.65	0.45	0.50	0.54	0.56	0.56	0.55	**20**
0.95	0.95	0.62	0.85	0.89	0.91	0.92	0.91	**30**
0.95	0.95	0.40	0.58	0.69	0.72	0.72	0.69	**40**
0.95	0.95	0.40	0.50	0.53	0.57	0.59	0.57	**50**
0.95	0.95	0.30	0.40	0.45	0.48	0.49	0.46	**60**
0.95	0.95	0.20	0.37	0.40	0.38	0.37	0.36	**70**
0.95	0.35	0.25	0.31	0.33	0.31	0.27	0.20	**80**

Profile is constructed from two circles that form the input and output edges, one of BC, which describes the pressure side, and the two BCs, describing the suction side. In this way, initial profiling parameters are listed in Section 5.2.1 (Fig. 5.1).

This information is sufficient to build the support polygons of the profile sections. Formulas for determining the coordinates of the corresponding points and angles do not differ from those given in the previous section. An algorithm for constructing the profile is very simple, but it has a major disadvantage: in the point of the throat, where two base curves are joined, it is possible discontinuity of curvature, which may lead to local deformation of profile velocity, and a sharp increase in the friction loss. There is a simple way to smooth BC docking at the throat. It lies in the selection of the unguided turning angle to match the curvature of parts at the throat point. Because of the high curvature sensitivity of the unguided turning angle, the variation turns minor. Determination of δ_{opt} is carried out by solving the equation

$$\kappa_{1D}(\delta) = \kappa_{2D}(\delta)$$

by secant method.

Elimination of the curvature jump in the throat requires only a few profile evolutions and a decision is reached very quickly. Built in such a way will be called the basic profile (BP). After a slight modification the algorithm also allows to construct suitable profiles with elongated front part.

It should be borne in mind that the BP is not yet the final product, it is only a semifinished product intended for optimization of all the others, except for the initial, data. This optimization can be performed according to different criteria.

In the process of BP constructing assumed the specified parameters with the exception of the unguided turning angle, which was chosen in such a way as to

eliminate the curvature jump at the throat. The remaining ten parameters can be varied to optimize a chosen cascade optimality criterion.

In general, the problem of optimal design of a flat cascade can be written as:

$$\min F(\mathbf{X}), \quad \mathbf{X} \in \Omega_X . \tag{5.10}$$

Vector of variable parameters X should in some way describe the shape of the profile. Criterion $F(X)$ is a functional on X. Restrictions on the range of admissible values of the vector X associated with strength and technological requirements cascade imposed on, which are, in particular, the shape and thickness of the input and output edges. Because of the sufficient simplicity of accepted method for calculating the tensile and bending stress in the blade section, they can be defined directly in the process of the profile shape optimization. However, we will stick to a different approach, considering approximately known basic cascade dimensions (chord, relative pitch, etc.) on the basis of the calculation described in section 5.1.

Specifically, a vector of variable parameters includes the following characteristics which influence the configuration of the profile that is based on the procedure described in the previous section:

- profile stagger angle;
- relative pitch;
- geometrical exit angle;
- the radius of the leading edge;
- wedge angle of the leading edge;
- wedge angle of the trailing edge.

Restrictions on the range of the parameter is written in the simplest form:

$$\bar{X}_{\min} < \bar{X} < \bar{X}_{\max} . \tag{5.11}$$

If you wish to fix a component X_i we believe $X_{i\min} = X_{i\max}$.

The most important point in the cascade optimization is the correct criterion of quality selection, which generally represents the minimum total loss of kinetic energy in the cascade taking into account the relative time of its operation at different flow regimes in a given stage of the turbine. In connection with this problem distinguish multi-mode and single-mode optimization solution requires the calculation of cascade flow and constituting losses therein, respectively, at set of modes or in one of them.

As shown by previous studies, in some cases, an alternative criterion of aerodynamic quality can be geometric criterion of the profile smoothness. One could even argue that this observation even more relevant to a multi-mode optimization, than single-mode. The original method was developed in relation to the profiles submitted by power polynomials.

5.3 Optimization of Geometric Quality Criteria

When used for the formation of the profile contour of polynomials of degree n ($n > 5$ for the convex part of the profile, and $n > 3$ for the concave part) the question arises about the correct choice of the missing n–5 (or n–3) boundary conditions which must be selected on the basis of the requirements of aerodynamic profile perfection.

One of the requirements of building the turbine profiles with good aerodynamic qualities is a gradually changing curvature along the outline of the profile [25]. Unfortunately, the question concerning the nature of the change of curvature along the profile's surface, is currently not fully understood.

As a geometric criterion for smooth change of curvature in the lowest range of change in the absence of kinks on the profile, you can take the value of the maximum curvature on the profile contour in the range $\left[x_{C_2}, x_{C_1}\right]$ for the

convex and for $\left[x_{K_2}, x_{K_1}\right]$ the concave parts, by selecting the minimum of all possible values at the profile designs with the accepted parameters and restrictions. The requirement for the absence of curvature jumps in the description of the profile contour by power polynomials automatically fulfilled as all the derivatives of the polynomial are continuous functions. Agree to consider determined based on the geometric quality criterion, the missing boundary conditions in the form of derivatives of high orders in points C_2, and K_2 components of a vector $\vec{Y}$. For the concave part of the profile vector of varied parameters $\vec{Y}$ is as follows:

$$\vec{Y}_K = \left\{ y''_{K_2}, y'''_{K_2}, \ldots, y^{(n-3)}_{K_2} \right\}.$$

For the convex part to the derivatives of high orders added geometrical exit angle β_{2g} and at constructor's option unguided turning angle δ:

$$\vec{Y}_C = \left\{ y''_{C_2}, y'''_{C_2}, \ldots, y^{(n-5)}_{C_2}, \beta_{2g}, \delta \right\}.$$

To construct the optimal profile is taken such a vector $\vec{Y}_{opt}$, which provides the minimum of the functional

$$F\left(\vec{Y}\right) = \max\left(k\right), \tag{5.12}$$

wherein k – the curvature of the profile, and the maximum is searched for in the range $\left[x_{C_2}, x_{C_1}\right]$ on the convex portion of the profile and $\left[x_{K_2}, x_{K_1}\right]$ – on the concave part of the profile using one of the one-dimensional search methods.

Formulated the problem of minimizing the functional (5.12) can be solved by the methods of nonlinear programming. In this case, a very successful was a flexible polyhedron climbing algorithm.

An algorithm for an optimal profile constructing using the geometric quality criterion is as follows:

1. For the given values of the inlet and outlet edge radii r_1 and r_2, chord *b*, received or estimated using particular one of the recommended dependencies profile's stagger angle β_s, the coordinates of the centers of inlet and outlet edges circles calculated using (5.1).

2. Set the leading edge wedge angle ω_1.

3. Select the initial approximation for β_{2g}, δ, by which and adopted value of ω_2 by the formulas (5.2), (5.6) the coordinates of the points C_1, C_2 and *D* are determined, as well as their first derivatives.

4. Determine the coefficients of the polynomial (5.7), which describes the convex portion of the profile. Wherein high order derivatives $y''_{C_2}, y'''_{C_2}, \ldots, y^{(n-5)}_{C_2}$ are set as the initial approximation in the first step and refined during the optimization.

5. By using one of the methods of one-dimensional search the maximum curvature $\max|k|$ objective function value is found. Next on the program for searching the extremes minimum of the functional sought

$$F\left(\vec{Y}\right) = \max|k|.$$

Minimum of the functional corresponds to the optimal value of the vector of varied parameters $\vec{Y}_{C_{opt}} = \left\{y''_{C_2}, y'''_{C_2}, \ldots, y^{(n-5)}_{C_2}, \beta_{2g}, \delta\right\}$ by which at this stage of the profile building the coefficients of the polynomial (5.7) describing the profile's convex part are determined.

6. From formulas (5.3) calculates the coordinates of the points K_1, K_2, and their first derivatives. Varying the vector $\vec{Y}_K = \left\{ y''_{K_2}, y'''_{K_2}, \ldots, y^{(n-3)}_{K_2} \right\}$ by the means of optimization program a value $\vec{Y}_{K_{opt}}$ and the coefficients of the polynomial that describes the profile concave portion are searched.

7. Determine the area of the profile $f(\omega_1)$ and the discrepancy $F = \left| f(\omega_1) - f \right|$. Setting a new ω_1 value, profiling process is performed again from step 3. As stated above, the minimum residual is achieved by using the "golden section" one-dimensional search of extremum procedure.

It was also developed somewhat different algorithm for constructing an optimal profile of the geometric quality criteria.

The main stages of the algorithm are as follows:

1. Setting a constructive exit angle $\beta_{2g} = \arcsin a/t$, define as a first approximation, the profile stagger angle in the cascade by the recommended [25] formula

$$\operatorname{tg}\beta_s = 0.2 + 0.8\left(\beta_{1g} - \beta_{2g}\right),$$

and the coordinates of the centers of inlet and outlet edges circles O_1 and O_2, by using the specified values of the radii r_1 and r_2, the chord *b*.

2. Calculating from the formula (5.4), (5.5) the edges wedge angles ω_1 and ω_2, determine the coordinates of the points of contact C_1 and C_2 on the convex side, K_1 and K_2 on the concave part of the profile, as well as the first derivatives in them.

3. We determine the coefficients of the polynomial (5.7), which describes the convex portion of the profile. The derivatives of higher orders $y''_{C_2}, y'''_{C_2}, \ldots, y^{(n-3)}_{C_2}$, necessary to determine the coefficients, are set as the initial approximation in the first step and refined during the optimization.

4. Using the method of one-dimensional search of extremum – the "golden section" method in the range x_{C_2}, x_{C_1} the value of maximum curvature $\max|k|$ is found, the minimum of which is determined by the Nelder-Mead nonlinear programming method, changing the vector of varied parameters $Y_C = \left\{ y''_{C_2}, y'''_{C_2}, \ldots, y^{(n-3)}_{C_2} \right\}$.

5. Constructing the convex portion of the profile, drop the perpendicular from the center of the circle O_2 of the neighboring cascade profile trailing edge and determine the size of inter-blade channel throat $O_2D - r_2$. Having the difference between the obtained value and the predetermined throat

$$\Delta a = \frac{x_D - x_{O_2}}{y'_D}\sqrt{1+\left[y'_D\right]^2} - \left(a + r_2\right),$$

refine by the recommendations [25], the profile stall angle β_s and constructive exit angle β_{2g}:

$$\operatorname{tg}\beta_s\left(i+1\right) = \frac{\operatorname{tg}\beta_{si} + \Delta\beta_{si}}{1 - \operatorname{tg}\beta_{si}\Delta\beta_{si}}; \quad \beta_{2g}\left(i+1\right) = \beta_{2gi} - \Delta\beta_{si},$$

where

$$\Delta\beta_{si} = \frac{\Delta a}{2\sqrt{\left(x_D - x_{O_2}\right)^2 + y_D^2}}.$$

The process of the profile convex portion constructing continue from step 1 until the throat is not held with the desired accuracy.

1. Varying the vector $\vec{Y}_K = \left\{ y''_{K_2}, y'''_{K_2}, \ldots, y^{(n-3)}_{K_2} \right\}$, using optimization in the range x_{K_2}, x_{K_1} the values of $\vec{Y}_{K_{opt}}$ are sought as well as the coefficients of the polynomial, describing the concave part of the profile (points 3, 4).

2. Determined the profile area $f(\omega_1)$ and the discrepancy $F = \left| f(\omega_1) - f \right|$. Given a new value ω_1 and profiling process is carried out again from step 2. Minimization of F residual is achieved by using an one-dimensional search of extreme.

3. Using one of possible methods, profile velocity distribution and boundary layer are calculated. Profile quality control is carried out by the nature of the velocity distribution around its contours, the value of profile loss and the boundary layer separation criteria.

The calculation of the velocity distribution around a plane cascade profile and loss coefficients made by sequentially the following tasks: calculation of potential ideal incompressible fluid flow around a flat cascade; approximate calculation of the compressibility of the working fluid; the boundary layer calculation and loss factor determination.

Methods for potential flow of an incompressible ideal fluid calculation in the plane cascade can be divided into methods based on conformal mapping of the flow domain and methods of solving tasks given to integral equations [8, 22].

Considering the profile loss ratio ζ_{pr} as the sum of the friction ζ_{fr} and edge losses ζ_e coefficients using proposed in [8] approximate formula for determining the value of the expression ζ_{pr} can be written as:

$$\zeta_{pr} = 2\frac{\delta_{ss}^{**} + \delta_{ps}^{**}}{t\sin\beta_2} + 0.1\frac{2r_2}{t\sin\beta_2}, \tag{5.12}$$

wherein $\delta_{ss}^{**}, \delta_{ps}^{**}$ – the momentum thickness on the convex (suction side) and the concave (pressure side) portions of profile.

The calculation of the boundary layer can be produced by known methods of boundary layer theory [22]. There is reason to believe the boundary layer in real turbomachinery cascades fully turbulent. At least the treatment the boundary layer as turbulence do not gives low loss coefficient values in the cascades. Before values of Mach numbers M < 0.5, calculation of the boundary layer on a single cascade profile can produce satisfactory accuracy as an incompressible fluid [22]. As a possible formulas for the momentum thickness calculation can take the expression obtained in the solution of the turbulent boundary layer by L.G. Loytsyanskiy method

$$\delta^{**} = 0.0159\,\mathrm{Re}^{-0.15}\, w_2^{-3.55}\left(\int_0^S w^4 dS\right)^{0.85}, \tag{5.14}$$

where Re – Reynolds number; w_2 – cascade output velocity; $w(S)$ – the profile countour velocity distribution function.

The integral in (5.14) is determined by a numerical method. Determined with the help of (5.14) the $\delta_{ss}^{**}, \delta_{ps}^{**}$ values, and substituting them into (5.12), we will find the profile loss ratio.

5.4 Minimum Profile Loss Optimization

A more rigorous formulation of creating an optimal cascade profile problem that provides design parameters of the flow at the exit and meet the

requirements of strength and workability, is the problem of profiling, which objective function is the profile (or even better – integral) losses.

As mentioned above, the profile loss ratio can be presented as the sum of the friction loss coefficients of the profile ζ_{fr} and edge loss coefficient ζ_e.

Given that the ratio of the edge losses associated with the finite thickness of trailing edges, the value of which is predetermined and is practically independent of the profile configuration, the objective function can be assumed as [8]

$$\zeta_{fr} = 2\frac{\delta_{ss}^{**} + \delta_{ps}^{**}}{t\sin\beta_2}. \tag{5.15}$$

In terms of flow profile, you must set a limit, excluding the boundary layer separation. Unseparated flow conditions according to Buri criterion can be written as [22]:

$$-\frac{\delta^{**}}{w}\frac{dw}{dS} \le B\left(\mathrm{Re}^{**}\right)^{-\frac{1}{m}}, \tag{5.16}$$

Where $\mathrm{Re}^{**} = \mathrm{Re}\,\delta^{**}/b$.

The constants B and m can be taken equal to: $B = 0.013\ldots0.020$, $m = 6$.

The task is set of determining the coefficients of the polynomials (5.7) for a description of the convex and concave profile with given geometric, strength and processability parameters so as to reach the minimum of the functional (5.15) and satisfy the constraints (5.16).

Formulated the optimal profiling problem is essentially non-linear with inequality constraints and mathematically formulated as follows:

$$\min f\left(\vec{Y}\right), \quad g\left(\vec{Y}\right) \ge 0, \tag{5.17}$$

where $\vec{Y} = \left\{ \beta_s, \beta_{2g}, \delta, \beta_{1g}, y''_{C_2}, y'''_{C_2}, \ldots, y^{(n-5)}_{C_2}, y_{K_2}, y'''_{K_2}, \ldots, y^{(n-3)}_{K_2} \right\}$ vector of varied parameters objective function, whose role in the problem plays an equation for the coefficient of friction (5.12); $g\left(\vec{Y}\right)$ – constraint, which on the basis of Buri separation criterion (5.14), is defined as follows:

$$g\left(\vec{Y}\right) = \max g_i\left(\vec{Y}\right); \tag{5.18}$$

$$g_i\left(\vec{Y}\right) = \begin{cases} G_i, \text{ at } G_i > 0; \\ 0, \text{ at } G_i < 0, \end{cases}$$

where

$$G_i = B\left(\mathrm{Re}^{**}\right)^{-\frac{1}{m}} + \frac{\delta_i^{**}}{w_i}\left(\frac{dw}{dS}\right)_i, \tag{5.19}$$

i = 0, 1, ..., 2n (2n – the number of points on the profile contour).

Applying to the problem solution method the penalty functions method [3], we reduce the problem of finding the extremum in the presence of constraints to the problem without restriction. Form the generalized functional I^*

$$I^* = \zeta_{fr} + \Lambda g\left(\vec{Y}\right), \tag{5.20}$$

where Λ – penalty coefficient.

For the unconstrained minimization of the functional (5.20) Nelder and Mead algorithm was used [3].

An algorithm for constructing an optimal profile of the minimum profile loss is as follows:

1. As the initial data for profiling on the basis of thermal calculation and the conditions of durability and adaptability the quantities are introduced:

a – throat inter-blade channel; b – chord; t – cascade step; f – profile square; r_1 and r_2 – input and output edges radii; ω_2 – trailing edge wedge angle.

2. An initial approximation for the leading edge wedge angle ω_1, the stagger angle of the profile β_s, geometric (constructive) entry β_{1g} and exit β_{2g} angles, unguided turning angle δ, derivatives of higher orders $y''_{C_2}, y'''_{C_2}, \ldots, y^{(n-5)}_{C_2}, y_{K_2}, y'''_{K_2}, \ldots, y^{(n-3)}_{K_2}$.

3. Determines the coordinates of the points C_1, C_2, D, K_1, K_2, and their first derivatives.

4. Sought the coefficients of polynomials describing the concave and convex portion of the profile according to the procedure set out in section 5.1.

5. The profile area determined and, using one of the one-dimensional search methods, varying angle ω_1, a minimum of residual $F = \left| f(\omega_1) - f \right|$ is found. The process of profiling is carried out from step 2.

6. Calculate the profile velocity distribution, as well as the coefficient of friction ζ_{fr} by (5.15) and the G_i value by (5.19).

7. We call the routine of optimization for finding the minimum of the functional (5.20), each time making the profile area fit before the calculation of the objective function. A minimum of the functional (5.20) corresponds to the optimum value of the vector of variable parameters

$$\vec{Y}_{opt} = \left\{ \beta_s, \beta_{2g}, \delta, \beta_{1g}, y''_{C_2}, y'''_{C_2}, \ldots, y^{(n-5)}_{C_2}, y_{K_2}, y'''_{K_2}, \ldots, y^{(n-3)}_{K_2} \right\}.$$

8. The optimal profile construction is made, satisfying the strength, geometrical and technological constraints, and provides a minimum profile loss while maintaining the unseparated flow. By the designer's wish optimization

may also be performed using the parameter *t*/*b*, and the trailing edge wedge angle ω_2.

5.5 Optimal Profiling Examples

The created profiling algorithms have allowed to design a series of profiles of turbine cascades.

As a starting (*1O*) was taken the standard profile *P2* with a high aerodynamic quality. Wherein were accepted such flow conditions that ensure the smallest possible profile *P2* (*1O*) losses: $\bar{t} = t/b = 0.722$, β_b = 76°26′, β_1 = 29°30′. Retaining the basic, necessary for the machine profiling raw data $(\bar{t}, \beta_b, b, a, f, r_1, r_2, \beta_1)$ with the help of the developed algorithms were obtained new profiles: *1MMC* (for the geometric quality criteria – the minimum of maximum curvature) and *1MPL* (the minimum of profile loss).

From technological considerations subsequently profile *1MMC* contour was approximated by the radii (Fig. 5.4, 5.5, Table 5.2). Fig. 5.6–5.8 shows the distribution of the velocity and the parameter *B* (the Buri boundary layer separation criterion) along the contours of the original and newly created profiles.

The calculated profile loss ζ_{pr} values correspondingly are 3.35, 3.16 and 3.00%. Attention is drawn to the different law of the parameter *B* variation along the profiles contours. Apparently, the possibility of the boundary layer separation, or the intensity of its thickening (which leads to increased losses) must be judged not only by the maximum value of the parameter *B*, which (usually) achieved at cascade's oblique cut, but also the character of its change within the channel prior bevel, particularly on the convex side of the profile.

For comparative testing of profiles *1O*, *1MMC* and *1MPL* were chosen conditions of the original flow profile *P2* (*1O*) which provide the smallest possible losses: $\bar{t} = t/b = 0.722$, β_b = 76°26′.

All nominal dimensions of the experimental blades and cascades of considered profiles adopted respectively the same, namely a chord b = 42 mm; length of blade l = 120 mm; pitch t = 30.32 mm; channel throat a = 10.85 mm; the thickness of the trailing edge δ = 0.66 mm. The stagger angles for the newly designed profiles *1MMK* and *1MPP* equaled stagger angle of the source profile *1O*.

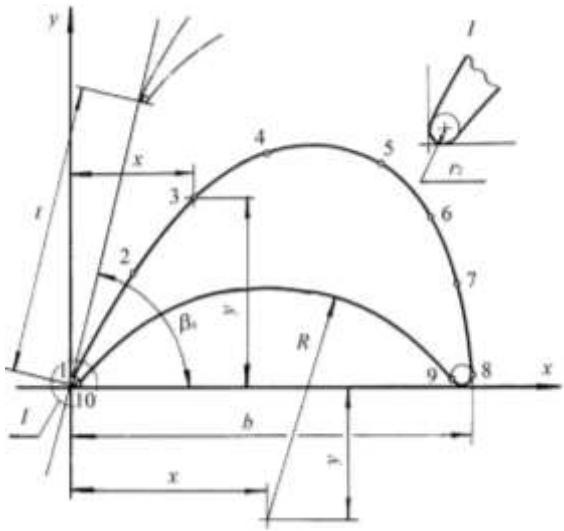

β_b ∘	76°26′	Bilateral points	Coordinates, mm		Bilateral points	Coordinates, mm	
b, mm	420,0		*x*	*y*		*x*	*y*
δ_{in}	6,66	1	0,3334	4,7837	6	377,3304	174,9175
δ_{out}	$1{,}59\cdot10^{-2}$	2	64,5584	118,8692	7	404,2919	104,6999
C, mm	153,6276	3	128,4423	196,9085	8	419,9	12,7715
t, mm	303,240	4	204,5439	244,4601	9	399,1575	4,6840
f, sm^2	479,962	5	324,6853	230,7689	10	6,0428	1,3995

Figure 5.4 *Profile 1MMC.*

Table 5.2 *1MMC profile parameters in the radiusographic form.*

Arcs	Radii and centers coordinates of arcs, mm			Arcs	Radii and centers coordinates of arcs, mm		
	R	***x***	***y***		***R***	***x***	***y***
1-2	1057,0	951,6247	–455,8897	6-7	277,5	134,1478	41,244
2-3	455,0	446,4076	–128,5415	7-8	750,0	–325,8325	–66,7955
3-4	210,0	275,1959	46,7023	8-9	11,55	408,4469	11,5460
4-5	137,7	250,8724	114,7901	9-10	242,99	203,8004	–139,8127
5-6	155,0	241,50	100,2534	10-1	3,33	3,33	3,33

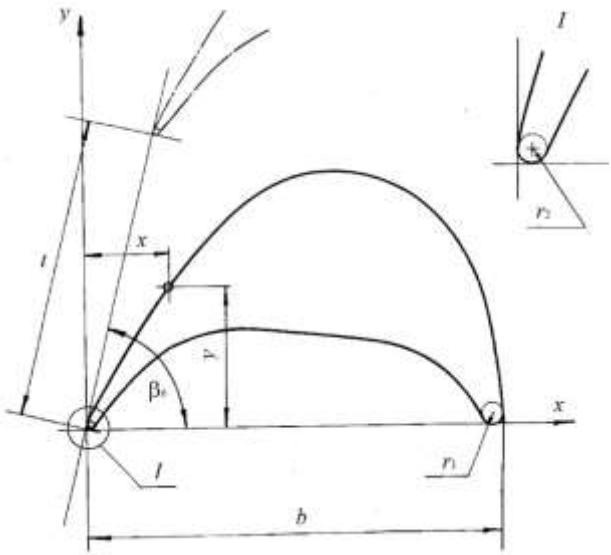

β_b °	76°26′
b, mm	420,0
δ_{out}, mm	6,66
δ_{in}, mm	$1{,}59 \cdot 10^{-2}$
C, mm	164
t, mm	303,240
f, sm^2	479,0

X_{O_2}, mm	3,33
Y_{O_2}, mm	3,33
r_2, mm	3,33
X_{O_1}, mm	408,451
Y_{O_1}, mm	11,55
r_1, mm	11,55

Figure 5.5 *Profile 1MPL.*

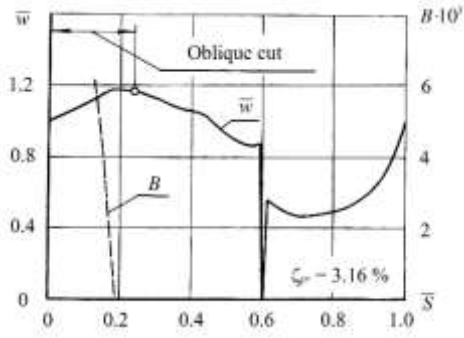

Figure 5.6 *Distribution of velocity and parameter B along the 1MMC profile contour. Calculated profile loss coefficient* ζ_{pr} *= 3.16%.*

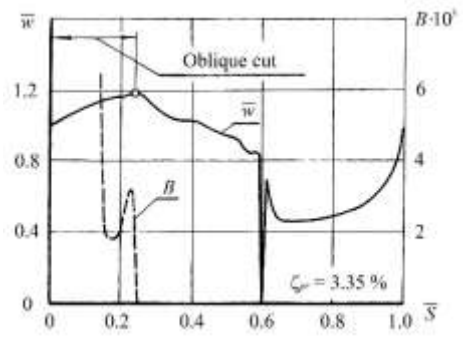

Figure 5.7 *Distribution of velocity and Buri separation criteria B along the 1MPL profile contour. Calculated profile loss coefficient* ζ_{pr} *= 3.35%.*

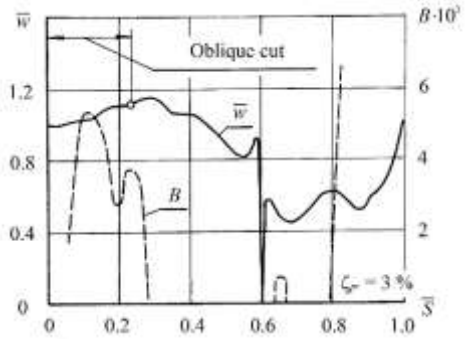

Figure 5.8 *Distribution of velocity and parameter B along the 1MPL profile contour. Calculated profile loss coefficient* ζ_{pr} *= 3.0%.*

In the blades manufacture the profile was controlled by the working patterns. The template fit appears on the projector using the drawing profile contour 10 times increased relatively to the blade profile. When fit the profile by template contour clearance allowed not more than 0.04 mm. It should be noted that the difference in the contours of the most similar profiles *1O* and *1MMC* reaches 0.6 mm, i.e. an order of magnitude greater of the blades manufacture tolerance. Particular attention was paid to ensure a predetermined trailing edge

thickness. The admission to the size of the throat when building cascades was ±0.03 mm. Effective angle downstream was $\beta_{2e} = \arcsin a/t = 20°55'$.

The aim of the tests was to obtain comparative data on the profile losses factors ζ_{pr} and exit flow angles β_2 in the subsonic region, at the range of Mach numbers 0.3…0.65, and different inlet flow angles β_1.

The comparability of the experimental results was ensured by making the blades and cascades in the same manner with the same requirements for precision and surface finish; cascade tests one the same test rig, using the same instrumentation and the measured data processing methods.

The main test was preceded by methodological tests. On expiration mode of Mach M_{2T} = 0.46, the measurements were carried out along the front of the cascade at different distances from the plane of output edges and in the three sections of the height of the blades. The values of certain kinetic energy loss factor ζ_{pr} is calculated for the measurement intervals along the cascade front multiple of two, three and four steps of the blades. The results of such averages practically coincided, indicating that careful manufacture of blades and high quality cascades assembly.

As a result of preliminary tests it was found that the averaged energy losses in the flow behind cascade will stabilize at a distance from the 0.25*b* of the trailing edges. Thus for a layer thickness of 20% of the blades height, symmetrical about their middle, the flow is very close to the flat.

Final testing data of three experimental cascades were obtained by measurements on the middle section of the height of the blades at a distance equal to 0.285*b* from the trailing edges in the three-step interval.

Fig. 5.9 shows the experimental dependences of the cascade profile losses versus inlet flow angle β_1 in the range of change from 26° to 41° at different Mach numbers ranging from 0.45 to 0.68, which corresponds to Reynolds numbers of Re = $3.9 \cdot 10^5$ to Re = $5.75 \cdot 10^5$. In these intervals profile losses curves of cascade made up of the original profile *1O*, are located above the profile losses curve of newly designed cascade *1MMC*. Both profiles have minimum profile loss at inlet flow angle β_1 = 35°. The magnitude of profile loss in the second cascade of 0.3…0.4% less than the first substantially throughout the whole range of variation of the input flow angle β_1 in the specified range of the Mach number values.

Wherein loss in each of the cascades *1O* and *1MMC* increasing against the minimum value of 0.8% in the case of 5° deviation of input flow from the optimum angle β_1 = 35°. The minimum profile losses amount of the cascade, composed from the newly designed blades *1MMC*, optimized for geometric quality criterion, is 2.2 %.

Profile losses of cascade, composed of profiles *1MPL*, were slightly lower of cascades *1O* and *1MMC* at the nominal input flow angle β_1 = 29°30′. With the inlet flow angle decreasing, *1MPL* profile advantage slightly increases. However, at the inlet flow angles β_1 > 30° profile *1MPL* is worse than others. It should be emphasized that this profile losses factor curve vs input flow angle β_1 in the investigated range of Mach numbers has a minimum at the angle β_1 = 29°30′, under which the profile *1MPL* was designed.

Fig. 5.10 shows the dependence of the angles downstream the cascades β_2 of the input flow angle β_1 at different Mach numbers. The newly designed cascade 1MMC has the better match of the output flow angle β_2 with the effective

angle $\beta_{2eff} = \arcsin a/t$ value in the entire tested range. A similar pattern is observed for the cascade of *1MPL* profiles within its region of advantages.

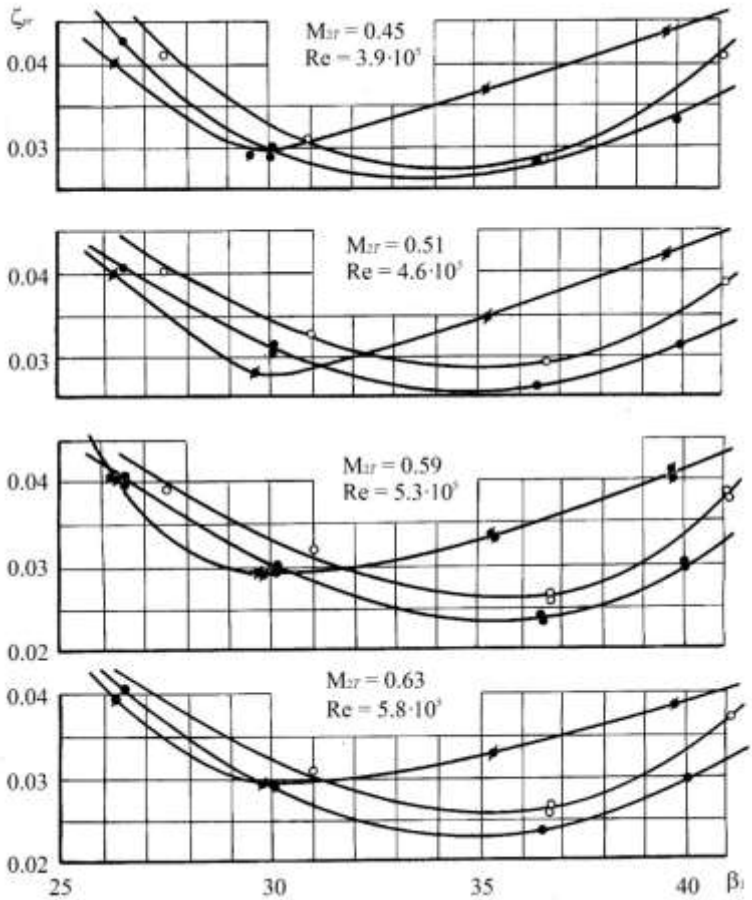

Figure 5.9 *Test results of cascades 1O (—o—), 1MMC (—● —) and 1MPL (—◕—). Test conditions: b = 42 mm; t/b = 0.722; l/b = 2.857; a = 10.87 mm;* $\bar{\delta} = 1.59 \cdot 10^{-2}$*;* $\beta_b = 76°26'$.

The another results of optimal profiling of cascades with converging and diffuser channels, as well as data of their experimental studies, can be found in [13].

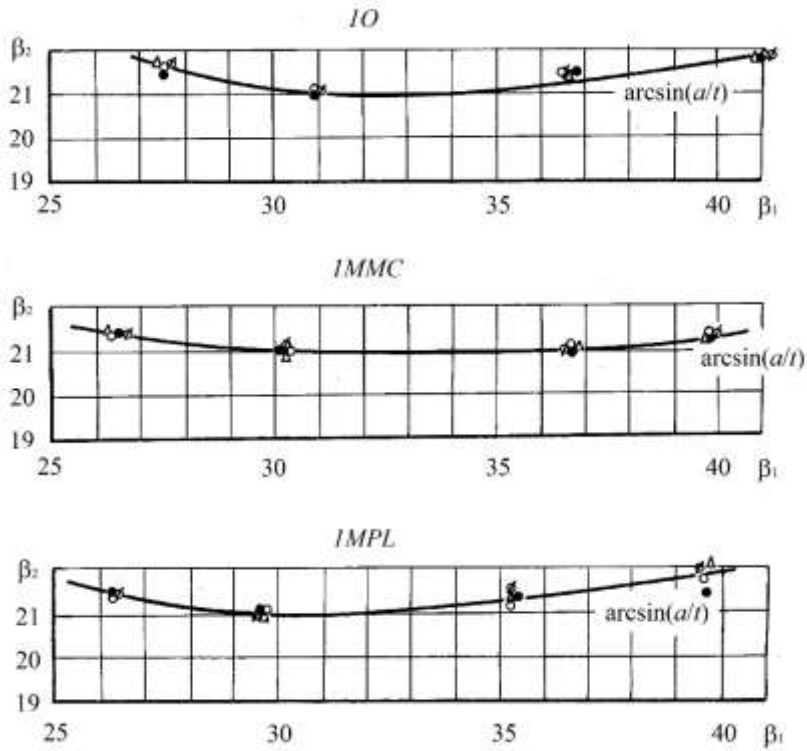

Figure 5.10 *Test results of cascades 1O, 1MMC and 1MPL at different Mach numbers:* $\Delta -\ \mathrm{M}_{2T}=0.37$; $\varnothing -\ \mathrm{M}_{2T}=0.45$; $O -\ \mathrm{M}_{2T}=0.51$; $\bullet\ -.\ \mathrm{M}_{2T}=0.59$.

The results obtained to build the turbine cascades of a minimum profile loss authenticate the proposed statement of the profiling problem. Of course, for such problems more correct to take as an objective function the integral loss, what is the most naturally achieved involving computational aerodynamics models.

6

Application of Computational Aerodynamics for Blades Shape Optimization

6.1 Problem Statement

The rapid development of computational aerodynamics methods not only puts on the agenda introduction of the spatial calculations into the turbines design practice, but also raises the need to develop the blades shape and other turbine flow path elements optimization methods taking into account 3*D* flow [24].

Formulations of the blades spatial optimization problems, which essentially cannot be solved by using one-dimensional and two-dimensional models, for minimization of the secondary flows loses, arising at the tip and the hub of the blades, are of the greatest interest [35].

Analyzing the results of the research, three main reasons for formation of the secondary flows in the turbine cascades could be singled out:

1) *Turning of the flow.* In channels with flow turning (including the turbine cascades) the transverse gradient of pressure arises, under influence of which whirlwind is forming at the ends of the channel.

2) *Interaction of the boundary layer, accumulated on the end wall in front of the blade* with the leading edge of the blade. For this reason, a horseshoe-shaped whirlwind is formed, which is then divided into two parts on both sides of the blade.

3) *Vortex wedge.* In almost every corner areas, which are generated between vortical structures and walls of turbine channel cascade, the forming or dissipating of corner vortexes may take place. Some from them are there constantly, some are dissipating depending rom the flow parameters and the type of the wedge.

To the most important causes inducing the secondary losses, relate the following factors:

1) natural accumulation of the boundary layer on end wall at the entrance till the lines of detachment;

2) braked the detachable bubble in the field of entrance edge between two lines of the detachment;

3) increasing the new boundary layer after the line of detachment;

4) losses in the corners between the high and low pressure sides and end wall (the most significant losses are situated in the corner between the low pressure side and end wall);

5) influence of tangential stresses along the 3*D* lines of detachment;

6) loss caused by tangential stresses between the channel vortex and the low pressure side of the blade, as well as the process of mixing of the crosscut flow with the flow in the channel along with a three-dimensional line of detachment;

7) dissipation of all vortexes and complete mixing of heterogeneous flow field at the cascade exit.

Such a complex character of the influence of secondary flows on cascade losses requires investigation of means of their minimization through appropriate selection of the blades shape in the end zones. Management of the end phenomena may be implemented by changing the shape of the profile along the height of the blades, using the complex tangential lean, profiling of the form of the flow path, utilization of the additional aerodynamic elements in channels between the blades.

The most evident way to control the flow nearby the ends of the blades is a lean. The simple problem statement of lean optimization involves parameterization of the blades shape by means of deformation of the stacking line in accordance with the chosen law. Selection of the deformation parameters, using one of the methods of direct search, leads to the definition of a profile

shape that ensures minimum integral losses in the cascade. Despite its apparent simplicity, this approach requires overcoming several problems associated with the efficiency of the solving of the putted task, in particular: rapid and reliable ways of building a parameterized blades and corresponding with them calculation grids in the blade passages; development of the mechanisms of data exchange with *CFD*-solvers; elaboration of recommendations for solver settings, providing sufficient accuracy and speed of calculations; the choice of optimization method, usable for solving the problems with difficult computable objective functions and with various kinds of restrictions.

6.2 Representation of Blades Geometry

6.2.1 File Formats for Blades Storage

Sources of geometric information related to turbines blades are quite varied.

These can be drawings in the paper or electronic form, the results of measurement of coordinates of the dots multitude, using mechanical or laser devices, coordinates of cross sections by flat or conical surfaces.

When the surface of the blade is represented by sets of dots its conical (cylindrical for axial machines) cross sections, it is assumed that the program, taking this information, will build the splines on cross sections and then will stretch the spline on surface. In this sense, this description is procedural.

In particular, the BladeGen preprocessor (*Ansys CFX*) offers two format of procedural form of the blades storing – *RTZT* and *CURVE*. Because the information in the *CURVE* file is not enough for permanent storage of data of the blade wheel, we have developed its extension – *CUR* format. It additionally includes the number of blades in the crown, the number of the cross sections and the number of the profile sectors in the cross sections, the number of dots in the sectors, etc.

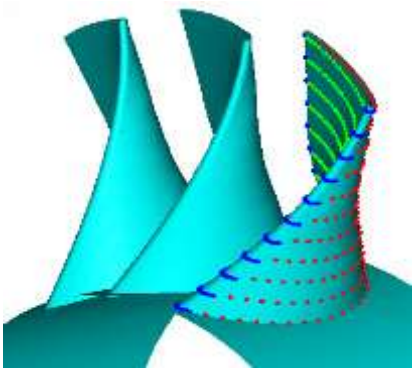

Figure 6.1 *Fragment of the blade wheel stored in the CUR format (4 sectors on the profile).*

The number of sectors on the contour of the cross section can be 1, 2 or 4. In the first case, the surface of the blade is formed by one spline. Accordingly, in the second and third cases, the blades is formed by two (suction and pressure sides) or four (suction side, leading edge, pressure side and trailing edge) spline segments.

The order and type of splines (for example, interpolation or approximation) are not stored in a file, because these options are implementation-dependent. They must be specified in the reading procedure. A fragment of the blade wheel, described using the CUR format with four sectors in each of the five initial cross sections of the blade, is shown at Fig. 6.1. The cross sections, shown at Fig. 6.1, came out as a result of spline-approximation of original dots (dots on the sites have different colors).

6.2.2 Stacking

The process of drawing up the blades from known cross sections (flat or cylindrical) is called *stacking*. To do this, specific point of each cross section, which coincides with the stacking line of this cross section, must be selected. Often, for convenience, the centers of the edges or the centers of gravity of the cross sections are chosen as stacking points (Fig. 6.2). In general, this selection can significantly change the shape of the blades.

Any deviation of the stacking line from radial location will be named *lean.* With a simple lean stacking line remains straight and is characterized by a single parameter –the angle of incline. When we have a complex lean it can take

a b c

Figure 6.2 *The simplest methods of the blade forming: a – radial center of gravity; b – radial center of inlet edge; c – radial center of outlet edge any form. There is distinguishing among axial and tangential lean.*

For easy use, it makes sense to limit parameterization of stacking line by Bezier curves.

6.2.3 Forming the Lateral Surfaces of the Blades

The surface of the blade is described by the parametric functions-interpolation or approximation *B*-splines based on two parameters: *u*-along the contour of each cross section and *v*-along the direction of stacking. Interpolation spline passes exactly through all dots of cross-section of the blade, and approximation spline – in accordance with supporting polygon, which is build using the dots of cross section or by least squares method [36]. All dots of the surface can be found, when *u* and *v* parameters taking the values from 0 to 1. In some cases, it is required to allow extrapolation towards the staking and then the *v* parameter may become a bit less than 0 or greater than 1.

The blade can be described either by one surface or by several. In our implementation (as already noted) 2 or 4 surfaces, that can be useful for some applications, in particular, when constructing grids, are allowed. Since there is no

joining on surface boundary, the junction's error could be managed only changing the spline order along u and v directions. It is usually within the range 2…5.

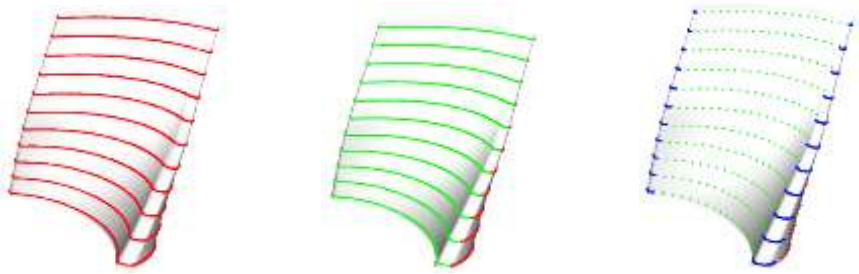

a *b* *c*

Figure 6.3 *The blade surface formation, using one (a), two (b) and four (c) surfaces.*

6.2.4 Three-Dimensional the Turbine Blade Parametric Model

One of the key elements of the 3*D* aerodynamic optimization of the turbine cascades algorithm is the turbine blade model parameterization, which consists in the possibility of changing blade shape (curvature) by variation of the limited number of numeric parameters that describes the stacking line.

The Bezier curve of 3-d (method I) and 4-th order (method 2) it seems convenient to use as the binding line. The second method allows creating a stacking line with practically straight-line the middle segment. (Fig. 6.4, 6.5). The number of independent variables in both cases can be reduced to two (Y_h and Y_s).

Parametric model of turbine blades must provide an opportunity to check the mass flow through the cascade. This requires incorporation in the model parameter, which allows controlling the mass flow during optimization. Most eventually the last gives the possibility to ensure equality of the mass flow between initial and optimized cascades with the same flow parameters before and after cascades. The changing of stagger angle of the blade, relative to the original, can be taken as such parameter.

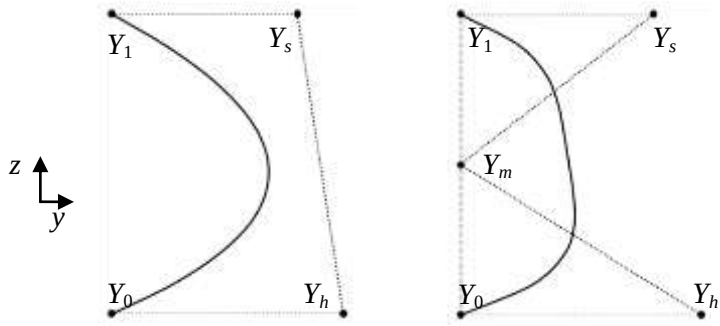

Figure 6.4 *Bezier curves of 3-rd and 4-th order.*

In addition to complex lean, the simple lean was implemented in methodical aim, which consists in turning of the turbine blades profiles relatively of the axis of rotation of the turbine on the specified angle. In general, developed parametric model of turbine blade allows producing its curvature in the circumferential (tangential) direction as well as in axial direction, simultaneously or separately.

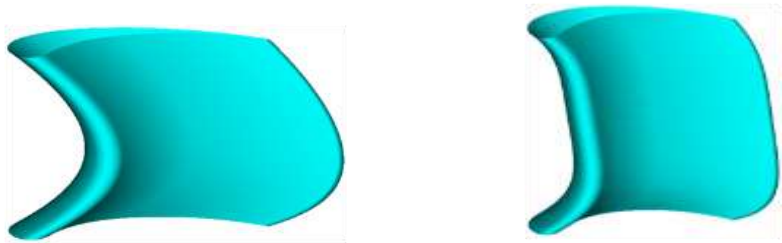

Method 1 Method 2

Figure 6.5 *Shapes of the blades with complex lean.*

6.2.5 The Grids Construction

As it is known, the results of the *CFD* calculations may depend on the type of calculation grids. One of the tasks, needing to be addressed, is to build up a three-dimensional parametric calculation grids, satisfying the form of parameterized blades.

Fast and reliable building of the parametric calculation grids is an integral part of the optimization studies as it implies the calculation of a large number of variants of the geometry of the turbine cascade. Since the developed algorithm of optimization should not be tied up with solitary *CFD*-solver, a specialized grids builder has been developed.

We will describe in details the work with *H*-grids, which represent a convenient compromise between complexity of the grids creation and quality of the obtained solutions when flows computation in turbomachine cascades occur. *H*-grid topologically is equivalent to the cube. Therefore, a data structure is simple enough for description. It intentionally is made redundant to accelerate frequently meeting operations. This, of course, slightly reduces the maximum size of the grid when a limited amount of RAM available to the computer, but it is not critical to the solving problem.

The structured calculation grid for channel between the blades is obtained because of deformation in the direction of each of the coordinate axes of a rectangular parallelepiped (in space) or rectangle (flat case).

Inter-blade channel is formed by concave and convex sides of the two adjacent blades (or profiles in the planar case). For selecting the high pressure and low pressure sides of the blade, the blade is made up by two splines, connecting in the points of minimum and maximum x-coordinate sections. Parametric lines v = const of these splines give the calculated coordinates of D sections of the grid in the radial direction. Next inter-blade channels are supplemented by input and output sections of the specified length, representing segments of the rings (for circumferential blade cascade) or parallelepiped (for flat cascade).The resulting area in each section is split up to cells of grids in the direction of x-coordinates dimension L. On the inlet and outlet sections is usually taken by $L/4$ cells. Other cells are located on the profile and coordinates

of the nodes are calculated by interpolation spline via dots of the splines of the high and low pressure sides.

Finally, channels are split on H sections along the directions x = const, that completes the structured grid formation. In the process of grid building a primitives numbering (nodes, edges, verges, and cells), topological ties formation and geometrical data calculation are made. All information is entered into a data structure.

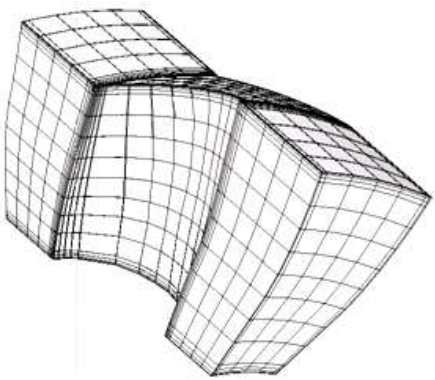

Figure 6.6 *The spatial H-grid of inter-blade channel 32×8×16 with thickening in three directions.*

As such, the calculated grids are not yet suitable for conducting reliable calculations of viscous flows in the blades cascades. They should be improved in order to fit the peculiarities of the flow near the walls of the channel.

Thickening structured grid is performed independently for each of the coordinate directions. Law of deformation of the grid can be different and should reflect the physical characteristics of the flow in the area of thickening. For example, near the wall polynomial law for changing the grid can be used, which corresponds to the rate of changing the velocity in the boundary layer. In the area of input and output edges the deformation may be exponential in nature that is less aggressive. In either case, a number of parameters controlling the

thickening as for the rate of deformation as well as the ratio of the sizes of areas of the channel subject to or not to distortion should be entered.

In general three-dimensional case, the grid, suitable for calculations of viscous flows, is presented at Fig. 6.6.

6.2.6 File Format for Grids Storage

The diversity of formats creates some difficulty in reading these files by different *CFD*-applications. *CGNS*-standard for *CFD* calculations data storage is positioned as a "common, portable and extensible". Software implementation of the standard is an open, cross-platform and well documented that, in principle, precludes differences of various applications.

Data in *CGNS* format are stored in binary form and access to it is implemented through a set of functions for reading, writing, and modifying of the contents of the files which can be called from application in different programming languages. In general case *CGNS* file can contain data which is associated with viscous compressible fluid flow, but suitable for solutions of the Euler equations and potential flows.

The standard includes the following data types: structured, unstructured hybrid grids; data of the *CFD* calculations; information on the sub-grids docking or overlapping; boundary conditions; descriptions of equations of state, turbulence models etc.; nonstationary solutions, including deformation of calculation grids in time; dimension of variables; variables reference points; history of calculations; user's and other data.

For the purpose of specific tasks solution there is no need to implement in full all the functionality, supported by the *CGNS* (this is not currently doing even such advanced products like *CFX*). It is enough, for example, organize saving of the structured grids and setting of the boundary conditions, satisfying the terms of the calculation task. This significantly speeds up the preparation of

data for *CFD* calculations. Analysis of output information, perhaps, you might need to implement by means of post-processors of used packages, since not all of them conserve the results of calculations in *CGNS* format.

6.3 *CFD* Tools

For realization of the optimization algorithm, using *CFD*-calculations, it is necessary to choose the right program product.

Well known program complex *ANSYS CFX* includes in it pre-processor, post-processor and the solver.

ANSYS CFX Solver has the following characteristics:

- *numerical methods*: finite volume discretization of equations; solution of the complete three-dimensional unsteady Navier-Stokes equations; difference schemes of 1-2order; the joint solution of the equations of conservation of mass and moment; algebraic multigrid method for solving the linearized equations; support of the elements of various types – hexahedrons, prisms, pyramids, tetrahedrons; adaptive thickening of grids; movable and changing grids;
- *model of turbulence*: algebraic model; model k–ε; k–ω model; model SST; Reynolds stress model; method of large vortices LES; method of not attached vortex DES.

The program complex *ANSYS CFX* has the following level of support for *CGNS* format:

- preprocessor supports only reading of grids and names of edges of the computational domain;
- solver does not support the reading of *CGNS* files, but allows to convert the results of calculation in *CGNS* format;

- post-processor supports the reading of the calculation results.

The preprocessor is used for entering the *CGNS* files and setting the boundary conditions for each variant of blades geometry, even when the boundary conditions and calculation parameters are identical.

Calculation in *ANSYS CFX*-Solver is made then.

Processing and the analysis of results takes place in postprocessor, using macros that are intended for determination of the values, required in the process of optimization.

6.4 Algorithm of Spatial Aerodynamic Optimization of the Blade Cascades of Axial Turbines

The proposed method of optimization of the cascades is based on the joint usage of the formal macromodeling and LPτ search and includes the following steps [37]:

The plan of computing experiment is created [1, 2]. In the given range of variable parameters, defining a stacking line, the points, in which computations will be carried out, are determined.

The blades matching of the plan points parameters are constructed and computation domain and grids are generated.

Values of objective function for each combination of parameters are determined. For this purpose *CFD* computation and post-processing of results are carried out.

Coefficients of a full square-law polynomial type (1.2) or (1.12) of objective function and restriction function in the set range of varied parameters are determined. Using LPτ search the minimum of value losses in the cascade

$\zeta\left(Y_h, Y_s, \Delta\beta_s\right)$ is determined, under condition that the mass flow through it satisfies the condition $\left|G\left(Y_h, Y_s, \Delta\beta_s\right) - Gorg\right| < \varepsilon$.

The scope of varied parameters has been changed:

a) if the minimum of the objective function appears on the border of the range of variation parameters, the last is displaced aside of this boundary;

b) if the minimum of the objective function are inside of the range, but macromodel is not sufficiently precise, the range decreases;

c) if the minimum function falls within the range and macro-model is accurate enough, checking *CFD*-calculation is carried out and if its results with sufficient accuracy coincide with optimization results on macromodel, optimization is completed, otherwise the range decreases. Repeat pt. 1–4.

6.5 The Impact of Simple Tangential Lean on the Flow Through the Turbine Circumferential Cascade

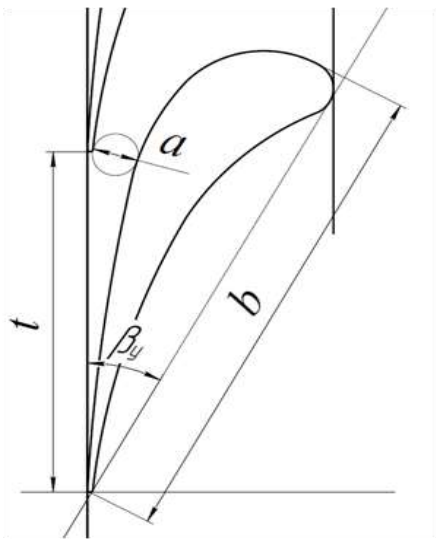

Figure 6.7 *Researched blade profile TC-1A.*

It is known that the lean along the flow leads to increasing secondary flow losses on the periphery and to reducing them at the root. Lean against the stream leads, correspondingly, to the opposite result.

The lean to the opposite flow direction allows to alter the distribution of flow parameters along height, so that the leakages in the axial gap is reduced on the periphery, that positively affects stage efficiency.

As an object of research the circumferential guide blade cascade was chosen with the profiles TC-1A (Fig. 6.7) with the following parameters:

$$b = 0.26\ \text{m};\quad \bar{t}_h = 0.715;\quad \bar{t}_t = 0.864;\quad \beta_s = 61^\circ;\quad l/b = 0.49$$

and centering on the input edge.

Boundary conditions:

- inlet: $P_0^2 = 102240\ \text{Pa}; T_0^* = 373.15\ \text{K}$;
- the degree of turbulence 1%;
- outlet: $P_2 = 81861\ \text{Pa}$;
- the blade and the ends of the channel: impermeable wall with condition of sticking the flow;
- working medium: air.

In the investigated guide blade cascade boundary conditions correspond to subsonic flow with Reynolds number at outlet equals $2 \cdot 10^6$.

Fig. 6.8–6.10 shows the results of calculations with lean angles γ = –30; –20; –10; 0; 10; 20; 30° (negative lean means the lean against the direction of the flow and positive – the lean in the direction of the stream).

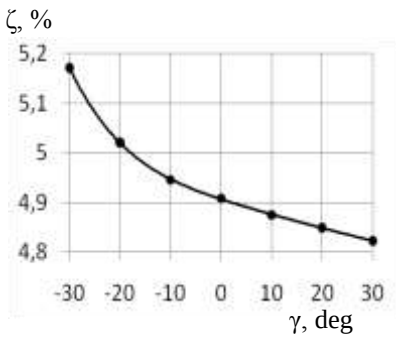

Figure 6.8 *Change of the integral losses coefficient from lean.*

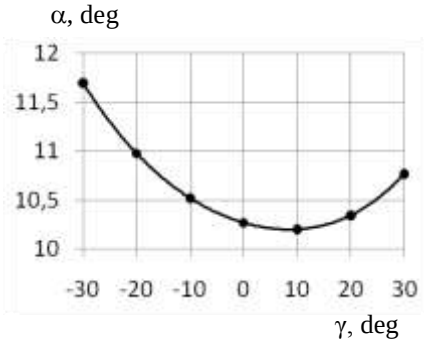

Figure 6.9 *Change of the integral actual outlet flow angle from lean.*

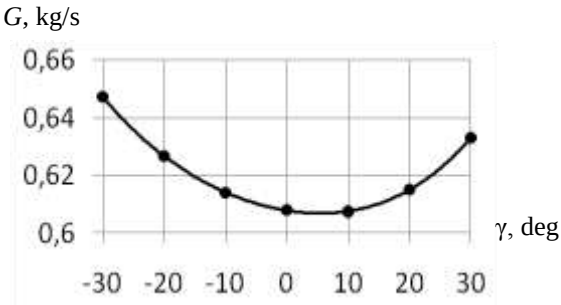

Figure 6.10 *Change of mass flow rate from lean.*

Obviously, that the total losses are increasing when there is negative lean and decreasing with the positive lean. Exit angle of the flow and the mass flow rate is increasing as with positive and with negative lean.

The mode of the changing of the actual outlet flow angle is shown at Fig. 6.11. Positive lean leads to an increase in the actual outlet flow angle near the root and decrease on the periphery; negative lean brings to the opposite effect. Given the nature of allocation of the losses along height of the blade as a lean result (Fig. 6.12), possible to say that an increase of the outlet flow angle leads to the secondary losses reducing.

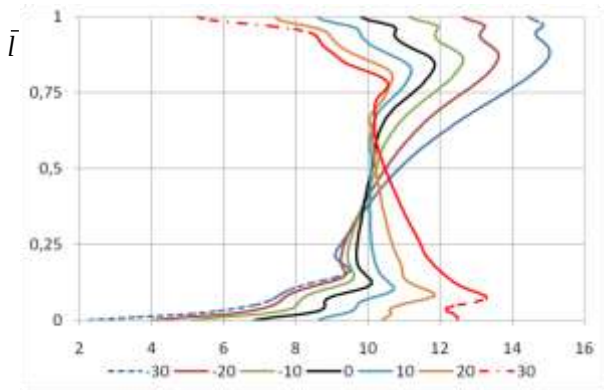

Figure 6.11 *Distribution of actual outlet flow angle along the blade height.*

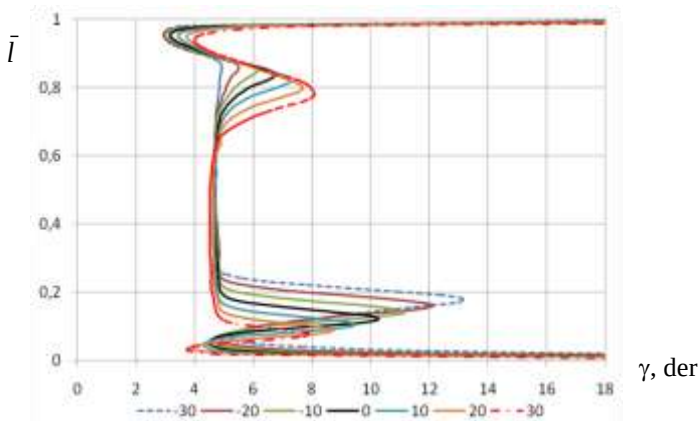

Figure 6.12 *Distribution of losses coefficient along the height behind cascade with different blades leans.*

An increase of the mass flow rate, as with a positive and with a negative lean occurs due to an increase in the integral actual outlet flow angle. In addition, with positive lean into increase of the mass flow rate also contributes reducing the integral losses and, accordingly, with a negative lean increasing of the losses slightly brings down increasing the mass flow rate, which takes place as a result of increase of the outlet flow angle.

The reasons for this significant changing of flow parameters with lean of the blades may be explained by the distribution of static pressure with various leans

in the control plane (Fig. 6.13). Isolines of static pressure in all cases are located almost vertically.

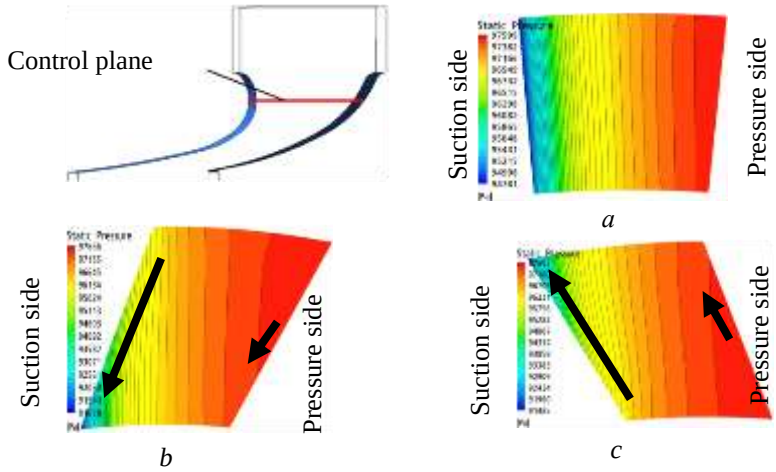

Figure 6.13 *The contours of the static pressure at control plane at different leans: a – 0 °; b – –30 °; c – 30 °.*

In the cascade without lean (Fig. 6.13) the pressure gradient along the height of the blade is virtually absent, unlike the blades with lean (Fig. 6.13*b* and Fig. 6.13*c*). Negative lean (see Fig. 6.13*b*) leads to pressure gradient appearance along the height of the blades, directed from the periphery to the root and on the suction side of the blade it is more substantial than on its pressure side. Positive lean brings to appearance of the opposite to the direction of pressure gradient at the surface of the blade (Fig. 6.13*c*).

6.6 The Influence of Complex Tangential Lean on the Flow in Circumferential Turbine Cascade

Object of study and boundary conditions are identical to the turbine cascade, that described in the previous section, with the exception of the relative height

of the blade, which in this case amounted to l/b = 0.714. Complex lean was carried out according to 2-nd method without changing the stagger angle of the profile.

Using proposed algorithm (section 6.4) the optimal blade's shape of the specified turbine guide blade was found on the sixth step of the variation parameters range refinement.

All 56 configurations of turbine blades shape were counted.

To solve the same problem using genetic algorithm, probably, hundreds of calculations would have required. The Table 6.1 shows the best value of the varied parameters and the best value of target function for each of the optimization stages.

At the 1–5 stages optimization of minimum objective function fall on the border range of variation parameters, at that on 4-th phase the function is minimal on the right edge of the border of variation parameters range, while on 5-th phase the function is minimal on the left edge. As a result, after the 6-th phase the values of the optimal parameters became $Y_s = 0.77$ and $Y_h = 0.80$.

Table 6.1 *History of optimization studies.*

Stage	**Initial**	**1**	**2**	**3**	**4**	**5**	**6**
Range, Y_s	0	0,02–0,18	0,16–0,25	0,25–0,38	0,38–0,73	0,73–1,58	0,65–0,94
Range, Y_h	0	0,02–0,18	0,16–0,25	0,25–0,38	0,38–0,73	0,73–1,58	0,67–0,98
Y_s	0	0,18	0,25	0,38	0,73	0,73	0,77
Y_h	0	0,18	0,25	0,38	0,73	0,73	0,8
ς, %	4,4010	4,3360	4,3025	4,2506	4,1688	4,1688	4,1687

Fig. 6.14 shows isolines of the objective function in the space of parameters Y_s and Y_h.

Lines of equal values of the objective function have incomplete shape due to the fact, that the obtained values of the function are distributed unevenly, and

most of them are situated in the neighborhood of line $Y_s = Y_h$. Dots on the Fig. 6.14 display the values of the parameters Y_s and Y_h on every stage of the optimization study. Comparison of Fig. 6.14 and Table 6.1 allows to see how the history of the changes Y_s and Y_h looks like.

Partial filling in by the calculation points of depicted area associated with large labour-intensive calculations and inability to evenly fill in the entire area. However, the carried out calculations are sufficient to argue that the domain of the minimum values of the target function was found. It is located near the center of the study area.

Fig. 6.14 shows that the objective function in the domain of minimum values has been changing slightly, which means that there is some freedom in choosing the optimal values of Y_s and Y_h.

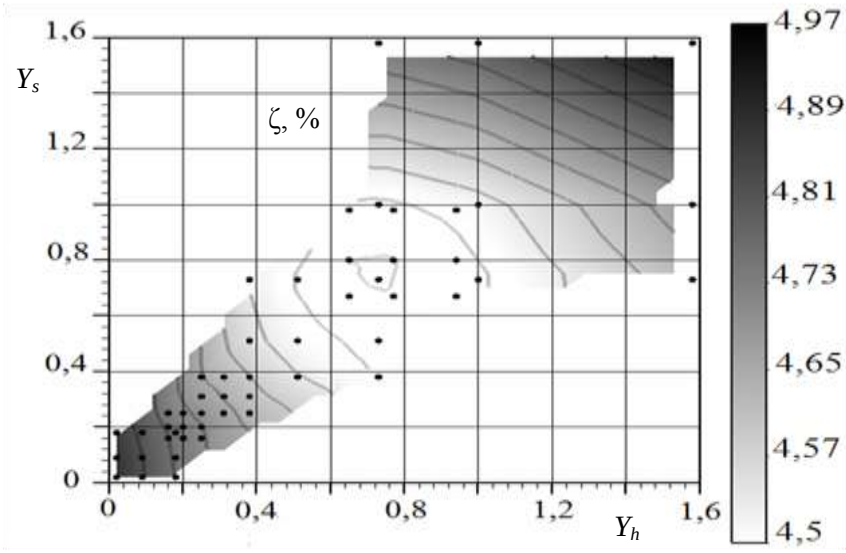

Figure 6.14 *Isolines of integral losses.*

Fig. 6.15 depicts the distribution of the losses coefficient of kinetic energy.

Analyzing these data, you can see that the peaks, characterizing horseshoe vortices in the optimal cascade, become less manifested and slightly have shifted in the direction of the flow center. Further confirmation of this is the distribution of the actual outlet flow angle in the optimal cascade (Fig. 6.16).

Indeed, looking at the optimized turbine blade (Fig. 6.17), we can see that in the bottom part of the blade the positive lean takes place and the negative lean has place at the top. It gave the possibility to obtain, predicted in the previous subsection, pressure distribution in the blade passage (Fig. 6.18) and on the suction side of the blade (Fig. 6.19), in other words, to combine the positive effects from simple leans, excluding the negative implications.

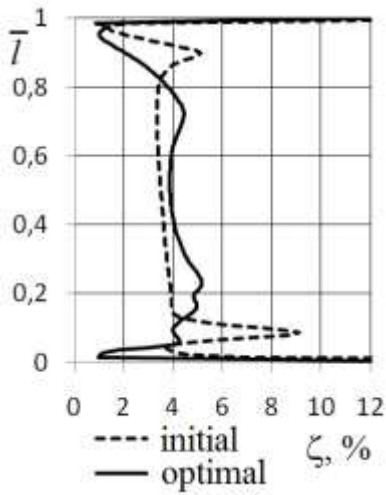

Figure 6.15 *Distribution of the losses coefficient along the blade height.*

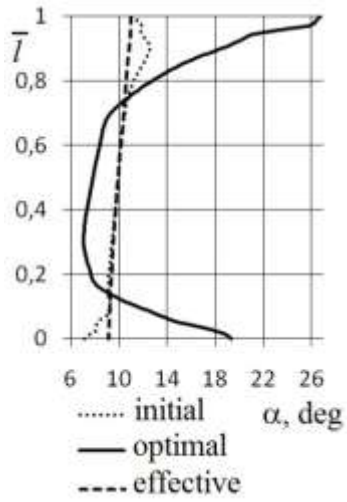

Figure 6.16 *Distribution of the outlet flow angle along the blade height.*

Some calculated characteristics of initial and optimized blade cascade has shown in the Table. 6.2. It is worth to note that mass flow rate and actual outlet flow angle has changed, and this changing is in the order of 10%. Changing of the outlet flow angle and, as a consequence, the mass flow rate is connected with changing of flow structure in the cascade and with reduced losses.

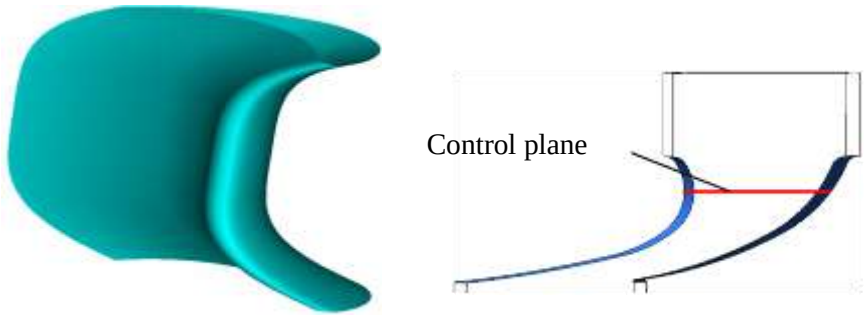

Figure 6.17 *Optimal cascade.*

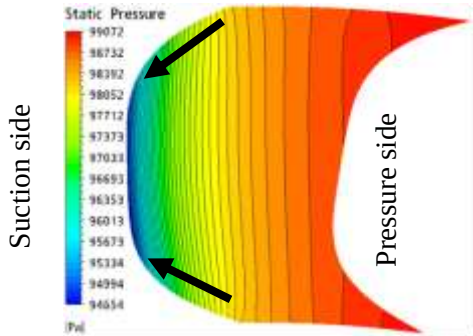

Figure 6.18 *The contours of the static pressures at the control plane in the optimal cascade.*

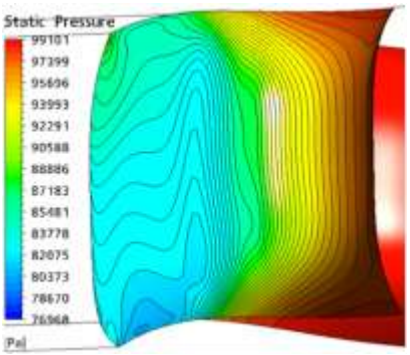

Figure 6.19 *The contours of the static pressures at the low pressure side of the optimal cascade.*

Table 6.2 *Characteristics of the initial and optimal cascade.*

Blade cascade	**Mass flow rate, kg/s**	**α_1, degree**	**ς_{total}, %**
Initial	0.9936	10.11	4.970
Optimal	1.0922	11.30	4.497

As a result, it can be stated that the proposed method gave the possibility to find the global minimum of the function, but the increase of the mass flow rate in the optimal cascade by almost 10% is unallowable.

So in further when conducting optimization this should be taken into account and the changing of the mass flow rate should be restricted by imposing an additional parameter of variation $\Delta\beta_s$.

6.7 Optimization with the Mass Flow Rate Preservation Through the Cascade

Review of research on the application of the complex tangential lean and its optimization, as well as conducted computational research has shown that using of complex lean gives the possibility to increase aerodynamic efficiency of turbine cascades. However, as previously noted, research on optimization of complex tangential lean with preserving mass flow rate through the cascade with high precision, currently we do not have. Using developed optimization approach it is possible to preserve in optimal cascade mass flow rate at the level of the initial cascade with a high accuracy.

Complex tangential lean reduces integral losses by reducing secondary losses. It is known, that with increasing l/b there is a reducing in the part of the secondary losses in integral losses and, accordingly, the benefit from optimization has to diminish.

Relative height criterion was taken not l/b, but the cascade's characteristic relation a/l, by analogy with the flows in the swivel tubes of rectangular cross-section.

Optimization problem is solved using two methods of stacking line parameterization. Research of the efficiency of the algorithm consists in attempts of optimization of turbine cascade at different $a/l = 0{,}16; 0{,}23; 044$ by changing of the blade height. It should be noted that for the blades with

$a/l \le 0.16$ optimization, using both methods of stacking parameterization, no longer led tot he reducing losses compared to the cascade without lean.

The size of the throat varies slightly due to the changing of stagger angle of the profile, which is associated with the preserving of the mass flow rate.

Special attention was given to the *FMM* accuracy, since it determines the validity of the results obtained with used optimization approach. Criterion of the accuracy is deviation of the values of the target function and the constraint function, which we obtain in *FMM* and in checking *CFD* calculation.

6.7.1 Optimization with Various *a/l* Using Method 1

The results of the optimization for *a/l = 0.44*

Taking into account the experience of previous studies, in Table 6.3 the ranges of parameters variation have shown. The correctness of their choice is confirmed by the fact that the optimal combination of varied parameters falls in this range already at the first step of the optimization.

Table 6.3 *Ranges of variation of parameters optimization.*

Parameter	min	max
Y_s	0.2	0.5
Y_h	0.6	0.9
$\Delta\beta_s$, degree	0	0.5

Then, a plan is created in accordance with the algorithm and relevant *CFD* calculations are produced (Table 6.4). The objective function – integral losses ζ, restriction function – mass flow rate through the calculation channel *G*.

A potential imperfection of the proposed optimization approach can be precision of the obtained *FMM*. Checking *CFD* calculation of optimal variant shows that the accuracy of the *FMM* is high because the objective function optimal values, projected by *FMM*, and restriction function with high enough

precision coincide with their values received as a result of *CFD* calculation (divergence in ζ is 0.005%, and in G – 0.017%). Differences of the mass flow rate in optimal and initial variant, based on the results of the *CFD* calculations, is 0.014%.

Table 6.4 *Results of the optimization using method 1 for* $a/l = 0.44$.

Parameters	Y_s	Y_h	$\Delta\beta_s$, **degree**	ξ, **%**	G, **kg/s**
Initial	0	0	0	6.46483	0.288864
1	0.500	0.900	0.250	6.06853	0.290430
2	0.500	0.600	0.250	6.12689	0.286293
3	0.200	0.900	0.250	6.12155	0.288312
4	0.200	0.600	0.250	6.19087	0.284589
5	0.500	0.750	0.500	6.17293	0.280340
6	0.500	0.750	0	6.01586	0.296079
7	0.200	0.750	0.500	6.23117	0.278370
8	0.200	0.750	0	6.07275	0.294141
9	0.350	0.900	0.500	6.17547	0.281387
10	0.350	0.900	0	6.01665	0.297062
11	0.350	0.600	0.500	6.23770	0.277339
12	0.350	0.600	0	6.08898	0.293340
13	0.350	0.750	0.250	6.11509	0.287041
opt. *FMM*	0.495	0.799	0.249	6.08030	0.288855
opt. *CFD*	0.495	0.799	0.249	6.08063	0.288905

Turbine cascade, obtained as the result of optimization, is shown at Fig. 6.20. The losses of the optimal cascade were reduced on 0.384% in absolute value or on 6.31% in relative value.

The distribution of the coefficients of losses and the actual outlet angles along the height of the blades for the initial and the optimal variants are represented at Fig. 6.21 and 6.22 respectively. These figures show that increasing of the losses in optimal variant took place in the central part of the cascade along with

reduction of the losses at the end areas, while actual outlet angle, on contrary, decreased in the central part and at the end areas.

Figure 6.20 *Optimal cascade obtained using method 1 for* $\boldsymbol{a/l} = 0.44$.

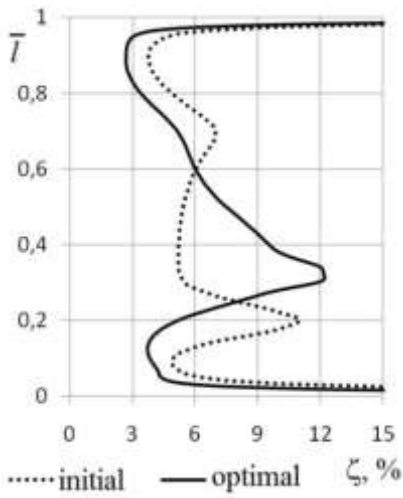

Figure. 6.21 *Distribution of the losses coefficient for a/l = 0.44.*

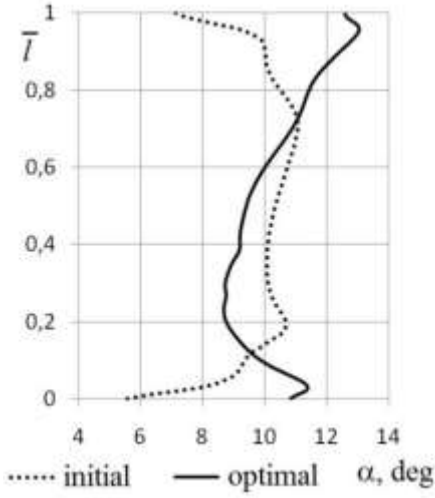

Figure 6.22 *Distribution of the outlet flow angle for* $a/l = 0.44$.

Table 6.5 *Ranges of the variation of optimization parameters.*

Parameter	min	max
Y_s	0.25	0.45
Y_h	–0.05	0.15
$\Delta\beta_s$, deg	–0.10	0.40

The results of the optimization for a/l = 0.23

Optimization results by method 1 at $a/l = 0.23$ were quite unexpected. Initial ranges of variation of parameters optimization were far from the final result. For this reason, the optimal variant was received only on the fifth stage of the optimization. Ranges of variation of parameters optimization of the fifth step are shown in the Table 6.5. Thus, to obtain the optimal variant in this case, 65 *CFD* calculations were required plus the calculation of initial variant and checking *CFD* calculation.

The appropriate calculation's plan for the fifth step with the results of determining the value of the target function, and restriction function listed in the Table 6.5.

Losses deviation between optimal variants for *FMM* and *CFD* made up 0.020% and the corresponding deviation of *G* in relative terms made up 0.006%. The mass flow rate was preserved with an accuracy of 0.004% in relative terms.

Table 6.6 *Results of the optimization using method 1 for a/l = 0.23.*

Parameters	Y_s	Y_h	$\Delta\beta_s$ **, degree**	ξ,**%**	*G*, **kg/s**
Initial	0	0	0	5.45888	0.603025
1	0.450	0.15	0.15	5.32876	0.604827
2	0.450	–0.05	0.15	5.37593	0.599889
3	0.250	0.15	0.15	5.38874	0.598860
4	0.250	–0.05	0.15	5.44175	0.595029
5	0.450	0.05	0.40	5.45634	0.586522
6	0.450	0.05	–0.10	5.25013	0.617545
7	0.250	0.05	0.40	5.51989	0.581216
8	0.250	0.05	–0.10	5.31001	0.611905
9	0.350	0.15	0.40	5.46201	0.585955
10	0.350	0.15	–0.10	5.25297	0.616883
11	0.350	–0.05	0.40	5.50755	0.581701
12	0.350	–0.05	–0.10	5.30059	0.612414
13	0.350	0.05	0.15	5.38528	0.598818
opt. *FMM*	0.408	–0.0379	0.0816	5.35769	0.603015
opt. *CFD*	0.408	–0.0379	0.0816	5.35660	0.603049

Turbine cascade, obtained as the result of the optimization, is shown at Fig. 6.23. The losses of the optimal cascade were reduced on 0.102% in absolute value or on 1.89% in relative value.

Figure 6.23 *Optimal cascade obtained using method 1 for a/l = 0.23.*

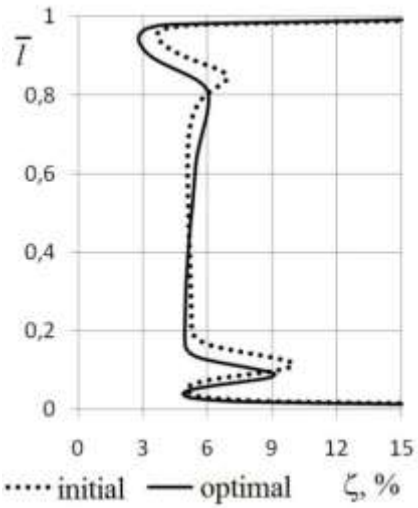

Figure 6.24 *Distribution of the losses coefficient for a/l = 0.23.*

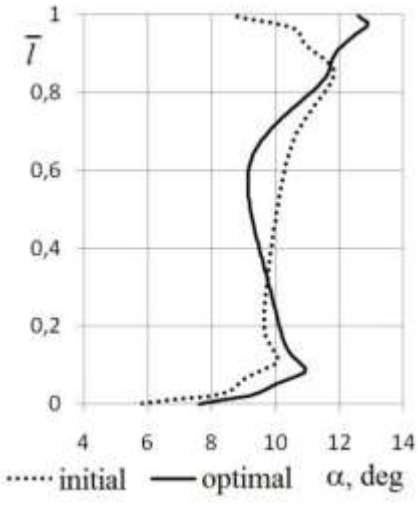

Figure 6.25 *Distribution of the outlet flow angle for a/l = 0.23.*

6.7.2 Optimization with Various *a/l* Using Method 2

The results of the optimization for a/l = 0.44

In this case were taken the ranges of parameters variation listed in the Table 6.7.

The solution was obtained in the first step of the optimization. The results of calculation using optimization method 2 have shown in the Table 6.8.

Table 6.7 *Ranges of variation of parameters optimization.*

Parameter	min	max
Y_s	0,2	0,5
Y_h	0,7	1
$\Delta\beta_s$, deg	0	0,5

In this case, losses deviation between optimal variants for *FMM* and *CFD* made up 0.006%, and the corresponding deviation of *G* in relative terms made up 0.017%. The mass flow rate was preserved with an accuracy of 0.017% in relative terms.

Table 6.8 *Results of the optimization using method 2 for a/l = 0.44.*

Parameters	Y_s	Y_h	$\Delta\beta_s$ **, degree**	**ξ, %**	***G*, kg/s**
Initial	0	0	0	6.46483	0.288864
1	0.5	1	0.25	6.22297	0.287388
2	0.5	0.7	0.25	6.24602	0.284416
3	0.2	1	0.25	6.27384	0.287651
4	0.2	0.7	0.25	6.28318	0.284258
5	0.5	0.85	0.5	6.29683	0.277681
6	0.5	0.85	0	6.15406	0.293667
7	0.2	0.85	0.5	6.36221	0.277942
8	0.2	0.85	0	6.19314	0.293665
9	0.35	1	0.5	6.33226	0.279469
10	0.35	1	0	6.16875	0.295172
11	0.35	0.7	0.5	6.34015	0.276185
12	0.35	0.7	0	6.18533	0.292074
13	0.35	0.85	0.25	6.24891	0.285655
opt. FMM	0.498	0.856	0.154	6.19839	0.288865
opt. CFD	0.498	0.856	0.154	6.19875	0.288914

Turbine cascade, obtained as the result of the optimization, is shown at Fig. 6.26. The losses of the optimal cascade were reduced on 0.266% in absolute value or on 4.20% in relative value.

Figure 6.26 *Optimal cascade obtained using method 2 for a/l = 0.44.*

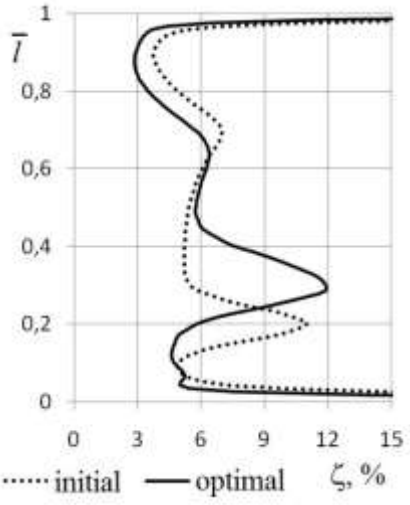

Figure 6.27 *Distribution of the losses coefficient for a/l = 0.44.*

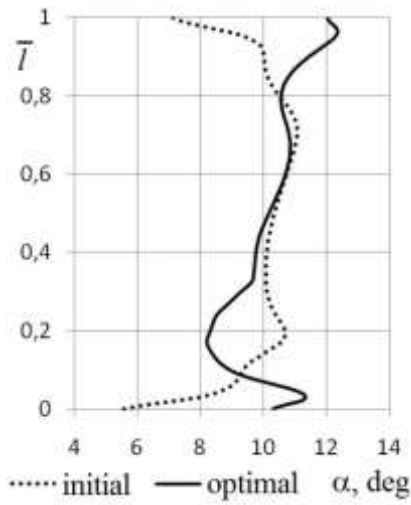

Figure 6.28 *Distribution of the outlet flow angle for a/l = 0.44.*

Comparing increasing of aerodynamic efficiency using methods 1 and 2, we can conclude that for this turbine cascade with a/l = 0.44 method 1 is more preferred because its use has significantly reduced integral losses.

The distribution of the coefficients of losses and the actual outlet angles along the height of the blades for the initial and the optimal variants are represented at Fig. 6.27 and 6.28 respectively. These figures show that increasing of the losses in optimal variant took place in the central part of the cascade along with

reduction of the losses at the end areas, while actual outlet angle, on contrary, decreased in the central part and at the end areas.

The results of the optimization for a/l = 0.23

Ranges of variation of parameters optimization are shown in the Table 6.5. In this case, the optimal variant was obtained at the first step of optimization.

Table 6.9 *Ranges of variation of parameters optimization.*

Parameter	min	max
Y_s	0.25	0.45
Y_h	0.40	0.60
$\Delta\beta_s$, deg	0	0.50

The plan of calculations with the results of determining the value of the objective function, and the restriction function listed in the Table 6.10.

In this case the losses deviation between optimal variants for *FMM* and *CFD* made up 0.032% and the corresponding deviation of *G* in relative terms made up 0.008%. The mass flow rate was preserved with an accuracy of 0.009% in relative terms.

Turbine cascade, received as the result of the optimization, is shown at Fig. 6.29. Losses in the new cascade made up 5.314% that on 0.145% in absolute value or on 2.69% in relative value is smaller than in the initial variant.

Application of the optimal complex lean by the method 2 when a/l = 0.23 resulted in a reduction of losses in end areas, but in the core of the flow losses remained almost unchanged. On contrary, actual outlet angle decreased in the central part of the cascade and increased in the end areas, the same as in the previous cases.

Thus, the optimization method 2 gave the possibility to reduce integral losses greater than method 1.

6.7.3 Reasons of Increasing the Efficiency of Optimized Cascades

Consider the flow in the initial cascade for *a/l*=0.23. Comparing the field of the total pressure at the value of $\overline{l} = 0.96$ and $\overline{l} = 0.5$ of the initial blade (Fig. 6.32), it can be seen that the thickness of the boundary layer in the similar areas much less at the height $\overline{l} = 0.96$ of the blade than in the core flow.

At the same time, the boundary layer thickness on its low-pressure side plays an essential role in the losses formation on the blade. This agrees well with the corresponding graphs of the losses coefficient distribution in height of the blade (see. Fig. 6.30).

Explanation of the reducing of boundary layer thickness in indicated areas at the periphery and the root can be given based on the analysis of the flow on the suction side of the blade (Fig. 6.33). On Fig. 6.33 line *S* marked the line of detachment of the channel vortex.

Table 6.10 *Results of the optimization using method 2 for a/l = 0.23.*

Parameters	Y_s	Y_h	$\Delta\beta_s$, **degree**	**ξ, %**	***G*, kg/s**
Initial	0	0	0	5.45888	0.603025
1	0.450	0.600	0.250	5.29505	0.602551
2	0.450	0.400	0.250	5.35124	0.596915
3	0.250	0.600	0.250	5.32629	0.601706
4	0.250	0.400	0.250	5.38373	0.594765
5	0.450	0.500	0.500	5.41731	0.583745
6	0.450	0.500	0	5.22568	0.615261
7	0.250	0.500	0.500	5.45064	0.582208
8	0.250	0.500	0	5.25427	0.613547
9	0.350	0.600	0.500	5.41036	0.586293
10	0.350	0.600	0	5.21395	0.617685
11	0.350	0.400	0.500	5.46167	0.579785
12	0.350	0.400	0	5.26454	0.610895
13	0.350	0.500	0.250	5.33404	0.598298
opt. *FMM*	0.407	0.408	0.143	5.31201	0.603023
opt. *CFD*	0.407	0.408	0.143	5.31373	0.602973

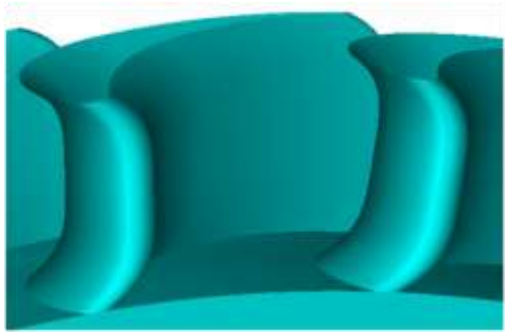

Figure 6.29 *Optimal cascade obtained using method 2 for a/l = 0.23.*

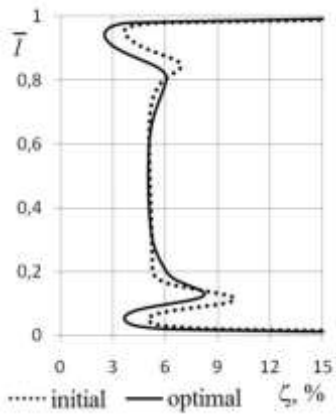

Figure 6.30 *Distribution of the losses coefficient for a/l = 0.23.*

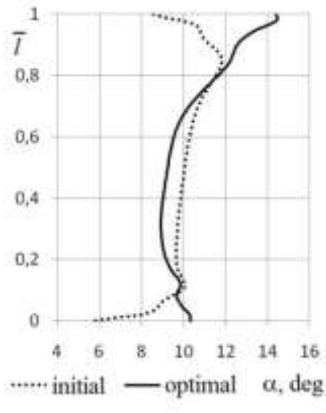

Figure 6.31 *Distribution of the outlet flow angle for a/l = 0.23.*

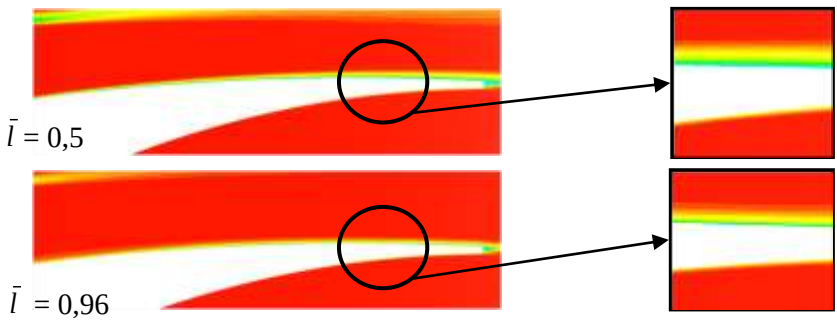

Figure 6.32 *The field of the total pressure in the initial cascade.*

It is the line of distinction of the two main border flows on the suction side of the blade:

1) flow along the blade from the leading edge to the trailing edge;

2) cross-over flow, that comes from the ends of the channel and penetrates, due to its inertia, on the blade (this flow is a part of the peripheral and root channel vortices) (Fig. 6.34).

Thus, on the suction side of the blades, there are areas with variously formed boundary layers. This explains the different thickness of the boundary layer in the appropriate places on the suction side of the blade.

As a result, the important conclusion can be formulated: the channel vortex leads to the formation on the suction side of the blade up to the line S of the boundary layer thickness less than the thickness of the boundary layer of the main flow around the blades. Thus the secondary flows have not only negative, but a positive effect, and properly distribution the stream structure can be used for creating optimal forms of turbine blades.

From the last considerations, it is possible to prove the reduction mechanism of aerodynamic losses for turbine cascade by applying optimal complex lean: the complex lean leads to the movement of the line *S* in the direction of the flow core and therefore to increasing the areas with smaller losses.

Figure 6.33 *Stream lines on the suction side of the initial blade.*

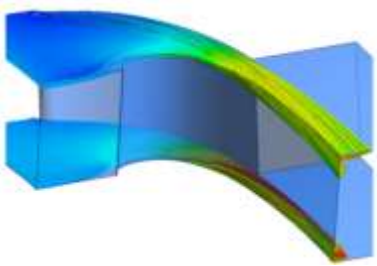

Figure 6.34 *Stream lines of the secondary flow of the initial blade.*

Displacement of the line *S*, when using complex tangential lean, takes place because of pressure gradient appearance on the suction side of the blade, which occurs when complex tangential lean is used. The result of this aerodynamic effect is certain offset of the saddle point from the pressure side of the blade to the suction side, therefore, to more earlier descent of the channel vortex from the end of the blade to the blade itself (Fig. 6.35). Descended on the blade, vortex, in turn, under the influence of pressure gradient slightly shifted on the blade toward the core of the flow, that leads to an increase of the part of the flow on the suction side of the blade with a smaller boundary layer than in the core of the flow.

As a result the proposed optimization algorithm made possible to find the optimum position of the line channel vortex detachment on the suction side of the blade by complex the lean optimization.

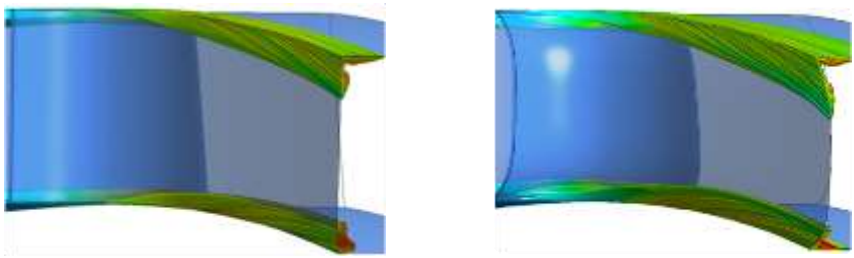

a b

Figure 6.35 *The move of the channel vortex on the suction side: a – initial cascade; b – optimal cascade using method 2.*

7

Experience and Examples of Optimization of Axial Turbines Flow Paths

In this chapter, as an example of practical use of the developed theory of optimal design of axial turbines flow paths, the results of the studies, related to the optimization of parameters of flow path of the high pressure cylinders (HPC) of 220, 330 and 540 MW capacities turbines, operating at nominal mode, as well as examples of optimization turbo-expander and low pressure turbine of gas turbine unit, taking into account the mode of its operation, are presented. The entire complex of calculation research was conducted using mathematical models of flow path (FP) of axial turbines, described in Chapter 2.

In addition, in the studies variants of mathematical models of FP "with the specified profiles" [38] were also used, which allowed with more accuracy determine geometric characteristics of turbine cascades, in particular, the inlet geometric angles of working and nozzle cascades, that are changing with the changing of stagger angles of the profiles. The latter had a significant impact on the amount of additional losses related to the incidence angle of inlet flow of working fluid.

7.1 Multi-Criterion Optimization of HPC of Powerful Steam Turbines at Nominal Operational Mode

7.1.1 A Preliminary Study of Influence of Quality Criteria Weights Coefficients on the Optimization Results

Practice of the optimal design of axial turbines cylinders has showed that when optimizing steam turbine cylinder with extraction of working fluid for regeneration and heat supplying at least two criteria – the efficiency of the cylinder flow path and its capacity must be taking into account [38, 40-42].

Using the convolution of quality criteria in accordance with (1.37) allows efficiently solve the multi-criterion optimization problems corresponding the Pareto front.

As an example of the effectiveness of the use of convolution (1.37) the results of the optimization of HPC FP of a powerful steam turbine by two criteria - power and cylinder efficiency for different values of the weight coefficients μ_i are presented in Table 7.1 and Fig. 7.1.

Table 7.1 *Optimization results with different weight coefficients of the optimization criteria for power (μ_N) and efficiency (μ_{η_d}).*

The optimization task number	μ_N	μ_{η_d}	N, MW	η_d , %
1	0	1	124.398	82.49
2	0.2	0.8	124.981	82.23
3	0.4	0.6	125.844	81.77
4	0.5	0.5	126.436	81.07
5	0.6	0.4	126.804	80.15
6	0.8	0.2	127.173	78.50
7	1	0	127.288	77.82

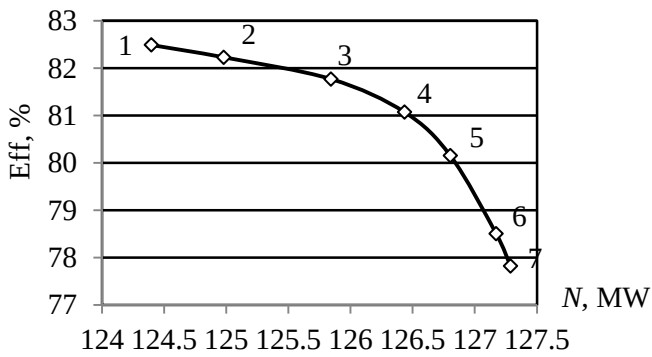

Figure 7.1 *Pareto front solutions of the optimization task with two criterions for HPC FP powerful steam turbine.*

Numbers on the curve corresponds to the numbers of optimization problem in the Table 7.1.

7.1.2 Optimization of HPC Parameters of the 220 MW Capacity Turbine for Nuclear Power Plant

The number of optimization parameters – 33:

- level 1 (cylinder) - optimized for 19 parameters:
  - Root diameter and height of the nozzle blades of the first stage of the cylinder.
  - Meridional disclosing of the channels of the nozzle and working cascades.
  - Effective exit angles of the nozzle and working cascades of all turbine stages.
- 2-nd level (stage) - optimized for 14 parameters:
  - The number of the blades in the nozzle cascades for all turbine stages.
  - The number of the blades in the working cascades for all turbine stages.

Quality criteria applied when optimizing – the criterion vector that inclu-des the normalized values of internal relative efficiency of the cylinder (η_{oi}) and its power (N) with equal weight coefficients.

The results of the optimization of the HPC FP of the 220 Mw capacity turbine [39] are listed in Table 7.2 and in Fig. 7.2, where η_d – Moliere diagram efficiency of FP; η' – the ratio of efficiency of the stages to Moliere diagram efficiency of the initial variant of the cylinder; η_{oi} – internal efficiency of FP; $\Delta\eta_{oi}$ – gain of the internal efficiency of the optimal FP; N – power; ΔN – the power gain of the optimal variant of the HPC FP.

Table 7.2 *The integral indicators of initial and optimal variants of FP.*

Variant of HPC FP	η_d	η_{oi}	N, MW	$\Delta\eta_{oi}$, %	ΔN, kW
1 Initial, 6 st.	0.7836	0.7690	119.425	0	0
2 Optimal, 7 st.	0.8096	0.8011	125.375	3.21	5949.45
3 Final, 7 st.	0.8063	0.7961	124.824	2.71	5399.06

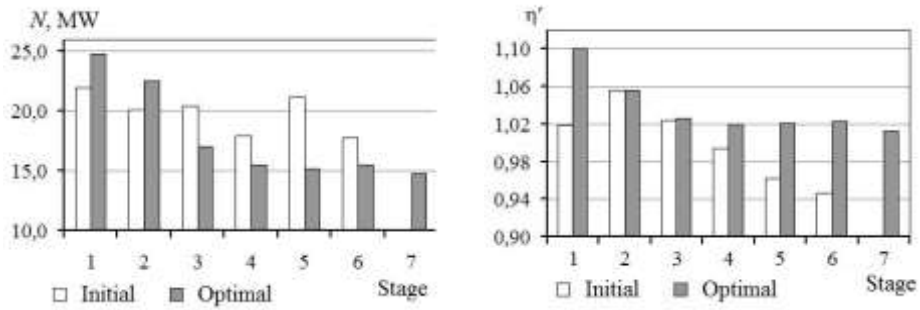

a b

Figure 7.2 *A comparison of the power (a) and (b) efficiency of the initial and optimal variants of stages of HPC FP 220 MW capacity turbine.*

Improvement of the quality indicators of the optimized FP obtained through:

- rational distribution of the cylinder heat drop, having in its disposal, between the stages;
- some decreasing of the axial speed components and ensuring closer to axial outlet working fluid from the stages, resulting in reducing the exit velocity losses;
- reducing the incidence angles, that provides the improving efficiency of the nozzle and working cascades;
- increasing the mean diameter of the stages, that led to obtaining the optimal values of the ratio of the velocities (u/C_0);
- reducing the specific weight of the losses near the hub and the shroud boundaries by increasing the height of the blades;

- the optimal value of the nozzle and working cascades relative pitch, which also led to an increase of their effectiveness.

The final variant is obtained by optimization taking into account the technological restrictions on the production of the flow path parts. This explains the slight decreasing of efficiency and cylinder capacity compared to the best option without restrictions.

The optimal variant of HPC FP of the 220 MW capacity turbine for nuclear power plant is obtained, which characterized by high perfection levels of aerodynamic indices, providing a boost of power on 5.4 MW, of internal efficiency on 2.71% and Moliere diagram efficiency on 2.27% as compared to the initial version of FP.

7.1.3 Optimization of High-Pressure Cylinder Parameters of the 330 MW Capacity Turbine

The number of optimization parameters – 55:

- level 1 (cylinder)-optimized for 44 parameters:
  - Root diameter and height of the nozzle blades of the first stage of the cylinder.
  - Meridional disclosing of the channels of the nozzle and working cascades.
  - Effective exit angles of the nozzle and working cascades of all turbine stages.
- 2-nd level (stage)-optimized for 11 parameters:
  - The number of the blades in the working cascades for all turbine stages.

Quality criteria applied when optimizing – the criterion vector that inclu-des the normalized values of Moliere diagram efficiency of the cylinder (η_d) and its power (N) with equal weight coefficients.

The results of the optimization of the HPC FP of the turbine 330 MW capacity turbine are listed in Table 7.3 and in Fig. 7.3, where η_d – Moliere diagram efficiency of FP; η' – the ratio of efficiency of the stages to Moliere diagram efficiency of the initial variant of the cylinder; η_{oi} – internal efficiency of FP; $\Delta\eta_{oi}$ – gain of the internal efficiency of the optimal FP; N – power; ΔN – the power gain of the optimal variant of the HPC FP.

Table 7.3 *Integral indicators of initial and optimal variant of HPC FP.*

Variant of HPC FP	η_d	η_{oi}	N, **MW**	$\Delta\eta_{oi}$, **%**	ΔN, **kW**
Initial	0.8595	0.8119	95.573	0	0
Optimal	0.8989	0.8656	101.773	5.37	6200.0

Improvement of the quality indicators of the optimized FP obtained through:

- more rational distribution of the cylinder heat drop, having in its disposal, between the stages;
- application of the optimal configuration of meridional shape of FP with a slightly reduced heights blades;
- increasing value of the effective nozzle exit angles, providing the reduction of the incidence angles on the working cascades;
- improving the efficiency of working cascades through the optimal choice of stagger angles and numbers of the blades, resulting in a significant reduction of losses from the incidence angle;
- reducing the degree of reaction level of the stages and, as a consequence, reducing the losses from root and radial leakages.

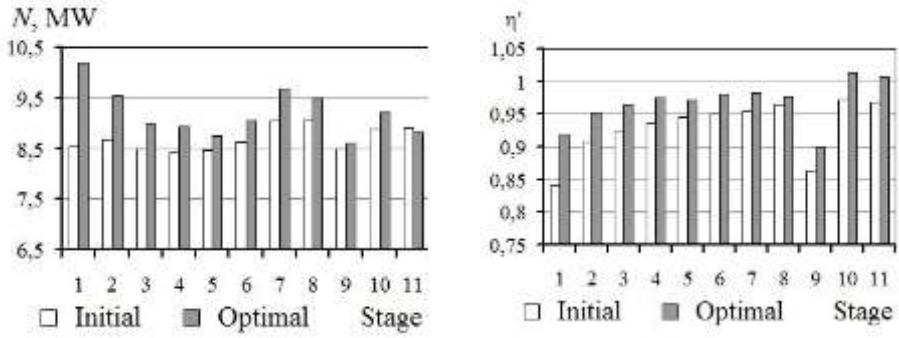

a *b*

Figure 7.3 *Comparison of the power (a) and (b) efficiency of the stages of initial and optimal variants of HPC FP of the 330 MW capacity turbine.*

Practical application of the developed optimization theory provided the solution of the task: the optimum variant HPC PF of the 330 MW capacity turbine was obtained, which characterized by high perfection levels of aerodynamic indices, providing a boost of power on 6.2 MW, of the relative internal efficiency on 5.76% and Moliere diagram efficiency on 3.94% in comparison with the initial version of FP.

7.1.4 Optimization of the HPC Flow Path Parameters of the 540 MW Capacity Turbine

Features of the initial variant of the HPC FP:

- FP of the 9 stages HPC has high enough quality integral indicators, which have been achieved thanks to the very high level of aerodynamic perfection of the flow path of the cylinder:
  - numbers of the nozzle and working cascades blades are close to the optimal values;

- the inlet flow incidence angles at the nozzle and work cascades are close enough to the possible minimum values given used profiles and blades production technology;
- the root degrees of reaction provide fairly low levels of hub leakages;
- the use of highly effective radial seals has significantly reduced radial leakages.

However, in the construction of FP reserves of possible efficiency gains were identified associated with not quite rationally distribution of disposable heat drop between the cylinder stages and somewhat inflated level of root leakages in first stage.

The number of optimization parameters of HPC FP of the turbine 540 MW capacity – 55:

- level 1 (cylinder) - optimized for 37 parameters:
  - Root diameter and height of the nozzle blades of the first stage of the cylinder.
  - Meridional disclosing of the channels of the nozzle and working cascades.
  - Effective exit angles of the nozzle and working cascades of all turbine stages.

Due to the fact that in the initial variant of the HPC FP number of the nozzle and working cascades blades near by the optimal values, the second level of optimization (stage) was not used in this task.

Quality criteria applied when optimizing – the criterion vector that includes the normalized values of Moliere diagram efficiency of the cylinder (η_d) and its power (N) with equal weight coefficients. The results of the optimization of the HPC FP of the turbine 540 MW capacity are listed in Fig. 7.4, where N – power

and η' – the ratio of efficiency of the stages to Moliere diagram efficiency of the initial variant of the cylinder.

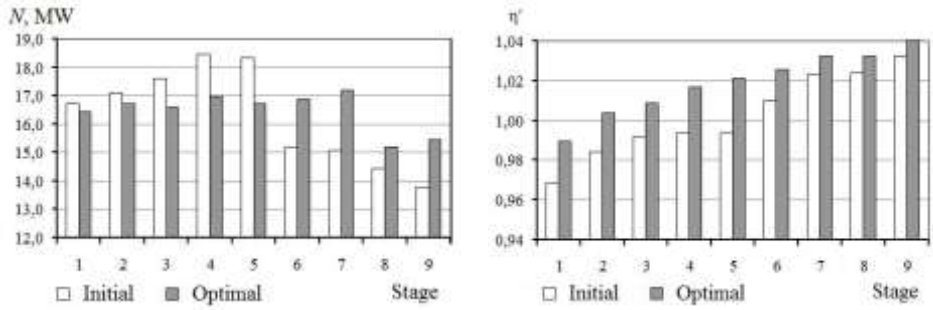

a *b*

Figure 7.4 *Comparison of the power (a) and efficiency (b) of the stages of initial and optimal variants of HPC FP of the 540 MW capacity turbine.*

Improvement of the quality indicators of the optimized FP obtained through:

- a more rational distribution of the disposal cylinder heat drop, between the stages, thereby improving the integral indicators of the cylinder quality;
- some decrease of axial velocity component and ensuring closer to axial outlet of working fluid from the stages, that reduced the exit velocity losses, improving inlet conditions for nozzles cascades (which led to an improvement in their effectiveness);
- close to optimal values of velocities ratio (u/C_0), obtained by incre-asing the mean diameter of the stages;
- reduction in the share of the losses near the hub and the shroud boundaries associated with increasing the heights of the blades;
- using in 6–9 stages of the blades a highly effective *1MMC* profile (Chapter 5), which provided a good matching flow inlet angles and the

geometric inlet angles of the working cascades, that resulted in increasing their efficiency;

- obtaining the optimal twist laws of the β_{2e} angles at the outlet of the working wheels of 6–9 stages that contributed to the rational distribution of the gas-dynamic parameters along the radius of these stages.

So, the practical application of the developed optimization theory secured the solution of the requested task: the optimum variant of HPC FP of the 540 MW capacity turbine was obtained, which characterized by high perfection levels of aerodynamic indices, providing a boost of power on 1.4 MW, of inner efficiency on 1.52% and Moliere diagram efficiency on 1.63% in comparison with the initial version of FP.

7.2 Optimal Design of the Axial Turbines Flow Paths Taking into Consideration the Mode of Operation

For demonstration of opportunities of the developed complex of the methods, algorithms and mathematical models for solving the problems of optimal design of the turbine units taking onto account their mode of operation [38, 40–42] the results of optimization research of turbine expander flow path and of gas turbine unit GTU GT-750-6M low pressure turbine flow path are presented below.

7.2.1 Optimization of Rendering Turbine Expander Unit (RTEU) Flow Path of 4 MW Capacity With Rotary Nozzle Blades

In gas pipelines, natural gas is transported under the pressure 35–75 atmospheres. Before serving the natural gas to the consumer its pressure must be lowered to the level of pressures local supply systems. At the moment gas distribution stations widely are using technologies of utilization of natural gas let-down pressure before serving the consumer. To extract energy from compressed gas the special rendering turbine expander units (RTEU) are used in

which the potential overpressure energy is converted into mechanical work of a rotor rotation of a turbine, which serves as generator drive.

Seasonal unevenness of natural gas consumption, usually caused by environmental temperature, leads to a deeply no projected RTEU operation modes and adversely affect their performance and service life. For example, the gas flow through the flow path of the RTEU during the year may vary in ranges from 0.25–0.35 to 1.05–1.25 from the rated value. The foregoing attests to the relevance and necessity of taking into account the factor variability of operation loads during the selection of the basic geometric parameters of the RTEU FP.

This section provides results of optimization of 4-stage flow path of existing design of RTEU taking into account real operation modes of it, using the developed algorithm [40].

Operating conditions of the considered RTEU are characterized by significant monthly uneven mass flow rate of the working fluid through the flow path of the unit with fixed heat drop and rotor speeds:

- full gas pressure at the inlet of FP ..... $P_0^* = 1.2$ MPa;
- full gas temperature at the inlet of FP ..... $t_0^* = 110\,°C$;
- static gas pressure at the outlet of FP ..... $P_2 = 0.19$ MPa;
- the rotor turbine speed ..... n = 8000 rpm.

The mass flow rate of natural gas, depending on the operating mode, changed in the range from 4.94 to 20.66 kg/s (the mass flow rate at the design mode is $G_{nom} = 16.66$ kg/s).

At present several ways to regulate the mass flow through the RTEU FP are known. The changing of the walk-through sections of nozzle cascade (NC), thanks to the use of rotary nozzle blades, is the most effective.

It is known that the implementation of the rotary nozzle blades can significantly extend the range of workloads of the turbine installation and improve performance indicators of FP. However, to get the maximum effect from the rotation of the nozzle blades, there is a need to further address the challenge of defining optimal angles α_{1e} for each stage, depending on the operating mode of the RTEU FP.

In accordance with the terms of the design, mass flow regulation of the working fluid through the flow path of the RTRU has been carried out by turning of the nozzle blades (changing the outlet angles α_{1e}) of all stages. Optimization was carried out taking into account the 12 operational modes of turbine expander (one month duration of each mode). The mass flows of natural gas through the FP for the specified modes are shown in the Table 7.4.

Table 7.4 ***T****he natural gas mass flows through the RTEU FP for specified operational modes.*

#	1	2	3	4	5	6	7	8	9	10	11	12
G_0, kg/s	18.71	20.66	18.71	10.18	6.33	6.28	4.94	6.14	7.17	10.55	17.57	20.35

Two levels of recursive optimization algorithm (section 1.2.1) – "Cylinder" (Layer 1 and Layer 2) and "Stage" were involved in the optimization process. At the level of "Cylinder" recursive optimization algorithm is called on not only for "Stage" level but for Layer 1 and Layer 2. As can be seen from Fig. 7.5, at the top level "Cylinder" (Layer 1) the vector of varied parameters of created *FMM* has been generated from 16 parameters, one of which is operational mode (the mass flow at the cylinder inlet – G_0) and the remaining 15 are design parameters.

They included effective outlet flow angles from nozzle and blades (α_{1e}, β_{2e}), and average diameters and heights of the blade wheel cascades (D_2 and l_2). Mean diameters and heights of nozzle wheel cascades (D_1 and l_1) for each

stage were determined based on values similar to the parameters of the blade wheel cascades taking into account recommendations about overlap size for each RTEU stage. At the below laying level "Stage" for each stage except the first the vector of varied parameters of *FMM* was formed of 9 parameters ($D_2, l_2, \alpha_1, \beta_2, u/C_0, z_{1,2}, b_{1,2}$). For the 1-st stage the dimension of *FMM* vector is equal 8 (angle α_1 isn't a member of *FMM* of the 1-st stage).

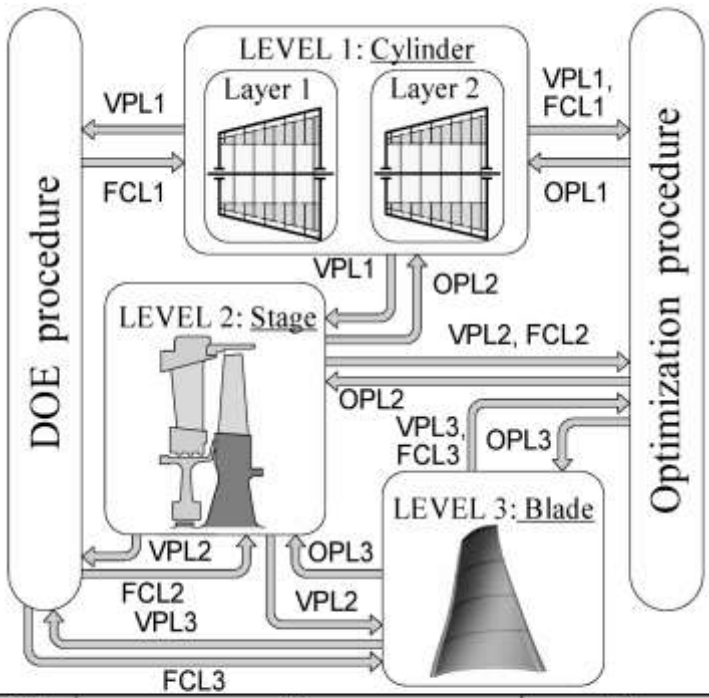

Level	VPL	OPL
Cylinder	$d_{1,2}; l_{1,2}; \alpha_1; \alpha_{0g}; \beta_2; \beta_{1g}; P_0; i_0; P_2; w/C_0$	$d_{1,2}; l_{1,2}; \alpha_1; \alpha_{0g}; \beta_2; \beta_{1g}$
Stage	$d_{1,2}; l_{1,2}; \alpha_1; \alpha_{0g}; \beta_2; \beta_{1g}; P_0; i_0; P_2; u/C_0; Z_{1,2}; b_{1,2}; m_{1,2}$	$Z_{1,2}; b_{1,2}; m_{1,2}$
Blade	$\alpha_1; \alpha_{0g}; \beta_2; \beta_{1g}; Z_{1,2}; b_{1,2}; m_{1,2}; r_1; \omega_{1,2}$	$r_1; \omega_{1,2}$

Figure 7.5 *The structure of optimal design technique.*

The sequence of the general optimization task solution looks as follows. Previously, using the DOE theory (paragraph 1.3) the *FMM*s of the level

"Stage" were created in the form of full quadratic polynomials (1.2). The *FMM* of the "Cylinder" level (Layer 1) was build next.

According to a design of experiment matrix from top level "Cylinder" to level "Stage" parametrical restrictions in the form of values $D_2, l_2, \alpha_{1e}, \beta_{2e}, u/C_0$ arrive. Concrete level of these parameters is defined by a current point of the plan of numerical experiment of level "Cylinder" (Layer 1). At level "Stage" taking into account the arrived parametrical restrictions local optimizing tasks by definition of optimal values of blades numbers ($z_{1,2}$) and chords values ($b_{1,2}$) of nozzle and blade wheel cascades of each stage are solved.

The received optimal values of these parameters are passed to the top level "Cylinder" (Layer 2) for calculation of the optimal angles α_{1e} along the FP depending on the mass flow of working fluid at the entrance to the turbine expander.

At the end of the optimization process under optimal values of "Cylinder"-level parameters, except values of chords and numbers of blades, inlet metal angles of nozzle and blade wheel cascades of each stage are specified. The values of the specified angles are defined taking into account a weight part of quality criterion of each operational mode.

As quality criterion for an estimation of the flow path efficiency at the level "Cylinder" the value equal to total work of the cylinder for a selected period of time one year (*T*)

$$U = \int_{t=0}^{t=T} N_{cyl}(t)\,dt\,, \tag{7.1}$$

defined according to the developed mathematical model (section 2.2.3), was used.

Given the assumption that the duration of the modes is the same, this criterion was reduced to the sum of the "regime" cylinder capacity ($\sum_{i=1}^{n} N_{cyl}^{i}$, where *n* is the number of modes). To assess the quality criterion at "Stage" level the internal relative efficiency of the corresponding stage was used.

Since this task was solved for the FP with standard type of the nozzles profiles H-2, changing the angle α_{1e} takes into account and corresponding changing of the inlet metal angle of the nozzle wheel cascade (α_{0g}). When calculating the losses, associated with incidence angles at the inlet of the cascade, the influence of the blade's inlet flow angle on the losses in accordance with experimental data was taken into account.

Inlet metal angles of the blade wheel cascade for each stage were determined by averaging their values across 12 modes of operations taking into account weight proportion of quality criterion of each mode.

The values of the "basic" design parameters, obtained by solving the general optimization task, are listed in the Table 7.5.

The received distributions of angles α_1 for each stage of the flow path as functions of mass flow change are presented in Fig. 7.6. Apparently from Fig. 7.6 optimal curves of angles differ greatly from the linear curve received at uniform simultaneous turn of nozzles.

Table 7.5 *Results of optimal design along stages of the turbine expander.*

Parameter	Stage number				Stage number			
	Prototype				Optimal design			
	1	2	3	4	1	2	3	4
D_1, m	0.48	0.48	0.48	0.48	0.481	0.483	0.489	0.498
D_2, m	0.48	0.48	0.48	0.48	0.482	0.484	0.49	0.499
l_1, m	0.0305	0.035	0.0425	0.051	0.029	0.036	0.045	0.056
l_2, m	0.031	0.0375	0.0465	0,056	0.032	0.039	0.049	0.06
β_2, degree	22	25.7	29.1	34	21.7	25.52	28.43	34.15
z_1	54	54	46	46	54	58	48	49
z_2	69	69	53	53	69	78	61	59
b_1, mm	35.099	35.099	42.118	42.118	35.345	35.257	42.034	42.761
b_2, mm	30.809	30.809	40.15	40.15	33.25	30.179	39.187	40.754
β_{1g}, degree	30.75	35.68	44.03	53.72	38.21	32.27	38.97	48.31

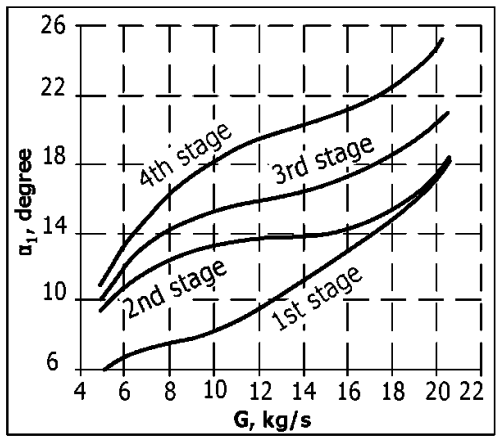

Figure 7.6 *Optimal distribution of angles α_1 along the flow path subject to mass flow.*

Efficiency of an initial design of the flow path with synchronous turn of all nozzles and efficiency of the design received as result of optimal design with the optimal law of angles α_1 change by operation modes are presented in Fig. 7.7. The efficiency of the received flow path essentially surpasses efficiency of initial flow path on all operation modes (Fig. 7.7). Significant improvements in efficiency has been observed in the low mass flow modes of

operation (up to 5%), as well as to the modes of mass flow greater than 18 kg/s. Additional generation of electricity for operating cycle is equal to 914.793 MWh (3.64%).

It is obvious, that it is impossible to create the flow path equally well working in a range of loadings from 30 to 125% of the nominal. So the efficiency of any flow path on modes with low mass flows remains at low enough level due to the great values of incidence angles, negative degrees of reaction, a substantial redistribution of disposable heat drop, offset u/C_0 of the stages aside from optimal values.

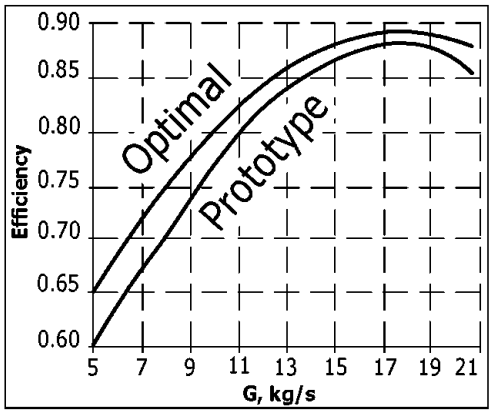

Figure 7.7 *Efficiencies of turbine expanders.*

The gain of optimal variant, in comparison with initial variant of design, on modes with low mass flows is provided by selection of optimal angles α_1 for all nozzle cascades along the flow path. As can be seen from Fig. 7.6 for optimal variant of RTEU FP, when small mass flow rate, value of the 1-st stage angle α_{1e} significantly lower compared to the values of the same angles of subsequent stages, that increases its heat drop and value of output velocity from the nozzle cascade (velocity c_1 close to the speed of sound M_{c_1} = 0.997).

Despite some deterioration in the effectiveness of 1-st stage, this solution allowed unload the subsequent stages and significantly improve their work conditions (positive degree of reaction on the mean radius of the second and third stages has been achieved) and get a positive final outcome.

On operation modes with the mass flow close to or surpassing on-design, increase of efficiency of the flow path became possible due to selection of an optimal combination of "base" design parameters ($D_{1,2}, l_{1,2}, \beta_{1g}, \beta_{2e}, z_{1,2}, b_{1,2}$) for each stage. This helped to reduce the losses associated with the inlet of the working fluid on the cascades and exit velocity losses, as well as to improve the efficiency of the nozzle and blade wheel cascades. Also on the considered operation modes there is a redistribution of heat drops between the stages: reducing load of 1-st and 4-th stages and increasing load of 2-nd and 3-rd.

7.2.2 Optimal Design of Gas Turbine Flow Path Considering Operational Modes

In the current section the example of applying developed methods and algorithms for the solution of the problem of optimization of gas turbine flow path taking into account the modes of operations is given. As the object of study the gas turbine installation GT-750-6M was chosen [40]. This *GTU* is used at the compressor station as a driver of gas-compressor unit. Selection of the specified unit is linked to the fact that such installations are quite widespread in the gas transportation system of Ukraine and more than 80% of them exhausted its resource.

In addition, the authors had at their disposal all the necessary project documentation and the results of the field tests of the manufacturer that was the necessary condition for optimization and the validation of the computational research results.

Optimization of FP of the low-pressure turbine installation GT-750M was carried out taking into account the actual operating loads and the inclusion in consideration of the thermal scheme (TS) of installation.

A direct one-dimensional flow model through the axial turbines FP (section 2.2.3) and the procedure of thermal schemes calculation of *GTU* (section 2.5) were involved in this case. A screenshot of a window of the specialized CAD system with active project of GT-750M installation is presented at Fig. 7.8. One-dimensional mathematical model of the turbine stages group is used in the process of solving common optimization tasks and to build the universal characteristics of the gas turbines, and the model of thermodynamic processes in thermal schemes of *GTU* – for thermodynamic calculation of the unit's thermal cycle (TC) for real operating modes.

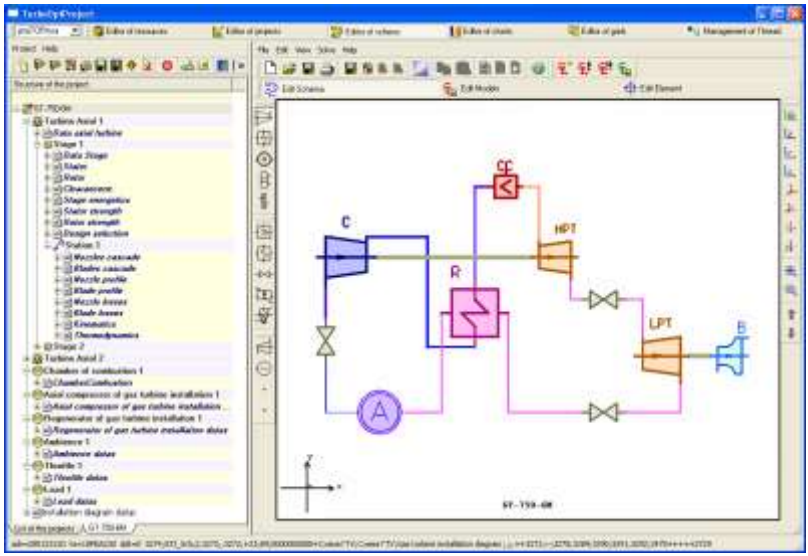

Figure 7.8 *Project of GT-750M installation in a specialized CAD system environment.*

Thermal cycle scheme consists of the following main elements: compressor (C); combustion chamber (CC); high pressure turbine (HPT), located on the

same shaft with compressor; free power turbine low pressure (LPT); regenerator (R); external consumer of net power – natural gas blower (B).

As can be seen from Fig. 7.8, GT-750-6M is a split-shaft gas turbine unit with waste-heat recovery.

Such a scheme, thanks to good surging characteristics, is more flexible, reliable and cost-effective in terms of variable operating mode and can be equally well applied for driving propeller, for ground transportation, for blast furnace production etc. When operating on the gas pipeline such a gas turbine unit can provide any mode of operation of the gas pipeline without throttling at the suction and without pressure lowering of the blower.

For operation modeling of the compressor and turbine, while calculating on the various modes the universal characteristics were used. Moreover, the characteristic of the compressor was built according to the manufacturer's data but turbines characteristics were obtained using specialized CAD system.

Fields on the characteristics of high and low pressure turbines covering ranges of operating modes of FP, obtained by calculating the GT-750-6M unit thermal scheme for one calendar year of real modes of operation.

Calculations have showed that area of the work of the HPT FP is close to the on-design regime, but LPT works in more wide range of operating modes.

The problem of flow path geometrical parameter multi-mode optimization with consideration of the thermal scheme of the unit is difficult and extremely labor-intensive. At present, in the available literature, recommendations and examples of the solution of optimization problems in similar papers are practically not existent. Considering the above, for the purpose of the development of approaches to finding solutions to specified problems, preliminary research directed at the consideration of the influence of the efficiency of high and low pressure flow paths of GT-750-6M on its integral

characteristics (fuel consumption, *GTU* efficiency, cycle initial parameters, etc.) have been carried out.

The increase of the efficiency of gas turbines flow paths is one of the preferable methods of increasing GTU efficiency and useful power. However, as studies have shown, in some cases the increase of the efficiency of gas turbine separately used in the thermal scheme within modernization does not produce the expected effect. It is connected with features of the configuration of turbines within GTU, and also with the interaction of turbines with other elements of the thermal scheme. The influence of gas turbines flow paths efficiency on GTU performance parameters using a GT-750-6M unit (Fig. 7.8) is considered as an example.

Increasing the efficiency of HPT

As can be seen from Fig. 7.8, HPT is located on the same shaft as the axial compressor and provides its work. The mass flow rate, temperature and pressure of combustion products behind HPT must be in strict conformity with the values necessary for generation by LPT power, set by the external consumer (the natural gas blower) in the current operation mode. An increase of HPT efficiency in the specified operating conditions of the turbine does not lead to the predicted improvement of the performance parameters of the turbine unit. For example, when saving the unit operation mode (useful power, the power turbine rotor speed and the air parameters), the increase of HPT efficiency leads to an increase of its power. The additional power of HPT is transmitted through the shaft to the axial compressor, which leads to the redistribution of the main parameters of the gas-turbine cycle, namely:

- the increase of power for compressor drive causes an increase in compressor rotor speed, which causes an increase of the air flow rate and a slight increase of the compression ratio (compressor efficiency decreases

because of the displacement of the compressor and HPT joint operation line takes place);

- the new air flow rate and pressure at the compressor outlet are superfluous for this thermal cycle and cause a fall in combustion products at the combustion chamber outlet, which inevitably leads to a decrease in cycle thermodynamic efficiency.

The specified changes in the unit's thermal scheme nullify the effect expected from HPT flow path optimization.

Increasing the efficiency of LPT

The calculations show that the increase of LPT efficiency has a favorable effect on the performance parameters of the GT-750-6M and allows getting increase the net power while maintaining fuel consumption or fuel economy while maintaining power, given to the external consumer. Considerable deviations of the gas-turbine cycle parameters from design are not observed in this case.

Thus, an increase in the efficiency of LPT flow path is the most rational variant of the GT-750-6M unit modernization. The specified modernization does not lead to an essential redistribution of the parameters of the gas-turbine cycle and therefore does not touch the expensive elements of the unit such as the compressor, combustor, regenerator and supercharger.

It is worth to note that these studies were carried out for the GT-750-6M unit but research results and conclusions are valid for all *GTUs* with a similar thermal scheme.

For the optimization of geometrical parameters of GT-750-6M LPT flow path, taking into account the actual modes of operation, three upper levels of developed recursive algorithm optimization, described in Chapter 1, were

involved. The distribution of the tasks and interaction between the local design levels are depicted in Fig. 7.9.

The highest level in the hierarchy of the design process "Scheme" is intended to calculate the distributions of parameters of GTU cycle (pressure, temperature, capacity, and cost) between elements in the scheme, as well as to determine the integral indicators of the unit at the off-design operation modes. As can be seen from Fig. 7.9, from the level "Scheme" to the level "Cylinder" the sets of mode parameters come that uniquely identify modes of the FP operation (consumption of combustion products at the entrance to the FP – G_0, full gas pressure at the inlet of FP – P_0^*, full gas temperature at the inlet to FP – T_0^*, full gas pressure at the outlet of the FP – P_2^*, turbine shaft speed – n).

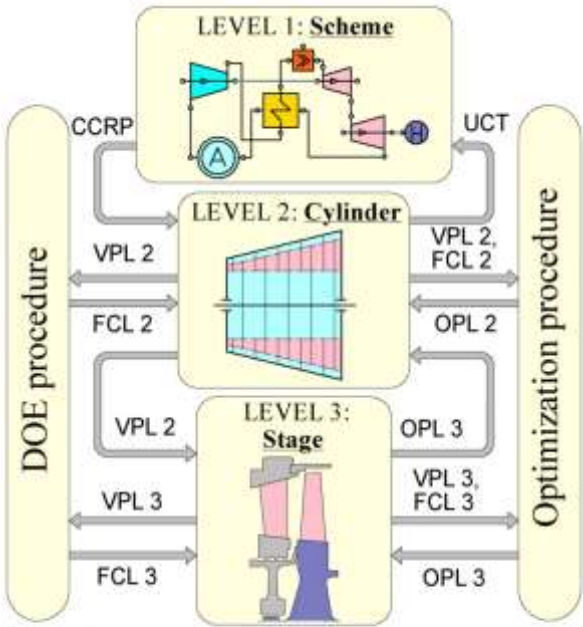

Level	VPL	OPL
Cylinder	$d_{1,2}$; $l_{1,2}$; α_1; α_{0g}; β_2; β_{1g}; P_0^*; h_0^*; P_2^*; P_2^*; G_0; n; u/C_0	$d_{1,2}$; $l_{1,2}$; α_1; α_{0g}; β_2; β_{1g}
Stage	$d_{1,2}$; $l_{1,2}$; α_1; α_{0g}; β_2; β_{1g}; P_0^*; h_0^*; P_2; u/C_0; n; $Z_{1,2}$; $b_{1,2}$; $m_{1,2}$	$Z_{1,2}$; $b_{1,2}$; $m_{1,2}$

Figure 7.9 *The structure of optimal design technique.*

At the "Cylinder" level optimal values of basic geometrical parameters such as mean diameters of the nozzle and blade wheel cascades (D_1, D_2), the heights of the nozzles and the blades (l_1, l_2), inlet/outlet flow angles in both absolute and relative motions for nozzle and blades wheel cascades ($\alpha_1, \alpha_{0g}, \beta_2, \beta_{1g}$) were defined.

As a functional limitation at the level of "Cylinder" the flow rate of combustion products at the entrance to the LPT was chosen, that should match to the flow rate through the initial FP of the unit. For assessing the quality criterion in the process of optimization the value equal to the total work of the gas turbine (GT) for one year of operation was used.

At the next level "Stage" the optimal values of the numbers of the nozzle and rotor blades (z_1, z_2) for their cascades were found, and optimized parameters on the "Cylinder" level were used as parametric constraints. Quality criterion is the internal efficiency of the stage.

A thermodynamic calculation of the *GTU* schemes procedure (section 2.5) is used as the mathematical model at the "Scheme" level. At the "Cylinder" and "Stage" levels a procedure for direct one-dimensional calculation of the axial turbines FP (section 2.2.3) is applied. When the optimal solution at the level of "Cylinder" was found, using direct one-dimensional model of FP, the universal characteristics of well-designed LPT are build. These characteristics are returning to the "Scheme" level for calculation of integral characteristics of the *GTU*.

Three iterations for refining the optimal solution were conducted during computation. The optimization task was solved taking into account 177 real operation modes of the *GTU*. Each mode corresponds to unit operation for 24 hours. Unit loading for the considered period varied in a range from 52 to 73% of the on-design mode, equal to 6 MW.

The calculations has shown that in the on-design operation mode of the *GTU* the gain of *LPT* useful capacity, without mass flow rate increase, was 1.5% (93.1 kW). Efficiency increase after optimization is caused by a decrease in the losses in nozzle and rotor cascades, exit energy losses, and a reduction of leakages in radial clearance. Therefore, in the on-design mode the velocity coefficient for nozzle and rotor cascades of an optimal flow path increased by 0.4 and 0.6% respectively, the absolute velocity downstream rotor (c_2) decreased by 22%, and the leakage in radial clearance decreased by 2.7%. There was an increase of heat drop for nozzle cascades and a decrease of heat drop for rotor cascades (reaction decreased from 0.478 to 0.368). When the optimal design of the turbine works within the thermal scheme of the studied unit, the reduced value of velocity c_2 leads to a corresponding decrease of total pressure losses in the exhaust diffuser.

The optimum values of variable parameters, obtained through the optimization, are shown in the Table 7.6.

Table 7.6 *Results of optimal design of the GT-750-6M high pressure turbine.*

Parameter	Initial design	Optimal design
1. Nozzle mean diameter – D_1, m	0.970	1.046
2. Blade wheel mean diameter – D_2, m	0.972	1.050
3. Nozzle blade height – l_1, m	0.210	0.203
4. Working blade height – l_2, m	0.211	0.222
5. Inlet metal angle of nozzle cascade – α_{0g}, deg	90.00	94.54
6. Inlet metal angle of blade wheel cascade – β_{1g}, deg	47.33	47.93
7. Outlet effective angle of nozzle cascade – α_1, deg	20.67	19.00
8. Outlet effective angle of blade wheel cascade – β_2, deg	25.18	24.12
9. Number nozzle blades – z_1, pcs	48	41
10. Number rotor blades – z_2, pcs	60	70

As the result of the optimization the efficiency increment depending on the operation mode of *GTU* is from 0.09 to 0.27%. The fuel economy (of natural gas) for *GTU* with optimal *LPT* flow path depending on operation modes is

given in Fig. 7.10. The total fuel economy for the considered period of 177 days amounted to 50831 kg.

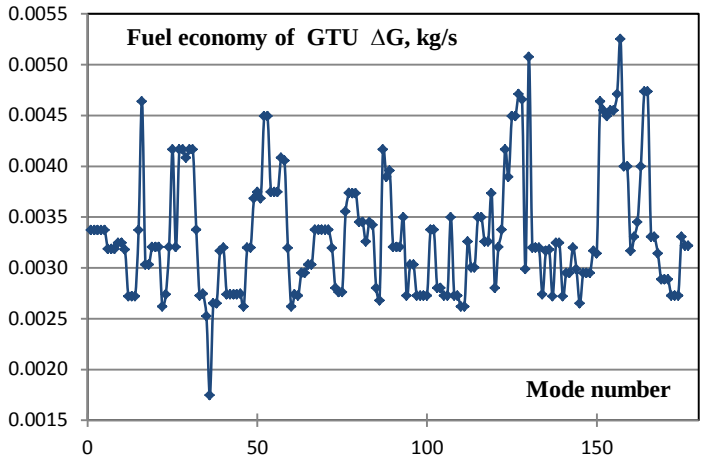

Figure 7.10 *Fuel economy for the GT-750-6M with optimal LPT by operation modes.*

Before performing the work of such complexity, as the above examples of optimal design of multi-stage cylinders, the authors made a huge amount of the work related to the verification of the developed and implemented mathematical models as well as proposed methods of optimization.

It should be emphasized that the criteria of the calculation results is an experiment. Full-scale experimental investigation of powerful turbines is very expensive. However, at one of the thermal power plants the test of turbine 200 MW capacity was conducted in a wide range of operational modes.

Comparison of results of the calculation research of the HPC FP turbines with experimental data obtained as a result of field tests of the same turbine in a wide range of operating modes, have strongly affirmed that used in optimization designed and implemented mathematical models have high accuracy and

adequately simulate physical processes of flow of the working fluid in axial turbine flow path.

According to the results of the conducted studies one important conclusion can be formulated.

The further improvement of the indicators level of the quality of existing and newly designed advanced multi-stage axial turbine installations is possible only using the most modern methods and software systems, capable of solving tasks of a multilevel object-oriented multi-criterion and multi-parameter optimization of the flow paths of axial turbines, taking into account their operational mode.

References

[1] Box, E. P., and D. W. Benken. "Some new three level design for the study of quantitative variables." *Technometrics.* Vol. 2.4. 1960. 455–475. Print.

[2] Rechtschaffner, R. L. "Saturated fractions of 2n and 3n factorial designs." *Technometrics.* Vol. 4. 1967. 569–575. Print.

[3] Himmelblau, D. M. *Applied Nonlinear Programming* / The University of Texas, Austin, Texas. New York: McGraw-Hill Book Company, 1972. Print.

[4] Sobol, I. M., and R. B. Statnikov. *Selection of optimal parameters in the multi- criterion problems*. Moscow: Nauka, 1981. Print (in Russian).

[5] Karaboga, D. "An idea based on honey bee swarm for numerical optimization". *Technical report - TR06, Erciyes University, Engineering Faculty, Computer Engineering Department,* 2005. Web. 15 October 2015 <http://mf.erciyes.edu.tr/abc/pub/tr06_2005.pdf>.

[6] Pham, D. T., A. Ghanbarzadeh, E. Koc, S. Otri, S. Rahim and Zaidi M. "The Bees Algorithm – A Novel Tool for Complex Optimisation Problems." *Technical Note, Manufacturing Engineering Centre, Cardiff University, UK*. 2005. CF24 3AA. Web. 15 October 2015 <https://svn-d1.mpi-inf.mpg.de/AG1/MultiCoreLab/papers/Pham06%20-%20The%20Bee%20Algorithm.pdf>.

[7] Yuza, Ya. "Equations of thermodynamic properties of water and steam, designed for computers." *Thermal Engineering*. Vol. 1. 1967. 80–86. Print (in Russian).

[8] Stepanov, G. Yu. *Hydrodynamics of the turbomachines cascades*. Moscow: 1962. Print (in Russian).

[9] Sirotkin, Ya. A. *Aerodynamic calculation of the axial turbomachines flow*. Moscow: Mashinostroenie, 1972. Print (in Russian).

[10] Shchegliaev, A. V. *Steam turbines*. Moscow: Energy, 1976. Print (in Russian).

[11] Kirilov, I. I. *Theory of turbomachines*. Leningrad: Mashinostroenie, 1972. Print (in Russian).

[12] Korn, G. A., and T. M. Korn. *Mathematical Handbook for Scientists and Engineers.* New York: McGraw-Hill Book Company, 1968. Print.

[13] Boiko, A. V., and A. V. Garkusha. *Aerodynamics of flow pass of steam and gas turbines: calculations, researches, optimization, designing*. Kharkov: NTU "KhPI", 1999. ISBN 966-593-059-3. Print (in Russian).

[14] Boiko, A. V., and Y. N. Govoruschenko. *The fundamentals of the theory of optimal design of axial turbines flow paths*. Kharkov: Vishcha Shkola, 1989. ISBN 5-11-000692-X. Print (in Russian).

[15] Boiko, A. V. *Optimal design of axial turbine flow path*. Kharkov: Vishcha Shkola, 1982. Print (in Russian).

[16] Craig, H. R. M., and H. J. A. Cox. "Performance Estimation of Axial Flow Turbines." *The Sust. Of Mech. Eng. Proc.* Vol. 185, No. 32/71. 1970. 407–424. Print.

[17] Boiko, A. V., Yu. N. Govorushchenko and A. P. Usaty. "The creation of an empirical methodology for determining the coefficients of energy losses in turbine cascades by using the theory of planning the experiment." *Miscellany "Power engineering"*. Issue 42. Kharkov, 1986. 8–14. Print (in Russian).

[18] Boiko, A. V., Yu. N. Govorushchenko, G. L. Romanov and A. P. Usaty. "Study on efficiency of axial turbine stages by using the formal macro modeling." *Thermal Engineering.* No. 6. 1988. 24–27. ISSN 0040-6015. Print

[19] Govoruschenko Y., L. Moroz and P. Pagur. "Axial turbine stages design: 1D/2D/3D simulation, experiment, optimization." *Design Of Single Stage Test Air Turbine Models And Validation Of 1D/2D/3D Aerodynamic Computation Results Against Test Data Proceedings of ASME Turbo Expo 2005, June 6-9, 2005*. Reno-Tahoe, Nevada, USA. GT2005-68614-2630. Web. 15 October 2015 <http://www.softinway.com/wp-content/uploads/2013/10/Axial-turbine-stages-design-1D2D3D.pdf>.

[20] *OST 108.260.01-84. The nozzles profiles of permanent section of the stationary steam turbines. The types, basic parameters and dimensions*. Leningrad: NPO CKTI, 1985. Print (in Russian).

[21] Abramov, V. I., G. A. Filippov and V. V. Frolov. *Thermal calculation of turbines*. Moscow: Mashinostroenie, 1974. Print (in Russian).

[22] Zhukovsky, M. I. *Aerodynamic calculation of flow in the axial turbomachines*. Leningrad: Mashinostroenie, 1967. Print (in Russian).

[23] Lojciansky, L. G. *Fluid and gas mechanics*. Moscow: Nauka, 1978, Print (in Russian).

[24] Boiko, A. V., Yu. N. Govorushchenko, S. V. Yershov, A. V. Rusanov and S. D. Severin. *Aerodynamic Computation and Optimal Projection of Turbomachine Flow Paths.* Kharkov: NTU "KhPI", 2002. ISBN 966-593-228-4. Print (in Russian).

[25] Aronov, B. M., M. I. Zhukovsky and V. A. Zhuravlev. *Profiling the blades of aviation gas turbines*. Moscow: Mashinostroenie, 1975. Print (in Russian).

[26] Govorushchenko, Yu. N., G. L. Romanov, E. E. Skibina and A. P. Usaty. "Assessment of geometrical parameters of turbine cascade using automated designing of flow path. Miscellany." *Power engineering.* Kharkov, 1990. Print (in Russian).

[27] Shubenko-Shubin, L. A. *Strength of steam turbines*. Moscow: Mashinostroenie, 1973. Print (in Russian).

[28] Hawtorne, W. R. "Thermodynamics of Cooled Turbines. Part I. The turbine stage. Part II. The Multistage Turbine." *Trans of ASME.* Vol. 78. 1956. Print.

[29] Govorushchenko, Yu. N., G. L. Romanov and E. E. Skibina. "Automated preliminary design of flow path of the multistage steam turbines." *Thermal Engineering*. No. 6. 1991. ISSN 0040-6015. Print.

[30] Baily, F. C., K. C. Cotton and R. C. Spencer. "Predicting the performance of large steam turbogenerator operating with saturated and low super heat steam conditions." *Proc. Amer. Power. Conf*. Vol. 29. 1967. 5–64. Print.

[31] Govorushchenko, Yu. N., G. L. Romanov, E. E. Skibina and A. P. Usaty. "The subsystem of automated design of steam turbine flow path." *Thermal Engineering*. No. 6, 1989. ISSN 0040-6015. Print.

[32] Boiko A. V., and Yu. N. Govorushchenko. "Design problems of axial turbine stages." *News of the Academy of Sciences of the USSR. Energy and Transport.* No. 3. 1985. 134–140. Print (in Russian).

[33] *OST 108.260.02-84. The working blades profiles of permanent section of the stationary steam turbines. The types, basic parameters and dimensions.* Leningrad: NPO CKTI. 1985. Print (in Russian).

[34] Boiko, A. V., S. N. Kozhevnikov and V. A. Meltiukhov. "Optimization of the shape subsonic profile cascades of axial turbine." *News of the Academy of Sciences of the USSR. Energy and Transport*. Vol. 6. 1984. 119–124. Print (in Russian).

[35] Boiko, A. V., Yu. N. Govorushchenko and M. V. Burlaka. *Application of Computational Fluid Dynamics to Optimization of Turbomachine Blades*. Kharkov: NTU "KhPI", 2012. ISBN 978-617-05-0010-6. Print (in Russian).

[36] Piegl, L., and W. Tyler. *The NURBS Book*. Springer, 1996. Print.

[37] Boiko, A. V., Yu. Govorushchenko and M. Burlaka. "New method and algorithm of three-dimensional turbine guide blade rim optimization." *Proceedings of ASME 2010 3rd Joint US-European Fluids Engineering Summer Meeting and 8th International Conference on Nanochannels, Microchannels and Minichannels FEDSM2010, August 1-5, 2010, Montreal, Canada*. Vol. I. FEDSM-ICNMM2010-30018. ISBN: 978-0-7918-4948-4.

[38] Boiko, A. V., A. P. Usaty, A. S. Rudenko. *Multi-criterion Multi-parametric Optimization of Flow Paths of Axial Turbines taking into Consideration their Mode of Operation: monograph*. Kharkov: NTU "KhPI", 2014. ISBN 978-966-2426-94-6. Print (in Russian).

[39] Shvetsov, V. L., I. I. Kozheshkurt, V. A. Konev, A. V. Boiko, A. P. Usaty, V. G. Solodov and A. A. Khandrimailov. "Improving the high-pressure cylinder of the K-220-44-2M turbine at the Loviisa nuclear power station." *Thermal Engineering*. Vol. 60, No. 2. 2013. 95–105. ISSN 0040-6015. Print.

[40] Boiko, A. V., Yu. N. Govorushchenko, A. P. Usaty and A. S. Rudenko. "Optimal design of turbines taking into consideration the mode of operation." *Proceedings of the 8th European Turbomachinery Conference, March 23-27, 2009.* Graz, Austria. 959–970. Web. 15 October 2015 <http://www.gbv.de/dms/tib-ub-hannover/599496002.pdf>.

[41] Boiko, A. V., and A. P. Usaty. "Optimal positioning the valves of the multiple steam nozzle control system of steam turbine." *Proceedings of an International Conference on Engineering and Applied Sciences Optimization (OPT-i), Kos Island, Greece, 4-6 June 2014*. ISSN 2241-9098, ISBN 978-960-99994-5-8.

[42] Boiko, A. V., Yu. N. Govorushchenko, A. P. Usaty and O. S. Rudenko. "Optimal Design of Gas Turbines Flow Paths Considering Operational Modes." *Proceedings of ASME 2014 4th Joint US-European Fluids Engineering Summer Meeting and 12th International Conference on Nanochannels, Microchannels and Minichannels, FEDSM2014, August 3-7, 2014, Chicago, Illinois, USA.* FEDSM2014-21012, ISBN 978-0-7918-4622-3.

Short Introduction to the Book

The fundamentals of the theory for the optimal design of flow paths of turbo-machines are presented, including mathematical models of flow path elements, determination of the optimal number of turbine stages and the distribution of the heat drop between them, optimization of the spin laws of the nozzles and blades of axial turbine stages, taking into account slope and curvature stream lines, as well as leaks. Methods for creating optimal profiles considering the strength limitations are given. The problem of the spatial optimization of the shape of turbine blades using computational aerodynamics is described. The examples of the application of the theory to the projection of the optimal flow path of modern steam and gas turbines, taking into account their operational mode, are presented.

Short Biography of the Author

Anatoli Boiko, D. Sc., Full Professor, is a Head of the Turbine Projection Chair. The founder of a new scientific approach to turbine projection - optimal design of turbomachines. Author of many articles and several books on one dimensional, 2D and 3D optimization of the axial turbines flow paths. Winner of the State Prize of Ukraine in science and technology.

Yuri Govorushchenko, is a Senior Research Fellow, Ph.D. The largest specialist in optimal design of turbomachines. Author of several books, articles and programs on one dimensional, 2D and 3D optimization of the turbine stages, modules and cylinders of the steam and gas turbines.

Alexander Usaty, is a Senior Research Fellow/lecturer, D.Sc. A well-known expert in the field of optimal design of turbomachines. Author of one book, several articles and programs on the multi-criterion, multimode and multi-parametric optimization of the steam and gas turbines cylinders.

ISBN 978-1-940366-67-8
9 781940 366678 >
Price: US $125

To order additional copies of this book, please contact:
Science Publishing Group
book@sciencepublishinggroup.com
www.sciencepublishinggroup.com